School of Doctoral Studies in Biological Sciences
University of South Bohemia in České Budějovice
Faculty of Science

Optimization and Application of Chromatographic and Mass Spectrometric Methods for Determination of Lipidome in Physiological, Nutritional and Biochemical Issues

Ph.D. Thesis

Ing. Ivana Schneedorferová

Supervisor: RNDr. Aleš Tomčala, Ph.D.
Institute of Parasitology, Biology Centre CAS, České Budějovice

České Budějovice 2019

This thesis should be cited as:

Schneedorferová, I, 2019: Optimization and Application of Chromatographic and Mass Spectrometric Methods for Determination of Lipidome in Physiological, Nutritional and Biochemical Issues. Ph.D. Thesis. University of South Bohemia, Faculty of Science, School of Doctoral Studies in Biological Sciences, České Budějovice, Czech Republic, 110 pp.

Annotation

This study defines a sequence of methods offering comprehensive information about the quality and quantity of lipid molecules. The proposed methodology, mostly based on HPLC-MS-MS data, is able to provide enough information to determinate the particular lipid species in a single run. The lipid and fatty acid determination procedure were suggested including sample preparation, instrumental measurement, and data processing with statistical implementation. The presented thesis consists of four publications and the proposed methodology was successfully applied to algal, insect and fish matrices. In the last publication, where the methodology was applied to algae matrix, were 289 lipid species from 9 lipid classes in total detected and identified. Proposed methodology represents a robust, reliable and accurate method for glycerolipid detection.

Declaration

I hereby declare that this thesis is based on my own work and all other sources of information have been acknowledged. I hereby declare that, I accordance with Article 47b of Act No. 111/1998 in the valid wording. I agree with the publication of my PhD thesis, in full to be kept in the Faculty of Science archive, in electronic form in the publicly accessible part of the STAG database operated by the University of South Bohemia in České Budějovice accessible through its web pages. Further, I agree to the electronic publication of the comments of my supervisor and thesis opponents and the record of the proceedings and results of the thesis of the text of my thesis with the Theses.cz thesis database operated by the National Registry of University Theses and a plagiarism detection system.

Date…….. Signature……

Ivana Schneedorferová

This thesis originated from a partnership of Faculty of Science, University of South Bohemia, and Institute of Parasitology, Institute of Entomology, Biology Centre CAS, supporting doctoral studies in the Physiology and Developmental Biology - Animal study programme.

Financial support by the Czech Science Foundation (P506/12/1522) and the University of South Bohemia Grant Agency (GAJU 038/2014/P) is gratefully acknowledged.

Acknowledgements

Primarily I would like to thank my supervisor RNDr. Aleš Tomčala, Ph.D. for everything he taught me, his support and personal approach. I would like to express my sincere gratitude to prof. Ing. Miroslav Oborník, Ph.D. for taking me into his crew. I am also very grateful to RNDr. Petr Šimek, CSc. for the opportunity to work and learn from all members of the Laboratory of Analytical Biochemistry and Metabolomics. Special thanks belong to Ing. Helena Zahradníčková, Ph.D. for help in both lab and writing. I would like to thank the Head of the Department prof. RNDr. Dalibor Kodrík, CSc. for his help and motivation during the study. Besides that, I am very thankful to Ing. Aleš Svatoš, CSc. for the opportunity to experience the research in Mass Spectrometry Group of Max Planck Institute for Chemical Ecology in Jena. Furthermore, I would like to extend thanks to all co-authors of the mentioned articles. Finally, I must express my very profound gratitude to my parents for providing me with unfailing support and continuous encouragement throughout my years of study. Thank you.

List of papers and author's contribution

The thesis is based on the following papers (listed chronologically):

I. Zahradníčková, H., Tomčala, A., Berková, P., **Schneedorferová, I.**, Okrouhlík, J., Šimek, P., Hodková, M., 2014. Cost effective, robust, and reliable coupled separation techniques for the identification and quantification of phospholipids in complex biological matrices: application to insects. Journal of Separation Science, 37: 2062-2068. (IF = 2.415)
Ivana Schneedorferová participated in sample preparation, extraction and pre-separation.

II. **Schneedorferová, I.**, Tomčala, A., Valterová, I., 2015. Effect of heat treatment on the n-3/n-6 ratio and content of polyunsaturated fatty acids in fish tissues. Food Chemistry, 176: 205-211. (IF = 4.946)
Ivana Schneedorferová participated in sample preparation, lipid extraction, derivatization, instrumental measurement, data evaluation and writing the manuscript.

III. Bajgar, A., Kučerová, K., Jonatová, L., Tomčala, A., **Schneedorferová, I.**, Okrouhlík, J., Doležal, T., 2015. Extracellular adenosine mediates a systemic metabolic switch during immune response. PLoS biology, 13. (IF = 9.163)
Ivana Schneedorferová participated in sample preparation and extraction for lipid analyses.

IV. Tomčala, A., Kyselová, V., **Schneedorferová, I.**, Opekarová, I., Moos, M., Urajová, P., Kručinská, J., Oborník, M., 2017. Separation and identification of lipids in the photosynthetic cousins of Apicomplexa *Chromera velia* and *Vitrella brassicaformis*. Journal of Separation Science, 40: 3402–3413. (IF = 2.415)
Ivana Schneedorferová was responsible for sample preparation, lipid extraction, pre-separation, derivatization, instrumental measurement, data assembly, data evaluation and drafting the manuscript.

Co-autor's agreement:

…….. …… …….

Ing. Helena Zahradníčková, Ph.D. Mgr. Adam Bajgar, Ph.D. RNDr. Aleš Tomčala, Ph.D.

CONTENT

1 INTRODUCTION

1.1 LIPIDS

The lipids are a group of very diverse substances that can be divided in many ways. They differ both structurally and functionally. Lipids can be defined as biological substances which are insoluble in water but often soluble in organic solvents. According to Fahy *et al.* (Fahy, 2005; Fahy, 2009), lipids can be classified into eight basic groups, namely fatty acids, glycerolipids, glycerophospholipids, sphingolipids, sterol lipids, prenol lipids, saccharolipids, and polyketides. This classification is based on the chemical character and, above all, the hydrophobic and hydrophilic properties of the lipid molecule (Fahy, 2005; Fahy, 2009). Lipid molecule examples are depicted in Figure 1. Due to the broad spectrum of diverse chemical compounds covering lipids, this work will be focused only on the first three groups.

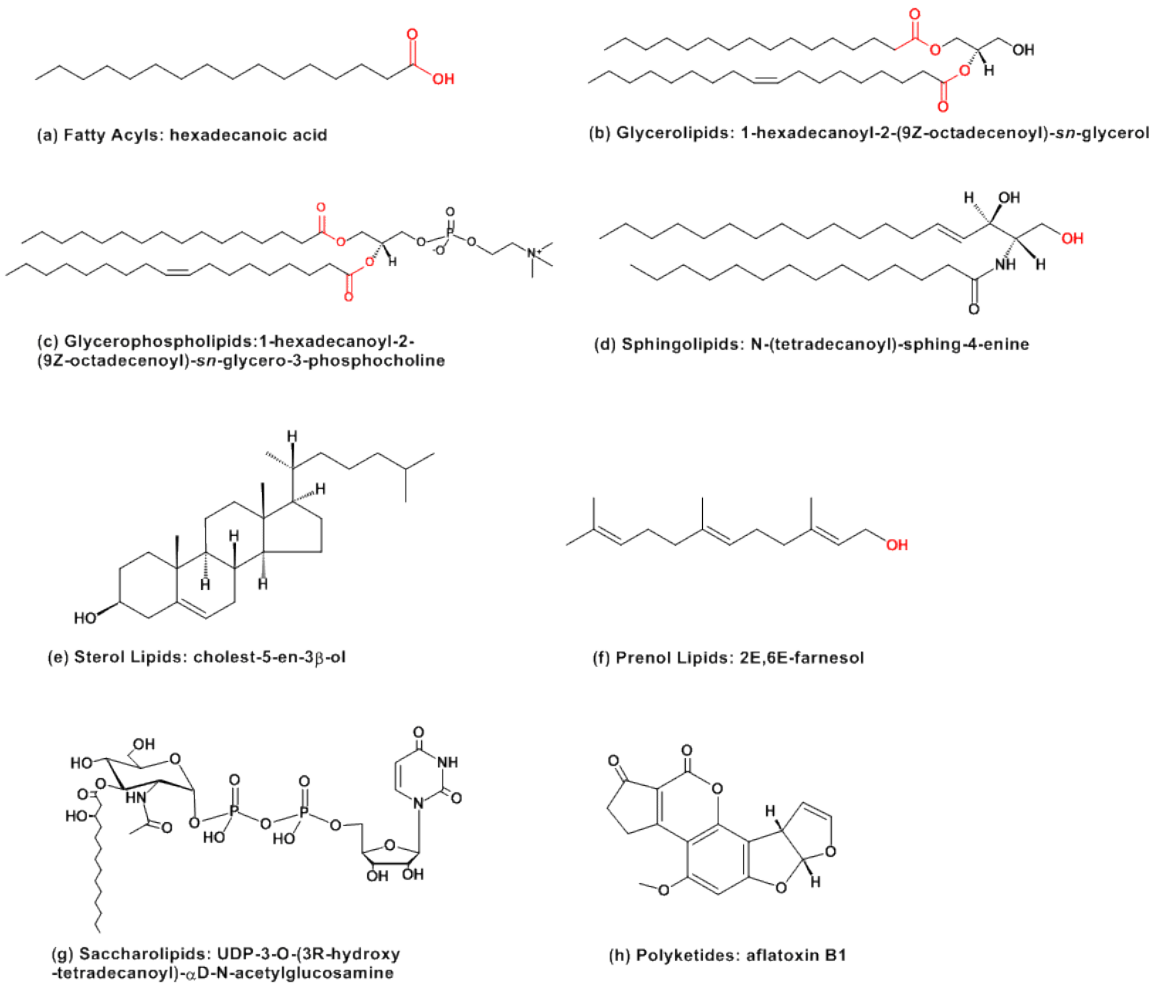

Figure 1: Lipid classification according to Fahy *et al.* (Fahy, 2005)

1.1.1 FATTY ACIDS (FAS)

Fatty acids are fundamental components of all lipid molecules, and moreover, they form a separate lipid group. They are composed of methylene units that provide hydrophobic character and carboxyl groups with hydrophilic character. Commonly, their aliphatic chain of 4-36 carbons is unbranched. Fatty acids include single carbon bonds and may include one or more double bonds. Physical and similarly chromatographic properties are dependent on the number of carbons and the number of double bonds. In gas chromatography systems the increasing number of carbons raises the retention time, and on the other hand the increasing number of double bonds decreases it. This study was focused on the straight-chain saturated and unsaturated fatty acids with a terminal carboxylic acid group, supposed to be the most abundant subclass. Figure 2 shows examples.

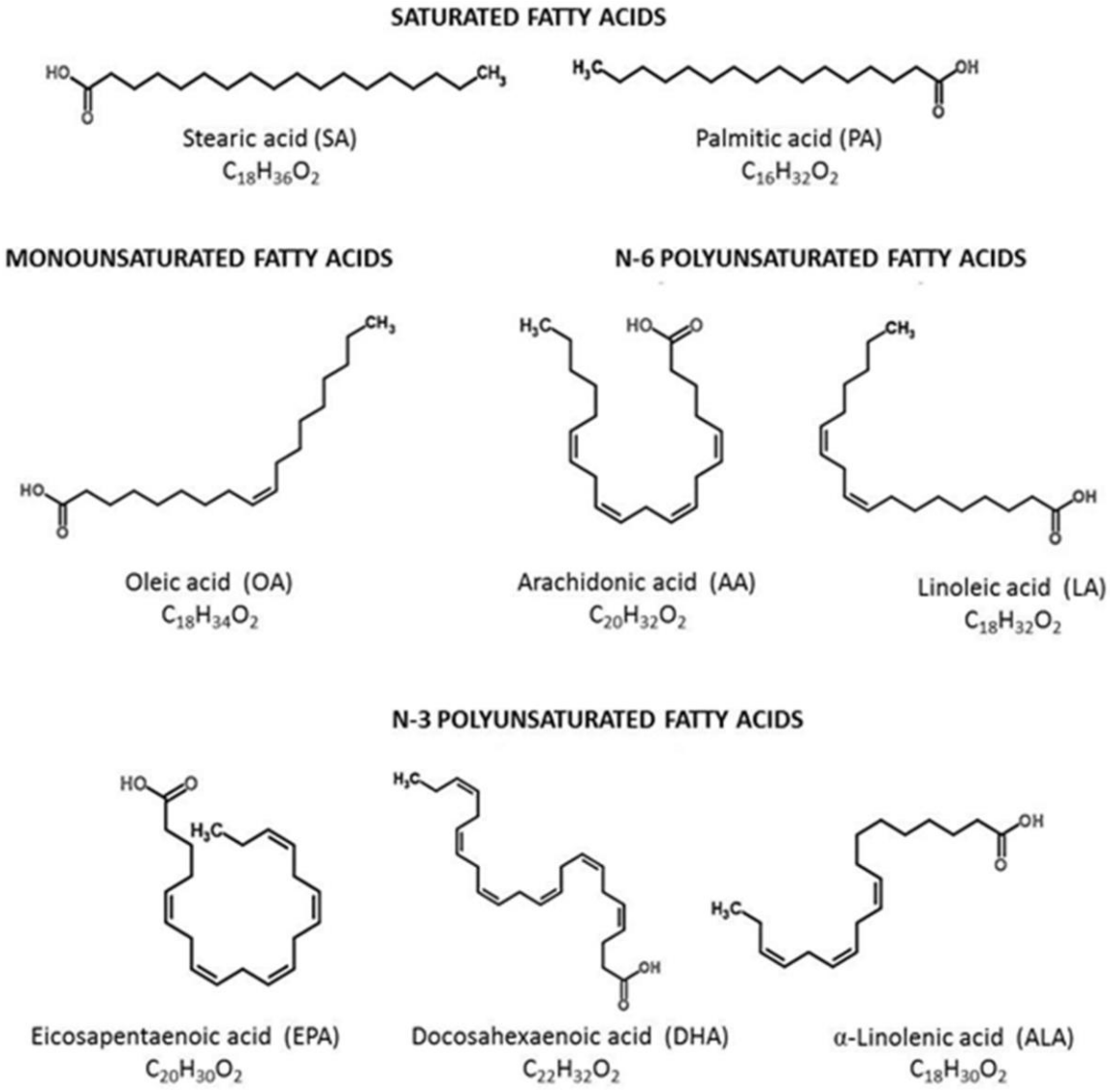

Figure 2: Representatives of saturated fatty acids (Sokoła-Wysoczańska, 2018)

Generally, FAs are synthesized by the repeated addition of two carbon units to a growing carboxylic acid chain attached to the acyl carrier protein (Goodman, 2007). The synthesis itself produces exclusively saturated FAs which are supposed to be further modified by desaturation (addition of double bond into the FA chain) and elongation (adding additional carbons to the FA chain) (Chirala, 2004; Fahy, 2005). Two types of elongases and several types of desaturases are recognized due to their mode of action. The first type of elongases can process only saturated and monounsaturated fatty acid, the second group is able to elongate only polyunsaturated fatty acids (Uttaro, 2006; Fritzler, 2007). Desaturase classes are divided according to the position of the double bond introduced to the carbon chain. If an organism possesses complete enzymatic equipment, then it is capable of producing polyunsaturated fatty acids (PUFAs) (Guschina, 2006). However, not all organisms are able to produce PUFAs. For instance, mammals lack Δ12 and 15 desaturases,

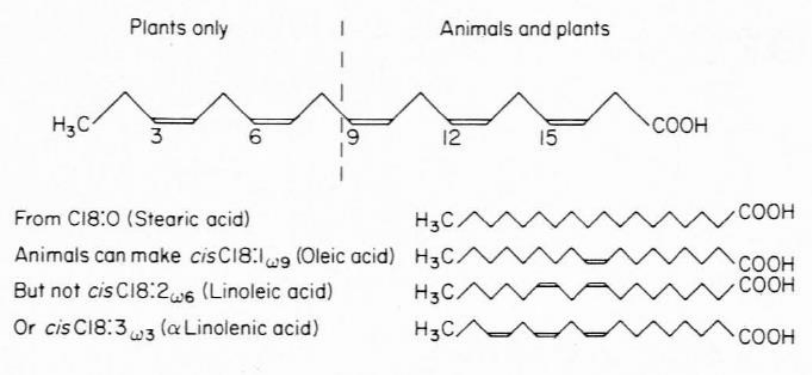

Figure 3: Formation of unsaturated fatty acids from precursors (Davidson, 1985)

therefore they are unable to synthetize important precursors for PUFAs - ω-6 linoleic acid (LA) and ω-3 linolenic acid (ALA) (Figure 3). These FAs have to be obtained from food and therefore are called essential. PUFAs such as eicosapentaenoic acid (EPA) and docosahexaenoic acid (DHA) are crucial for eukaryotes. PUFAs play a role in the regulation of fluidity, flexibility, and selective permeability of membranes. PUFAs, in general, have functions in many cellular and physiological processes such as cold adaptation and survival, modulation of ion channels, endo/exocytosis, pathogen defence, chloroplast development and activities of membrane-associated enzymes sensitive to biophysical properties of lipid membranes (Wallis, 2002). The key roles of PUFAs have been and are being studied widely. Their effect on the human organism is monitored closely. Basically, two types of PUFAs according to the position of the last double bond can be distinguished - of ω-3 and ω-6 FAs. Furthermore, the physiological impact of a particular group is very different. The latest

research points to the importance of ω-3 and ω-6 FAs ratio rather than their amount because of the fact that ω-3 and ω-6 synthetic paths are competitive (SanGiovanni, 2005). For instance, a diet of human ancestors contains much more ω-3 FAs, which could lead to human brain evolution (Zhu, 2010). On the other hand, nowadays the western diet has a much higher content of ω-6 PUFAs and has negative impacts on the organism. The highlighted example could be human metabolic syndrome (Poudyal, 2011). The positive effects of ω-3 PUFA on the cardiovascular system (Adkins, 2010; Russo, 2009; Casula, 2013), obesity and diabetes prevention (Wu, 2014; Simopoulos 2002), cancer progression (Sarotra, 2010; Sala-vila, 2011), brain development and function (Suominen-Taipale, 2010; Branbury, 2011), by a number of various mechanisms were confirmed.

1.1.2 OTHER LIPID CLASSES

The target lipid molecules of this study are glycerolipids and glycerophospholipids (PLs). The best-known glycerolipids are mono-, di- and triacylglycerols. Those are esters of glycerol and one or more fatty acids. Glycosyldiacylglycerols (GLs) containing one or more residues of sugar attached to glycerol by glycosidic bond and betaine lipids (BLs) possessing N-permethylated hydroxyamino acid in the polar headcan be placed into glycerolipids group as well (Figure 4). Glycerophospholipids are classified separately because they are widely represented in nature and have a number of important functions.

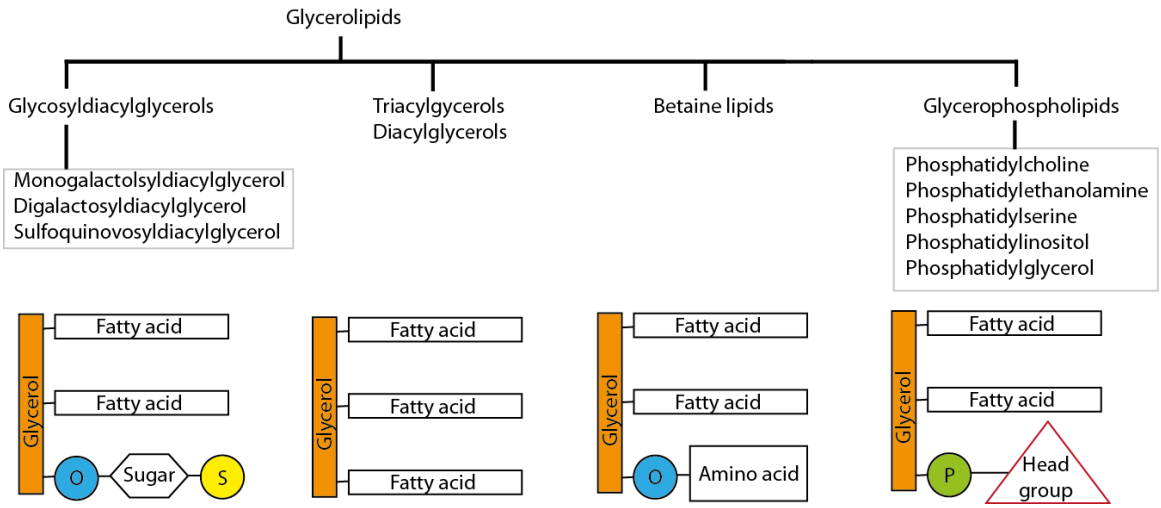

Figure 4: Classification and structure of glycerolipids with respect to polarity (Cox, 2000 modified in accordance with LIPIP MAPS)

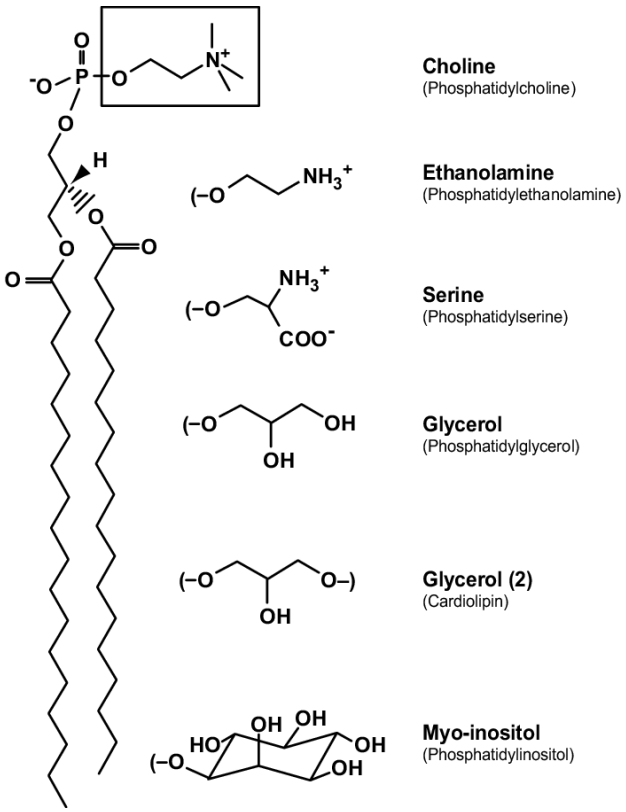

Figure 5: Structure of glycerophosphate-based lipids (Dowhan, 2015)

From another point of view, lipids can be divided into two groups, storage and structural, in a simplified way. Energy in living systems is mostly stored in the form of sugars as glycogen, or in glycerolipids - triacylglycerols (TGs). TGs serve as a pool of fatty acids which is used for energy production via β-oxidation. The gain of chemical energy by cleaving the hydrogen-carbon bond is enormous. Especially in terrestrial organisms, TGs have several advantages as storage molecules compared to sugars. TGs are stored in the anhydrous form, produce high caloric content per unit and release almost two times more metabolic water (Arrese, 2010). TGs also represent a group of lipids with biotechnological potential. For instance, many microalgae are able to produce a huge amount of TGs (e.g. 20-50% dry cell weight) under several types of environmental stress conditions. This feature has recently been very carefully investigated for possible biofuel production. (Rismani-Yazdi, 2012; Slocombe, 2015).

Structural lipids are the essential components of every cell, cell compartment, and organelle lipid bilayer including primarily GLs, BLs, and PLs but also sphingolipids or sterols. However, this study is focused only on the first three lipid groups. The presence of a particular structural lipid group is derived from the life-style of the organism. PLs mostly occur in heterotrophs, whilst, GLs exclusively occur in a photosynthetic organism.

The molecules of PLs includes glycerol with phosphoric acid residue and two fatty acids (as shown in Figure 5). They can be further divided by chemical properties of the polar molecule part into several classes: phosphatidyl-cholines (PCs), -ethanolamines (PEs), -serines (PSs), -glycerols (PGs) and -inositols (PIs) (Fahy, 2005). The distribution of the PL classes among the organelles differs due to the chemical and physiological properties of the particular class. The reason is that phospholipid membrane composition influences the action of proteins embedded in these membranes. PCs are the most abundant phospholipid in mammalian cells reaching 40-50% of all phospholipids. Also, the distribution of PLs differs in the outer and inner leaflet of the bilayer. For instance, the inner leaflet is normally highly enriched by PE and PS. The asymmetrictransbilayer distribution of PLs is very importantdue to several physiological functions. For example, the movement of PS from the inner to external leaflet of the plasma membrane of platelets is crucial for the initiation of the blood clotting cascade (Vance, 2014).

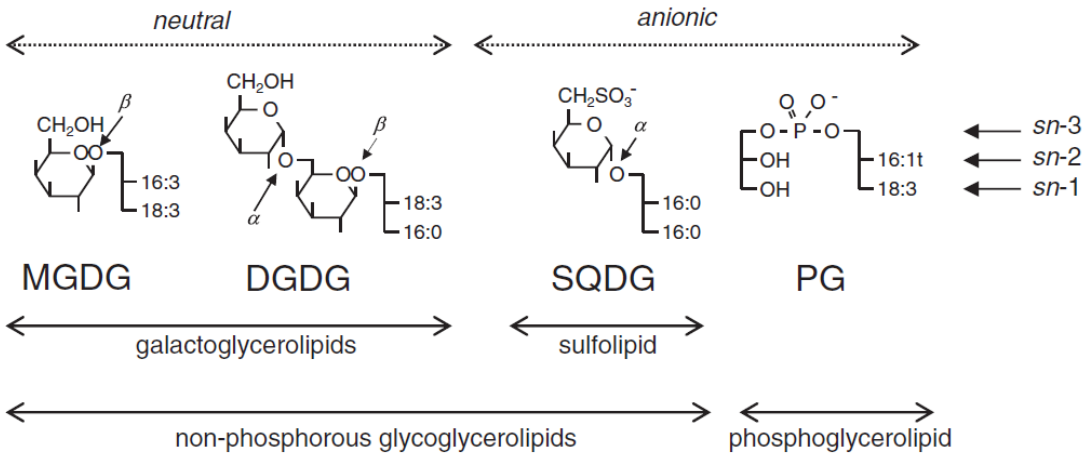

Figure 6: Glycosyldiacylglycerol classes conserved in photosynthetic membranes (Boudiere, 2014)

The photosynthetic membranes of prokaryotes and also eukaryotes first of all consist of three GLs, monogalactosyldiacylglycerol (MGDG), digalactosyldiacylglycerol (DGDG), and sulfoquonovosyldiacylglycerol (SQDG) and sole phospholipid – PG (Figure 6) (Sato, 2004; Boudiere, 2014). Thylakoid membranes harbour enzymatic machinery of photosynthesis and each lipid class plays its own swift role based on its physicochemical properties. MGDG has the ability to form the reverse micelles which helps to maintain membrane stability in highly curved regions nearby the large protein complexes. On the other hand, DGDG stabilizes the membrane bilayer. The absence of charges in MGDG and

DGDG and negative charge in SQDG and PG is also very important. One of the evolutionary theories speculates that since chloroplast is an organelle with swift phosphate turn-over, the GLs could replace the PLs to save the phosphate. This phenomenon was recorded in vascular plants during the phosphate starvation. DGDG was exported to several extraplastidial membranes to replace the phospholipids. Furthermore, phosphate shortage leads to the replacement of PG by SQDG in photosynthetic membranes (Boudiere, 2014). The replacing of PG by other non-phosphorus glycerolipids is common in algae and lower plants during phosphorus starvation where the BL are utilized (Sato, 1992). However, in some species, for instance, green alga *Chlamydomonas reihardtii*, phospholipids are replaced constitutively rather than facultatively (Murakami, 2018). Betaine lipids are glycerolipids characterised by the presence of N-permethylated hydroxyamino acids. To date, three types of BL have been recognised: diacylglyceryl-*N*,*N*,*N*-trimethylhomoserine (DGTS), diacylglyceryl-hydroxymethyl-*N*,*N*,*N*-trimethyl-β-alanine (DGTA), and diacylglyceryl-carboxyhydroxymethylcholine (DGCC) (Murakami, 2018).

1.2 PROCEDURE OF LIPID DETERMINATION

The scheme illustrating the lipid determination procedure is depicted in Figure 7. The individual steps are described in the following chapters.

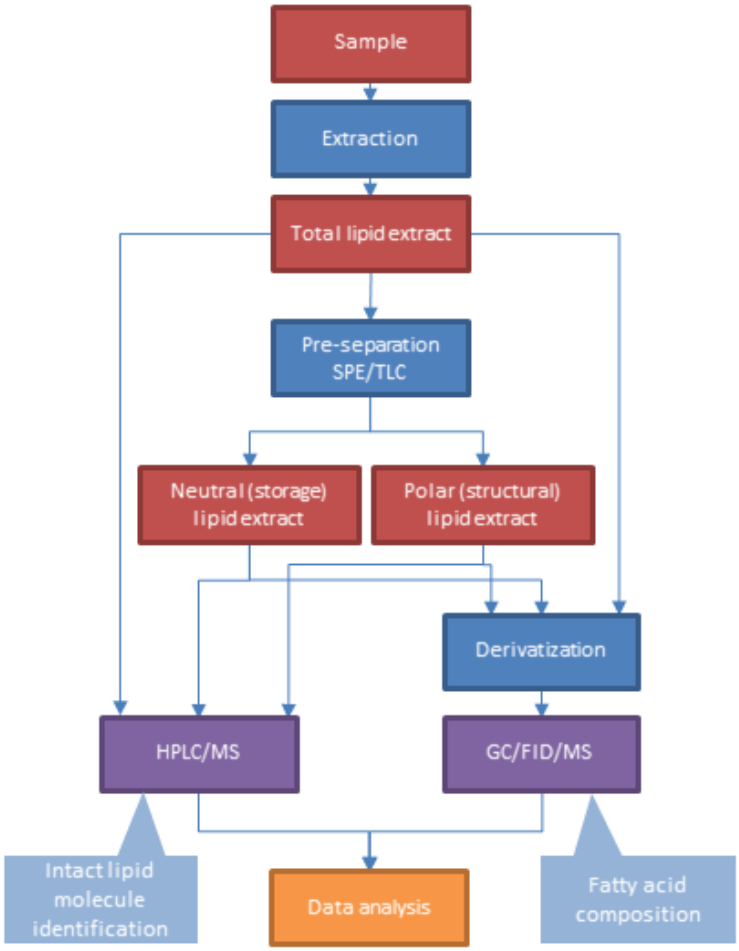

Figure 4: Procedure of lipid determination

1.2.1 LIPID EXTRACTION

Biological samples for the lipidomic analysis ordinarily come in the form of a frozen pellet, for instance, whole insect bodies, insect organs, fish tissue, or whole algal cells. Therefore, homogenization is one of the crucial steps in the extraction process. Various procedures for lipid extraction from biological samples can be followed. The so-called golden standard method (and the most commonly used) was published by Folch *et al.* in 1957. The brain tissue of mammals was utilized as the matrix. Initially, tissue was homogenized in extraction medium chloroform:methanol in the ratio 2:1. The separation and collection of the supernatant were followed by another rehomogenization of the pellet. The

first and second collected supernatant was mixed and water or a solution of mineral salts was subsequently added, which led to the separation of two phases in the resulting solution. Then an upper phase containing non-lipidic molecules with only an insignificant amount of lipids and the lower lipid-containing organic phase was obtained. The ratio of chloroform, methanol and water was 8:4:3. Another widely used method is the Bligh and Dyer method from 1959, which was designed mainly to extract lipids from the tissues of sea fish. In 2001, Iverson *et al.* compared these two methods applied to the matrix acquired from the marine ecosystem. The Bligh and Dyer method use the same solvents, but they intended to reduce their volume. Unlike Folch, Bligh and Dyer used a ratio of 1:2:0,8 or 2:2:1,8 chloroform, methanol and water. The initial ratio of solvent:the sample was (3+1):1 (Bligh and Dyer) and 20:1 (Folch). Data received from Iverson suggested that the results obtained by both methods are not different but only in samples with lipid content reaching less than 2%. In these samples Bligh and Dyer managed to achieve a 95% yield of total lipids. However, the extraction of samples containing more lipids showed a lower yield. Meanwhile the Folch method recorded the same yield range. (Folch, 1957; Bligh, 1959; Iverson, 2001)

Extraction using methyl-*tert*-butyl ether (MTBE) was published by Mathyash *et al*. in 2008. The authors guaranteed the same or even higher yield of lipids than the two previous methods. Moreover, the method has two other benefits. Lipids were kept in the top layer during MTBE extraction and thus this method is suitable for automatization. Also, unlike the extraction media of the previous methods, MTBE is not carcinogenic and consequently dangerous for laboratory personnel. Besides that, MTBE does not require special disposal like chlorinated solvents. In 2012, Ryckebosch *et al.* described the method of sample preparation and lipid extraction optimized on the matrix of unicellular algae. The authors designed the optimal extraction solution, pre-treatment of algal samples, and cell membrane disruption method. Among them, sonication, crushing after nitrogen freezing, and bead beater, i.e. homogenization by sharply shaking the culture with glass beads, were listed. Chloroform:methanol 1:1 was evaluated as the most appropriate extraction medium since the number of biological samples such as unicellular algae has a lipid content higher than 10%. Pre-treatment of the sample by lyophilization to inactivate lipases was tested. The advantage of lyophilization was an easier weighing of the sample, however, it did not bring a higher yield of lipids and did not affect the fatty acid content. All the mentioned methods of cell membrane disruption gave nearly identical results (Mathyash, 2007; Ryckebosch, 2012; Dunstan, 1993).

1.2.2 PRE-SEPARATION

1.2.2.1 SOLID PHASE EXTRACTION (SPE)

Solid phase extraction is one of the sample preparation processes. This method provides separation of dissolved compounds from the liquid mixture in accordance with their chemical and physical properties. In addition, it can be used to purify, concentrate or isolate analyte out of the complex. The SPE method depends on small cartridges filled with a solid phase that is flushed by various solvents to achieve the gradual release of individual lipid groups. The resulting eluates are in a liquid state; thus the connection of SPE and HPLC is advantageous. The device employed for the creation of suction is referred to as SPE manifold and it is shown in Figure 8. The cartridges are located on the top of a vacuum chamber equipped with a stand and collecting containers. The separation of lipid classes is affected by the type of solid phase and selection of mobile phases. SPE columns bonded with aminopropyl phase are frequently utilized for lipid molecule separation. The mobile phase system has been described many times (Hamilton, 1992; Kalužný, 1985; Kim, 1990; Bateman, 1997). Based on that, the optimization of the mobile phase composition was done and has been described previously (Schneedorferová, 2012; Zahradníčková 2014). The primary cartridge was conditioned by hexane and then flushed by a solution of chloroform and 2-propanol in ratio 2:1 to obtain neutral lipids (TG, DG). The cartridge was washed with 2% acetic acid in diethyl ether to acquired free fatty acids consequently and then with methanol and water to obtain phospholipids.

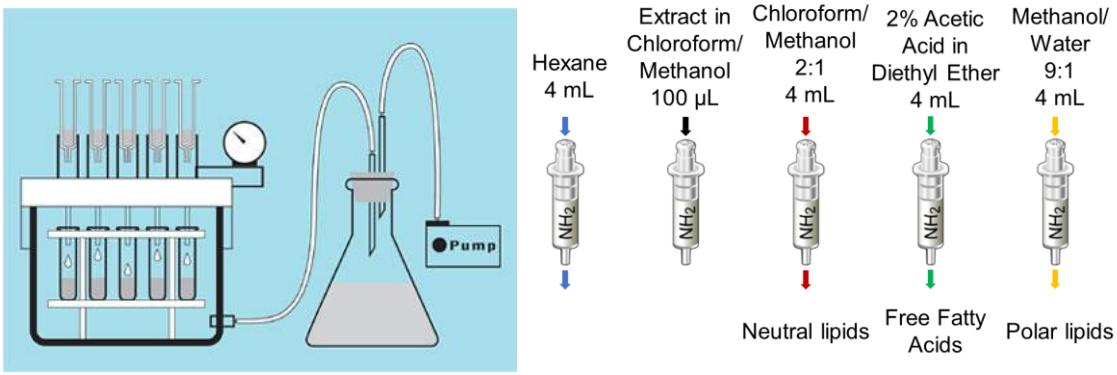

Figure 5: SPE manifold (Phenomenex) and modified lipid separation illustration (Sandra, 2016)

1.2.2.2 THIN LAYER CHROMATOGRAPHY (TLC)

TLC is a rapid analytical method not requiring complicated laboratory equipment. The principle of this method has been known for a long time, but it appeared that the method had come into the overshadow in analytical laboratories. Lately, with the expansion of matrix-assisted laser desorption and ionization time-of-flight (MALDI-TOF) technique, the popularity of TLC is coming back. These methods are mutually beneficial to each other (Vieler, 2007; Lobasso, 2012). The resulting chromatogram is in the solid state and thus the connection of TLC and MALDI-TOF is advantageous. TLC is a chromatographic method, and therefore the principle lies in the distribution of individual substances between the mobile phase of the solvent and stationary phase of a thin layer. The method is suitable for non-volatile samples. The stationary phase can be an aluminium, glass or plastic plate coated with the sorbent of silica gel, aluminium oxide or cellulose. The range of organic solvents constitutes the so-called development system. The application of standards is appropriate as well as with other chromatographic methods. The sample or samples are applied to the marked starting position and the plate is then positioned into the developing chamber. Thus only the bottom of the plate is soaked into the solvent (as is shown in Figure 9). The mobile phase immediately starts to rise through capillary attraction. Final spots are observed in the UV radiation or visualized by e.g. iodine vapours or sulfuric acid. For lipid molecule classes separation can be used; for instance, chloroform-ethanol-water-triethylamine (Fuchs, 2011; Lessig, 2004) or chloroform-methanol-acetic acid-water (Kuypers, 1991) as the solvent system. The procedure we used is depicted in Figure 9 (Zahradníčková, 2014).

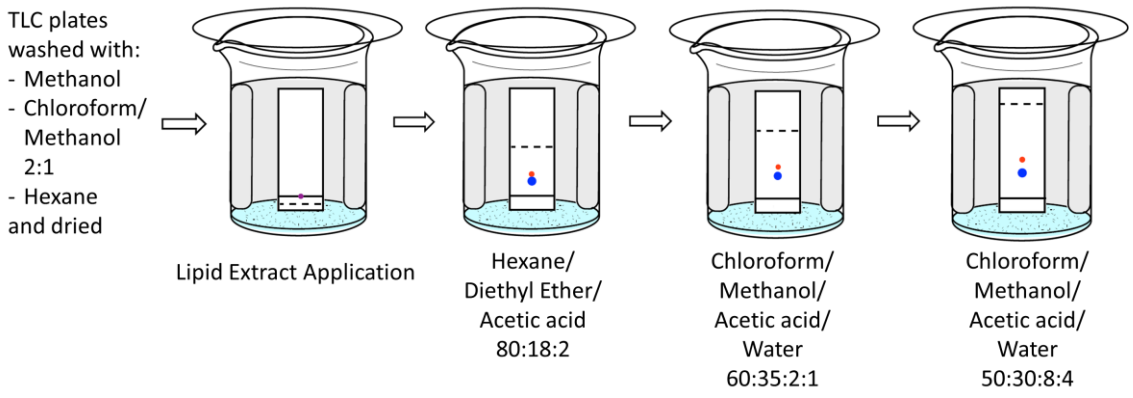

Figure 6: Modified visualization of TLC progress (Nichols, 2017)

1.2.3 DERIVATIZATION

Gas chromatography allows the determination of fatty acid composition along with the information about the position of double bonds. Admittedly this technique requires more complicated sample preparation. It is necessary to convert fatty acids (FA) into fatty acids methyl esters (FAME), or other volatile compounds with a lower boiling point. The transesterification reaction can be catalyzed by acid or base. The majority of biological samples contain predominantly long fatty acids with a very nonpolar hydrocarbon chain. Hexane or isooctane, for instance, is a suitable medium for the esterification of these fatty acids. The reaction is repeated two times and an aqueous saline solution is used to increase the yield of FAME. Preparation of butyl esters is recommended for biological samples with short fatty acids which have a higher boiling point and are less soluble in water. Hydrochloric or sulfuric acid is employed for acid catalyzed transesterification reaction. The base-catalyzed esterification reagent is sodium methoxide or, for example, sodium hydroxide in methanol. The transesterification reaction using 2M sodium methanolate was described in 1984 by Nováková and Kubišta. The reaction mixture was neutralized with acetic acid. Extracted methyl esters are in the upper hexane phase. The reaction is depicted in Figure 10 (Nováková, 1984; Eder, 1995).

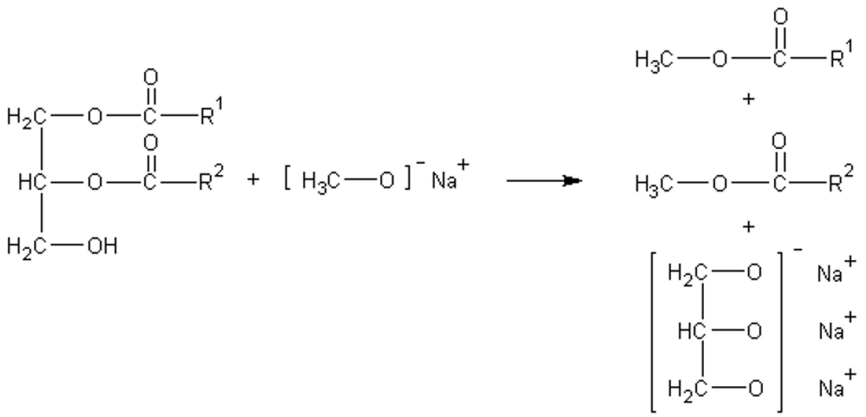

Figure 7: Transmethylation reaction scheme using sodium methanolate

The method employing acetyl chloride was published a couple of years later by Lepage. The mixture of methanol and benzene in ratio 4:1 was added to the sample with an internal standard in the glass tube. Acetyl chloride was slowly added and mixed with a magnetic stirrer. The tube was sealed and exposed to 100 °C for one hour. Subsequently, the samples were cooled with water and 6% solution of potassium carbonate to stop the

reaction. Further, samples were centrifuged, and the upper benzene layer was prepared for GC analysis. Another transesterification procedure was published by Stránský and Jursík (Stránský, 1996), in which the sample was heated with a mixture of chloroform, methanol and acetyl chloride. The reaction was catalyzed by hydrogen chloride and its scheme is shown in Figure 11. Derivatization ordinarily involves many steps. The method reproducibility decreases with increasing number of steps in the quantitative analysis of fatty acids with medium-length chain and decreases the probability of the short-length chain fatty acid detection. The suggested procedure of Stránský involves only three steps. The mixture of chloroform, methanol (2:3) and acetyl chloride was added to the sample and internal standard into the glass ampule. Sealed ampules were heated in a water bath at 70 °C for 90 min. Then the ampule contents were neutralized with silver carbonate and all centrifuged (Lepage, 1986; Stránský, 1996).

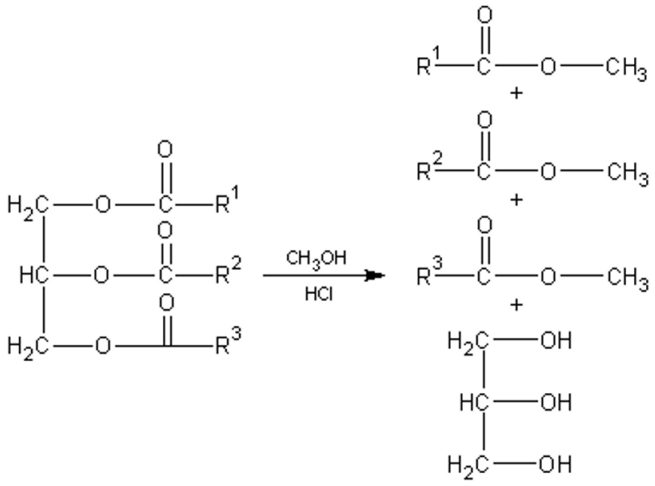

Figure 8: Transmethylation reaction scheme using acetyl chloride

A process involving potassium hydroxide catalysis was described by Ichibara*et al*. It is intended for fatty acids included in glycerolipid molecules. Hexane, 2M methanolic potassium hydroxide was added to the sample, mixed, centrifuged, and the upper hexane layer containing the FAME can be analyzed by GC-FID or GC-MS (Ichibara, 1996).

1.2.4 INSTRUMENTATION

1.2.4.1 GAS CHROMATOGRAPHY (GC)

Gas chromatography is an instrumental analytical technique that has been an important tool in biochemical laboratories for many decades. This robust technique provides the determination of the quality and the quantity of many substances (both organic and inorganic). Simplicity, high separation efficiency and sensitivity are major benefits in comparison with other instrumental techniques. The principle of GC is simple. Measured samples containing unknown compounds have to be firstly gasified. The crucial part is the separation. The gaseous mixture is transported by a carrier gas into the chromatographic column which is filled with a specific stationary phase. Different stationary phases can be used, and separation depends on their chemical properties. Chromatographic separation is based on the affinity between individual components and particles of the stationary phase. The compound with the highest affinity for stationary phase interacts more firmly; therefore, it exits the column the last. In other words, the frequency and the strength of interactions determine the order of column-leaving constituents primarily due to different polarities. The separation of analytes by GC is primarily influenced by the setting of column temperature gradient, unlike liquid chromatography (LC) where the setting of mobile phases gradient is crucial. GC is a technique suitable for the determination of small and volatile molecules that remain stable at high temperatures.

The separation of FAMEs can proceed in columns with several types of stationary phases – non-polar (Golebiowski, 2008; Sauvage, 2012; Zoerner, 2009), medium-polar (Basconcillo, 2008), polar (Abalos, 2000; Ecker, 2012), and very polar (Liu, 2010). The polarity of the sorbent influences retention times of FAMEs, particularly unsaturated FAMEs. Therefore, length and degree of fatty acids saturation have to be taken into consideration in the selection process. Very polar columns are the most appropriate for the separation of long and more unsaturated FA. However, these columns have a shorter lifetime and a long retention time (Eder, 1995). The carrier gas called mobile phase is an inert gas, i.e. helium (Kangani, 2008; Pinho, 2002), nitrogen (Zhu, 2010; Feng, 2008), and less often hydrogen (Candela, 1998).

The flame ionization detector (FID) (Nevigato, 2012) and the mass spectrometer (MS) (Tan, 2010) are common detectors used in combination with gas chromatograph. FID is a robust instrument especially appropriate for quantitative analysis. The carrier gas passes from the column into an oxygen-hydrogen flame where the sample is gasified and ionized.

Charged particles are detected on electrodes. The detector response to fatty acids is directly proportional to the number of analyte molecules. The value of retention time, calibration curves of standards and the internal standard method allows the analytes identification. The advantage of FID in comparison with MS is a better broad linear dynamic range. However, MS provides not only retention times but also the mass spectra of analytes. Libraries of mass spectra have a significant contribution to the identification of the analyte. (Pacchiarotta, 2010)

1.2.4.2 HIGH-PERFORMANCE LIQUID CHROMATOGRAPHY (HPLC)

The technique of high-performance liquid chromatography has been a significant instrument in analytical chemistry for many years. Versatility and high resolution and sensitivity are major benefits in comparison with other instrumental techniques. The principle of HPLC is similar to the GC principle. The main difference is in the state of the mobile phase. Measured samples of unknown compounds are transported by the mobile phase stream at high pressure into the chromatographic column that is filled with a specific stationary phase. Subsequently, the chromatographic separation proceeds in accordance with the affinity between individual components and particles of the stationary and mobile phase. The gradient of mobile phases ordinarily varies from low to high eluting strength. This technique is appropriate for the identification of substances that can be dissolved in liquid and have high molecular weight.

HPLC columns also have a wide range of sorbents with different functional groups. Columns C18 (Larsen, 2002; Kim, 1994, Qiu, 2000) and then C8 (Adachi, 2004; Marcato, 1996) are commonly used for the separation of lipids. The reverse phase system (stationary phase nonpolar and mobile phase increasingly polar) is the most usual for lipid molecule separation (Patton, 1982). Some studies have presented a comparison of lipid analysis with normal and reversed phase. The results established, that the reverse phase is evidently more suitable for the neutral lipid analysis (Buchgraber, 2004). Acetonitrile and 2-propanol in different ratios (Cvačka 2006; Lísa, 2008), chloroform, methanol, and water in various ratios and combined with previous solvents (Uran, 2001; Mchowat, 1996; Fang, 1998), and e.g. n-hexane and isooctane (Graeve, 2009; Landi, 1998) are among the most commonly used mobile phases. Various additives such as ammonium hydroxide or sodium buffers are added to improve ionization (Caboni, 1996).

HPLC technique employs various detection systems. The UV/VIS detector (Wang, 2007), the evaporative light scattering detector (ELSD) (Donot, 2013), and above all the mass spectrometer (Kofroňová, 2009) are often employed for the lipid analysis. The principle of the spectrophotometric detector is based on different radiation absorption (approximately 100-700 nm) by different biological molecules. The response of the detector is given by analyte concentration and the rate of absorption itself. ELDS finds the application to analyse a wide range of analytes. As the name indicates, it detects the scattering of light on the aerosolized analyte particles after the mobile phase solvent evaporation. This detection requires the supplementation of volatile additives such as ammonium hydroxide or sodium buffers to the mobile phase.

1.2.4.3 MASS SPECTROMETRY (MS)

MS has been high-end technology in analytical chemistry for a long time and it has an indisputable and irreplaceable position in lipidomics. MS plots individual compounds according to their mass to charge ratio. MS data could be generated by several MS techniques and the complexity of the obtained data depends on it. In the case of shotgun lipidomics (the sample is introduced to the MS without prior separation) obtained data is two-dimensional (m/z values x intensity). When a GC or LC is involved the generated data are three-dimensional (retention time x m/z values and intensity) (Checa et al., 2015). The reason is to sort the mixture and not to see everything at once. The principle of MS is quite simple. The injected sample is transferred immediately or gradually to the ionizer and subsequently to the analyzer that sorts the ions and sent them to the detector. A common method of ionization is e.g. the electrospray ionization (ESI) (Pang, 2008) or the atmospheric pressure chemical ionization (APCI) (Cvačka, 2008). Methods of ionization are different but aim at one thing: to break molecules of samples into charged fragments, in other words, add a proton to every molecule. APCI is particularly suitable for the ionization of neutral lipids, but less suitable for phospholipid ionization. ESI is a “softer” methodology and therefore is an efficient tool for the ionization of nearly all lipid classes and the additives mentioned above are used to support ionization. An overwhelming majority of glycerolipids, when using ammonium ions, are ionized in the form of molecular ions or ammonium adducts, and then characteristic fragmentation patterns determine the structural composition (Han, 2005). An ion trap (Thomas, 2006), a quadrupole (Hsu, 2003), time of flight detector (TOF) (Schwundke, 2006), and high-resolution orbitrap (Yamada, 2013) are analyzers which

employ magnetic and electric field for ion separations. Based on electro-physical principles the detector estimates the exact weight of all charged molecules in the sample, and after this mathematical optimization records it into the plot. Such a graph has yet to be interpreted, and even though attempts to automate this process are being made, it still has to be done by researchers.

1.2.5 DATA ANALYSIS

Recent improvements in instrumental robustness and sensitivity are responsible for the rapid development of the lipidomic field. As in other - omics studies, HPLC coupled with MS-MS as a current analytical technique provides a huge number of raw data. The higher number of identifying analytes is better for a true view of testing the organism state, however it also, complicates the interpretation of obtained data. Therefore, the advanced data analysis tools have to be used (Niemla, 2009; Oresic, 2009; Checa, 2015). Prepared data for the statistical analysis is commonly pre-processed by noise reduction, signal alignment, and peak picking (Checa, 2015). The basic analytical tool is the hypothesis testing which is focused on the differences between the means of two groups of samples. Univariate significance test (*t-tests* family) and ANOVA related methods could be employed for hypothesis testing (Checa, 2015).

The clustering statistical analyses cover supervised (canonical) or unsupervised (uncanonical) methods. In supervised techniques, the information about the group is used to guide the segregation of the groups by variables with the exclusion of grouping factors. (Niemla, 2009) Cluster statistical analysis provides a statistical framework organizing the samples to the groups according to a set of variables. The main goal is to group samples that have two complementary characteristics - similarities and differences. The result is a tree-structured graph (dendrogram) visualizing groups based on the similarity of the samples (Oresic, 2009; Checa, 2015).

Principal component analysis (PCA) is the most commonly utilized unsupervised explorative multivariate statistical approach. This method primarily aims to explain the variation in pre-processed raw data using a reduced place, defined by principal components, the variables which remain most of the relevant information from the original data. The principal components are a linear combination of the original variables that hierarchically describe the directions of maximum variation in the data. In other words, this method

reduces the multidimensional dataset into lower dimensions (Oresic, 2009; Checa, 2015). Redundancy analysis (RDA) is the canonical or supervised version of PCA (Lepš, 2000). The mentioned methods are based on the linear response of species on the environmental gradient - variables. Therefore, they are suitable for homogeneous data sets. On the other hand, for heterogeneous data sets, suitable methods are based on the unimodal response and these are methods of weighted averaging. Correspondence analysis (CA) and constrained correspondence analysis (CCA) and eventually detrended correspondence analysis (DCA) belongs to the second group. The statistical significance designation was done by Monte-Carlo permutation test. This test is based on randomness; it uses repeated random sampling to obtain numeric results (Meloun, 2004; Lepš, 2000).

Linear discriminant analysis (LDA) is an example of another commonly used supervised method. In contrast to PCA that maximizes the identifiers directions with maximum explain variance, the LDA maximize the separation between the classes (Niemla, 2009; Checa, 2015). The samples which overcome the limitation of LDA are classified by the partial least square discriminant analysis (PLS-DA) (Oresic, 2009).

2 OBJECTIVES

The aim of the study is to:

- combine known chromatographic and mass spectrometric methods to yield the best information about analytes
- prepare a chemical analytical setup experiment to determinate a particular lipid molecule
- propose a raw data processing methodology
- apply the proposed methodology to different matrices.

3 SUMMARY

This study defines a sequence of methods offering comprehensive information about the quality and quantity of lipid molecules which are not expensive, equipment-demanding and time-consuming (Paper I). HPLC-ESI-MS^2 (Papers I-IV) is an irreplaceable method for separation and determination of the lipid class. However, it has two major disadvantages. The first is its incapability to define the position of the double bond in the fatty acid chain, and the second is the inaccuracy to determine the quantity of lipid class and even lipid species due to the different efficiency of the analytes to ionize. Nevertheless, it should be noted, that in biological studies relative changes in particular lipid abundances are more important than their exact quantities due to individual variability inside the testing group. However, the quantification of lipid classes is possible in association with the HPTLC technique and inorganic phosphorus quantification (Paper I). Contrariwise, GC-FID technique is suitable for the quantification of FAMEs due to its detection principle, and also is able to distinguish FAs with a different double bond position.

The proposed methodology, mostly based on HPLC-MS-MS data, is able to provide enough information to determinate the particular lipid species in a single run. Basically, three-dimensional data is obtained (retention time x m/z value x intensity) by proposed HPLC separation. Ionization setup (+/- polarity) gives data about analytes behaviour in different polarities, and MS-MS analysis provides information about their fragmentation patterns (listen in table 1 of Paper IV). If necessary, high-resolution technology must be employed to determine the exact m/z value correct to four decimal places; for instance when analyte has very low or trace abundance. The limitation of the HPLC-MS-MS could be compensated by the other presented methods. The utilization of the pre-separation technique (TLC, SPE) along with the use of internal standards can be beneficial. The determination of a particular fatty acid with the knowledge of the double bond position is allowed by 20 minutes of GC separation. Application of standards in six concentration levels allows the acquisition of a concrete fatty acid concentration in the sample. For analytical purposes, the library of mass spectra is very useful for FAME identification in GS-MS technique.

The tested datasets in the first publication were small, containing only two variables and 14 species. Therefore no advanced statistical analysis was involved. On the other hand, the other two publications focused on the physiology of *D. melanogaster* and a nutrition study of fish are dealing with more than two variables and a hundred analytes. The Canoco 4.5 (Biometrics, Plant Research International, Wageningen UR, Netherlands) software was

chosen for the data processing due to the presence of this program and also expert lecturers at the University of South Bohemia. This program covers DCA analysis for linearity or unimodality determination, PCA and its supervised version RDA for linear data, and CA and supervised CCA for unimodal data. The statistical significance was tested by Monte-Carlo permutation test. The raw data was pre-processed by peak area recalculation on the internal standard peak area to exclude the LC-MC system errors. Prior to all analysis, the pre-processed peak areas were subjected to logarithmic transformation, scaling was focused on inter-species correlation, the species scores were divided by standard deviation, and the data were centred by species.

The combined analytical methods were applied to the insect *Pyrrhocoris apterus*. Pre-separation by TLC allowed to identify individual PL classes (PC, PE, PS, PI, PG). Subsequent GC-FID technique provides information about the composition of particular FA including double bonds description within particular PL class. However, HPLC-MS-MS technique was able to determinate only 14 dominated PL molecules (7 PEs and 7 PCs) in the thorax and fat body of *Pyrrhocoris apterus* (Paper I). The limitations of the proposed methodology lay in the short separation time, mass spectrometer sensitivity and accuracy, and also the matrices used. Previous studies on this type of insect revealed precisely the same results (Šlachta, 2002; Tomčala, 2006).

The demands of a nutrition study (Paper II) require a more precise approach then the HPLC was optimised to allow determination of storage lipids (DGs, TGs). A comparison between the results obtained in Paper II and other publications is fairly complicated. The determination of fatty acid and lipid molecule content was often focused on FAs metabolism and measured in a liver matrix (Wodtke, 1978; Henderson, 1996; Farkas, 1976). Our study was nutritional and therefore only the fish fillet was used as a sample. The FAs composition of the muscle tissue was described; however, a comparison is not possible due to the different locations (Rahman, 1995; Rasoarahona, 2004) which means a different diet and subsequent major impact on lipid composition (Kmínková, 2001; Mráz, 2012; Schwalme, 1992; Navarro, 1993; Kirsch, 1998). This fact is reflected in studies comparing the lipid profile of wild and farmed fish (Janowska, 2007; Kucska, 2006). In addition to diet, the seasonal changes during a year are significant (Bulut, 2010; Schwalme, 1993; Hamre, 2003). The stadium of development and changes related to spawning, for instance, also have substantial impact (Huynh, 2007; Tocher, 1985; Fraser, 1988). Moreover, the number of specimens included in the study is not often sufficient to cover wide species variability.

The same method was verified on insect tissue of *Drosophila melanogaster* in 2015 (Paper III). The physiologicalstudy revealed more than 200 lipids and multivariate statistic analyses were also performed. However, the aim of the study was not lipid determination. Due to the complexity of the project only summarized data were published.

The same methodology has been employed on completely different matrix - photosynthetic algae *Chromera velia* and *Vitrella brassicaformis.* These tiny algae which were relatively recently discovered occupy a very interesting evolutionary position. They are supposed to be the closest photosynthetic relatives of apicomplexans parasites. Despite this fact, their lipid profiles were only studied slightly. The methodology has to be extended to more complicated identification of other glycerolipid groups, specifically GLs (MGDG, DGDG, SQDG) and BLs. The intact lipid profile of these algae was published in 2017 (Paper IV). The study revealed 14 FAs and 9 glycerolipid classes. Lukeš *et al*. (Lukeš, 2017) detected the same 12 species of FAs as in Paper IV. Some publications dealing with fatty acid and lipid composition in *Chromera velia* did not mention specific fatty acid content (Huerlimann, 2014) or an intact lipid molecule list (Botté, 2011). Dahmen *et al.* (Dahmen, 2013) determined 3 molecules of MGDG and 4 molecules of DGDG in contrast with 15 types of MGDG and 14 types of DGDG identified with the results obtained by the described methodology in Paper IV.

4 CONCLUSION

The proposed analytical procedure has evolved over the time, experience, and application of advanced mass spectrometers. Despite the utilization of several pre-separation techniques and considerable effort, only 14 PLs molecules (7 PCs and 7 PEs) in the fat body and thorax tissue of insect *Pyrrhocoris apterus* (Paper I); were successfully identified. Further work was focused on the optimization of HPLC technique for the separation of as many lipid species as possible in a single run. This effort resulted in the methodology further successfully used in fish, insect, and algal matrices. In total 164 lipid species from 7 lipid classes in fish were identified. The lipidome of *Drosophila melanogaster* contains 241 lipid molecules- 96 PLs (5 lyso PCs, 5 lyso PEs, 30 PCs, 26 PEs, 11 PGs, 14 PIs, and 6 PSs), and 16 DGs and 128 TGs. Finally, in algae, 289 lipid species from 9 lipid classes were detected and identified (for details see supplementary data). The application of a set of statistical approaches powered by Canoco allows the testing of the hypothesis, and in case of nutrition study, provides clear results about the influence of cooking treatment on the quality of the meat. The proposed methodology seems to be time-consuming; however, it also seems to be universal through different matrices and is able to separate hundreds of analytes in a single run. Additionally, it could provide information about non-lipidic compounds, like for example chlorophyll a and b, its derivates, and vitamin K.

5 LIST OF ABBREVIATIONS

ALA	ω-3 Linolenic Acid
APCI	Atmospheric Pressure Chemical Ionization
BLs	Betaine lipids
CA	Correspondence Analysis
CCA	Constrained Correspondence Analysis
DCA	Detrended Correspondence Analysis
DGDG	Digalactosyldiacylglycerol
DGs	Diacylglycerols
DHA	Docosahexaenoic Acid
ELDS	Evaporative Light Scattering Detector
EPA	Eicosapentaenoic Acid
ESI	Electrospray Ionization
FAs	Fatty Acids
FID	Flame Ionization Detector
GC	Gas Chromatography
GLs	Glycosyldiacylglycerols
HPLC	High-performance Liquid Chromatography
HPTLC	High-performance TLC
LA	ω-6 Linoleic Acid
LDA	Linear Discriminant Analysis
MALDI-TOF	Matrix-assisted Laser Desorption with Time-of-flight Detector
MGDG	Monogalactosyldiacylglycerol
MS	Mass Spectrometer
MTBE	Methyl-*tert*-butyl Ether
PCA	Principal Component Analysis
PCs	Phosphatidylcholines
PEs	Phosphatidylethanolamines
PGs	Phosphatidylglycerols
PIs	Phosphatidylinositols

PLs	Glycerophospholipids
PLS-DA	Partial Least Square Discriminant Analysis
PSs	Phosphatidylserines
PUFAs	Polyunsaturated Fatty Acids
RDA	Redundancy Analysis
SPE	Solid Phase Extraction
SQDG	Sulfoquonovosyldiacylglycerol
TGs	Triacylglycerols
TLC	Thin Layer Chromatography

6 REFERENCES

ABALOS, M.; BAYONA, J., M.; PAWLISZYN, J.: Development of a headspace solid-phase microextraction procedure for the determination of free volatile fatty acids in waste waters. *Journal of Chromatography A*. 2000: vol. 873, p. 107-115.

ADACHI, J.; YOSHIOKA, N.; FUNAE, R.; NUSHIDA, H.; ASANO, M.; UENO, Y.: Determination of phosphatidylcholine monohydroperoxides using quadrupole time-of-flight mass spectrometry. *Journal of Chromatography B*. 2004, vol. 806, p. 41-46.

ADKINS, Y.; KELLEY, D. S: Mechanism underlying the cardioprotective effects of omega-3 polyunsaturated fatty acids. *Journal of nutritional biochemistry*. 2010, vol. 21 (9), p. 781-792.

ARRESE, E., L.; SOULAGES, J., L.: Insect Fat Body: Energy, Metabolism, and Regulation. *Annual Review of Entomology*. 2010: vol. 55, p. 207-225.

BASCONCILLO, L., S.; MCCARRY, B., E.: Comparison of three GC/MS methodologies for the analysis of fatty acids in *Sinorhizobium meliloti*: Development of a micro-scale, one-vial method. *Journal of Chromatography B*. 2008: vol. 871, p. 22-31.

BATEMAN, H., G.; JENKINS, T., C.: Method for Extraction and Separation by Solid Phase Extraction of Neutral Lipid, Free Fatty Acids, and Polar Lipid from Mixed Microbial Cultures. *Journal of Agricultural and Food Chemistry*. 1997: vol. 45, p. 132-134.

BLIGH, E., G.; DYER, W., J.: A rapid method of total lipid extraction and purification. *Canadian Journal of Biochemistry and Physiology*. 1959: vol. 37, issue 8, p. 911-917.

BOTTÉ, C., Y.; YAMARYO-BOTTÉ, Y.; JANOUŠKOVEC, J.; RUPASINGHE, T.; KEELING, P., J.; CRELLIN, P.; COPPEL, R., L.; MARÉCHAL, E.; MCCONVILLE, M., J.; MCFADDEN, G., I.: Identification of Plant-like Galactolipids in *Chromera velia*, a Photosynthetic Relative of Malaria Parasites. *Journal of Biological Chemistry*. 2011: vol. 286 (34), p. 29893–29903.

BOUDIERE, L.; MICHAUD, M.; PETROUTSOS, D.; REBEILLE, F.; FALCONET, D.; BASTIEN, O.; ROY, S.; FINAZZI, G.; ROLLAND, N.; JOUHET, J.; BLOCK, M., A.; MARÉCHAL, E.: Glycerolipids in photosynthesis: Composition, synthesis and trafficking. *Biochimica Et Biophysica Acta-Bioenergetics.* 2014: vol. 1837 (4), p. 470-480.

BRADBURY, J.: Docosahexaenoic Acid (DHA): An Ancient Nutrient for the Modern Human Brain. *Nutrients*. 2011: vol. 3 (5), p. 529–554.

BUCHGRABER, M.; ULBERTH, F.; EMONS, H.; ANKLAM, E.: Triacylglycerol profiling by using chromatographic techniques. *European Journal of Lipid Science and Technology*. 2004: vol. 106, p. 621-648.

BULUT, S.: Fatty acid composition and 6/3 ratio of the pike (*Esox lucius*) muscle living in Eber Lake, Turkey. *Scientific Research and Essays*. 2010: vol. 523, p. 3776-3780.

CABONI, M., F.; MENOTTA, S.; LERCKER, G.: Separation and analysis of phospoholipids in different foods with a light-scattering detector. *Journal of the American Oil Chemists Society*. 1996: vol.73 (11), p. 1561-1586.

CANDELA, M.; ASTIASARÁN, I.; BELLO, J.: Deep-Fat Frying Modifies High-Fat Fish Lipid Fraction. *Journal of Agricultural and Food Chemistry*. 1998: vol. 46, p. 2793-2796.

CASULA, M.; SORANNA, D.; CATAPANO, A. L.; CORRAO, G.: Long-term effect of high dose omega-3 fatty acid supplementation for secondary prevention of cardiovascular outcomes: A meta-analysis of randomized, double blind, placebo controlled trials. *Atherosclerosis Supplements*. 2013: vol. 14 (2), p. 243–251.

CHECA, A.; BEDIA, C.; JAUMOT, J.: Lipidomic data analysis: Tutorial, practical guidelines and applications. *Analytica Chimica Acta*. 2015: vol. 885, p. 1-16.

CHIRALA, S., S.; WAKIL, S., J.: Structure and function of animal fatty acid synthase. *Lipids*. 2004: vol. 39, p. 1045-1053.

COX, M.; NELSON, D.: *Lehninger Principles of Biochemistry*. 6th Ed. New York: Worth Publishers, 2000, 10.1007/978-3-662-08289-8.

CVAČKA, J.; HOVORKA, O.; JIROŠ, P.; KINDL, J.; STRÁNSKÝ, K.; VALTEROVÁ, I.: Analysis of triacylglycerols in fat body of bumblebees by chromatographic methods. *Journal of Chromatography A*. 2006: vol. 1101, p. 226-237.

CVAČKA, J.; KOFROŇOVÁ, E.; VAŠÍČKOVÁ, S.; STRÁNSKÝ, K.; JIROŠ, P.; HOVORKA, O.; KINDL, J.; VALTEROVÁ, I.: Unusual fatty acid in the fat body of the early nesting bumblebee, *Bombus pratorum. Lipids*. 2008: vol. 43, p. 441-450.

DAHMEN, J., L.; KHADKA, M.; DODSON, V., J.; LEBLOND, J., D.: Mono- and digalactosyldiacylglycerol composition of dinoflagellates. VI. Biochemical and genomic comparison of galactolipid biosynthesis between *Chromera velia* (Chromerida), a photosynthetic alveolate with red algal plastid ancestry, and the dinoflagellate, *Lingulodinium polyedrum*. *European Journal of Phycology*. 2013: vol. 48 (3), 268–277.

DAVIDSON, B.; CANTRILL, R.: Fatty acid nomenclature. A short review. *South African medical journal*. 1985: vol. 67 (16), p. 633-634.

DONOT, F.; GAZALS, G.; GUNATA, Z.; ERGON, D.; MALINGE, J.; STRUB, C.; FONTANA, A.; SCHORR-GALINDO, S.: Analysis of neutral lipids from microalgae by HPLC-ELSD and APCI-MS/MS. *Journal of Chromatography B*. 2013: vol. 942-943, p. 98-106.

DOWHAN, W.; BOGDANOV, M.; MILEYKOVSKAYA, E.: *Biochemistry of Lipids, Lipoproteins and Membranes - Functional Roles of Lipids in Membranes*. 6th Ed. Elsevier, 2015, 10.1016/B978-0-444-63438-2.00001-8.

DUNSTAN, G., A.; VOLKMAN, J., K.; BARRETT, S., M.: The effect of lyophilization on the solvent extraction of lipid classes, fatty acids and sterols from the oyster *Crassostrea gigas*. *Lipids*. 1993: vol. 28: 937.

ECKER, J.; SCHERER, M.; SCHMITZM, G.; LIEBISCH, G.: A rapid GC-MS method for quantification of positional and geometric isomers of fatty acid methyl esters. *Journal of Chromatography B*. 2012: vol. 897, p. 98-104.

EDER, K.: Gas chromatographic analysis of fatty acid methyl esters. *Journal of Chromatography B*. 1995: vol. 671, p. 113-131.

FAHY, E.; SUBRAMANIAM, S.; BROWN, H., A.; GLASS, C., K.; MERRILL, A., H.; MURPHY, R., C.; RAETZ, C., R., H.; RUSSELL, D., W.; SEYAMA, Y.; SHAW, W.; SHIMIZU, T.; SPENER, F.; MEER, G.; VANNIEUWENHZE, M., S.; WHITE, S., H.; WITZTUM, J., L.; DENNIS, E., A.: A comprehensive classification system for lipids. *Journal of Lipid Research*. 2005: vol. 46, p. 839-861.

FAHY, E.; SUBRAMANIAM, S.; MURPHY, R., C.; NISHIJIMA, M.; RAETZ, C., R.; SHIMIZU, T.; SPENER, F.; VAN MEER, G.; WAKELAM, M., J.; DENNIS, E., A.: Update of the LIPID MAPS comprehensive classification system for lipids. *Journal of lipid research*. 2009: vol. 50 Suppl, S9-14.

FANG, J.; BARCELONA, M., J.: Structural determination and quantitative analysis of bacterial phospholipids using liquid chromatography/electrospray ionization/mass spectrometry. *Journal of Microbiological Methods*. 1998: vol. 33 (1), p. 23-35.

FARKAS, T.; CSENGER, I.: Biosynthesis of fatty acids by the carp, *Cyprinus carpio L*., in relation to environmental temperature. *Lipids*. 1976: vol. 11 (5), p. 401–407.

FENG, L.; HUANG, Y.; WANG, H.: Solid-Phase Microextraction in Combination with GC-FID for Quantification of the Volatile Free Fatty Acids in Wastewater from Constructed Wetlands. *Journal of Chromatographic Science*. 2008: vol. 46, p. 577-583.

FOLCH, J.; LEES, M.; STANLEY, G., H., S.: A simple method for the isolation and purification of total lipides from animal tissues. *Journal of Biological Chemistry*. 1957: vol. 226, issue 1, p. 497-509.

FRASER, A., J.; GAMBLE, J., C.; SARGENT, J., R.: Changes in lipid content, lipid class composition and fatty acid composition of developing eggs and unfed larvae of cod (*Gadus morhua*). *Marine Biology*. 1988: vol. 99 (3), p. 307–313.

FRITZLER, J., M.; ZHU, G.: Functional characterization of the acyl- acyl carrier protein ligase in the Cryptosporidium parvum giant polyketide synthase. *International Journal for Parasitology*. 2007: vol. 37, p. 307-316.

FUCHS, B., SÜß, R., TEUBER, K., EIBISCH, M., & SCHILLER, J. Lipid analysis by thin-layer chromatography - A review of the current state. *Journal of Chromatography A*. 2011: vol. 1218 (19), p. 2754–2774.

GOLEBIOWSKI, M.; MALINSKI, E.; BOGUS, M., I.; KUMIRSKA, J.; STEPNOWSKI, P.: The cuticular fatty acids of *Calliphora vicina*, *Dendrolimus pini* and *Galleria mellonella* larvae and their role in resistance to fungal infection. *Insect Biochemistry and Molecular Biology*. 2008: vol. 38, p. 619-627.

GOODMAN, C., D.; MCFADDEN, G., I.: Fatty acid biosynthesis as a drug target in apicomplexan parasites. *Current Drug Targets*. 2007: vol. 8 (1), p. 15-30.

GRAEVE, M.; JANSSEN, D.: Improved separation and quantification of neutral and polar lipid classes by HPLC-ELSD using a monolithic silica phase: Application to exceptional marine lipids. *Journal of Chromatography B*. 2009: vol. 877 (20-21), p. 1815-1819.

GUSCHINA, I., A.; HARWOOD, J., L.: Lipids and lipid metabolism in eukaryotic algae. *Progress in Lipid Research*. 2006: vol. 45, p. 160-186.

HAMILTON, R., J.; HAMILTON, S. *Lipid Analysis: A Practical Approach*. 1st Ed. New York: Oxford University Press, 1992, s. 310. ISBN 0-19-963099-2.

HAMRE, K.; LIE, Ø.; SANDNES, K.: Seasonal development of nutrient composition, lipid oxidation and colour of fillets from Norwegian spring-spawning herring (*Clupea harengus L.*). *Food Chemistry*. 2003: vol. 82 (3), p. 441–446.

HAN, X.; GROSS, R., W.: Shotgun lipidomics: Electrospray ionization mass spectrometric analysis and quantitation of cellular lipidomes directly from crude extracts of biological samples. *Mass Spectrometry Reviews*. 2005: vol. 24 (3), p. 367-412.

HENDERSON, R., J.: Fatty acid metabolism in freshwater fish with particular reference to polyunsaturated fatty acids. *Archiv Für Tierernaehrung*. 1996: vol. 49 (1), p. 5–22.

HSU, F.-F.; TURK, J.; THUKKANI, A., K.; MESSNER, M., C.; WILDSMITH, K., R.; FORD, D., A.: Characterization of alkyl, alk-1-enylacyl and lyso subclasses of glycerophosphocholine by tandem quadrupole mass spectrometry with electrospray ionization. *Journal of Mass Spectrometry*. 2003: vol. 38, p. 752-763.

HUERLIMANN, R.; STEINIG, E., J.; LOXTON, H.; ZENGER, K., R.; JERRY, D., R.; HEIMANN, K.: The effect of nitrogen limitation on acetyl-CoA carboxylase expression and fatty acid content in *Chromera velia* and *Isochrysis aff. galbana* (TISO). *Gene*. 2014: vol. 543 (2), p. 204–211.

HUYNH, M., D.; KITTS, D., D.; HU, C.; TRITES, A., W.: Comparison of fatty acid profiles of spawning and non-spawning Pacific herring, Clupea harengus pallasi. *Comparative Biochemistry and Physiology Part B: Biochemistry and Molecular Biology*. 2007: vol. 146 (4), p. 504–511.

ICHIBARA, K.; SHIBAHARA, A.; YAMAMOTO, K.; NAKAYAMA, T.: An Improved Method for Rapid Analysis of the Fatty Acids of Glycerolipids. *Lipids.* 1996: vol. 31, no. 5, p. 535-539.

IVERSON, S., J.; LANG, S., L., C.; COOPER, M., H.: Comparison of the Bligh and Dyer and Folch methods for total lipid determination in a broad range of marine tissue. *Lipids*. 2001: vol. 36, issue 11, p. 1283-1287.

JANKOWSKA, B.; ZAKĘŚ, Z.; ŻMIJEWSKI, T.; SZCZEPKOWSKI, M.: Fatty acid composition of wild and cultured northern pike (*Esox lucius*). *Journal of Applied Ichthyology*. 2008: vol. 24 (2), p. 196–201.

KALUŽNÝ, M., A.; DUNCAN, L., A.; MERRITT, M., V.; EPPS, D., E.: Rapid separation of lipid classes in high yield and purity using bonded phase columns. *Journal of Lipid Research*. 1985: vol. 26, p. 135-144.

KANGANI, C., O.; KELLEY, D., E.; DELANY, J., P.: New method for GC/FID and GC-C-IRMS analysis of plasma free fatty acid concentration and isotopic enrichment. *Journal of Chromatography B.* 2008: vol. 873, p. 95-101.

KIM, H., Y.; SALEM, N., JR.: Separation of lipid classes by solid phase extraction. *Journal of Lipid Research*. 1990: vol. 31, p. 2285-2290.

KIM, H., Y.; WANG, T., C., L.; MA, Y., C.: Liquid Chromatography/Mass Spectrometry of Phospholipids Using Electrospray Ionization. *Analytical Chemistry*. 1994: vol. 66, p. 3977-3982.

KIRSCH, P., E.; IVERSON, S., J.; BOWEN, W., D.; KERR, S., R.; ACKMAN, R., G.: Dietary effects on the fatty acid signature of whole Atlantic cod (*Gadus morhua*). *Canadian Journal of Fisheries and Aquatic Sciences*. 1998: vol. 55 (6), p. 1378–1386.

KMÍNKOVÁ, M.; WINTEROVÁ, R.; KUČERA, J.: Fatty acids in lipids of carp (*Cyprinus carpio*) tissues. *Czech Journal of Food Science*. 2001: vol. 19, p. 177-181.

KOFROŇOVÁ, E.; CVAČKA, J.; VRKOSLAV, V.; HANUS, R.; JIROŠ, P.; KINDL, J.; HOVORKA, O.; VALTEROVÁ, I.: A comparison of HPLC/APCI-MS and MALDI-MS for characterizing triacylglycerols in insect: Species-specific composition of lipids in the fat bodies of bumblebee males. *Journal of Chromatography B*. 2009: vol. 877, p. 3878-3884.

KUCSKA, B.; PAL, L.; MULLER, T.; BODIS, M.; BARTOS, A.; WAGNER, L.; HUSVÉTH, F.; BERCSENYI, M. Changing of fat content and fatty acid profile of reared pike (*Esox lucius*) fed two different diets. *Aquaculture Research*. 2006: vol. 37 (1), p. 96–101.

KUYPERS, F., A.; BÜTIKOFER, P.; SHACKLETON, C., H., L.: Application of liquid chromatography-thermospray mass spectrometry in the analysis of glycerophospholipid molecular species. *Journal of Chromatography A*. 1991: vol. 562, p. 191-206.

LANDI, L.; GALLI, M., C.; CABRINI, L.; HAKIM, G.; CARRU, C.; FIORENTINI, D.: HPLC and light scattering detection allow the determination of phospholipids in biological samples and the assay of phospholipase A(2). *Biochemistry and Molecular Biology International.* 1998: vol. 44 (6), p. 1157-1166.

LARSEN, A.; MOKASTET, E.; LUNDANES, E.; HVATTUM, E.: Separation and identification of phosphatidylserine molecular species using reversed-phase high-performance liquid chromatography with evaporative light scattering and mass spectrometric detection. *Journal of Chromatography B*. 2002: vol. 774, p. 115-120.

LEPAGE, G.; ROY, C., C.: Direct transesterification of all classes of lipids in a one-step reaction. *Journal of Lipid Research*. 1986: vol. 27, p. 114-119.

LEPŠ, J.; ŠMILAUER, P.: *Mnohorozměrná analýza ekologických dat*. České Budějovice, 2000. 101 p.

LEßIG, J.; GEY, C.; SÜß, R.; SCHILLER, J.; GLANDER, H.-J.; ARNHOLD, J.: Analysis of the lipid composition of human and boar spermatozoa by MALDI-TOF mass spectrometry, thin layer chromatography and 31P NMR spectroscopy. *Comparative Biochemistry and Physiology Part B: Biochemistry and Molecular Biology*. 2014: vol. 137 (2), p. 265–277.

LÍSA, M.; HOLČAPEK, M.: Triacylglycerols profiling in plant oils important in food industry, dietetics and cosmetics using high-performance liquid chromatography-atmospheric pressure chemical ionization mass spectrometry. *Journal of Chromatography A*. 2008: vol. 1198-1199, p. 115-130.

LIU, L.; LI, Y.; GUAN, C.; LI, K.; WANG, C.; FENG, R.; SUN, C.: Free fatty acid metabolic profile and biomarkers of isolated post-challenge diabetes and type 2 diabetes mellitus based on GC-MS and multivariate statistical analysis. *Journal of Chromatography B*. 2010: vol. 878, p. 2817-2825.

LOBASSO, S.; LOPALCO, P.; ANGELINI, R.; VITALE, R.; HUBER, H.; MÜLLER, V.; CORCELLI, A.: Coupled TLC and MALDI-TOF/MS Analyses of the Lipid Extract of the Hyperthermophilic Archaeon Pyrococcus furiosus. *Archaea*. 2012: p. 1–10.

LUKEŠ, M.; GIORDANO, M.; PRÁŠIL, O.: The effect of environmental factors on fatty acid composition of *Chromera velia* (Chromeridae). *Journal of Applied Phycology*. 2017: vol. 29 (4), p. 1791–1799.

MARCATO, B.; CECCHIN, G.: Analysis of mixtures containing free fatty acids and mono-, di- and triglycerides by high-performance liquid chromatography coupled with evaporative light-scattering detection. *Journal of Chromatography A.* 1996: vol. 730, p. 83-90.

MATYASH, V.; LIEBISCH, G.; KURZCHALIA, T., V.; SHEVCHENKO, A.; SCHWUDKE, D.: Lipid extraction by methyl-*tert*-butyl ether for high-throughput lipidomics. *Journal of Lipid Research*. 2008: vol. 49, issue 5, p. 1137-1143.

MCHOWAT, J.; JONES, J., H.; CREER, H., M.: Quantification of individual phospholipid molecular species by UV absorption measurements. *Journal of Lipid Research.* 1996: vol. 37, p. 2450 – 2460.

MELOUN, M.; MILITKÝ, J. *Kompendium statistického zpracování dat*: *Metody a řešené úlohy*. Vyd. 2. přeprac. a rozš. Praha: Academia, 2006. 984 p. ISBN 80-200-1396-2.

MRÁZ, J.; MÁCHOVÁ, J.; KOZÁK, P.; PICKOVA, J.: Lipid content and composition in common carp - optimization of n-3 fatty acids in different pond production systems. *Journal of Applied Ichthyology*. 2011: vol. 28 (2), p. 238–244.

MURAKAMI, H.; NOBUSAWA, T.; HORI, K.; SHIMOJIMA, M.; OHTA, H.: Betaine Lipid Is Crucial for Adapting to Low Temperature and Phosphate Deficiency in Nannochloropsis. *Plant Physiology.* 2018, vol. 177, p. 181-193.

NAVARRO, J., C.; BATTY, R., S.; BELL, M., V.; SARGENT, J., R.: Effects of two Artemia diets with different contents of polyunsaturated fatty acids on the lipid composition of larvae of Atlantic herring (*Clupea harengus*). *Journal of Fish Biology*. 1993, vol. 43 (4), p. 503–515.

NICHOLS, L. Overview of TLC [online]. Butte Community College. 2017 [2019-03-25]. Available at: https://chem.libretexts.org/Bookshelves/Organic_Chemistry/Book%3A_Organic_Chemistry_Lab_Techniques_(Nichols)/2%3A_Chromatography/2.2%3A_Thin_Layer_Chromatography_(TLC)/2.2.A%3A_Overview_of_TLC

NEVIGATO, T.; MASCI, M.; ORBAN, E.; DI LENA, G.; CASINI, I.; CAPRONI, R.: Analysis of Fatty Acids in 12 Mediterranean Fish Species: Advantages and Limitations of a New GC-FID/GC-MS Based Technique. *Lipids.* 2012: vol. 47, p. 741-753.

NIEMELA, P., S.; CASTILLO, S.; SYSI-AHO, M.; ORESIC, M.: Bioinformatics and computational methods for lipidomics. *Journal of Chromatography B-Analytical Technologies in the Biomedical and Life Sciences.* 2009: vol. 877, p. 2855-2862.

NOVÁKOVÁ, O.; KUBIŠTA, V.: Effect of Early Denervation on the Phospholipid-Metabolism of Insect Flight-Muscle. *Comparative Biochemistry and Physiology B-Biochemistry & Molecular Biology*. 1984: vol. 77, issue 3, p. 579-582.

ORESIC, M.: Bioinformatics and computational approaches applicable to lipidomics. *European Journal of Lipid Science and Technology.* 2009: vol. 111, p. 99-106.

PACCHIAROTTA, T.; NEVEDOMSKAYA, E.; CARRASCO-PANCORBO, A.; DEELDER, A., M.; MAYBORODA, O., A.: Evaluation of GC-APCI/MS and GC-FID as a complementary platform. *Journal of biomolecular techniques*. 2010: vol. 21 (4), p. 205-213.

PANG, L.-Q.; LING, Q.-L.; WANG, Y.-M.; PING, L.; LUO, G.-A.: Simultaneuos determination and quantification of seven major phospholipid classes in human blood using normal-phase liquid chromatography coupled with electrospray mass spectrometry and the application in diabetes nephropathy. *Journal of Chromatography B.* 2008: vol. 569, p. 118-125.

PATTON, G., M.; FASULO, J., M.; ROBINS, S., J.: Separation of phospholipids and individual molecular species of phospholipids by high-performance liquid chromatography. *Journal of Lipid Research*. 1982: vol. 23 (1), p. 190-196.

PINHO, O.; FERREIRA, I., M., P., L., V., O.; FERREIRA, M., A.: Solid-Phase Microextraction in Combination with GC/MS for Quantification of the Major Volatile Free Fatty Acids in Ewe Cheese. *Analytical Chemistry*. 2002: vol. 74, p. 5199-5204.

POUDYAL, H.; PANCHAL, S., K.; DIWAN, V.; BROWN, L.: Omega-3 fatty acids and metabolic syndrome: Effects and emerging mechanisms of action. *Progress in Lipid Research*. 2011: vol. 50 (4), p. 372-387.

QIU, D., F.; GAMES, M., P., L.; XIAO, X., Y.; GAMES, D., E.; WALTON, T., J.: Characterisation of membrane phospholipids and glycolipids from a halophilic archaebacterium by high-performance liquid chromatography/electrospray mass spectrometry. *Rapid communication in mass spectrometry*. 2000: vol. 14 (17), p. 1586-1591.

RAHNAN, S., A.; HUAH, T., S.; NASSAN, O.; DAUD, N., M.: Fatty acid composition of some Malaysian freshwater fish. *Food Chemistry*. 1995: vol. 54 (1), p. 45–49.

RASOARAHONA, J., R., E.; BARNATHAN, G.; BIANCHINI, J.-P.; GAYDOU, E., M.: Annual Evolution of Fatty Acid Profile from Muscle Lipids of the Common Carp (*Cyprinus carpio*) in Madagascar Inland Waters. *Journal of Agricultural and Food Chemistry*. 2004: vol. 52 (24), p. 7339–7344.

RISMANI-YAZDI H.; HAZNEDAROGLU, B., Z.; HSIN, C.; PECCIA, J.: Transcriptomic analysis of the oleaginous microalga *Neochloris oleoabundans* reveals metabolic insights into triacylglyceride accumulation. *Biotechnology for Biofuels.* 2012: vol. 5 (74).

RUSSO, G., L.: Dietary n−6 and n−3 polyunsaturated fatty acids: From biochemistry to clinical implications in cardiovascular prevention. *Biochemical Pharmacology*. 2009, vol. 77 (6), p. 937-946.

RYCKEBOSCH, E.; MUYLAERT, K.; FOUBERT, I.: Optimalization of an Analytical Procedure for Extraction of Lipids from Microalgae. *Journal of the American Oil Chemists Society*. 2012: vol. 89, issue 2, p. 189-198.

SALA-VILA, A.; CALDER, P., C.: Update on the Relationship of Fish Intake with Prostate, Breast, and Colorectal Cancers. *Critical Reviews in Food Science and Nutrition*. 2011: vol. 51 (9), p. 855–871.

SANGIOVANNI, J., P.; CHEW, E., Y.: The role of omega-3 long-chain polyunsaturated fatty acids in health and disease of the retina. *Progress in Retinal and Eye Research*. 2005: vol. 24 (1), p. 87-138.

SAROTRA, P.; SHARMA, G.; KANSAL, S.; KUMARI NEGI, A.; AGGARWAL, R.; SANDHIR, R.; AGNIHOTRI, N.: Chemoprotective Effect of Different Rations of Fish Oil and Corn Oil in Experimental Colon Carcinogenesis. *Lipids.* 2010, vol. 45, p. 785-798.

SATO, N.: Betaine lipids. *The botanical Magazine-Tokyo.* 1992: vol. 105 (1), p. 185-197.

SATO, N.: Roles of the acidic lipids sulfoquinovosyl diacylglycerol and phosphatidylglycerol in photosynthesis: their specificity and evolution. *Journal of Plant Research.* 2004: vol. 117, p. 495-505.

SANDRA, K.; T'KINDT, R.; DEVOS, C.; TIENPONT, B.; SANDRA, P.; DAVID, F.: Automated Sample Preparation Using the GERSTEL MPS WorkStation. Automated Lipid Fractionation Using Solid Phase Extraction. Metabolomics (Part 2). [online] 2016. [2019-03-25] Available at: http://www.gerstel.com/pdf/ GST_GSW_16_8-10_en.pdf

SAUVAGE, F.-L.; GASTINEL, L., N.; MARQUET, P.: Untargeted screening of urinary peptides with liquid chromatography coupled to hybrid linear-ion trap tandem mass spectrometry. *Journal of Chromatography A*. 2012: vol. 1259, p. 138-147.

SCHNEEDORFEROVÁ, I.: Essential Fatty Acid Diagnostics Using Modern Analytical Methods for Nutrition Studies. Thesis. Czech Technical University in Prague, Kladno, Czech Republic, 2012, 107 pp.

SCHWALME, K.; MACKAY, W., C.: Seasonal changes in the neutral and polar lipid fatty acid content of female northern pike (*Esox lucius L.*). *Canadian Journal of Zoology*. 1992: vol. 70 (2), p. 280–287.

SCHWALME, K.; MACKAY, W., C.; CLANDININ, M., T.: Seasonal dynamics of fatty acid composition in female northern pike (Esox lucius L.). *Journal of Comparative Physiology B*. 1993: vol. 163 (4), p. 277–287.

SCHWUDKE, D.; OEGEMA, K.; BURTON, L.; ENTCHEV, E.; HANNICH, J., T.; EJSING, C., S.; KURYCHALIA, T.; SHEVCHENKO, A.: Lipid profiling by multiple precursor and neutral loss Scanning driven by the data-dependent acquisition. *Analytical Chemistry*. 2006: vol. 78, p. 585-595.

SIMOPOULOS, A., P.: The importance of the ratio of omega-6/omega-3 essential fatty acids. *Biomedicine & Pharmacotherapy*. 2002: vol. 56 (8), p. 365-379.

ŠLACHTA, M.; BERKOVÁ, P.; VAMBERA, J.; KOŠŤÁL, V.: Physiology of cold acclimation in the non-diapausing adults of *Pyrrhocoris apterus* (Heteroptera). *European Journal of Entomology*. 2002: vol. 99, p. 181-187.

SLOCOMBE, S., P.; ZHANG, Q., Y.; ROSS, M.; ANDERSON, A.; THOMAS, N., J.; LAPRESA, A.; RAD-MENENDEZ, C.; CAMPBELL, C., N.; BLACK, K., D.; STANLEY, M., S.; DAY, J., G.: Unlocking nature's treasure-chest: screening for oleaginous algae. *Scientific Reports*. 2015: vol. 5.

SOKOŁA-WYSOCZAŃSKA, E.; WYSOCZAŃSKI, T.; WAGNER, J.; CZYŻ, K.; BODKOWSKI, R.; LOCHYŃSKI, S.; PATKOWSKA-SOKOŁA, B.: Polyunsaturated Fatty Acids and Their Potential Therapeutic Role in Cardiovascular System Disorders-A Review. *Nutrients*. 2018: vol. 10 (10), p. 1561.

STRÁNSKÝ, K.; JURSÍK, T.: Simple Quantitative Transesterification of Lipids. *Fett/Lipid*. 1996: vol. 98, p. 65-71.

SUOMINEN-TAIPALE, A. L.; PARTONEN, T.; TURUNEN, A. W.; MANNISTO, S.; JULA, A.; VERKASALO, P. K.: Fish consumption and omega-3 polyunsaturated fatty acids in relation to depressive epizodes: a cross sectional analysis. *PloS One*. 2010, vol. 5 (5), e10530.

TAN, B., B.; LIANG, Y., Z.; YI, L., Z.; LI, H., D.; ZHOU, Z., G.; JI, X., Y.; DENG, J., H.: Identification of free fatty acids profiling of type 2 diabetes mellitus and exploring possible biomarkers by GC-MS coupled with chemometrics. *Metabolomics*. 2010: vol. 6 (2), p. 219-228.

THOMAS, M., C.; MITCHELL, T., W.; BLANKSBY, S., J.: Ozonolysis of phospholipids double bound during electrospray ionization: A new tool for structure determination. *Journal of American Chemical Society*. 2006: vol. 128, p. 58-59.

TOCHER, D., R.; FRASER, A., J.; SARGENT, J., R.; GAMBLE, J., C.: Lipid class composition during embryonic and early larval development in Atlantic herring (*Clupea harengus, L.*). *Lipids*. 1985: vol. 20 (2), p. 84–89.

TOMČALA, A.; TOLLAROVÁ, M.; OVERGAARD, J.; ŠIMEK, P.; KOŠŤÁL, V.: Seasonal acquisition of chill tolerance and restructuring of membrane glycerophospholipids in an overwintering insect: triggering by low temperature, desiccation and diapause progression, *Journal of Experimental Biology*. 2006, vol. 209, Issue 20, s. 4102-4114.

URAN, S.; LARSEN, A.; JACOBSEN, P., B.; SKOTLAND, T.: Analysis of phospholipid species in human blood using normal-phase liquid chromatography coupled with electrospray ionization ion-trap tandem mass spectrometry. *Journal of Chromatography B*. 2001: vol. 758 (2), p. 265-275.

UTTARO, A., D.: Biosynthesis of polyunsaturated fatty acids in lower eukaryotes. *IUBMB Life*. 2006: vol. 58 (10), p. 563-571.

VANCE, J., E.: Phospholipid Synthesis and Transport in Mammalian Cells. *Traffic*. 2015: vol. 16, p. 1-18.

VIELER, A.; WILHELM, C.; GOSS, R.; SÜß, R.; SCHILLER, J.: The lipid composition of the unicellular green alga *Chlamydomonas reinhardtii* and the diatom *Cyclotella meneghiniana* investigated by MALDI-TOF MS and TLC. *Chemistry and Physics of Lipids*. 2007: vol. 150 (2), p. 143-155.

WALLIS, J., G.; WATTS, J., L.; BROWSE, J.: Polyunsaturated fatty acid synthesis: what will they think of next? *Trends in Biochemical Sciences*. 2002: vol. 27, p. 467-473.

WANG, X.; ZHANG, Z.-R.; FU, H.; LIU, J.; CHEN, Q.; NIE, Y.; DENG, L.; GONG, T.: Simultaneous determination and pharmacokinetic study of water-soluble and lipid soluble components of danshen in rat plasma using HPLC-UV method. *Biomedical Chromatography*. 2007: vol. 21, p. 1180-1185.

WODTKE, E.: Lipid adaptation in liver mitochondrial membranes of carp acclimated to different environmental temperatures. *Biochimica et Biophysica Acta (BBA) - Lipids and Lipid Metabolism*. 1978: vol. 529 (2), p. 280–291.

WU, L.; PARHOFER, K., G.: Diabetic dyslipidemia. *Metabolism*. 2014: vol. 63 (12), p. 1469–1479.

YAMADA, T.; UCHIKATA, T.; SAKAMOTO, S.; YOKOI, Y.; FUKUSAKI, E.; BAMBA, T.: Development of a lipid profiling system using reverse-phase liquid chromatography coupled to high-resolution mass spectrometry with rapid polarity switching and an automated lipid identification software. *Journal of Chromatography A*. 2013: vol. 1292, p. 211–218.

ZAHRADNÍČKOVÁ, H.; TOMČALA, A.; BERKOVÁ, P.; SCHNEEDORFEROVÁ, I.; OKROUHLÍK, J.; ŠIMEK, P.; HODKOVÁ, M.: Cost effective, robust, and reliable coupled separation techniques for the identification and quantification of phospholipids in complex biological matrices: application to insects. *Journal of Separation Science*. 2014: vol. 37, p. 2062-2068.

ZHU, H.; FAN, C.; XU, F.; TIAN, C.; ZHANG, F.; QI, K.: Dietary fish oil n-3 polyunsaturated fatty acids and alpha-linoleic acid differently affect brain accretion of docosahexanoic acid and expression of desaturases and sterol regulatory element-binding protein 1 in mice. *Journal of nutritional biochemistry*. 2010: vol. 21 (10), p. 954-960.

ZHU, H.; FAN, C.; XU, F.; TIAN, C.; ZHANG, F.; QI, K.: Dietary fish oil n-3 polyunsaturated fatty acids and alpha-linolenic acid differently affect brain accretion of docosahexaenoic acid and expression of desaturases and sterol regulatory element-binding protein 1 ibn mice. *Journal of Nutritional Biochemistry*. 2001: vol. 21, p. 954-960.

ZOERNER, A., A.; GUTZKI, F., M.; SUCHY, M., T.; BECKMANN, B.; ENGELI, S.; JORDAN, J.; TSIKAS, D.: Targeted stable-isotope dilution GC-MS/MS analysis of the endocannabionoid anandamide and other fatty acid ethanol amides in human plasma. *Journal of Chromatography B.* 2009: vol. 877, p. 2909-2923.

[online] Phenomenex. SUNGMOON SYSTECH LTD., CO. [2019-03-25]. Available at: http://www.phenomenex.co.kr/main/page.php?no=31

7 RESEARCH ARTICLES

Paper I

Cost effective, robust, and reliable coupled separation techniques for the identification and quantification of phospholipids in complex biological matrices: application to insects

Zahradníčková, H., Tomčala, A., Berková, P., Schneedorferová, I., Okrouhlík, J., Šimek, P., Hodková, M.

Journal of Separation Science 37, 2062-2068

2014

Helena Zahradníčková[1]
Aleš Tomčala[1,2]
Petra Berková[1]
Ivana Schneedorferová[1,3]
Jan Okrouhlík[3]
Petr Šimek[1]
Magdalena Hodková[1]

[1]Biology Centre, Academy of Sciences of the Czech Republic, České Budějovice, Czech Republic
[2]Institute of Organic Chemistry and Biochemistry, Academy of Sciences of the Czech Republic, Czech Republic
[3]Faculty of Science, University of South Bohemia, České Budějovice, Czech Republic

Received February 5, 2014
Revised April 7, 2014
Accepted April 24, 2014

Research Article

Cost effective, robust, and reliable coupled separation techniques for the identification and quantification of phospholipids in complex biological matrices: Application to insects

The quantification of phospholipid classes and the determination of their molecular structures are crucial in physiological and medical studies. This paper's target analytes are cell membrane phospholipids, which play an important role in the seasonal acclimation processes of poikilothermic organisms. We introduce a set of simple and cost-effective analytical methods that enable efficient characterization and quantification of particular phospholipid classes and the identification and relative distribution of the individual phospholipid species. The analytical approach involves solid-phase extraction and high-performance thin-layer chromatography, which facilitate the separation of particular lipid classes. The obtained fractions are further transesterified to fatty acid methyl esters and subjected to gas chromatography coupled to flame ionization detection, which enables the determination of the position of double bonds. Phospholipid species separation is achieved by high-performance liquid chromatography with mass spectrometry, which gives information about the headgroup moiety and attached fatty acids. The total content of each phospholipids class is assessed by phosphorus determination by UV spectrophotometry. The simultaneous analysis of phosphorus, fatty acid residues, and phospholipid species provides detailed information about phospholipid composition. Evaluation of these coupled methods was achieved by application to an insect model, *Pyrrhocoris apterus*. High correlation was observed between fatty acid compositions as determined by gas chromatography and high-performance liquid chromatography analysis.

Keywords: Insects / Mass spectrometry / Phospholipids / Thin-layer chromatography
DOI 10.1002/jssc.201400113

Additional supporting information may be found in the online version of this article at the publisher's web-site

1 Introduction

Researchers in the fields of physiology, pharmacology, and medicine desire quick, cheap, and reliable methods for polar lipid analysis. We present such a technique using the insect model *Pyrrhocoris apterus*. Insect tissues possess similar lipid compositions of polar lipids and nonpolar lipids (NLs) to other animals including mammalian tissues [1], therefore insects provide a suitable system for testing this technique. Moreover, obtaining insect samples is cheap and safe and no legal restrictions are involved.

Temperature is one of the most important abiotic factors for poikilothermic organisms, especially insects. Biological membranes assembled from phospholipids (PLs) are responsible for a wide variety of vital functions and their primary structure is influenced by temperature. Since membranes have to maintain structural and functional cell integrity during fluctuations of environmental temperature, the study of the effects of temperature on membrane lipids is particularly important for understanding organism temperature adaptation mechanisms. Changes in distribution of individual PLs involving fatty acid (FA) acyl chain and PL head group restructuring seem to be an integral part of the adaptation of cell membranes to environmental changes in temperature

Correspondence: Dr. Helena Zahradníčková, Biology Centre ASCR, v.v.i., Branišovská 31, České Budějovice 370 05, Czech Republic
E-mail: helenaz@bclab.eu
Fax: +420387775287

Abbreviations: CL, cardiolipin; **FA**, fatty acid; **FAME**, fatty acid methyl ester; **FID**, flame ionization detector; **HPTLC**, high-performance TLC; **MP**, mobile phase; **NL**, nonpolar lipid; **PC**, phosphatidylcholine; **PE**, phosphatidylethanolamine; **PI**, phosphatidylinositol; **PL**, phospholipid; **PS**, phosphatidylserine; **SM**, sphingomyelin

and have been reported in fish [2, 3]. Insect studies, focused on the effect of temperature on membrane intact PL composition with PL class quantification, remain an important part of physiological research [4–8].

To investigate the changes in membrane lipids during *P. apterus* overwintering, we focused on the main membrane components—PLs. Recently, the lipidome investigation of *Drosophila melanogaster* was introduced by Carvalho et al. [9]. The determination of the lipidome was achieved by quantitative shotgun profiling by high-resolution MS. This approach requires expensive instrumentation and does not directly provide information about the position of FA chain double bonds. Additionally, in the Carvalho study expensive labeled internal standards were essential for the quantification process. The purpose of our work, therefore, is to develop a cost effective and affordable methodology by coupling "classical" optimized techniques.

Most researchers use conventional methods of total lipid extraction introduced by Folch [10]. Common sample processing methods such as SPE [11–17] or high-performance thin-layer chromatography (HPTLC) [4, 16, 18–20] are used to separate NLs and PLs from the sample. PL species are often separated and identified by HPLC–ESI-MS^2, enabling the characterization of polar head groups and the identification of FAs moiety, in particular intact PL molecules [5, 8, 11, 21–34]; this methodology, however, is not able to directly determine the position of double bonds in FA carbon chains. For this purpose, other methods of GC FA characterization and quantification were widely used [34–37]. However, these techniques require hydrolysis of lipids and transesterification of FAs [38–40], and therefore the FA composition of individual PL molecular species cannot be determined. The quantification of particular PL classes is effectively achieved by HPTLC separation [6, 16, 18–20] followed by inorganic phosphorus spectrometric concentration elucidation [20]. The most abundant PLs that occur in insects and other animals are phosphatidylcholines (PCs) and phosphatidylethanolamines (PE); phospahatidylserines, phosphatidylinositoles (PIs), and sphingomyelins (SMs) occur less frequently [2, 8, 16] and are therefore not considered in this study. The FAs present in samples depend on the biological material used [41–43].

We offer here a cost-effective and reliable method to complete quantification of PL classes and identification of PL species, suitable for physiological, medical, and nutrition studies dealing with PLs in broad spectrum of biological samples.

2 Materials and methods

2.1 Reagents and standards

All chemicals and solvents were of analytical grade. Methanol Suprasolv, hexane Suprasolv, and water Lichrosolv were purchased from Merck (Germany); isooctane, chloroform, perchloric acid, KH_2PO_4, HCl, and ammonium acetate from Fluka (Germany); acetic acid, ascorbic acid, iodine, NaCl, $(NH_4)_8Mo_7O_{24}{\cdot}4H_2O$, and sodium from Lachema (Czech Republic); 2-propanol LC–MS Chromasolv grade from Riedel-deHaen (Germany); diethyl ether (EC 200–467), chloroform stabilized by ethanol (Chromasolv purity), fatty acids and their methyl esters: C16:0, C16:1, cis-9, C17:0, C18:0, C18:1, cis-9 (oleic), C18:1, cis-11, C18:2, cis-9, 12, C18:3, cis-9, 12, 15, C20:0, tetracosane, PC from egg yolk, PE from egg yolk, PI ammonium salt from bovine liver, SM from bovine brain, cardiolipin (CL) CA sodium salt from bovine heart, phosphatidylserine (PS) from bovine heart, PC C16:0/C16:0, PC C18:1, cis-9/C18:1, cis-9, PC C18:0/C18:2, cis-9,12, PC C16:0/C18:0, PC C18:2, cis-9,12/C18:2, cis-9,12, PE C16:0/C16:0, PE C18:2, cis-9,12/C18:2, cis-9,12, PE C18:0/C18:1, cis-9, PE C18:2, cis-9,12/C18:0, TG C16:0/C16:0/C16:0 (where TG is triacylglycerol), and DG C16:0/C18:1 (where DG is diacylglycerol) were obtained from Sigma–Aldrich (Germany). Separation was achieved using HPTLC silica gel plates Si 60 F254 10 × 10 cm from Merck, and aminopropyl bonded phase columns Bond Elut with 500 mg of sorbent from Varian (USA).

2.2 Sample collection and preparation

Pyrrhocoris apterus adult insects were collected from fields around České Budějovice (South Bohemia, Czech Republic) over the course of one year. The dissection of thoraces and fat bodies was performed within 3 min to prevent PL degradation and were subsequently stored under liquid nitrogen prior to analysis. Each sample consisted of ten thoraces or ten fat bodies and varied from 10 to 25 mg of raw tissue.

2.3 Sample processing and time schedule

Workflow 1 shows the methodology used and complementarity of presented methods. The time frames of particular techniques under routine laboratory conditions are depicted in the diagram. Coupling of these "classical" techniques provides identification and quantification of PLs in an unknown sample within a single day. The time frame is calculated for a set of samples because the methods are designed for parallel sample processing.

2.4 Lipid extraction

Lipids were extracted from various insect tissues using the procedure based on chloroform and methanol described by Folch [10] and adjusted by Kostal and Simek [6]. Extracts were dried under a stream of nitrogen and dissolved in 500 μL of chloroform/methanol mixture (2:1, v/v). A 300 μL aliquot of each extract was used for phosphorus determination of PL classes by HPTLC and the remaining 200 μL was subjected to SPE treatment followed by HPLC–ESI-MS and GC with flame ionization detection (FID) for PL detailed structure characterization.

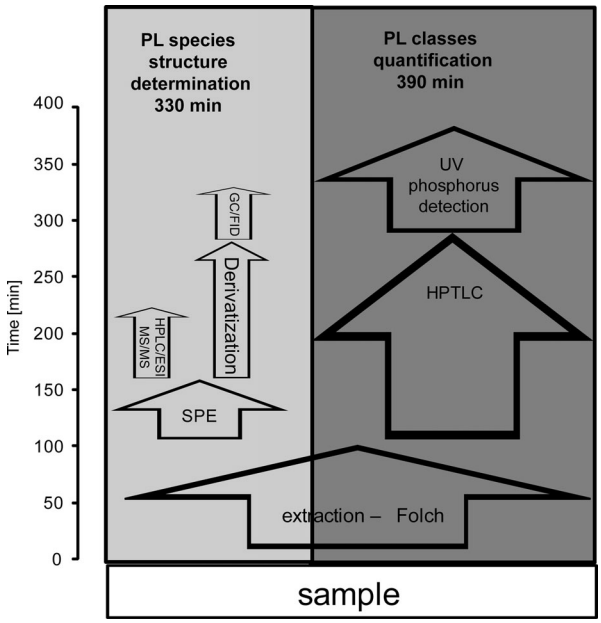

Workflow 1. The fate of the sample treated by coupled separation and detection techniques to obtain detailed information including PL species structure determination and quantification of PL classes. Arrows show the direction of the sample through analytical methods; the total time required for each analytical process is shown at the top.

2.5 PL structure elucidation

To determine PL structure, it was necessary to remove neutral lipids by SPE. Then intact PL identification by HPLC–ESI-MS preceded GC–FID FA double bond position elucidation. SPE is based on previous work introduced by Kaluzny [13] and redesigned in the following manner: extractions on aminopropyl-bonded phase columns were performed on the SPE device (Baker), which allowed several extractions to be processed simultaneously. Columns were conditioned with 4 mL of hexane. The 100 μL of chloroform/methanol solution with a sample or a mixture of standards was then applied. Mobile phase (MP) A (chloroform and 2-propanol, 2:1, v/v) and B (2% acetic acid in diethyl ether, v/v) were the same as Kaluzny described, but the MP C was modified to contain methanol and water in a 9:1 ratio v/v (Supporting Information Section 1). All three fractions were dried by a stream of nitrogen and stored at −22°C. The PL fraction was dissolved in 500 μL of chloroform and divided into two aliquots: 250 μL was dried and diluted with 250 μL of methanol for HPLC–ESI-MS analysis and the rest was derivatized for GC–FID analysis as described below.

HPLC–ESI-MS was performed on an ion trap LTQ mass spectrometer coupled to an Allegro ternary HPLC system equipped with an Accela autosampler and a thermostat chamber (all from Thermo, San Jose, CA, USA). Five microliters of sample was injected into a Gemini column 250 × 2 mm × 3 μm (Phenomenex, Torrance, CA, USA). The MPs were (A) 5 mmol/L ammonium acetate in methanol, (B) water, and (C) 2-propanol. The analysis was completed within 38 min with a flow rate of 200 μL/min by gradient of 95% A and 5% B in 0–5 min, than 100% A until 12 min, subsequently increasing phase C to 30% until 29 min and back to the 95:5% A/B ratio for column conditioning. The column temperature was maintained at 30°C. The mass spectrometer was operated in the positive and negative ion detection modes at +4 and −4 kV with capillary temperature at 220°C. A mass range of 440–1100 Da was scanned every 0.5 s to obtain the full scan ESI mass spectra of PLs. For the investigation of PL structure, the collision-induced decomposition ion trap mass spectra MS^2 in both polarities were simultaneously recorded with a 3 Da isolation window. Normalized collision energy was 30%. Main detected PL molecular species were separated by RP-HPLC. The structure of each entity was identified by MS^2 experiments [44]. Peak areas for each detected PL component were summarized and their relative contents were estimated to sum of all obtained peaks.

FAs were determined in the PL SPE fraction by transesterification to fatty acid methyl esters (FAMEs) with sodium methoxide (2 mol/L) [4]. The procedure was modified in the following manner: the PL fractions were transferred directly into glass derivatization vessels (1 mL). Tetracosane (5 μg) was subsequently added as an internal standard (50 μL of solution of 100 ng/μL in isooctane). Then, 50 μL hexane and 100 μL sodium methoxide (2 mol/L solution prepared by dissolving 0.46 g Na in 10 mL dried methanol) were added. The vessels were tightly closed, vigorously mixed for 10 s and then gently mixed for 15 min. After that, hexane (100 μL) and HCl (220 μL, 1 mol/L aqueous solution) were added, the content was mixed, pH was set to 5, and the upper hexane layer was aspirated. Hexane (200 μL) was added repeatedly; both hexane layers were collected, dried under the nitrogen stream and dissolved in isooctane (100 μL). FAMEs were then analyzed by GC–FID. The calibration curves were prepared for the following FAMEs: C16:0, C16:1, cis-9, C17:0, C18:0, C18:1, cis-9, cis- C18:1, cis-11, C18:2, cis-9, 12, C18:3, cis-9,12,15, C20:0 reaching the interval 2–50 μg of each standard in the injection. The concentration was set according to the levels of FAs acids presented in insect samples. GC analyses were performed on a GC Varian 3400 equipped with split/splitless injector and FID (USA). A capillary column BPX-70, 30 m × 0.22 mm, 0.25 μm film thickness (SGE – SciTech, Prague, Czech Republic) was used with the following settings: oven temperature program from 120 to 260°C at a rate of 10°C/min, the injector 260°C, FID detector 280°C, the helium carrier gas flow rate 30 cm/s with a split flow rate of 15 mL/min.

2.6 PL class quantification

The quantification is based on robust separation and on the measurement of inorganic phosphorus content; in particular those of PL class HPTLC spots. HPTLC plates were washed step by step with methanol, chloroform/methanol (2:1, v/v), and hexane, and used immediately after short air-drying for sample application by Linomat IV (CAMAG, Switzerland). Then, the plates were washed several times in the MP I

(hexane/diethyl ether/acetic acid 80:18:2, v/v/v) to remove neutral lipids, and developed gradually in two MPs—MP II consisted of chloroform/methanol/acetic acid/water (60:35:2:1, v/v/v/v), the developing path 9 cm, and MP III consisted of chloroform/methanol/acetic acid/water (50:30:8:4, v/v/v/v), the developing path 6 cm [4, 18]. One-dimensional developments were performed vertically at 25°C in a saturated twin-trough developing chamber (CAMAG). The spots of SM, PC, PS, PI, PE, and CL in the plates were visualized by iodine vapors and then the spots were densitometrically measured at 205 nm using Linomat IV and TLC Scanner II from CAMAG and integrator SP 4270 Spectra Physics (San Jose, CA, USA) and subsequently scraped from the plates. The silica gel materials of individual fractions was divided into two aliquots for phosphorus quantification and post-transesterification GC FA analysis. In order to quantify each main PL class, the separated PLs were converted into inorganic phosphate (as phosphomolybdate complex) and the phosphorus content was determined by UV spectrophotometric method [20] (see Supporting Information Section 2). The calibration was based on spectrophotometric measurement of the KH_2PO_4 standard solutions, processed in the same way as PLs. The PL recovery of the HPTLC method was estimated as follows: PC dioleoyl standard (20 μg) was applied eight times on HPTLC plate and processed as described above. Spots were scraped, extracted three times in a mixture of chloroform/methanol/H_2O, 5:5:1 (400 μL, v/v/v), dried under a stream of nitrogen and dissolved in chloroform/methanol/H_2O, 5:5:1 (60 μL, v/v/v). One half of each extract (30 μL, corresponding of 10 μg of PC–dioleoyl) was applied to another HPTLC plate together with the PC–dioleoyl (10 μg) standard ($n = 8$). After developing and drying, the plate was immediately densitometrically scanned. The recovery was determined from peak heights, 100% being the average from peak heights of 10 μg of the PC–dioleoyl standard.

2.7 Comparison of the C16 FA acyl composition measured by GC and by HPLC–ESI-MS

The proportions of PL C 16:0 FA determined by GC and HPLC–ESI-MS were compared. The value for the former case was calculated from peak area of C16:0 methyl ester recalculated to weight percent. The latter value was obtained by recalculation. Each PL contains two FAs in their molecule structure. In the case of molecules with the same FAs, the whole peak area was used for calculation. In the case of different FAs the area was divided into two parts, each dedicated to the particular FA. The total content of a given FA was acquired by summarization of peak areas donated from each PL. The weight percent values from ESI-MS were plotted against values acquired by GC–FID analysis.

2.8 Data processing, data analysis

Acquired data were processed by Xcalibur 2.1 (Thermo Fisher Scientific). Further data analysis was accomplished using statistics in MS Excel (Microsoft).

3 Results and discussion

3.1 PL structure elucidation

Several SPE methods employing reversed and normal phase were tested for the separation of PL classes but only the method described by Kaluzny et al. [13] provided satisfactory results due to separation of NLs from PLs. Our experiments, however, did not yield the same PL values as those performed by Kaluzny and colleagues. A similar situation was described by other authors [14]. We therefore experimented with MP composition and elution volumes, achieving the following yields: the percentage recovery was 67.6% (RSD = 12.7%) for PE and 85.4% (RSD = 4.0%) for PC. This SPE method also prevented NL contamination of the chromatographic column, ion source, and spectrometer optics.

Efficient HPLC separation and simultaneous +ESI and −ESI MS scanning provided characterization of the main PL classes and species occurring in the PL fraction of insect tissue (Supporting Information Fig. S3). The whole analysis took 38 min, and PEs were eluted during the first 12 min followed by PCs and finally by neutral lipids. The satisfactory separation of the main PLs enabled us to capture full scan mass spectral data of both polarities and MS^2 data in a single analysis. More than 90% of all PLs were successfully identified and their ratios are shown in Table 1 and Supporting Information Fig. S3. It should be noted, however, that HPLC–ESI-MS acquires data about intact PLs and this technique is unable to determine the double bond positions in FA acyls directly. GC–FID, on the other hand, is capable of determining double bond positions.

FAs were determined in the SPE PL fraction by GC–FID after direct transmethylation. More detailed investigation of particular PL class can be achieved by assessment of FAs contained in silica gel scraped from PL class spots obtained from the HPTLC separation. Calibration curves were prepared in different concentration ranges: 0.05–0.5 μg for C16:1, cis-11, C17:0, C18:1, cis-11, C18:3, cis-9,12,15, C20:0 fatty acids, 1–25 μg for C16:0, C18:0, C18:1, cis-9 fatty acids, and 2–50 μg for C18:2, cis-9,12 fatty acids. Linear relationships were obtained with a correlation coefficient >0.997. The GC–FID technique is a robust, easy, and cost effective way to obtain information about double bond positions in FA carbon chains [36, 37].

3.2 PL class quantification

The absolute quantification of a particular PL species by MS is difficult owing to their variable ESI ionization efficiencies, which hinder the analysis [45, 46]. The real content of PL classes in a sample can be easily obtained by HPTLC and subsequent inorganic phosphorus determination. The HPTLC procedure of Dibiase et al. [18] was adapted for the PL fractionation of insect extracts. An additional step, the triple prewashing of HPTLC plates with methanol, chloroform/methanol 2:1, and hexane before the application of

Table 1. Summary of measured and identified PCs and PEs. Data were obtained by HPLC–ESI-MS of SPE PLs fractions from the total lipid extract

Lipid		RT (min)	Ionization (*m/z*)		Fat body (%)		Thorax (%)	
Class	Species		ESI+	ESI−	August	February	August	February
PC	16:0/18:2	14.69	758.6	816.6	7.4	8.7	9.7	10.4
	16:0/18:1	16.34	760.6	818.6	0.1	1.1	0.2	0.1
	18:2/18:2	13.57	782.6	840.6	27.2	20.5	30.5	25.0
	18:1/18:2	15.01	784.6	842.6	6.5	2.7	5.7	3.4
	18:1/18:1	16.73	786.6	844.6	2.0	0.6	0.5	0.2
	18:0/18:2	17.22	786.6	844.6	8.5	3.3	5.6	1.2
	18:0/18:1	19.23	788.6	846.6	0.4	0.0	0.1	0.0
PE	16:0/18:2	12.14	716.4	714.4	8.0	27.1	8.8	25.5
	16:0/18:1	13.35	718.4	716.4	1.6	1.5	1.0	0.5
	18:2/18:2	11.3	740.4	738.4	12.8	14.5	11.6	10.8
	18:1/18:2	12.42	742.4	740.4	3.4	4.1	4.0	4.3
	18:1/18:1	13.98	744.4	742.4	0.9	0.5	0.3	0.3
	18:0/18:2	14.41	744.4	742.4	19.2	13.8	19.9	16.5
	18:0/18:1	15.37	746.4	744.4	2.0	1.6	2.3	1.7

The retention time (RT), ionization behavior ESI$^+$ (PC $[M+H]^+$, PE $[M+H]^+$) and ESI$^-$ (PC $[M+CH3OO]^-$, PE $[M\text{-}H]^-$) and relative ratio of particular PLs in summer and winter samples for a given tissue are shown. For clarity, the fragmentation data and SDs are not included in this table.

insect extracts to HPTLC plates, was appended in our previous paper [6]. In this work, we extended the procedure of repetitive removal of NLs by the mixture of hexane/diethyl ether/acetic acid 80:18:2 (MP I) after the application of insect extracts. Prewashing of the HPTLC plates increased the sensitivity and reproducibility of PL separation. Precleaning with MP I multiple times to completely remove neutral lipids was shown to be unavoidable. Without perfect elimination of NLs, good separation of PLs was unfeasible and subsequent FA quantification by GC was impossible. In performed HPTLC analyses, PL classes possessed the following retardation factors: 0.94 SM, 0.91 PC, 0.88 PS, 0.82 PI, 0.68 PE, 0.46 CL, and 0.07 NL (Supporting Information Fig. S1). Scraped spots of particular PL class were mineralized and measured. Calibration curves were obtained by standard solutions of KH_2PO_4 and were linear from 0.025 to 0.2 μmol/mL of phosphorus (correlation coefficient >0.998). Recoveries of the UV spectrophotometric method were obtained for PC–dioleoyl 88.2% with the RSD 5.2% and for PE–dioleoyl 86.9% with 7.2% ($n = 14$). The recovery reported previously [16] was higher and varied from 95 to 101.7% but the methodology used incorporated time-consuming 2D TLC and annoying H_2SO_4 spraying followed by heating of the plates. Our proposed technique does not yield complete recovery but is more environmentally friendly. To speed up PL quantification, we proposed comfortable and time-saving densitometric measurement, enabling high throughput of samples. The PC–dioleoyl standard showed the recovery of 76.5% with the RSD of 5.1% ($n = 8$) after prewashing HPTLC plates and removing NLs. The recovery is lower; however the methodology proposed by previous authors [16, 20] covers time consumption and skill required to scrape PL spots. The use of the densitometric method is more user-friendly and saves time. HPTLC combined with subsequent phosphorus analysis by UV detection or densitometric measurement of PL spots are important parts of the presented analytical approach, because neither mass spectrometric analysis of PL molecular species nor FA analysis by GC–FID are able to provide direct information about the real quantity of the particular PL classes in the biological tissue owing to the variable ionization efficiency of particular PL classes [45, 46]. In addition, proper quantification of particular PL classes/species using MS requires labeled internal standards [47]. Purchasing these compounds is very expensive and therefore decreases cost efficiency.

3.3 Comparison of FA acyl distribution by GC–FID and LC–ESI-MS

We compared the data obtained using both methods and found a good correlation between the FA C16:0 distribution estimated in the same insect tissue extract (Fig. 1). This shows that the relative proportion obtained from HPLC–MS analysis is a valuable indicator of the restructuring of PL molecular species in cold acclimation studies.

3.4 Application of optimized PL methodology to biological samples

The described HPLC–ESI-MS approach enabled identification of seven major PEs and seven PCs in the thoracic muscles and fat bodies of *P. apterus* (Table 1 and Supporting Information Fig. S2). GC–FID revealed that two unsaturated

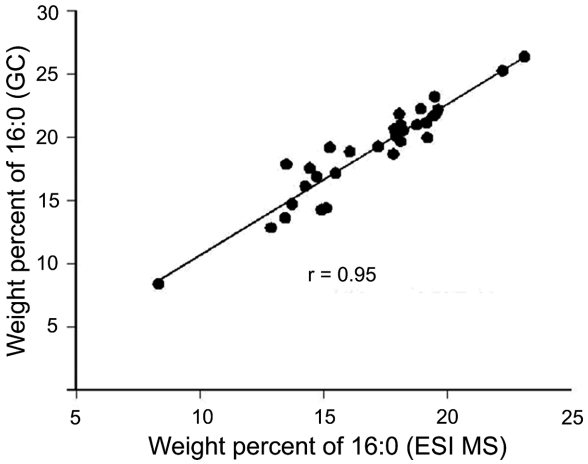

Figure 1. The correlation between FA acyl distributions in *P. apterus* thoraces determined by GC–FID and HPLC–ESI-MS. Proportions of C16:0 FAs calculated from ESI-MS profiles are expressed as weight percentages of PLs plotted against proportions of C16:0 FAs directly measured by GC–FID.

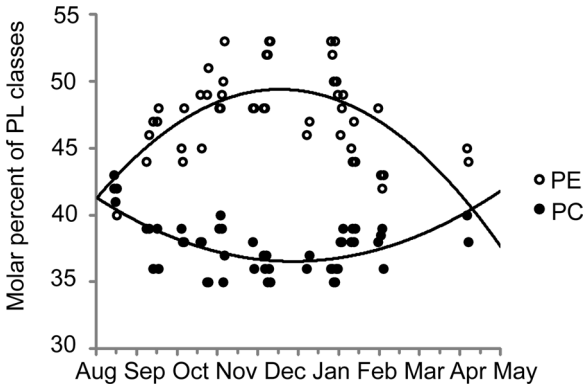

Figure 2. Seasonal changes of PLs expressed as molar percentages in thoraces of *P. apterus*. Molar percent composition of PLs were determined from phosphorus content in a given month. The most abundant classes (PC, PE) are shown here.

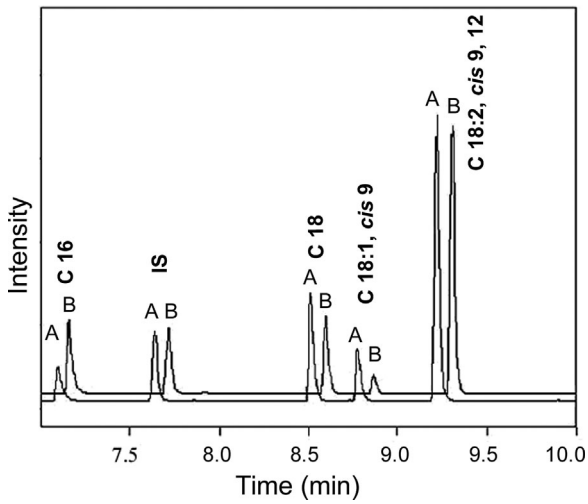

Figure 3. A part of the overlaid GC–FID chromatograms obtained by the analysis of FA profiles in a PE fraction isolated from thoraces of *P. apterus* using HPTLC. The chromatograms show that the C18:1, cis 9 double bond position and also C18:2, cis 9, 12 are only present in these samples. The figure clearly indicates differences between FA profiles. (A) August collection, (B) February collection. Workflow 1, the fate of the sample treated by coupled separation and detection techniques to obtain detailed information including PL species structure determination and quantification of PL classes. Arrows show the direction of the sample through analytical methods; the total time required for each analytical process is shown at the top.

FAs, C18:2, cis-9, 12 and C18:1, cis-9, and two saturated FAs, C16:0 and C18:0, were the most abundant FAs in all samples of *P. apterus*. The following FAs were found in minor amounts (<1%): C14:0, C17:0, and C18:1, cis-11. In some samples, C16:1, cis-9 and C18:3, cis-9, 12, 15 were also found in trace amounts (<0.2%). Detected FAs represented >97% of all FA residues present in the PL fraction (see Supporting Information Fig. S3) [5].

The phosphorus analyses in insect tissue extracts revealed that PLs with PE and PC head groups represented >80% of total PLs in *P. apterus* [4,5]. The less abundant PLs had SM, PS, PI, and CL headgroups (Supporting Information Fig. S1). By monitoring of the phosphorus content in particular PL classes throughout the whole year, distinct changes were observed in the PE and PC distribution in thoraces (Fig. 2). The results of PL species were expressed in molar percent (sum of μmol of PLs = 100%).

The measurements revealed (i) cold acclimation of *P. apterus* results in an increase of the proportion of PE at the expense of PC [3–5,8] (Fig. 2), (ii) a higher proportion of C16:0 in total PL content of winter samples ([4] and Fig. 3), (iii) accumulation of PE molecular species with the C16:0/C18:2 in winter samples, and (iv) a decreased ratio of PC 18:2/18:2, PC 18:1/18:2, and PE 18:0/18:2 (Table 1). These results are in accordance with previously published data [2–6, 8, 48].

4 Conclusions

This work describes a set of simple, cost-effective methods for PL analyses and their detailed characterization and quantification in insect tissues without the use of expensive high-resolution mass spectrometers and isotopically labeled standards. After NL removal by SPE, the intact PL species are easily detected by HPLC–ESI-MS^2. However, the limitation of this technique does not allow for the determination of double bond positions in FA moieties of intact PLs. A second limitation is the poor quantification of PL classes as a result of different ionization efficiencies. These shortcomings are compensated for by using GC–FID and HPTLC, respectively, coupled with inorganic phosphorus quantification.

Nearly perfect correlation was found between FA compositions as determined by GC and the data obtained using our newly developed HPLC–ESI-MS method. Although these

techniques were optimized for insect species, they can be employed for a wide spectrum of biological samples.

This study was supported by the Technological Grant Agency of Czech Republic (TA01020969) and the Czech Science Foundation (13–18509S and P502/10/1612.). We would like to kindly acknowledge Heather Esson for language correction.

The authors have declared no conflict of interest.

5 References

[1] Gennis, R. B., *Biomembranes: Molecular Structure and Function*, Springer-Verlag, New York 1989.

[2] Hazel, J. R., *Adv. Comp. Environ. Physiol.* 1989, *4*, 1–50.

[3] Hazel, J. R., *Annu. Rev. Physiol.* 1995, *57*, 19–42.

[4] Hodkova, M., Simek, P., Zahradnickova, H., Novakova, O., *Insect Biochem. Mol. Biol.* 1999, *29*, 367–376.

[5] Hodkova, M., Berkova, P., Zahradnickova, H., *J. Insect Physiol.* 2002, *48*, 1009–1019.

[6] Kostal, V., Simek, P., *J. Comp. Physiol. B* 1998, *168*, 453–460.

[7] Slachta, M., Berkova, P., Vambera, J., Kostal, V., *Eur. J. Entomol.* 2002, *99*, 181–187.

[8] Tomcala, A., Tollarova, M., Overgaard, J., Simek, P., Kostal, V., *J. Exp. Biol.* 2006, *209*, 4102–4114.

[9] Carvalho, M., Sampaio, J. L., Palm, W., Brankatschk, M., Eaton, S., Schevchenko, A., *Mol. Syst. Biol.* 2012, *8*, 600.

[10] Folch, J., Lees, M., Stanley, G. H. S., *J. Biol. Chem.* 1957, *226*, 497–509.

[11] Neron, S., El Amrani, F., Potus, J., Nicolas, J., *J. Chromatogr. A* 2004, *1047*, 77–83.

[12] Fuchs, B., Schiller, J., Suess, R., Schuerenberg, M., Suckau, D., *Anal. Bioanal. Chem.* 2007, *389*, 827–834.

[13] Kaluzny, M. A., Duncan, L. A., Merritt, M. V., Epps, D. E., *J. Lipid Res.* 1985, *26*, 135–140.

[14] Cascone, A., Eerola, S., Ritieni, A., Rizzo, A., *J. Chromatogr. A* 2006, *1120*, 211–220.

[15] Janero, D. R., Burghardt, C., *J. Chromatogr.* 1990, *526*, 11–24.

[16] Abramson, D., Blecher, M., *J. Lipid Res.* 1964, *5*, 628–631.

[17] Fauland, A., Troetzmueller, M., Eberl, A., *J. Sep. Sci.* 2013, *36*, 744–751.

[18] Dibiase, A., Salvati, S., Crescenzi, G. S., *Neurochem. Res.* 1989, *14*, 153–156.

[19] Touchstone, J. C., *J. Chromatogr. B* 1995, *671*, 169–195.

[20] Rouser, G., Fleische, S., Yamamoto, A., *Lipids* 1970, *5*, 494–496.

[21] Qiu, D. F., Games, M. P. L., Xiao, X. Y., Games, D. E., Walton, T. J., *Rapid Commun. Mass Spectrom.* 2000, *14*, 1586–1591.

[22] Jensen, N. J., Gross, M. L., *Mass Spectrom. Rev.* 1988, *7*, 41–69.

[23] Kerwin, J. L., Tuininga, A. R., Ericsson, L. H., *J. Lipid Res.* 1994, *35*, 1102–1114.

[24] Matsubara, T., Hayashi, A., *Prog. Lipid Res.* 1991, *30*, 301–322.

[25] Han, X. L., Gross, R. W., *J. Amer. Chem. Soc.* 1996, *118*, 451–457.

[26] Uran, S., Larsen, A., Jacobsen, P. B., Skotland, T., *J. Chromatogr. B* 2001, *758*, 265–275.

[27] Kim, H. Y., Wang, T. C. L., Ma, Y. C., *Anal. Chem.* 1994, *66*, 3977–3982.

[28] Hvattum, E., Rosjo, C., Gjoen, T., Rosenlund, G., Ruyter, B., *J. Chromatogr. B* 2000, *748*, 137–149.

[29] Fang, J. S., Barcelona, M. J., *J. Microbiol. Methods* 1998, *33*, 23–35.

[30] Duffin, K. L., Henion, J. D., Shieh, J. J., *Anal. Chem.* 1991, *63*, 1781–1788.

[31] Kuksis, A., Myher, J. J., *J. Chromatogr. B*1995, *671*, 35–70.

[32] Ekroos, K., Ejsing, C. S., Bahr, U., Karas, M., Simons, K., Schevchenko, A., *J. Lipid Res.* 2003, *44*, 2181–2192.

[33] Ecker, J., *J. Sep. Sci.* 2012, *35*, 1227–1235.

[34] Hellmuth, C., Uhl, O., Segura-Moreno, M., Demmelmair, H., Koletzko, B., *J. Sep. Sci.* 2011, *34*, 3470–3483.

[35] Novakova, O., Kubista, V., *Comp. Biochem. Physiol.* 1984, *77*, 579–582.

[36] Eder, K., *J. Chromatogr. B* 1995, *671*, 113–131.

[37] Ichihara, K., Shibahara, A., Yamamoto, K., Nakayama, T., *Lipids* 1996, *31*, 889–889.

[38] Myher, J. J., Kuksis, A., Marai, L., Yeung, S. K. F., *Anal. Chem.* 1978, *50*, 557–561.

[39] Harvey, D. J., in: Christie, W. W. (Ed.), *Advanced in Lipid Mehodology – One*, The Oily Press, Dundee 1992, pp. 19–80.

[40] Murphy, R. C., *Mass Spectrom. Lipids*, Springer 1993.

[41] Ansell, G. B., Spanner, S., *New Comprehensive Biochemistry,* Volume 4*, Phospholipids*, Elsevier Biomedical Press, Amsterdam 1982.

[42] Hori, T., Nozawa, Y., *New Comprehensive Biochemistry, Volume 4, Phospholipids*, Elsevier Biomedical Press, Amsterdam 1982.

[43] Gamo, S., Kawabe, A., Kohara, H., Yamaguchi, H., Tanaka, Y., Yagi, S., *J. Mass Spectrom.* 1999, *34*, 590–600.

[44] Hsu, F.-F., Turk, J., *J. Chromatogr. B* 2009, *877*, 2673–2695.

[45] Han, X. L., Yang, K., Yang, J. Y., Fikes, K. N., Cheng, H., Gross, R.W., *J. Am. Soc. Mass Spectrom.* 2006, *17*, 264–274.

[46] Koivusalo, M., Haimi, P., Heikinheimo, L., Kostiainen, R., Somerharju, P., *J. Lipid Res.* 2001, *42*, 663–672.

[47] Xiong, Y. P., Zhao, Y. Y., Goruk, S., Oilund, K., Field, C. J., Jacobs, R. L., Curtis, J. M., *J. Chromatogr. B* 2012, *911*, 170–179.

[48] Harwood, J. L., Jones, A. L., Perry, H. J., Rutter, A. J., Smith, K. L., Williams, M., in: Cossins, A. R. (Ed.), *Temperature Adaptation of Biological Membranes*, Portland Press, London 1994, pp. 107–118.

Paper II

Effect of heat treatment on the n-3/n-6 ratio and content of polyunsaturated fatty acids in fish tissues

Schneedorferová, I., Tomčala, A., Valterová, I.

Food Chemistry, 176: 205-211

2015

The original publication is available at:
http://dx.doi.org/10.1016/j.foodchem.2014.12.058

Effect of heat treatment on the n-3/n-6 ratio and content of polyunsaturated fatty acids in fish tissues

Ivana Schneedorferová,[1,2] Aleš Tomčala,[1,3] and Irena Valterová[3*]

[1] Biology Centre, Institute of Parasitology, Academy of Sciences of the Czech Republic, Branišovská 31, 370 05 České Budějovice, Czech Republic

[2] University of South Bohemia, Faculty of Science, Branišovská 31, 370 05 České Budějovice, Czech Republic

[3] Institute of Organic Chemistry and Biochemistry, Academy of Sciences of the Czech Republic, Flemingovo náměstí 2, 166 10, Prague 6, Czech Republic

Abstract

The aim of this study was to compare the effect of different heat treatments (pan frying, oven baking, and grilling) on the contents of polyunsaturated fatty acids (PUFAs) in fish tissue. Four fish species were examined: pike, carp, cod, and herring. High performance liquid chromatography, coupled with electrospray ionization and mass spectrometric detection (HPLC/ESI/MS) was employed for determination of intact lipid molecules containing n-3 and n-6 PUFAs. Although mostly non-polar lipids (triacylglycerols, TGs) were present in the fish tissue, the PUFAs were present preferentially in the phospholipid fraction. Omnivorous fish species (carp, herring) contained more TGs than did predatory ones (pike, cod). Higher amounts of PUFAs were detected in the marine species than in the freshwater ones. The impact of heat treatments on the lipid composition in the fish tissue seems to be species-specific, as indicated by multivariate data analysis. Herring tissue is most heat-stable, and the mildest heat treatment for PUFA preservation was oven baking.

Keywords: n-3 PUFA, n-6 PUFA, Heat treatment, Fish tissue, HPLC/MS, GC/MS

1. Introduction

Recent nutrition studies are increasingly focused on prevention and reduction of obesity caused by western dietary habits. Intake of an appropriate ratio of essential fatty acids (FAs) appears to be critical for achieving these aims. Polyunsaturated fatty acids (PUFAs) are a focus of nutritionists. Two classes of PUFAs are recognized: n-3 and n-6. These are referred to as "essential" FAs because mammals lack the Δ12- and Δ15-desaturases necessary to introduce double bonds at specific positions on the FA carbon chain. Double bonds in n-3 and n-6 PUFAs are located toward the methyl-end of the chain (Adkins & Kelley, 2010; Simopoulos, 1991). In mammalian systems, longer-chain FAs can be synthesized from two essential FA precursors: α-linolenic acid (ALA; 18:3 n-3), leading to n-3 PUFA, and linoleic acid (LA; 18:2 n-6), resulting in n-6 PUFA (Adkins & Kelley, 2010; Zhu, Fan, Xu, Tian, Zhang, & Qi, 2010). Both precursors are transformed by a similar enzymatic system in a competitive reaction. Thus, the western diet, which contains large amounts of n-6 precursors, leads to enhanced production of long-chain n-6 PUFAs and suppressed production of n-3 PUFAs. The most studied long-chain n-3 PUFAs are eicosapentaenoic acid (EPA; 20:5 n-3) and docosahexaenoic acid (DHA; 22:6 n-3) (Lopez-Huertas, 2010; Simopoulos, 2002) while, among n-6 PUFAs, it is arachidonic acid (AA; 20:4 n-6) (Heissenberger, Watzke, & Kainz, 2010). A high intake of ALA supports the elongation of n-3 PUFAs and reduces the elongation of n-6 PUFAs (Adkins & Kelley, 2010).

Human genes have changed little from those of our ancestors 40,000 years ago, but living conditions and lifestyle have changed significantly (Simopoulos, 2002). Evolutionary studies show that the hunter-gatherer's diet of our ancestors was rich in PUFAs with a n-3/n-6 ratio of approximately 1-2/1 (Zhu, Fan, Xu, Tian, Zhang, & Qi, 2010). In contrast, the modern western diet is characterized by consumption of high amounts of saturated fats, *trans*-fatty acids, and n-6 PUFAs and a low intake of n-3 PUFAs. The n-3/n-6 PUFA ratio in the western diet ranges from 1/15 to 1/25. This decrease in the n-3/n-6 PUFA ratio has been associated with development of numerous diseases (Simopoulos, 1991, 2002; Zhu, Fan, Xu, Tian, Zhang, & Qi, 2010).

Metabolic syndrome is a complex of metabolic abnormalities connected to obesity, which is a consequence of overnutrition. Metabolic syndrome increases a person's risk for a constellation of health problems, such as hypertension, insulin resistance, dyslipidemia, hypertriglyceridemia, hyperglycemia, oxidative stress, and inflammation (Poudyal, Panchal, Diwan, & Brown, 2011). It also may lead to type 2 diabetes or cardiovascular diseases (Puglisi, Hasty, & Saraswathi, 2011). EPA and DHA have been shown to reduce LDL-cholesterol levels, which closely relate to risk of coronary heart disease (Weintraub, 2013). Adipose tissue plays an important role in lipid homeostasis. The supply of free FAs controls lipolysis and storage of triacylglycerols (TGs). Long-chain n-3 PUFAs are associated with effective energy storage and secretory functions, and they have a preventive and curative effect on obesity (Puglisi, Hasty, & Saraswathi, 2011). Cardiovascular diseases are the most frequent causes of death in western countries (Mann, O'Connell, Baldwin, Singh, & Meyer, 2010). The intake of n-3 PUFAs reduces the incidence (Kris-Etherton, Harris, Appel, & Nutrition, 2002) and decreases the risk of fatal coronary heart disease or sudden cardiac death (Brouwer, Geelen, & Katan, 2006). Some of the underlying mechanisms for this protective effect include prevention of arrhythmia; reduction of blood pressure and heart rate, improvement of endothelial function, vascular reactivity and cardiac electrophysiology; and reduced platelet aggregation (Lopez-Huertas, 2010). Long-chain n-3 PUFAs, especially DHA, which is present at high levels in brain tissue, are significant contributors to brain development and function. Deficiency of n-3 PUFAs decreases the DHA concentration in the brain and has a negative effect on neural development and visual acuity. Lack of DHA is also associated with disorders of the nervous system, including Alzheimer's disease, schizophrenia, and depression (Zhu, Fan, Xu, Tian, Zhang, & Qi, 2010). Other research has focussed on the importance of diet for patients with cancer. Several studies have indicated that a high saturated fat intake increases the risk of cancer and that n-6 PUFAs have a proinflammatory and procarcinogenic effect (Sarotra, Sharma, Kansal, Negi, Aggarwal, Sandhir, et al., 2010). On the other hand, n-3 PUFAs seem to have chemopreventive properties in breast and colon cancers. Several mechanisms, such as suppression of neoplastic transformation, cell growth inhibition, antiangiogenicity, and enhanced apoptosis, may be involved (Rose & Connolly, 1999).

The primary source of n-3 PUFAs is marine algae, which are rich in enzymes involved in n-3 PUFA biosynthesis. These enzymes elongate FAs to EPA and DHA. Humans consume these long-chain FAs in marine fish, which are rich in PUFAs obtained through the food chain (Kim, Khan, McMurray, Prior, Wang, & Chapkin, 2010). Freshwater fish and other products of aquatic ecosystems are valuable source of PUFAs as well (Bhouri, Harzallah, Dhibi, Bouhlel, El Cafsi, Hammami, et al., 2010; Gladyshev, Sushchik, Gubanenko, Demirchieva, & Kalachova, 2007).

In some countries, it is common to consume raw fish meat, in which PUFAs retain their quality and nutritional value. However, this is not the case in middle Europe, where fish meat is consumed cooked. Long-chain PUFAs, such as EPA and DHA, are susceptible to oxidation during heating and other culinary treatments. Therefore, several studies have focused on the effects of different cooking procedures on the flesh FA composition of total lipids in various fish species from different parts of the world (Garcia-Arias, Pontes, Linares, Garcia-Fernandez, & Sanchez-Muniz, 2003; Gladyshev, Sushchik, Gubanenko, Demirchieva, & Kalachova, 2006; Nikoo, Rahimabadi, & Salehifar, 2010; Sharma, Kumar, Sinha, Ranjan, Kithsiri, & Venkateshwarlu, 2010). It was found that the EPA and DHA levels in the food vary with the fish species and cooking treatment (Candela, Astiasaran, & Bello, 1998).

Our study focusses on four fish species selected as representatives of different ecological demands. Pike and cod are predators standing on a high level of the food chain; thus, higher levels of PUFAs in their meat can be expected. On the other hand, cod and herring are marine animals that feed on primary sources of PUFAs. Carp was selected as a representative of omnivorous freshwater fish. We tested whether cod, as a marine predator, would have the highest levels of PUFAs in its meat, as well as the influence of several cooking procedures on the FA composition in fish tissues.

2. Materials and Methods

2.1. Chemicals

All chemicals and solvents were of analytical grade. Methanol Suprasolv, 2-propanol LC-MS Chromasolv, and hexane Suprasolv were purchased from Merck; isooctane, chloroform, and ammonium acetate from Fluka; and a mixture of 37 fatty acid methyl ester (FAME) standards from Supleco. Triacylglycerol and diacylglycerol standards and acetyl chloride were purchased from Sigma-Aldrich and phospholipid standards from Avanti® Polar Lipids, Inc.

2.2. Fish samples

We sampled the four fish species most frequently purchased in the Czech Republic. Pike (*Esox lucius*) and carp (*Cyprinus carpio*) (freshwater species) originated from the Czech Republic; cod (*Gadus morhua*) and herring (*Clupea harengus*) (marine species) originated from the North Atlantic region. All fish samples were bought at the local market either freshly killed or kept on ice. Samples were taken randomly from the fish fillets. Nine raw samples and nine samples after each cooking procedure (see below), of approx. 3 g of wet tissue, were collected (i.e., 36 samples for each fish species).

2.3. Heat treatment and sample preparation

Three common cooking procedures were investigated: (i) frying in extra virgin olive oil in a non-stick (Teflon) pan for 5 min, (ii) baking at 200 °C for 10-15 min in an electric oven without addition of fat, and (iii) grilling on a EGC8000 contact electric grill (Electrolux, Switzerland) for 2-5 min without addition of fat. Processing times were fish species-dependent.

Each sample was homogenized in chloroform:methanol (2:1), using a Diax 100 electric homogenizer (Heidolph, Germany). The liquid was evaporated by Speedvac (Labconco, USA) and the sample was weighed. Lipids were extracted using the method described by Folch, Lees, & Stanley (1957). Each sample was divided into three equal aliquots, which were subjected directly to HPLC/MS analysis, solid phase extraction (SPE), and acid transesterification according to Stranský and Jursík (1996). The resulting FAMEs were analyzed and identified by gas chromatography. SPE was performed to separate the total lipid extract into two fractions: non-polar and polar lipids. The olive oil used in the cooking treatments was analyzed in the same way as fish samples.

2.4. Analytical techniques

FAMEs were analyzed by gas chromatography and mass spectrometry (GC/MS) using a Focus GC gas chromatograph (Thermo Scientific) coupled with a MD 800 quadrupole mass spectrometer (Fisons Instruments, Beverly, USA). The instrument was equipped with a SLB IL 111 capillary column (100 m x 0.25 mm, film thickness 0.2 μm; Supelco, Inc., Bellefonte, PA, USA). The temperature gradient started at 140 °C (held for 5 min). Then, the temperature was increased to 180 °C at a rate of 8 °C/min. This was followed by a second temperature ramp to 250 °C at a rate of 5 °C min. The analysis duration was 20 min. Identification of a particular FAME and determination of the double bond positions was based on mass spectra as well as the retention time and comparison with standards. A mixture of 37 standards (Supleco Inc.) was used for FAME identification.

High performance liquid chromatography (HPLC), combined with electrospray ionization mass spectrometry (ESI-MS), was used for analyses of intact lipids. A linear ion trap LCQ Fleet mass spectrometer (Thermo Scientific, San Jose, CA, USA), coupled to a Rheos Allegro ternary system (Flux instruments, Basel, Switzerland) and to an Accela autosampler (Thermo Scientific), was used. Samples (100 μl aliquots) were dried under nitrogen flow and dissolved in methanol (1 ml). The samples (5 μl) were injected into a Gemini column (150 mm x 2 mm x 3 μm; Phenomenex, Torrance, CA, USA). The mobile phase consisted of (A) 5 mM ammonium acetate in methanol, (B) water, and (C) 2-propanol. The analysis took 80 min, with a flow rate of 200 μl/min. The linear gradient was set as follows: 0-5 min, 92% A and 8% B; 5-12 min, 100% A; 12-50 min, 100-40% A and 0-60% C; 50-65 min, 40% A and 60% C; and 65-80 min back to 92% A and 8% B. The column temperature was maintained at 30 °C. The mass spectrometer was operated in a positive ion detection mode at +4 kV with a capillary temperature of 220 °C. A mass range of 440-1100 Da was scanned every 0.5 s to obtain the full scan and MS^2 ESI mass spectra of separated lipids. The collision-induced decomposition multi-stage ion trap tandem mass spectra MS^2 were recorded with a 3 Da isolation window and normalized collision energy of 35%. The structure of each entity was identified by full scan and MS^2 experiments. Peak areas of detected lipids were used for estimation of their relative proportions.

2.5. Calculation of FA proportions in lipids

Each lipid contains two (phospholipids, PL) or three (triacylglycerols, TG) FA moieties per molecule. For molecules with the same FAs, we used the total peak area for calculation. For molecules with different FAs, the area was divided into two (PL) or three (TG) parts, each dedicated to the particular FA. The total content of a given FA was acquired by summation of the corresponding peak areas in each lipid molecule.

2.6. Data processing and analysis

The acquired data were processed with Xcalibur 2.1 (Thermo Fisher Scientific, Inc.). Identification was performed with the QualBrowser module and quantifications – peak areas – were performed with the QuanBrowser module. Further data analyses were performed in MS Excel (Microsoft) and multivariate statistical analysis software.

2.7. Statistical analysis

The data obtained from chemical analysis (N = 9) of each fish species were statistically evaluated. The peak areas of detected compounds were used as variables in statistical analyses. Differences in the compositions of the samples from various fish species were analyzed by principal component analysis (PCA). Prior to PCA analysis, the peak areas were subjected to logarithmic transformation, scaling was focused on inter-species correlation, the species scores were divided by standard deviation, and the data were centerd by species. The statistical significance was assessed using redundancy analysis (RDA), a canonical variant of PCA, and the Monte Carlo permutation test (unrestricted permutations, n = 999). In the RDA analysis, raw samples and each heat treatment stood as categorical predictors. The multivariate data analysis software CANOCO 4.5 (Biometris, Plant Research International, Wageningen UR, Netherlands) was used for both the PCA and the RDA analyses.

3. Results and Discussion

3.1. General

The four examined fish species differ in ecological features. Cod and herring vs. pike and carp represented marine vs. freshwater fish; cod and pike vs. herring and carp are representatives of carnivore vs. omnivore fish. As a consequence of their different lifestyle, we expected differences in their raw meat with regard to the lipid content and studied the lipid stability/changes after three heating procedures. Obtained samples were subjected to LC/MS analysis for semi-quantification and identification of intact lipids, while GC/FID analysis allowed determination of double bond positions in the FA carbon chain. The peak areas of particular lipids were subjected to multivariate statistical analysis.

3.2. Composition of fatty acids in fish muscle (raw tissue)

Although the present study deals with only one specimen from a particular species (Fig. 1), the acquired data agree with previous studies with broader sampling (Guler, Aktumsek, Cakmak, Zengin, & Citil, 2011; Guler, Kiztanir, Aktumsek, Citil, & Ozparlak, 2008; Jankowska, Zakes, Zmijewski, & Szczepkowski, 2008; Memon, Talpur, Bhanger, & Balouch, 2011; Molnar, Kucska, Szabo, Biro, Bercsenyi, & Hancz, 2012; Serini, Piccioni, Rinaldi, Mostra, Damiani, & Calviello, 2010; Zajic, Mraz, Sampels, & Pickova, 2013). The contents of particular FAs are influenced by environmental factors, such as season, locality, life phase, and sex (Bulut, 2010; Guler, Kiztanir, Aktumsek, Citil, & Ozparlak, 2008; Huynh, Kitts, Hu, & Trites, 2007; Memon, Talpur, Bhanger, & Balouch, 2011; Szlinder-Richert, Usydus, Wyszynski, & Adamczyk, 2010). The average n-3/n-6 PUFA ratio varied widely among the species studied and was highest in herring (34.5) and lowest in pike (3.6). This ratio was higher in the Czech carp specimen (5.3) than those reported in the literature for several carp species (1.7-1.9) (Memon, Talpur, Bhanger, & Balouch, 2011; Nikoo, Rahimabadi, & Salehifar, 2010). The pike n-3/n-6 ratio was in agreement with analyses performed earlier in Turkey (Bulut, 2010), which found that the ratio was season-dependent, varying between 0.97 and 3.65 during the year. Cod meat contained the highest amounts of n-3 FAs, with DHA dominating among the chain lengths. DHA was the main FA in cod, herring, and pike muscles, while EPA dominated in carp meat (Fig. 1). Meat of the freshwater species carp and pike contained significantly more n-6 FAs than did the marine fish cod and herring. The marine species studied did not contain 18:3 n-6 (γ-linolenic acid). Thus, our analytical results support the nutritive value of marine fish described by nutritionists.

The HPLC/ESI-MS chromatograms (total ion current, TIC) of experimental fish show differences in the contents of polar (muscle) and non-polar (fat) lipids among fish species (Fig. 2). The carp and herring chromatograms (Fig. 2A, C) show a high content of TGs. The reason likely lies in the food and lifestyle of these two species, which are both omnivores with a preference for small marine or freshwater crustaceans. The chromatograms in Fig. 2 B and D show the pike and

cod lipids, respectively. Cod and pike tissue contain very few TGs. Both of these species are strictly carnivorous. The type of nutrition, rather than the marine or freshwater factor, seems responsible for the TG content. Marine or freshwater factor also seem to be important for the contents and ration of n-3 and n-6 PUFAs. The reason probably lies in marine algae, which are considered to be major producer of n-3 PUFAs and serve as nutrition for marine fish (Kim, Khan, McMurray, Prior, Wang, & Chapkin, 2010). The influence of nourishment on lipid content in fish meat has been reported in several fish species (Hvattum, Rosjo, Gjoen, Rosenlund, & Ruyter, 2000; Jankowska, Zakes, Zmijewski, & Szczepkowski, 2008; Memon, Talpur, Bhanger, & Balouch, 2011). Several previous studies on fish meat dealt only with FA composition and did not consider intact molecules (Memon, Talpur, Bhanger, & Balouch, 2011; Serini, Piccioni, Rinaldi, Mostra, Damiani, & Calviello, 2010; Sharma, Kumar, Sinha, Ranjan, Kithsiri, & Venkateshwarlu, 2010). Intact lipids have been investigated only in studies focussing on thermal or seasonal changes in the membrane PL composition. Additionally, these studies focussed on liver tissue (Brooks, Clark, Wright, Trueman, Postle, Cossins, et al., 2002) and dealt with physiological issues rather than nutritive ones. The HPLC/ESI-MS techniques provide us with novel insight into the FA distribution in the lipid molecular species (Fig. 3). Our analysis revealed that the essential and nutritionally valuable FAs mostly occur in PLs.

A full table of identified intact lipid molecules, based on MS fragmentation (Hsu & Turk, 2009), is provided in the Supplementary Material (Table S1). These data were used for multivariate statistical analyses.

The olive oil used in the pan-frying consist mostly of triolein. In terms of the FA composition, it is formed by oleic acid (18:1, 85.1%), palmitic acid (16:0, 10.6%), and stearic acid (18:00, 4.3%). No PUFAs were detected in the oil.

3.3. PUFA occurrence in intact lipids and particular fish species

Visualization of complex data about intact lipid molecules is not straightforward, and therefore, only FA ratios in particular lipid classes are shown in Fig. 3. These data were obtained by recalculation (Zahradníčková et al., 2014). The data were also supported by GC analysis after transesterification of particular SPE fractions (data not shown). GC data revealed the double bond positions in FA carbon chains. The n-3 double bond was detected in 22:6, 22:5, and 20:5 FAs and partly in 18:3. The n-6 double bond was detected in 20:4 and partly in 18:3. Fig. 3 shows that one of major FA in all fish species is palmitic acid (16:0), but oleic (18:1) and docosahexaenoic (22:6) acid dominate in carp and herring, respectively. A comparison of marine and freshwater fish indicates that marine fish possess more PUFAs than do freshwater fish. Furthermore, PLs bear more PUFAs than non-polar lipids (TGs) (Fig. 3). Recent studies in the field of mammalian physiology show that PUFAs bound in PLs are more beneficial for health (e.g., prevention of metabolic syndrome) than are PUFAs incorporated in TGs (Rossmeisl et al., 2012).

3.4. Statistical analysis of the influence of heat treatment on fish tissue lipid composition

The heat treatments had different impacts on the tissues of different fish. Oven treatment had the lowest effect on intact lipid molecules in fish tissue, as evaluated with PCA (Fig. 4). PCA is an excellent tool for visualizing a complex data matrix, such as the relative content of intact lipid molecules. In PCA analyses, samples with similar chemical profiles cluster together and segregate from those that are different, while redundancy analysis (RDA) determines the sample segregation significance. RDA of cooking treatments of particular fish species revealed significant differences in the composition of intact lipid molecules ($p < 0.001$). The effect of heat treatments has been reported in previous studies (Gladyshev et al., 2006; Neff, Bhavsar, Braekevelt, Arts, 2014; Sioen, Haak, Raes, Hermans, De Henauw, De Smet, et al., 2006). Gladyshev et al. (Gladyshev, Sushchik, Gubanenko, Demirchieva, & Kalachova, 2006) showed that boiling and frying do not significantly decrease the content of EPA and DHA compared to raw fish. In our treatments, however, the cod samples showed the most prominent segregation of the data after different treatments (Fig. 4D), indicating that the cooking procedures influenced the lipid composition significantly. The opposite was true for the carp samples, which formed more-or-less one group without any clear separation between the different treatments (Fig. 4A). Thus, we can conclude that carp possess thermally stable lipids, while cod lipids are heat-sensitive (Sioen, et al., 2006).

Of the thermo-processes tested, oven-baking turned out to be the best heat treatment for preservation of all lipid features of the meat, including the PUFA content and n-3/n-6 ratio (Fig. 5). Garcia-Arias et al. (Garcia-Arias, Pontes, Linares, Garcia-Fernandez, & Sanchez-Muniz, 2003) reached a similar conclusion in a study dealing with *Sardina pilchardus*. Pan-frying seems to be the most harmful procedure for freshwater fish, causing the most significant decrease in PUFA content (Fig. 5 A and B). However, we observed a drastic decrease in the n-3/n-6 ratio in marine fish after

grilling (Fig. 5 C and D). Similarly, lipids of carnivorous fish (pike and cod) were more susceptible to heat treatment than were those of omnivorous ones, as expressed by decreasing n-3/n-6 PUFA ratio and content (Fig. 5). Several mechanisms can be suggested to explain these changes, including: (i) water loss in the food, (ii) leaching of fat soluble molecules from the food, and (iii) oxidation reactions (Sioen, et al., 2006). These effects are dependent on the type of cooking (Garcia-Arias, Pontes, Linares, Garcia-Fernandez, & Sanchez-Muniz, 2003), as well as on the fish species (Gladyshev, Sushchik, Gubanenko, Demirchieva, & Kalachova, 2006; Sioen, et al., 2006). Herring seems to be very resistant to heat, as the lipid abundance and composition are almost identical in the baked and raw meat (Fig. 4C). A similar phenomenon was observed in the carp samples (Fig. 4A). Baked carp had an even higher relative amount of n-3 PUFAs than had the raw fish. Clearly, no PUFAs are generated during heat treatment. The change in the PUFA relative percentage can be explained by a loss of saturated FAs present in TGs *via* leaching of fat from the meat. Since the PUFAs are predominantly bound in the muscle tissue, they stay in the muscle and do not leach out as observed by (Garcia-Arias, Pontes, Linares, Garcia-Fernandez, & Sanchez-Muniz, 2003).

A primary target of this study was investigation of changes in the intact lipid content during exposure of raw fish meat to three cooking processes. Only a few specimens (1-3) of each species were used for experiment. For a more accurate statistical evaluation that would cover the species variability, more specimens from each species will be used in future research.

4. Conclusion

Raw fish meat was compared for n-3 and n-6 PUFA composition and ratio. The intact lipid study shows that (1) PUFAs are dominantly distributed in PL classes and (2) the amount of non-polar lipids is higher in omnivorous species than in carnivores. The GC study of particular FAs revealed that marine fish possess a nearly 10-fold higher n-3/n-6 PUFA ratio than do freshwater species.

Our results show that the effects of heat treatment are species-specific with regard to the composition and abundance of PUFAs. The largest changes due to cooking treatment were recorded in cod samples, in particular a decrease in the amount and ratio of n-3 and n-6 PUFAs. On the other hand, the smallest changes were observed in the sample of oven-baked herring, in which the ratio of particular PUFAs did not change. The baking process seems to be least harmful for herring, carp, and pike.

The quality of fish meat can also be influenced by the season, locality, and sex and diet of the fish. Therefore, it is difficult to draw a general conclusion about the best cooking treatment. Studies of particular fish species in particular localities are needed to establish optimal heat treatment for preservation of PUFAs and their ratio.

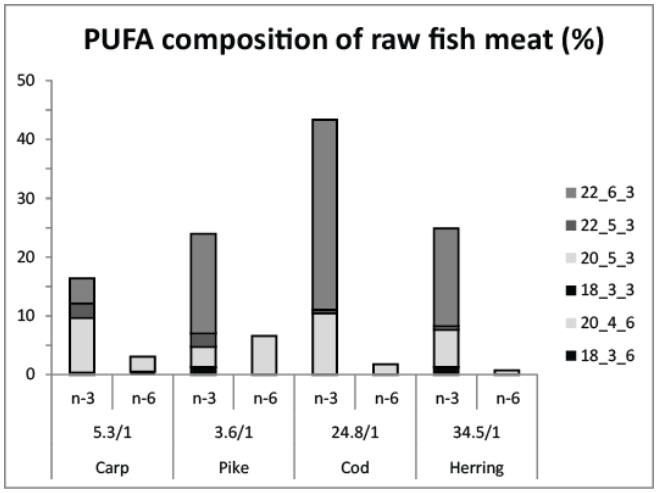

Fig. 1. Content of n-3 and n-6 PUFAs in fish muscles. Comparison of FAs of different chain lengths in four fish species. The n-3/n-6 ratio is given below the corresponding columns. 22_6_3: docosa-4,7,10,13,16,19-hexaenoic acid (DHA), 22_5_3: docosa-7,10,13,16,19-pentaenoic acid (DPA), 20_5_3: eicosa-5,8,11,14,17-pentaenoic acid (EPA), 18_3_3: octadeca-9,12,15-trienoic acid (α-linolenic acid, ALA), 20_4_6: eicosa-5,8,11,14-tetraenoic acid (arachidonic acid, AA), and 18_3_6: octadeca-6,9,12-trienoic acid (γ-linolenic acid, GLA).

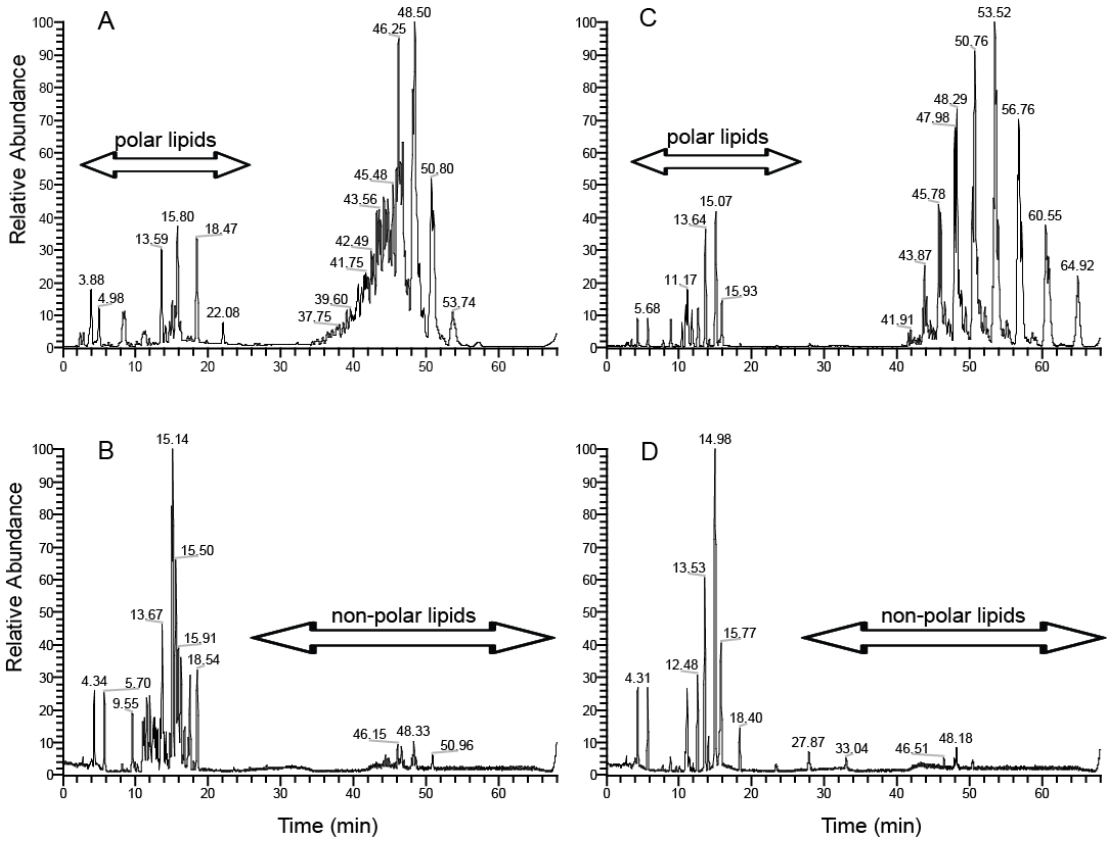

Fig. 2. HPLC/ESI TIC chromatograms of total raw meat extracts obtained from A) Carp, B) Pike, C) Herring, and D) Cod. Arrows indicate the elution time of polar lipids (phospholipids, present in the muscle tissue) and non-polar lipids (triacylglycerols, commonly called “fat”).

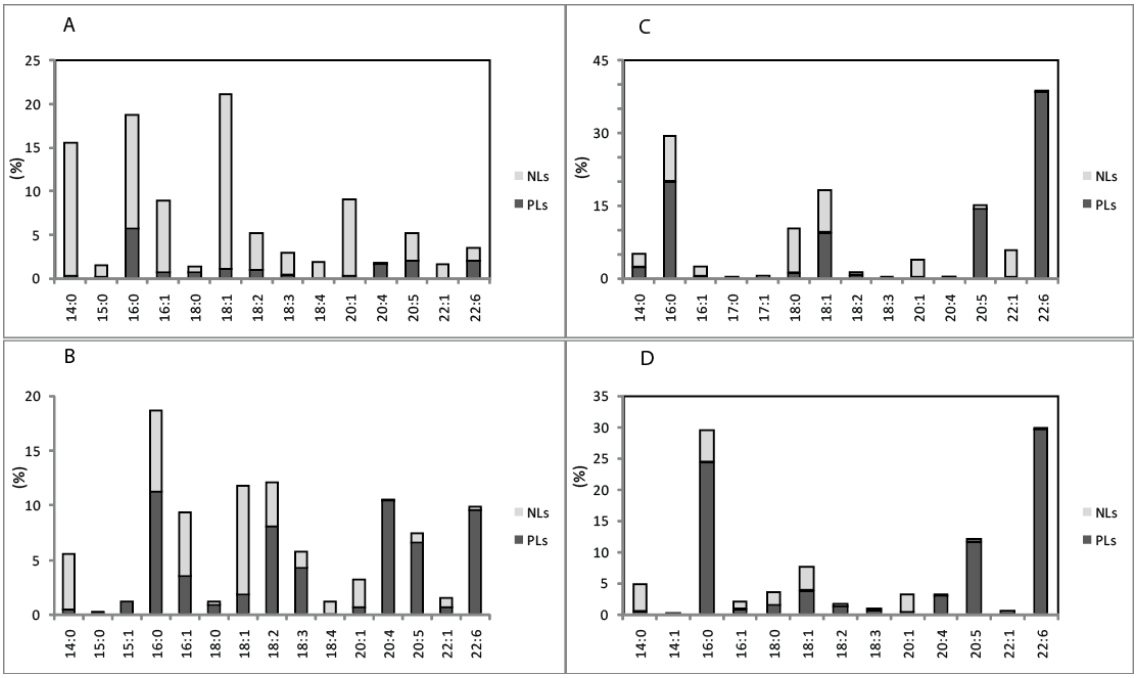

Fig. 3. Ratio of particular FAs in raw fish meat and their presence in intact lipid molecules (NLs, non-polar lipids; PLs, phospholipids). Data were obtained by recalculation of HPLC MS data (see Material and Methods); therefore, no information about double bond positions can be given.

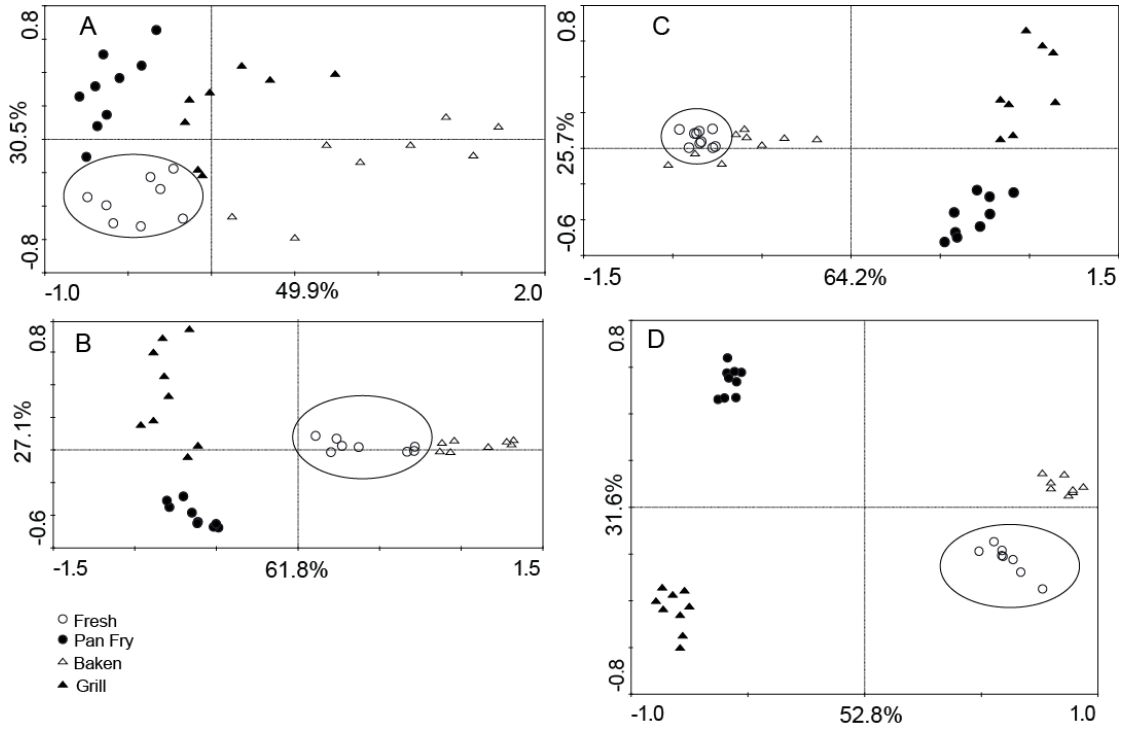

Fig. 4. Visualization of HPLC/ES/MS data produced by multivariate statistical analysis. A) Carp, B) Pike, C) Herring, and D) Cod. The % of the x and y axis represent the percentage of explained variation in the data sets.

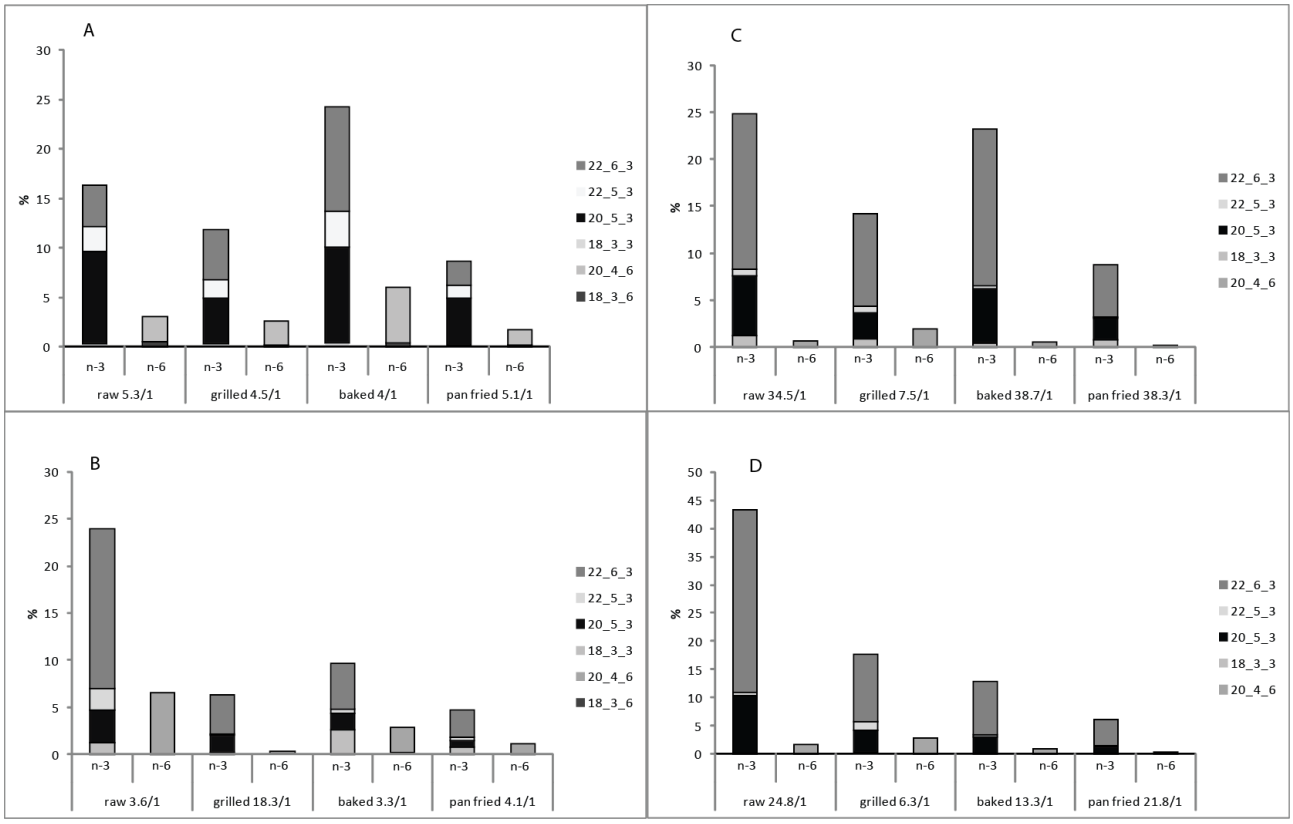

Fig. 5. Ratio of n-3 and n-6 FAs obtained by GC/MS in four fish species: A) Carp, B) Pike, C) Herring, and D) Cod before (raw meat) and after heat treatments (grilled, baked, pan fried fish meat). The n-3/n-6 ratio is given below the corresponding columns.

Acknowledgements

Financial support from the Institute of Organic Chemistry and Biochemistry (research project RVO: 61388963) is gratefully acknowledged. The authors thank Hillary Hoffman for proofreading of the manuscript.

References

Adkins, Y., & Kelley, D. S. (2010). Mechanisms underlying the cardioprotective effects of omega-3 polyunsaturated fatty acids. *Journal of Nutritional Biochemistry, 21*(9), 781-792.

Bhouri, A. M., Harzallah, H. J., Dhibi, M., Bouhlel, I., El Cafsi, M., Hammami, M., & Chaouch, A. (2010). Effects of different cooking treatments on flesh fatty acid composition of total lipids in farmed Sea bass Dicentrarchus labrax (Moronidae). *Cybium, 34*(1), 29-36.

Brooks, S., Clark, G. T., Wright, S. M., Trueman, R. J., Postle, A. D., Cossins, A. R., & Maclean, N. M. (2002). Electrospray ionisation mass spectrometric analysis of lipid restructuring in the carp (Cyprinus carpio L.) during cold acclimation. *Journal of Experimental Biology, 205*(24), 3989-3997.

Brouwer, I. A., Geelen, A., & Katan, M. B. (2006). n-3 fatty acids, cardiac arrhythmia and fatal coronary heart disease. *Progress in Lipid Research, 45*(4), 357-367.

Bulut, S. (2010). Fatty acid composition and omega 6/omega 3 ratio of the pike (Esox lucius) muscle living in Eber Lake, Turkey. *Scientific Research and Essays, 5*(23), 3776-3780.

Candela, M., Astiasaran, I., & Bello, J. (1998). Deep-fat frying modifies high-fat fish lipid fraction. *Journal of Agricultural and Food Chemistry, 46*(7), 2793-2796.

Folch, J., Lees, M., & Stanley, G. H. S. (1957). A simple method for the isolation and purification of total lipides from animal tissues. *Journal of Biological Chemistry, 226*(1), 497-509.

Garcia-Arias, M. T., Pontes, E. A., Linares, M. C. G., Garcia-Fernandez, M. C., & Sanchez-Muniz, F. J. (2003). Cooking-freezing-reheating (CFR) of sardine (Sardina pilchardus) fillets. Effect of different cooking and reheating procedures on the proximate and fatty acid compositions. *Food Chemistry, 83*(3), 349-356.

Gladyshev, M. I., Sushchik, N. N., Gubanenko, G. A., Demirchieva, S. M., & Kalachova, G. S. (2006). Effect of way of cooking on content of essential polyunsaturated fatty acids in muscle tissue of humpback salmon (Oncorhynchus gorbuscha). *Food Chemistry, 96*(3), 446-451.

Gladyshev, M. I., Sushchik, N. N., Gubanenko, G. A., Demirchieva, S. M., & Kalachova, G. S. (2007). Effect of boiling and frying on the content of essential polyunsaturated fatty acids in muscle tissue of four fish species. *Food Chemistry, 101*(4), 1694-1700.

Guler, G. O., Aktumsek, A., Cakmak, Y. S., Zengin, G., & Citil, O. B. (2011). Effect of Season on Fatty Acid Composition and n-3/n-6 Ratios of Zander and Carp Muscle Lipids in Altinapa Dam Lake. *Journal of Food Science, 76*(4), C594-C597.

Guler, G. O., Kiztanir, B., Aktumsek, A., Citil, O. B., & Ozparlak, H. (2008). Determination of the seasonal changes on total fatty acid composition and omega 3/omega 6 ratios of carp (Cyprinus carpio L.) muscle lipids in Beysehir Lake (Turkey). *Food Chemistry, 108*(2), 689-694.

Heissenberger, M., Watzke, J., & Kainz, M. J. (2010). Effect of nutrition on fatty acid profiles of riverine, lacustrine, and aquaculture-raised salmonids of pre-alpine habitats. *Hydrobiologia, 650*(1), 243-254.

Hsu, F.-F., & Turk, J. (2009). Electrospray ionization with low-energy collisionally activated dissociation tandem mass spectrometry of glycerophospholipids: Mechanisms of fragmentation and structural characterization. *Journal of Chromatography B-Analytical Technologies in the Biomedical and Life Sciences, 877*(26), 2673-2695.

Huynh, M. D., Kitts, D. D., Hu, C., & Trites, A. W. (2007). Comparison of fatty acid profiles of spawning and non-spawning Pacific herring, Clupea harengus pallasi. *Comparative Biochemistry and Physiology B-Biochemistry & Molecular Biology, 146*(4), 504-511.

Hvattum, E., Rosjo, C., Gjoen, T., Rosenlund, G., & Ruyter, B. (2000). Effect of soybean oil and fish oil on individual molecular species of Atlantic salmon head kidney phospholipids determined by normal-phase liquid chromatography coupled to negative ion electrospray tandem mass spectrometry. *Journal of Chromatography B, 748*(1), 137-149.

Jankowska, B., Zakes, Z., Zmijewski, T., & Szczepkowski, M. (2008). Fatty acid composition of wild and cultured northern pike (Esox lucius). *Journal of Applied Ichthyology, 24*(2), 196-201.

Kim, W., Khan, N. A., McMurray, D. N., Prior, I. A., Wang, N., & Chapkin, R. S. (2010). Regulatory activity of polyunsaturated fatty acids in T-cell signaling. *Progress in Lipid Research, 49*(3), 250-261.

Kris-Etherton, P. M., Harris, W. S., Appel, L. J., & Nutrition, C. (2002). Fish consumption, fish oil, omega-3 fatty acids, and cardiovascular disease. *Circulation, 106*(21), 2747-2757.

Lopez-Huertas, E. (2010). Health effects of oleic acid and long chain omega-3 fatty acids (EPA and DHA) enriched milks. A review of intervention studies. *Pharmacological Research, 61*(3), 200-207.

Mann, N. J., O'Connell, S. L., Baldwin, K. M., Singh, I., & Meyer, B. J. (2010). Effects of Seal Oil and Tuna-Fish Oil on Platelet Parameters and Plasma Lipid Levels in Healthy Subjects. *Lipids, 45*(8), 669-681.

Memon, N. N., Talpur, F. N., Bhanger, M. I., & Balouch, A. (2011). Changes in fatty acid composition in muscle of three farmed carp fish species (Labeo rohita, Cirrhinus mrigala, Catla catla) raised under the same conditions. *Food Chemistry, 126*(2), 405-410.

Molnar, T., Kucska, B., Szabo, A., Biro, J., Bercsenyi, M., & Hancz, C. (2012). Effect of graded dietary fish oil supplementation on body composition and fillet fatty acid composition of pike (*Esox lucius* L.). *Acta Alimentaria, 41*(1), 86-93.

Nikoo, M., Rahimabadi, E. Z., & Salehifar, E. (2010). Effects of Frying-Chilling-Reheating on the Lipid Content and Fatty Acid Composition of Cultured Sturgeon (Huso huso, Beluga) Fillets. *Journal of Aquatic Food Product Technology, 19*(2), 120-129.

Poudyal, H., Panchal, S. K., Diwan, V., & Brown, L. (2011). Omega-3 fatty acids and metabolic syndrome: Effects and emerging mechanisms of action. *Progress in Lipid Research, 50*(4), 372-387.

Puglisi, M. J., Hasty, A. H., & Saraswathi, V. (2011). The role of adipose tissue in mediating the beneficial effects of dietary fish oil. *Journal of Nutritional Biochemistry, 22*(2), 101-108.

Rose, D. P., & Connolly, J. M. (1999). Omega-3 fatty acids as cancer chemopreventive agents. *Pharmacology & Therapeutics, 83*(3), 217-244.

Rossmeisl, M., Jilkova, Z. M., Kuda, O., Jelenik, T., Medrikova, D., Stankova, B., Kristinsson, B., Haraldsson, G. G., Svensen, H., Stoknes, I., Sjovall, P., Magnusson, Y., Balvers, M. G. J., Verhoeckx, K. C. M., Tvrzicka, E., Bryhn, M., & Kopecky, J. (2012). Metabolic Effects of n-3 PUFA as Phospholipids Are Superior to Triglycerides in Mice Fed a High-Fat Diet: Possible Role of Endocannabinoids. *Plos One, 7*(6).

Sarotra, P., Sharma, G., Kansal, S., Negi, A. K., Aggarwal, R., Sandhir, R., & Agnihotri, N. (2010). Chemopreventive Effect of Different Ratios of Fish Oil and Corn Oil in Experimental Colon Carcinogenesis. *Lipids, 45*(9), 785-798.

Serini, S., Piccioni, E., Rinaldi, C., Mostra, D., Damiani, G., & Calviello, G. (2010). Fish from an artificial lake: n-3 PUFA content and chemical-physical and ecological features of the lake. *Journal of Food Composition and Analysis, 23*(2), 133-141.

Sharma, P., Kumar, V., Sinha, A. K., Ranjan, J., Kithsiri, H. M. P., & Venkateshwarlu, G. (2010). Comparative fatty acid profiles of wild and farmed tropical freshwater fish rohu (Labeo rohita). *Fish Physiology and Biochemistry, 36*(3), 411-417.

Simopoulos, A. P. (1991). OMEGA-3-FATTY-ACIDS IN HEALTH AND DISEASE AND IN GROWTH AND DEVELOPMENT. *American Journal of Clinical Nutrition, 54*(3), 438-463.

Simopoulos, A. P. (2002). The importance of the ratio of omega-6/omega-3 essential fatty acids. *Biomedicine & Pharmacotherapy, 56*(8), 365-379.

Sioen, I., Haak, L., Raes, K., Hermans, C., De Henauw, S., De Smet, S., & Van Camp, J. (2006). Effects of pan-frying in margarine and olive oil on the fatty acid composition of cod and salmon. *Food Chemistry, 98*(4), 609-617.

Stransky, K., & Jursik, T. (1996). Simple quantitative transesterification of lipids .1. Introduction. *Fett-Lipid, 98*(2), 65-71.

Szlinder-Richert, J., Usydus, Z., Wyszynski, M., & Adamczyk, M. (2010). Variation in fat content and fatty-acid composition of the Baltic herring Clupea harengus membras. *Journal of Fish Biology, 77*(3), 585-599.

Weintraub, H. (2013). Update on marine omega-3 fatty acids: Management of dyslipidemia and current omega-3 treatment options. *Atherosclerosis, 230*(2), 381-389.

Zahradníčková, H., Tomčala, A., Berková, P., Schneedorferová, I., Okrouhlík, J., Šimek, P., & Magdalena, H. (2014). Cost effective, robust and reliable coupled separation techniques for the identification and quantification of phospholipids in complex biological matrices: Application to insects. *Journal of Separation Science*, in press.

Zajic, T., Mraz, J., Sampels, S., & Pickova, J. (2013). Fillet quality changes as a result of purging of common carp (Cyprinus carpio L.) with special regard to weight loss and lipid profile. *Aquaculture, 400*, 111-119.

Zhu, H. Y., Fan, C. N., Xu, F., Tian, C. Y., Zhang, F., & Qi, K. M. (2010). Dietary fish oil n-3 polyunsaturated fatty acids and alpha-linolenic acid differently affect brain accretion of docosahexaenoic acid and expression of desaturases and sterol regulatory element-binding protein 1 in mice. *Journal of Nutritional Biochemistry, 21*(10), 954-960.

Paper III

Extracellular adenosine mediates a systemic metabolic switch during immune response

Bajgar, A., Kučerová, K., Jonatová, L., Tomčala, A., Schneedorferová, I., Okrouhlík, J., Doležal, T.

PLoS biology, 13

2015

PLOS | BIOLOGY

RESEARCH ARTICLE

Extracellular Adenosine Mediates a Systemic Metabolic Switch during Immune Response

Adam Bajgar[1], Katerina Kucerova[1], Lucie Jonatova[1], Ales Tomcala[2], Ivana Schneedorferova[1,2], Jan Okrouhlik[1], Tomas Dolezal[1]*

1 Faculty of Science, University of South Bohemia in Ceske Budejovice, Ceske Budejovice, Czech Republic, **2** Institute of Parasitology, Biology Centre, Academy of Sciences of the Czech Republic, Ceske Budejovice, Czech Republic

* tomas.dolezal@prf.jcu.cz

OPEN ACCESS

Citation: Bajgar A, Kucerova K, Jonatova L, Tomcala A, Schneedorferova I, Okrouhlik J, et al. (2015) Extracellular Adenosine Mediates a Systemic Metabolic Switch during Immune Response. PLoS Biol 13(4): e1002135. doi:10.1371/journal.pbio.1002135

Academic Editor: Marc S. Dionne, King's College London, UNITED KINGDOM

Received: December 12, 2014

Accepted: March 18, 2015

Published: April 27, 2015

Data Availability Statement: All relevant data are within the paper and its Supporting Information files.

Funding: This work was supported by the Grant Agency of the Czech Republic (Project P305-12-0115; www.gacr.cz) and Marie Curie International Outgoing Fellowship within the EU Seventh Framework Programme for Research and Technological Development 2007-2013 (Project 298186; http://ec.europa.eu/research/mariecurieactions/). The funders had no role in study design, data collection and analysis, decision to publish, or preparation of the manuscript.

Abstract

Immune defense is energetically costly, and thus an effective response requires metabolic adaptation of the organism to reallocate energy from storage, growth, and development towards the immune system. We employ the natural infection of Drosophila with a parasitoid wasp to study energy regulation during immune response. To combat the invasion, the host must produce specialized immune cells (lamellocytes) that destroy the parasitoid egg. We show that a significant portion of nutrients are allocated to differentiating lamellocytes when they would otherwise be used for development. This systemic metabolic switch is mediated by extracellular adenosine released from immune cells. The switch is crucial for an effective immune response. Preventing adenosine transport from immune cells or blocking adenosine receptor precludes the metabolic switch and the deceleration of development, dramatically reducing host resistance. Adenosine thus serves as a signal that the "selfish" immune cells send during infection to secure more energy at the expense of other tissues.

Author Summary

The immune response is energetically costly and often requires adaption of the whole organism to ensure it receives enough energy. It is not well understood how distribution of energy resources within the organism is regulated during an immune response. To understand this better, we used parasitoid wasp infection of fruit fly larvae—the host larvae have 48 h before they pupate to destroy the infecting "alien" or face destruction by the parasitoid that will consume the developing pupa. Here we find a signal, generated by the host immune cells, which mediates a systemic energy switch. This signal—adenosine—suppresses processes driving larval to pupal development of the host, thereby freeing up energy for the immune system. We show that the resulting developmental delay in the fruit fly larvae is crucial for an efficient immune response; without the adenosine signal, resistance to the parasitoid drops drastically. Generation of this signal by immune cells demonstrates that in response to external stressors, the immune system can mobilize reallocation to itself of energy and nutrients from the rest of the organism.

Competing Interests: The authors have declared that no competing interests exist.

Abbreviations: ADGF-A, adenosine deaminase-related growth factor A; AdoR, adenosine receptor; AMPK, AMP-activated protein kinase; e-Ado, extracellular adenosine; hpi, hours postinfection; SEM, standard error of measurement; TAG, triacylglycerol

Introduction

Immune response is energetically costly [1,2]. Immune cells, upon activation, favor glycolysis over oxidative phosphorylation for fast, albeit inefficient, energy generation and macromolecule synthesis [3,4]. This metabolic shift requires extra glucose as glycolysis produces much less ATP than does oxidative phosphorylation [5]. Therefore, at the organismal level, the energy shifts from storage and nonimmune processes towards the needs of the immune system [6–9].

Regulation of energy during the immune response is critical—full response requires a significant amount of energy, and inability to provide it with nutrients can lead to immune system suppression and reduced resistance [10–12]. In mammalian systems, the inflammatory cytokines TNF-α, IFN-γ, IL-1, and IL-6 are released upon recognition of the pathogen and, besides modulating immune functions, they also stimulate energy release [2,13–16]. Immune cells must respond rapidly to the activating signals, and thus they change their metabolism, which involves, at least in mammalian systems, the preferential use of aerobic glycolysis, known as the Warburg effect [3,4,17]. The increased demand for energy by the immune system requires, both in vertebrates and invertebrates, adaptation of the whole organism, which is associated with an overall metabolic suppression and a systemic insulin resistance in all tissues except the immune cells [2,12,18]. The importance of the systemic regulation of energy is demonstrated by examples of certain infections leading to depletion of energy reserves (wasting) and eventually death of the organism [15,19]. Despite the importance of the systemic regulation of energy, we have only fragmentary knowledge about the molecular mechanisms involved in the regulation of energy during immune response at the organismal level and about the communication between different parts of the organism mediating the shift of energy from storage and growth towards immunity [12,20,21].

Extracellular adenosine (e-Ado) is a signal originating from damaged or stressed tissues. Acting as an energy sensor, e-Ado is released from metabolically stressed cells with depleted ATP [22,23] or made from extracellular ATP leaking from damaged tissues [24]. e-Ado then works as a local or systemic hormone, adjusting metabolism by acting either via adenosine receptors or by the uptake into the cells and conversion to AMP activating AMP-activated protein kinase (AMPK) [24,25]. These actions lead to a suppression of energy consuming processes [22,26–29] and to a release of energy from stores [30].

Damaged tissues and metabolically stressed cells are very likely to occur during immune response and thus it is not surprising that elevated levels of e-Ado are also detected, for example, during sepsis in humans [31]. The capacity of e-Ado to regulate energy metabolism, to "measure" the level of tissue and organismal stress, and to adapt the energy use to the actual situation all make e-Ado a perfect candidate for an energy regulator during immune response. However, the mode of e-Ado action under immune challenge is unclear, as the role of e-Ado in energy regulation has mainly been studied in relation to anoxia in anoxia-tolerant organisms such as turtles and hypoxia and ischemia in rodent models and human patients [22,30], while e-Ado has thus far been associated with mammalian immune response only through its immunomodulatory and anti-inflammatory function [24,32].

We, and others, have previously shown that adenosine regulatory and signaling network in *Drosophila* is similar to mammalian systems [33–37]. In addition, we have shown that e-Ado regulates energy metabolism in *Drosophila*. Increase of e-Ado levels caused by a deficiency of adenosine deaminase-related growth factor A (ADGF-A) leads to hyperglycemia and reduced energy storage [38]. We have also found that the regulation of e-Ado by ADGF-A is particularly important during parasitoid wasp infection in *Drosophila* larvae; ADGF-A is strongly

expressed in immune cells that encapsulate the invading wasp egg [39]. These findings further support a potential role of e-Ado in energy regulation during immune response.

Here, we use the parasitoid wasp infection as a model to study the energy regulation during immune reaction. Parasitoid wasps inject their eggs into *Drosophila* larvae, and if the fly larva does not destroy the egg in time, the hatched wasp larva will consume the host [40]. The fly larva recognizes the egg and mounts a robust immune response that involves proliferation and differentiation of specialized immune cells, lamellocytes, which eventually encapsulate the parasitoid egg. Using this immune response as a model, we traced the dietary glucose destinations, measured selected metabolites and gene expressions, and analyzed host resistance and the impact of the immune response on its development.

We describe here the systemic changes in energy metabolism during the immune challenge and the role of e-Ado in the regulation of these changes. We have found that e-Ado, released from the immune cells, mediates a metabolic switch characterized by the suppression of nutrient storage and developmental growth in favor of the immune defense. This metabolic switch—a tradeoff between development and defense—is crucial for the resistance to infection. In *Drosophila* larvae lacking adenosine signaling, development is not suppressed, and the resistance dramatically drops.

Results

Immune Response to Parasitoid Wasp Egg

The endoparasitoid wasp *Leptopilina boulardi* injects its egg in early third-instar *Drosophila* larva. The egg, usually hiding in gut folds, is first recognized by the host-circulating hemocytes (Fig 1A) and the recognition triggers immune response [40]. This involves production of specialized cells called lamellocytes (Fig 1A and 1B) within the first 24 h postinfection (hpi; 0 hpi is the time of infection and corresponds to 72 h after egg laying; the time in hpi is also used for the uninfected control). Lamellocytes are then released into circulation, and the egg gets encapsulated with subsequent melanization by 48 hpi (Fig 1A). Production of lamellocytes involves a transient proliferation of prohemocytes in the lymph gland and their terminal differentiation into lamellocytes [41]. The efficiency of egg encapsulation depends on the ability to produce lamellocytes and thus varies among different genetic strains of *Drosophila* [42,43]. Our model was based on the Canton S strain of *Drosophila melanogaster* bearing the w^{1118} mutation (hereafter *w*), which served as a control genotype in all our experiments (the term "control" is reserved hereafter for uninfected situations, i.e., control *w* means uninfected *w* larvae). On average, 42% of these *w* host larvae succeeded to destroy the wasp egg and 38% survived to adulthood while 42% parasitoids developed to adult wasps (Fig 1C).

Immune Response to Parasitoid Egg Invasion Demands Energy

Parasitoid-infected third-instar larvae experienced a 15% developmental delay, pupating on average 7 h later than uninfected controls (Fig 1D). Such a delay might result from redistribution of energy from development towards immune defense. We therefore examined various energy aspects during infection.

Without infection, circulating glucose was kept below 0.04 μg per μg protein (Fig 2A). Both the glycogen and triacylglycerol (TAG) stores kept increasing, while circulating and tissue trehalose levels remained steady (Fig 2A). Trehalose is a nonreducing disaccharide source of glucose, which is liberated by the action of trehalase [44]. To trace the fate of glucose, we employed dietary radiolabeled D[U-^{14}C]-glucose. The glucose-derived ^{14}C became evenly distributed in the larvae among saccharides, proteins, and lipids (Fig 2B). About 84% of ^{14}C was found in developing tissues (Fig 2C). We divided the organism here in a simplified way into

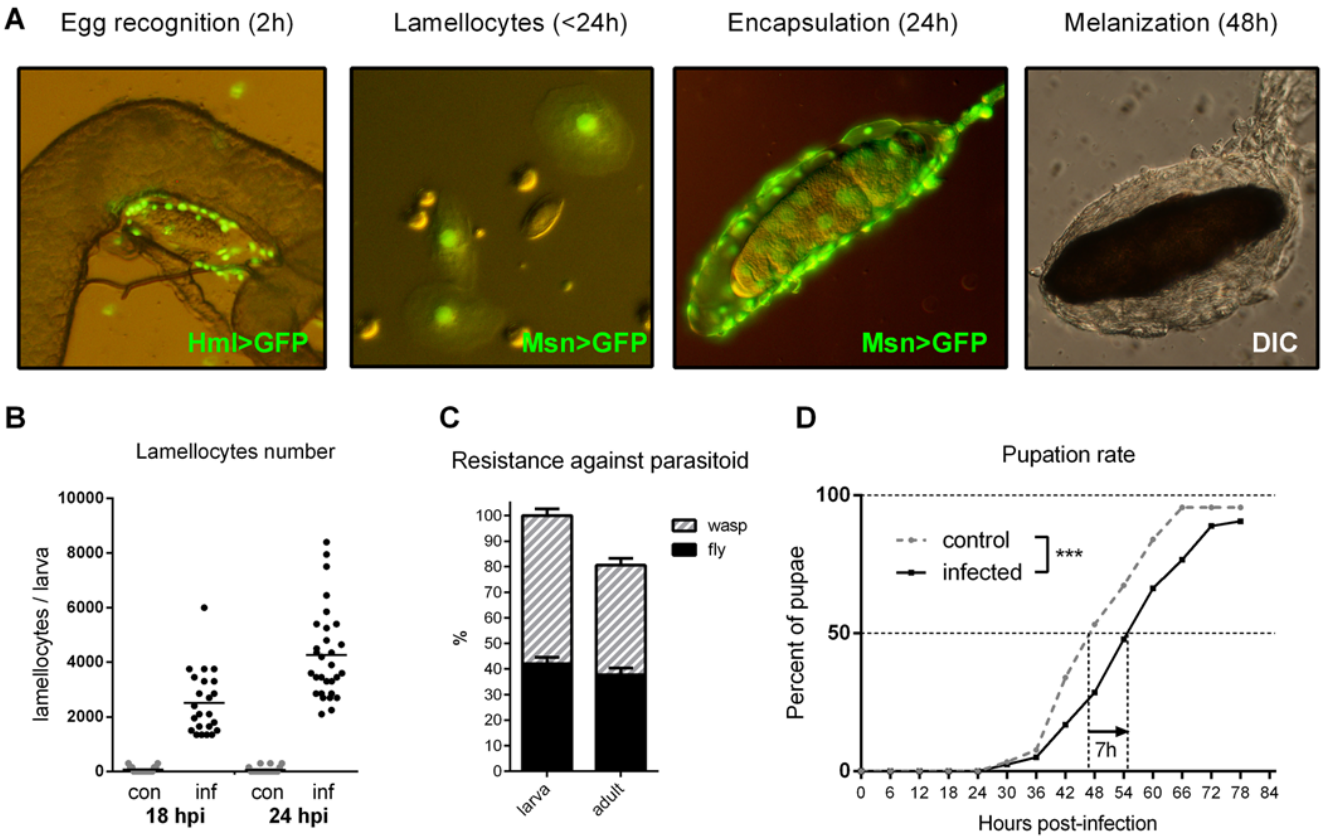

Fig 1. Immune response to parasitoid wasp intrusion. (A) Progressive stages of the response. The wasp egg is recognized by plasmatocytes (green, Hml>GFP) within 2 hpi. Lamellocytes, labeled by the Msn>GFP marker appear in circulation (<24 hpi) and start to encapsulate the egg. At 48 hpi, the egg is fully encapsulated by a multilayer of immune cells and melanized (original image of encapsulation published in [39]). (B) Number of lamellocytes per larva in control (con, grey) and infected (inf, black) larvae at 18 and 24 hpi. Each dot represents an individual larva; the horizontal lines indicate mean. (C) Percentage of host larvae with melanized wasp eggs (black, left column, mean 42%) and surviving host adults (black, right column, mean 38%) against winning wasp larvae and adults (hatched columns). Values are mean ± standard error of measurement (SEM). (D) Pupation of infected larvae ($n = 316$) was significantly delayed compared to control larvae ($n = 344$). Log-rank survival analysis ($p < 0.0001$).

doi:10.1371/journal.pbio.1002135.g001

the immune system (represented by cellular immunity, the most important defense against parasitoids, including circulating hemocytes and lymph gland), the circulation (hemolymph), and the rest of the tissues representing mainly development, growth, and energy storage.

In infected larvae, the accumulation of TAG and glycogen reserves ceased (Fig 2A). This was accompanied by down-regulation of glycogen synthase (CG6904; FlyBase ID: FBgn0266064) and up-regulation of glycogen phosphorylase expression (CG7254; FlyBase ID: FBgn0004507)(Fig 3A). The amount of tissue trehalose decreased (Fig 2A), and less dietary glucose was incorporated into lipids and proteins (Fig 2B and S2 Fig). These hallmarks of suppressed energy storage and growth were corroborated by reduced incorporation of ^{14}C into developing tissues from 84% in uninfected larvae to 77% at 6 hpi and 63% at 18 hpi (Fig 2C and S2 Fig).

The above effects were associated with hyperglycemia as indicated by elevated hemolymph glucose and ^{14}C at the expense of developing tissues (Fig 2A and 2C). Incorporation of ^{14}C into lipids and proteins (at the whole organism level) was also suppressed during infection (Fig 2B), which was accompanied by down-regulation of specific glycolytic enzyme genes in the fat body (Fig 3B and S3 Fig). The diversion of metabolism from building energy reserves and from fat

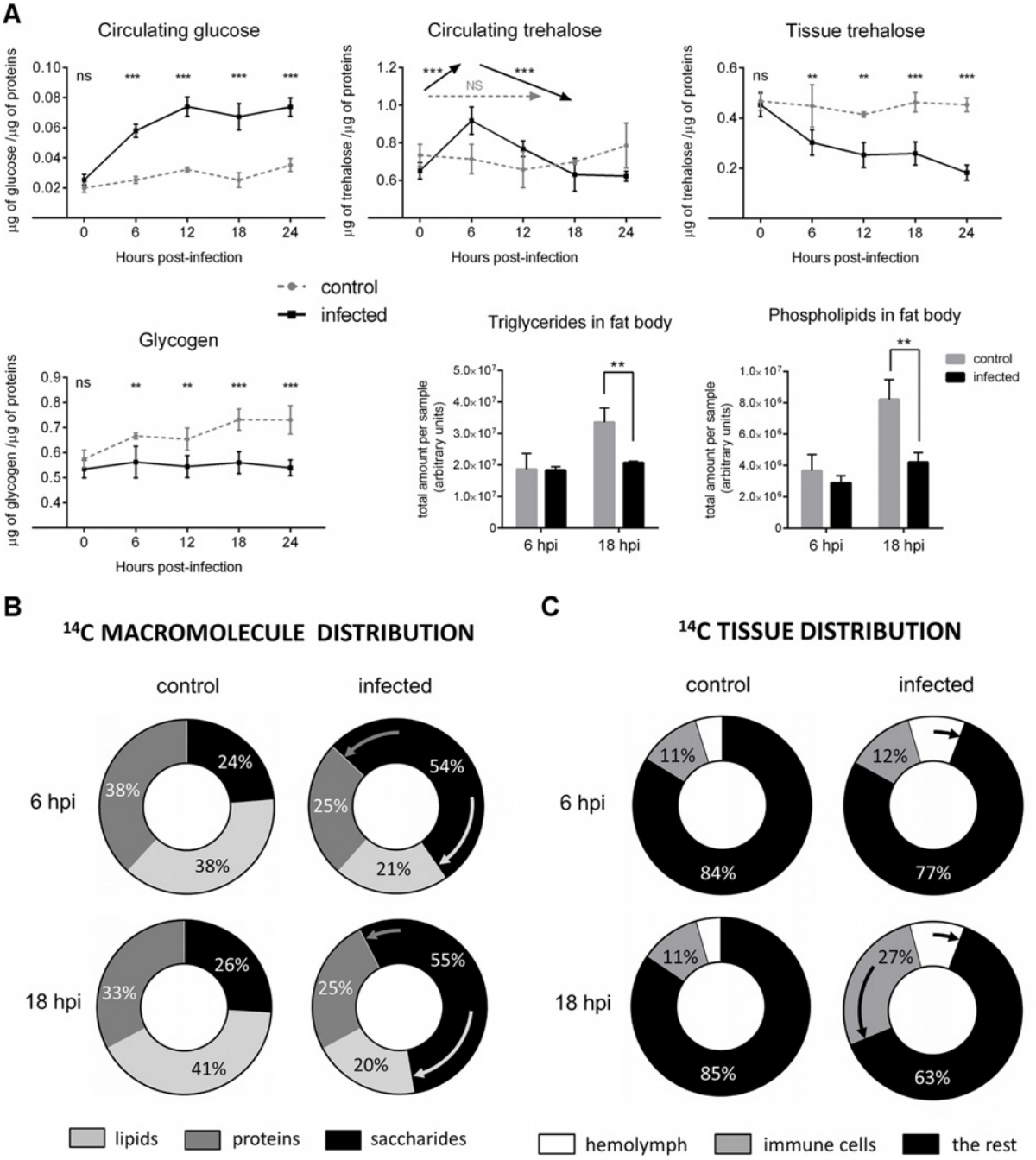

Fig 2. Metabolic changes during immune response in *w* flies. (A) Nutrient contents in the hemolymph, whole larval lysates, and fat body at different time points after infection (uninfected control: grey dashed line and grey column; infected: solid black line and column). Circulating glucose increases, tissue trehalose decreases, glycogen and lipids accumulation ceases upon infection; circulating trehalose first increases and then decreases making a 6 hpi peak. Values are mean ± SEM of four experiments (three for lipids). Asterisks show statistical significance (*$p < 0.05$; ** $p < 0.005$; *** $p < 0.0005$; ns, not significant) when compared between infected and control samples at indicated time points; arrows (Circulating trehalose, middle) indicate increase, decrease, and no change (NS), respectively, between time points. Significance of differences was tested by two-way ANOVA. (B) Percent incorporation of ^{14}C-labeled dietary glucose into lipids, proteins, and saccharides in whole larvae. Incorporation into lipids and proteins decreases upon infection, enlarging saccharide fraction as indicated by arrows. (C) Percent distribution of ^{14}C into the hemolymph, immune cells (circulating hemocytes, and lymph gland) and the rest of the larvae (brain, imaginal discs, gut, fat body, and carcass). ^{14}C first increases in hemolymph at 6 hpi (from 5% to 10%) and then also in immune cells (from 11% to 27%) at the expense of the rest of the organism upon infection; arrows indicate infection-induced changes. This figure shows data for the *w* genotype; the same values are shown in subsequent figures when compared with other genotypes. See S2 Fig for statistical analysis.

doi:10.1371/journal.pbio.1002135.g002

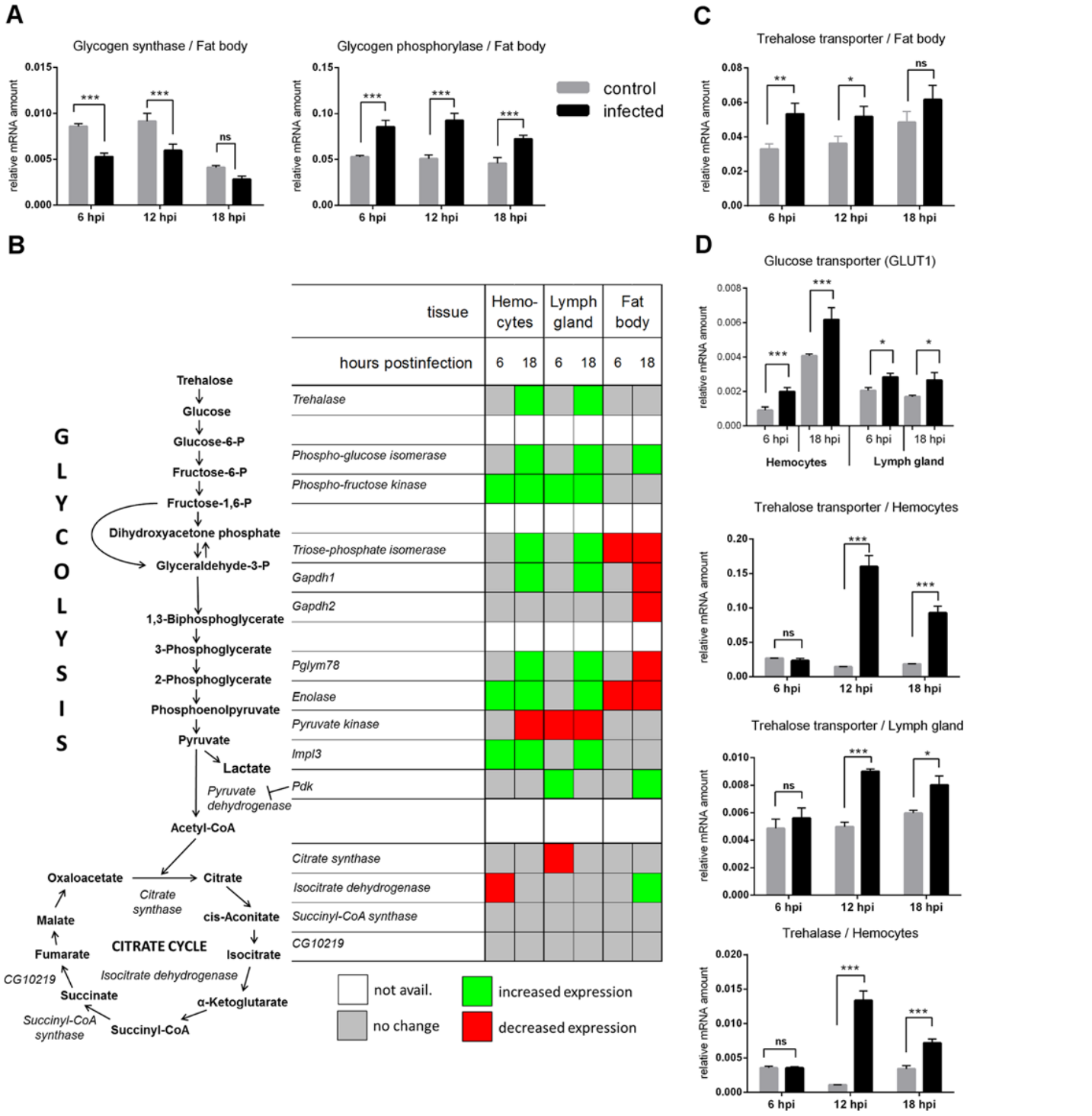

Fig 3. Gene expression during immune response of *w* larvae measured by q-PCR. (A) Reciprocal changes in mRNA expression of glycogen synthase and glycogen phosphorylase enzymes in the fat body. (B) Summary of significant changes in expression of glycolytic and citrate cycle enzymes in the hemocytes, lymph gland, and fat body (see S3–S5 Figs for corresponding graphs). Heat map indicates a tendency of glycolytic genes to increase in immune cells and to decrease in fat body. (C) Expression of trehalose transporter Tret1-1 in the fat body. (D) Expression of GLUT1, TreT1-1, and trehalase in the circulating hemocytes and lymph gland. All graphs except (B) show mean values of expression relative to *Rp49* ± SEM from three independent experiments; grey columns: control larvae, black columns: infected larvae; asterisks indicate significant changes (tested by two-way ANOVA).

doi:10.1371/journal.pbio.1002135.g003

body glycolysis was thus in agreement with extra ^{14}C in the carbohydrate form and with the increase of circulating glucose and trehalose. Circulating trehalose peaked at 6 hpi (Fig 2A) concomitantly with increased expression of a trehalose transporter in the fat body, the organ where trehalose is produced (Fig 3C).

At the same time, the immune cells changed their behavior during infection in the opposite direction, leading to increased energy consumption. Around one-tenth of ^{14}C is normally allocated to immune cells, leaving almost 90% to the rest of the organism, but immune cells demanded up to one-third of nutrients during immune response (Fig 2C). Expression of several glycolytic genes including lactate dehydrogenase *Impl3* (CG10160; FlyBase ID: FBgn0001258) increased both in the circulating hemocytes and in the lymph gland (Figs 3B, S4, and S5). This resembled the glucose-demanding aerobic glycolysis, the Warburg effect, in activated mammalian immune cells. Both the lymph gland and the circulating hemocytes expressed elevated amounts of glucose transporter Glut1 (CG43946; FlyBase ID: FBgn0264574) and trehalose transporter Tret1-1 (CG30035; FlyBase ID: FBgn0050035) mRNAs (Fig 3D). Interestingly, later during infection (12–18 hpi), the circulating hemocytes together with already differentiated lamellocytes strongly increased expression of both Tret1-1 and trehalase (CG9364; FlyBase ID: FBgn0003748) (Fig 3D). This suggests that differentiated immune cells preferentially uptake energy in the form of trehalose, which may be linked to the decline of circulating trehalose after 6 hpi (Fig 2A). These results demonstrate a shift of energy distribution away from storage and growth, first towards circulating glucose and trehalose, and then towards the immune cells (Fig 2).

e-Ado Signaling via AdoR Is Required for Hyperglycemia and Effective Immune Response

We have previously shown that e-Ado increases circulating glucose via adenosine receptor (AdoR; CG9753; FlyBase ID: FBgn0039747) signaling [38]. Here, we tested if e-Ado was involved in the observed effects of infection on the metabolic shift. While the circulating glucose increased more than 2-fold during infection in *w* larvae, this increase was suppressed in *adoR* (FlyBase ID: FBal0191589) mutant larvae (Fig 4A), indicating that AdoR was indeed necessary for the energy redistribution during infection. Therefore, we compared the number of lamellocytes as a measure of immune response. While *w* larvae produced 5–6 thousand lamellocytes by 24 hpi, the *adoR* mutants contained less than a third of this amount (Fig 4B). Yet the *adoR* mutants were clearly capable of differentiating functional lamellocytes that displayed normal morphology, expressed a lamellocyte-specific MSNF9>GFP marker (FlyBase ID: FBtp0064497), and were capable of encapsulating the wasp egg (Fig 4C and S16 Fig). Therefore, *adoR* larvae were impaired in efficiency or speed of lamellocyte production, and this corresponded with their reduced resistance against the parasitoid invasion relative to *w* larvae. Indeed, the *adoR* mutants were three times less successful at neutralizing the wasp eggs and surviving to adult flies (Fig 4C). Thus, AdoR signaling is crucial for effective immune defense against the parasitoid.

The impaired defense in the *adoR* mutants was not due to affected recognition of the wasp egg, as the number of plasmatocytes attached to the egg surface within the first few hpi was similar in *w* and *adoR* larvae (S7 Fig). Therefore, we tested if shortage of energy could be the problem as suggested by failure to increase circulating sugar levels in *adoR* larvae (Fig 4A). When we fed these larvae a high-glucose diet (12% instead of the regular 5%), the hemolymph glucose significantly increased even without infection in both *w* and *adoR* larvae (Fig 4D). This dietary treatment significantly increased the number of lamellocytes in the infected *adoR* larvae (Fig 4B), suggesting that it was the lack of energy causing inefficient differentiation of lamellocytes in the absence of AdoR.

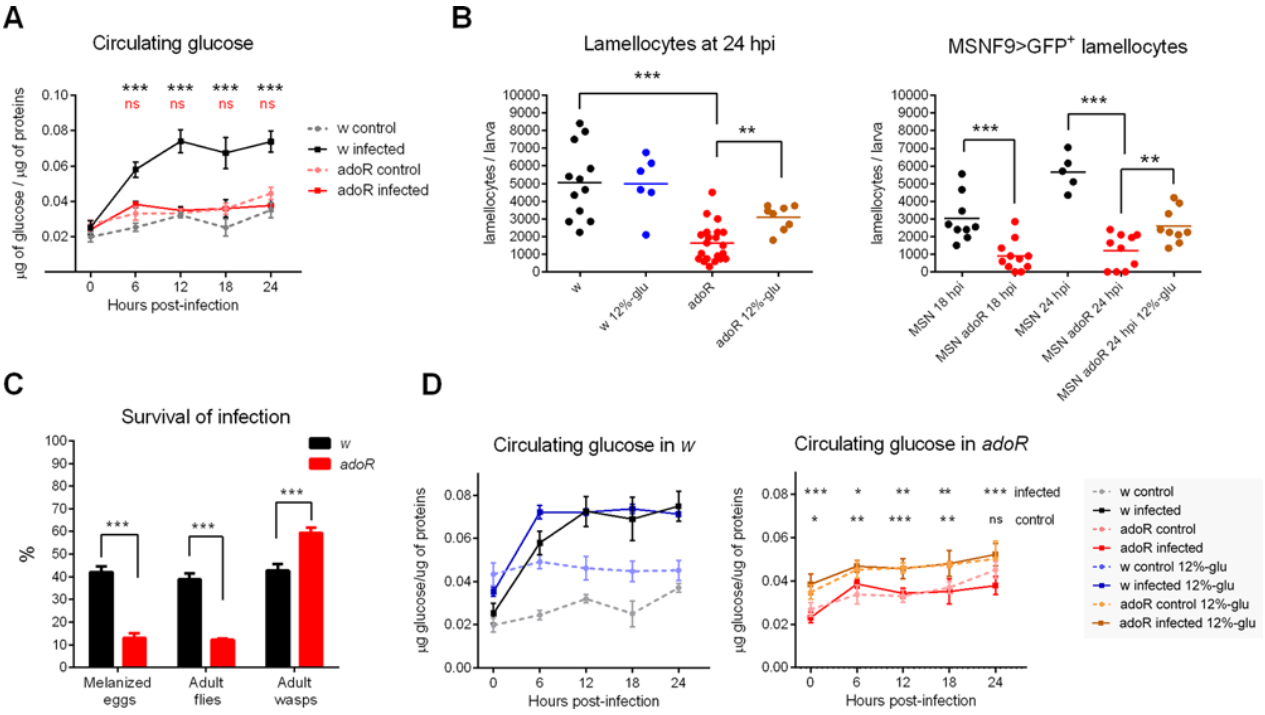

Fig 4. Effects of blocking signaling through *adoR* on immune response. (A) Increase in circulating glucose level during infection is suppressed in the *adoR* mutant. Values are mean ± SEM of four experiments; black asterisks—comparison of *w;* red "ns" (not significant)—comparison of *adoR;* tested by two-way ANOVA. (B) Number of lamellocytes based on cell morphology and a lamellocyte-specific MSNF9>GFP marker. *adoR* larvae contain fewer lamellocytes than *w* or *MSN* controls. High-glucose diet (12%-glu) increases lamellocyte number in *adoR* larvae. Each dot represents lamellocyte count per larva, the lines are mean values; tested by unpaired *t* test. (C) *adoR* mutation significantly reduces the host resistance to parasitoid wasp as assessed from frequency of melanized eggs (*adoR*—13% versus *w*—42%; $n = 100$ *Drosophila* larvae per genotype in five experiments), emerged adult flies (*adoR*—12% versus *w*—38%; $n = 310$ for *adoR*, 316 for *w*, in three experiments). Values are mean ± SEM; tested by unpaired *t* test. (D) High-glucose diet (12%-glu) significantly increases circulating glucose both in uninfected *w* and *adoR* larvae and in infected *adoR* larvae (graph with *w* does not show statistical significance). Values are mean ± SEM of three experiments; tested by two-way ANOVA. In all panels, statistical significance of differences is indicated as *$p < 0.05$; ** $p < 0.005$; *** $p < 0.0005$; and ns, not significant.

doi:10.1371/journal.pbio.1002135.g004

Interestingly, adding glucose to the diet did not further increase the level of circulating glucose during infection. In fact, the increase induced by infection was greater than that achieved with dietary glucose (Fig 4D), and consistently the number of lamellocytes in infected *w* larvae was the same on both diets (Fig 4B). Since the glucose increase induced by the dietary treatment was not as high as the one induced by the infection, the number of lamellocytes in *adoR* did not reach, even on the high-glucose diet, the levels observed in *w* (Fig 4B). This suggests that the glucose available in circulation is the limiting factor for the lamellocyte differentiation.

AdoR Signaling Mediates the Metabolic Switch

Upon infection, more glucose was retained in the saccharide fraction in the *w* larvae (Fig 2B), indicating that this glucose was available for energy needs of the immune response and less used for storage and growth. Little (at 6 hpi) or no (18 hpi) such retention was observed in *adoR* mutants (Fig 5A and S2 Fig), suggesting that storage and/or growth were not suppressed during infection in the absence of AdoR. This notion was supported by the relative distribution of ^{14}C among individual tissues (Fig 5B). The distribution was the same in uninfected *w* and *adoR* animals. The incorporation of ^{14}C did not change at 6 hpi in infected *adoR* (as opposed to *w*), and the shift from storage and growth (red part) towards immune cells (blue part) was much smaller in infected *adoR* compared to *w* at 18 hpi (Fig 5B). Importantly, the comparison

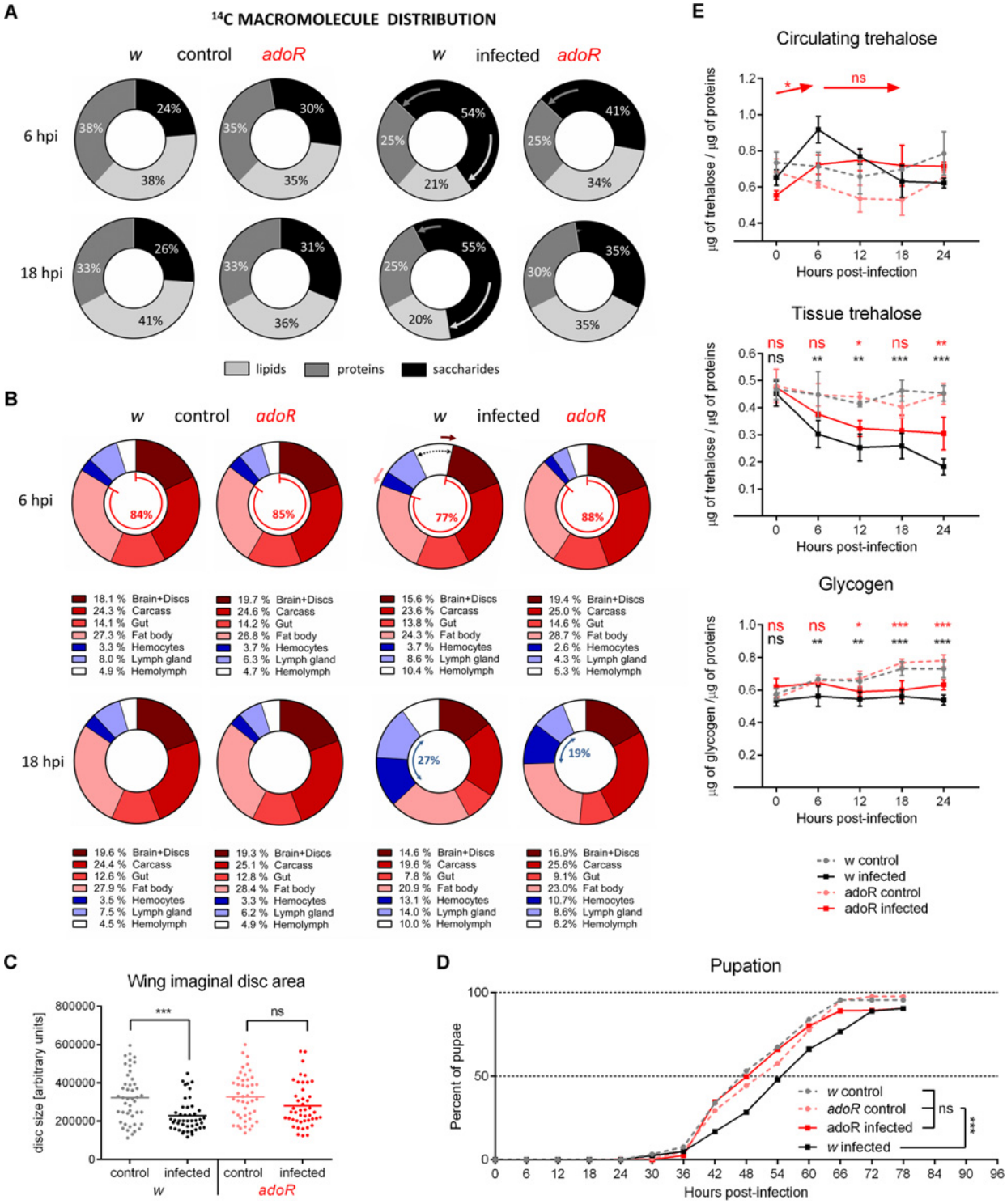

Fig 5. Metabolic changes and developmental effects of AdoR deficiency. (A) Incorporation of ^{14}C-glucose into lipids and proteins is reduced upon infection in *w* but not in *adoR* larvae. Arrows indicate infection-induced changes. For statistical analysis, see S2 Fig. (B) Relative distribution of ^{14}C in the hemolymph (white), immune cells (circulating hemocytes, dark blue; lymph gland, light blue), and the remaining body parts (brain with imaginal discs—brown; carcass, i.e., all the remnants after dissecting all other presented tissues—red; gut—light red; fat body—pink). Arrows indicate increasing ^{14}C in hemolymph (black dashed arrow) of *w* at 6 hpi at the expense of brain+discs (brown arrow) and fat body (pink arrow); these changes are missing in *adoR*. Increase in hemolymph and in immune cells (blue arrow) of *w* at 18 hpi at the expense of all other tissues is smaller in *adoR* (less in immune cells and more in

the rest). Legends below graphs show percentages in body parts. For detailed analysis, see S9 Fig and S10 Fig. (C) Growth of the wing imaginal discs is delayed by infection in *w* (unpaired *t* test $p < 0.0001$) but not in *adoR* larvae ($p = 0.06$). Each dot represents measured area of an individual disc at 18 hpi; horizontal lines indicate mean. (D) Pupation is delayed upon infection in *w* larvae ($n = 316$, control and 344, infected) but not in *adoR* larvae ($n = 310$, control and 293, infected). The rates were compared using Log-rank survival analysis; the *p* values are: *w* < 0.0001; *adoR* = 0.74; *w* control versus *adoR* control = 0.053; *w* control versus *adoR* infected = 0.054. (E) Nutrient contents in the hemolymph and whole larval lysates. Values are mean ± SEM of four experiments. Circulating trehalose in *adoR* does not form the 6 hpi peak of *w*; arrows show increase and no change (ns), respectively, when levels of infected *adoR* are compared between time points. Tissue trehalose show smaller differences for *adoR* and glycogen shows similar pattern to *w*. Asterisks show statistical significance when compared between infected and control animals at indicated time points (black for *w*, red for *adoR*). Tested by two-way ANOVA; for statistical analysis, see S2 Fig.

doi:10.1371/journal.pbio.1002135.g005

of relative distribution of ^{14}C into tissues was allowed by equal total uptake of ^{14}C-glucose from diet in *w* and *adoR* larvae (S8 Fig). Interestingly, the comparison of absolute numbers of ^{14}C entering the system also revealed anorexia during infection (lower uptake of ^{14}C; S8 Fig), supporting a common observation during immune responses [45]. This anorexia did not seem to depend on AdoR. Besides the lymph gland with slightly lower ^{14}C in *adoR* mutants, the tissue distribution of ^{14}C was similar in uninfected *w* and *adoR* larvae at both time points (Fig 5B and S10 Fig).

Upon infection, only the brain and imaginal disc complex and fat body of *w* larvae contained significantly less ^{14}C while hemolymph contained significantly more ^{14}C at 6 hpi (Fig 5B and S9 Fig). While ^{14}C incorporation into brain+discs significantly decreased in *w* larvae, it did not change in the *adoR* mutant upon infection (Fig 5B and S9 Fig), demonstrating that the suppression of developmental growth, which occurred during infection, was missing in *adoR*. This is supported by the measurement of the wing imaginal disc growth. While the growth of discs was significantly delayed in *w* control upon infection, the delay did not occur in the *adoR* mutant (Fig 5C). Similarly, the delay in development observed in infected *w* (as measured by pupation rate) did not occur in *adoR*, which pupated as there would be no infection (Fig 5D).

At 18 hpi, all tissues were affected by infection, significantly increasing ^{14}C in immune cells and hemolymph and decreasing in the rest (Fig 5B and S9 Fig). In all cases but gut, the changes were significantly smaller in *adoR* than in *w* (S10 Fig), indicating that the AdoR signaling was involved in the overall suppression of nonimmune processes.

The missing suppression of development in *adoR* larvae resulted in shortage of energy available for the immune system as documented first by almost no increase of ^{14}C in the hemolymph at 6 hpi and then by much lower ^{14}C incorporation into the immune cells at 18 hpi compared to infected *w* larvae (Fig 5B). Weak suppression of nonimmune processes in the absence of AdoR may also be linked to the missing peak of circulating trehalose at 6 hpi (Fig 5E and S2 Fig). Functional AdoR signaling seems to lower glucose transport and to increase trehalose transport in the fat body (suggested by expression levels of the respective transporter genes; S11 Fig), leading to increased trehalose at 6 hpi. The trehalose peak probably serves as a reservoir for fast glucose production, which will be increasingly needed for immune defense. The rapid lamellocyte differentiation is lagging in *adoR* larvae, likely reflecting lower consumption of trehalose relative to *w* larvae (Fig 5E).

Effect of Ado Transport on Energy Regulation during Immune Response

The AdoR signaling reallocates energy towards immune defense, suggesting that e-Ado is released upon immune challenge. Therefore, we next wanted to determine the source of e-Ado during wasp invasion. We individually knocked down the Equilibrative nucleoside transporters, *ENT1* (CG11907; FlyBase ID: FBgn0031250) and *ENT2* (CG31911; FlyBase ID: FBgn0263916), which are expressed in *Drosophila* larvae [36,46]. We delivered RNAi to various tissues utilizing the Gal4-UAS system [47], and as a simple readout we used lamellocyte

count at 24 hpi (S12 Fig). Among the tested combinations, only *ENT2* knockdown driven by *Srp-Gal4* (FlyBase ID: FBtp0020112) in cells of the hematopoietic lineage achieved a reduction in the number of lamellocytes that resembled the effect of *adoR* deficiency (Figs 4B, 6A, and S12). *Srp-Gal4* was expressed in all hematopoietic cells, including the circulating hemocytes and all cells of the lymph gland that also contained precursors of lamellocytes (S13 Fig). In contrast, knocking down *ENT2* in already differentiated hemocytes (by *Hml-Gal4* and *Upd3*-Gal4 drivers; FlyBase ID: FBtp0040877 and FBtp0020110) did not affect the lamellocyte number (S12 Fig).

ENT2 mRNA was abundant in the lymph gland and brain but weakly expressed in circulating hemocytes and virtually undetected in the fat body (Fig 6B). During infection, *ENT2* expression increased in all these tissues except the fat body (Fig 6B) and, consistently, *ENT2* RNAi delivered using a fat body-specific *C7-Gal4* driver did not affect the number of lamellocytes (S12 Fig). The increasing expression of *ENT2* during infection in the brain leaves a possibility that the nervous system contributes e-Ado; however, undetectable expression of *Srp-Gal4* in the brain, except for minor signal in some nerve cords (S13 Fig), makes the observed effects of ENT2 removal attributable to the immune cells.

The results above suggest that Ado transport from immune cells, including the differentiating ones, is important for efficient lamellocyte differentiation. As in the case of *adoR* mutation (Fig 4B), the loss of lamellocytes was rescued by increasing dietary glucose in the *Srp>ENT2-RNAi* larvae (Fig 6A). Similarly to *adoR* mutation, *ENT2* knockdown in immune cells also cancelled changes in nutrient distribution that normally take place in infected *w* larvae; there was no peak of circulating trehalose at 6 hpi and no increase in circulating glucose (Fig 6C and S2 Fig). The partition of ^{14}C into saccharides, proteins, and lipids also resembled the pattern seen in *adoR* mutant larvae (compare Fig 6D with Fig 5A and S2 Fig with S14 Fig).

Together, the above data indicate that deficiency in e-Ado release and in its receptor, AdoR, consistently lead to the same failure of energy reallocation during immune challenge. Indeed, like loss of AdoR, knocking down *ENT2* also reduced the host resistance against wasp invasion (Fig 6E), while the normal developmental delay observed in *w* controls upon infection did not occur in *Srp>ENT2-RNAi* larvae (Fig 6F). Interestingly, pupation occurred earlier in *Srp>ENT2-RNAi* compared to *w* or *adoR* animals even without infection (Fig 6F); the size of pupae was unaffected implying faster growth instead of precocious pupation of *Srp>ENT2-RNAi*.

While glycogen storage was suppressed similarly upon infection in *adoR* mutant and *w* larvae (Fig 5E), there was no significant difference in glycogen content between infected and uninfected *Srp>ENT2-RNAi* larvae (Fig 6C). Even more apparent was the effect on lipid storage where the accumulation of TAG in the fat body was suppressed both in *w* and *adoR* but not at all in *Srp>ENT2-RNAi* larvae (Fig 6G). Blocking Ado transport thus led to continued nutrient storage even upon immune challenge, suggesting that energy storage during infection might be regulated by e-Ado independently of AdoR.

Discussion

An overall metabolic suppression is a common host response to infection [18,12,6]. A likely purpose for the suppression is to conserve energy for the immune response that is energetically costly [2,12]. The defense of the *Drosophila* larva against the parasitoid wasp requires a rapid production of specialized immune cells (lamellocytes) that encapsulate the parasitoid egg. This has provided us with a unique in vivo model to study the metabolic changes and their regulation during immune response. We show here that the production of lamellocytes is an energetically demanding process, and that a systemic metabolic switch is required for their effective

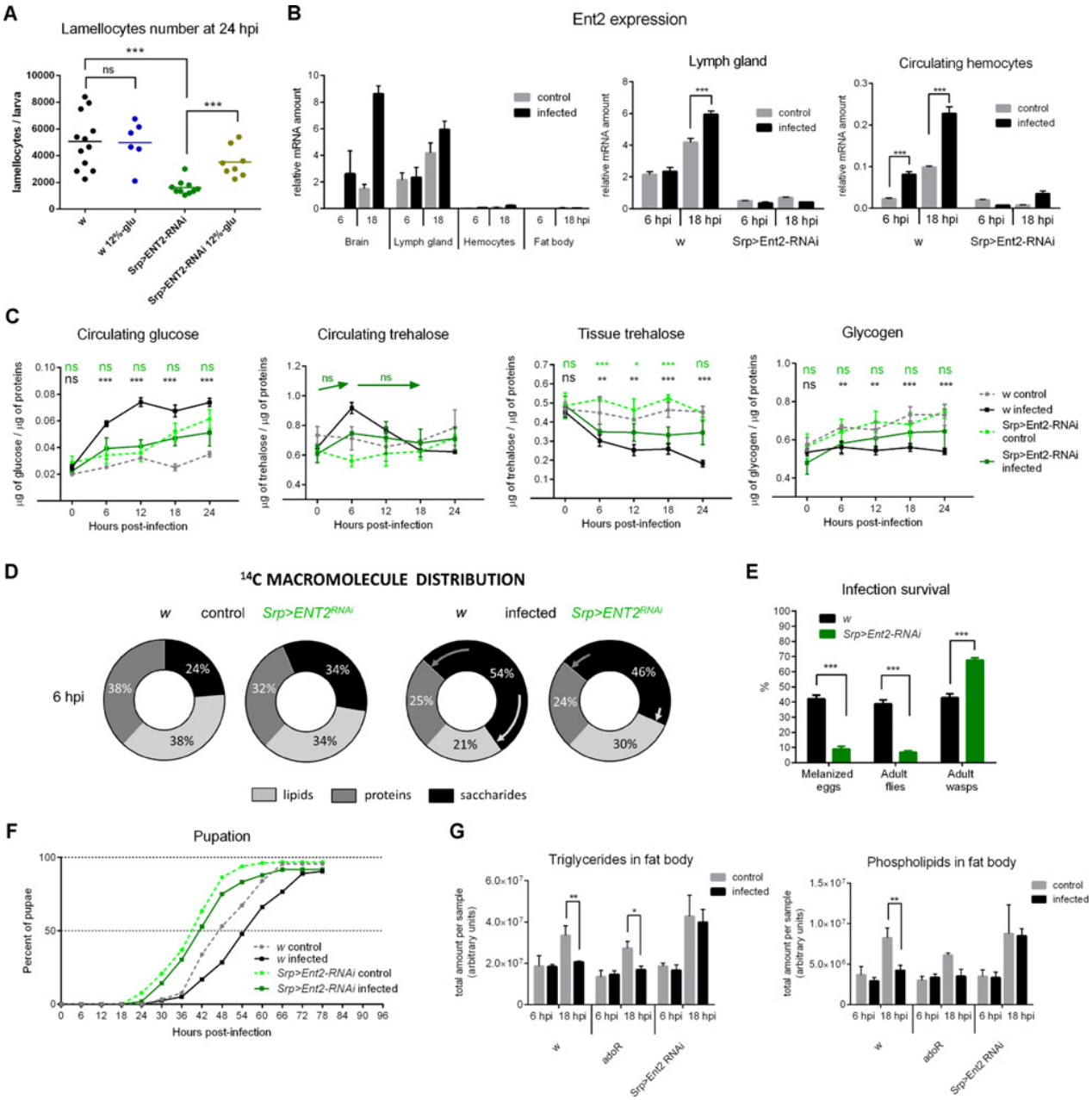

Fig 6. Effects of blocking adenosine transport in immune cells by *ENT2* RNAi. (A) *Srp>ENT2-RNAi* reduces lamellocyte number compared to *w* larvae, and high dietary glucose (12%-glu) significantly increases the lamellocyte number in *Srp>ENT2-RNAi*. Each dot represents lamellocyte count per larva; lines indicate mean. Differences were tested by unpaired *t* test. (B) *ENT2* mRNA expression. Comparison of *ENT2* mRNA expression in various tissues in *w* larvae shows a strong expression in brain and lymph gland, increasing in both upon infection. *Srp>ENT2-RNAi* reduces the *ENT2* expression below 20% both in the lymph gland and hemocytes. Values are mean ± SEM of relative expression (normalized to *Rp49* mRNA) of three experiments; tested by two-way ANOVA. (C) Nutrient contents in the hemolymph and whole larval lysates. Circulating glucose does not increase in *Srp>ENT2-RNAi* upon infection. Circulating trehalose in *Srp>ENT2-RNAi* does not form the 6 hpi peak of *w*; arrows indicate no change (ns) in levels of infected *Srp>ENT2-RNAi* when compared between time points. Tissue trehalose shows similar pattern to *w*. Glycogen does not differ between control and infected *Srp>ENT2-RNAi* indicating an accumulation of stores even upon infection. Asterisks show statistical significance when compared between infected and control animals at indicated time points (black for *w*, green for *Srp>ENT2-RNAi*). Values are mean ± SEM of four experiments; tested by two-way ANOVA. For statistical analysis, see S2 Fig. (D) Incorporation of ^{14}C-glucose into lipids and proteins is reduced upon infection in *w* larvae but significantly less so in *Srp>ENT2-RNAi* larvae. Arrows indicate infection-induced changes. For statistical analysis, see S14 Fig. (E) *Srp>ENT2-RNAi* significantly reduces the host resistance to parasitoid wasp as assessed from frequency of melanized eggs (9% versus 42%; $n = 100$ *Drosophila* larvae per genotype in five experiments) and emerged adult flies (7% versus 38%; $n = 316$ for *w*, 343 for *Srp>ENT2-RNAi* in three experiments). Values are mean ± SEM; tested by unpaired *t* test. (F) Uninfected *Srp>ENT2-RNAi* larvae ($n = 377$) pupate 8 h earlier than uninfected *w* larvae, and infection only delays their pupation by 2 h ($n = 343$). Compared using Log-rank survival

analysis ($p < 0.0001$ for all comparisons). (G) Total amount of TAG and phospholipids in the fat body of *w*, *adoR*, and *Srp>ENT2-RNAi* larvae. While infection suppresses TAG storage in *w* and *adoR*, TAG grows unaffected by infection in *Srp>ENT2-RNAi*. Data are mean values of mass spectra peak area per sample ± SEM; tested by two-way ANOVA.

doi:10.1371/journal.pbio.1002135.g006

differentiation. This switch includes (1) suppression of energy storage and developmental growth, (2) retaining more energy in circulation, and (3) increased consumption of energy by the immune system (Fig 7).

Suppression of energy storage (glycogen and lipids) and suppression of growth, as documented by slower growth of imaginal discs, lead to a developmental delay. We show here that e-Ado is a signal mediating this metabolic switch. Blocking this signal then demonstrates that the metabolic switch is crucial for an effective immune response. Without this signal, development and growth proceed at a normal speed, thus reducing energy available to the immune cells. Insufficiency of immune cells due to the shortage of energy then leads to a drastically reduced resistance against the parasitoid. Experimental interference with e-Ado or its receptor, AdoR, thus demonstrates the importance of tradeoff between development and immune response, and identifies e-Ado as a signal responsible for the switch.

Blocking Ado transport from immune cells by knocking down the equilibrative nucleoside transporter ENT2 identified the differentiating immune cells as an important source of the signal for the metabolic switch. This suggests that the immune cells could autonomously regulate energy influx based on their acute needs. Ado is a fine sensor of the cellular energy state, as it becomes produced when the ATP:AMP ratio decreases [23]. This scenario is appealing mainly because immune cells dramatically change their metabolism upon activation, leading to increased aerobic glycolysis akin to the Warburg effect [3,4]. Our expression analysis of glycolytic genes, glucose and trehalose transporters, and ^{14}C uptake by immune cells suggested a similar

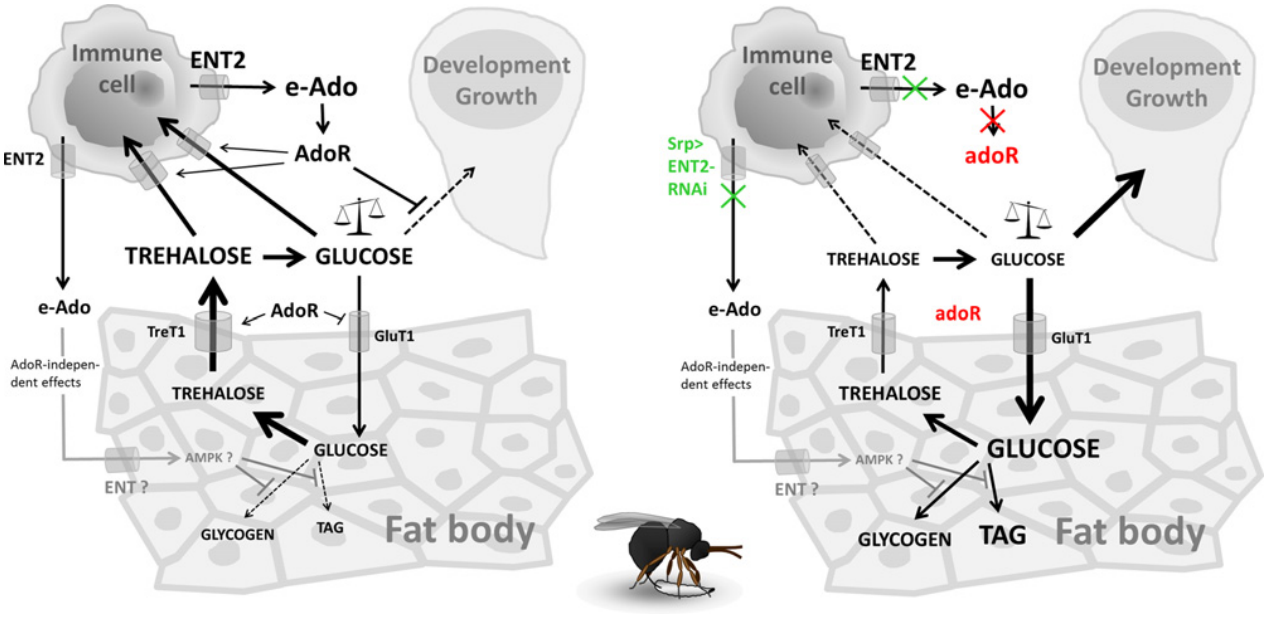

Fig 7. Model of metabolic shifts mediated by e-Ado during immune response. Left—wild-type situation upon infection. Right—situation without e-Ado upon infection; blocking AdoR signaling by *adoR* mutation is marked in red, blocking Ado transport from immune cells by *Srp>ENT2-RNAi* is marked in green. See text for details.

doi:10.1371/journal.pbio.1002135.g007

behavior for the differentiating immune cells upon wasp attack. The ability to rapidly react to a metabolic stress could be why ENT2 is strongly expressed in the lymph gland and the brain, both privileged organs from the energy point of view.

AdoR signaling is important for the suppression of developmental growth. Normally, infection leads to lower consumption of energy by the brain and imaginal discs (later also by other tissues), but the consumption continues in *adoR*-deficient larvae as if they were uninfected. At the same time, AdoR signaling seems to lower glucose transport and to increase trehalose transport in the fat body as inferred from expression levels of the respective transporter genes. The fat body is the site where trehalose is produced from glucose [44]; trehalose is then released back to the hemolymph, and more so during infection. The *adoR* mutation causes a misbalance of glucose and trehalose transport in the fat body, causing more nutrients to be retained there. The effect of AdoR signaling on the fat body combined with the suppression of developmental growth leads to hyperglycemia that in turn ensures enough energy to supply the immune cells. If the growth suppression fails to occur, as in the *adoR* mutant, the immune cells are unable to compete with developing tissues that consume the majority of energy. By analogy to the selfish brain theory [48], "selfish" immune cells may usurp energy to themselves by way of AdoR-mediated silencing of nonimmune processes. Our work thus brings experimental evidence and explains the molecular mechanism for recently published theoretical concept of selfish immune system [49].

Interestingly, the AdoR signaling does not mediate the suppression of energy storage (glycogen and TAG) during infection. However, increasing glycogen and TAG stores in infected *Srp>ENT2-RNAi* larvae with blocked Ado transport from immune cells indicates that the storage suppression is also under e-Ado control but through an AdoR-independent mechanism. Such a mechanism, which needs to be further studied, may involve e-Ado uptake, conversion to AMP by adenosine kinase, and activation of AMPK [25]. The *Srp>ENT2-RNAi* larvae proceeded faster through development not only during infection but even without infection when compared to control larvae. This suggests that the regulation of energy storage by e-Ado may play a role even during normal development.

e-Ado signaling was previously associated with regulation of hemocyte differentiation, and blocking the AdoR signaling was suggested to lower the differentiation in the lymph gland under noninfectious conditions [50]. The hallmark of lamellocyte differentiation upon parasitoid wasp infection is the turning off the Jak-Stat signaling in the medullary zone of the lymph gland containing the prohemocytes [51]. Expression of cytokine Upd3 (CG33542; FlyBase ID: FBgn0053542) is down-regulated, and the ratio of Jak-Stat receptor Domeless (CG14226; FlyBase ID: FBgn0043903) and its negative coreceptor Latran (CG14225; FlyBase ID: FBgn0031055) is switched upon wasp infection leading to turning off the Jak-Stat and to induction of lamellocyte differentiation [52]. The expression patterns of *Upd3*, *Domeless* and *Latran* mRNAs normally and during infection are unaffected both in *adoR* and *Srp>ENT2-RNAi* (S15 Fig), indicating that the induction of lamellocyte differentiation is functional in these lines. In addition, the lymph glands develop normally in both *adoR* and *Srp>ENT2-RNAi* ([50] and S17 Fig). Our results demonstrate that the *adoR* and *Srp>ENT2-RNAi* larvae are capable of lamellocyte differentiation; they are just less effective, and the reason is most likely the lack of energy as indicated by the rescue of this phenotype with extra dietary glucose.

An important part of the global energy switch observed upon parasitoid invasion is the AdoR-mediated suppression of developmental growth. Although AdoR is relatively strongly expressed in imaginal discs [34], we do not know if it is the tissue-autonomous signaling of AdoR, or whether AdoR acts systemically on metabolism as AdoR is also strongly expressed in the larval endocrine glands and brain; both scenarios may apply simultaneously. It is known that the activation of adenosine receptor leads to metabolic suppression—at the individual cell

level, the activation can inhibit growth of tumor cells [26], but it can also cause a systemic suppression during anoxia [28,29] or torpor [27]. Our work demonstrates that the AdoR-mediated suppression plays an important role also during immune response. It will be important to identify the target cells and signaling cascades mediating the observed suppression in future studies.

We show here that the metabolic switch is mediated by e-Ado and that the switch is crucial for an effective immune response. It is of interest to see if this e-Ado role is common to other organisms including humans. e-Ado plays the same role in energy regulation in flies and mammalian systems [30,38]. For example, sepsis is associated with hyperglycemia and insulin resistance as well as with increased e-Ado [31,53], suggesting that e-Ado could indeed mediate the systemic metabolic switch in higher organisms. However, analyzing this role of e-Ado in mammals will be complicated by the existence of multiple adenosine receptors with partly contradicting functions [54,55] and by diverse roles of e-Ado in immunomodulation [24,56,57].

In conclusion, our study demonstrates that extracellular adenosine, released from immune cells, mediates a systemic metabolic switch leading to suppression of energy storage and developmental growth, thus leaving more energy to the immune cells. This switch is crucial for the effective immune response and blocking adenosine signaling drastically reduces host resistance to the pathogen. This may resemble a selfish brain theory in a way that the immune system, like the brain, is a privileged part of the organism, capable of suppressing energy consumption by other tissues in its own interest. Such a selfish immune system [49] would use e-Ado as a signal to appropriate extra energy resources during immune challenge.

Materials and Methods

Fly Stocks, Culture, and Infection

All strains were backcrossed at least ten times to w^{1118} genetic background; w^{1118} was used as a control in all experiments. *adoR* mutant was homozygous for $adoR^{1}$ mutation (FBal0191589). RNAi lines originated from VDRC: *UAS-Ent1-RNAi* (ID 109885) and *UAS-Ent2-RNAi* (ID 100464). *SrpD-Gal4*, *Upd3-Gal4*, and *MSNF9-GFP* were obtained from Michele Crozatier, *HmlΔ-Gal4* from Bruno Lemaitre and *C7-Gal4* from Marek Jindra. Flies were grown on cornmeal medium (8% cornmeal, 5% glucose, 4% yeast, 1% agar) at 25°C. For dietary treatment, larvae were transferred upon infection to cornmeal diet with 12% instead of 5% glucose. Early 3rd instar larvae were infected by parasitoid wasp *L. boulardi*. Weak infection (1–2 eggs per larva) was used for resistance and pupation analysis; strong infection (4–7 eggs per larva) was used in all other cases.

Resistance and Pupation

To determine pupation rate and resistance to parasitoids, infected and control larvae were placed into fresh vials (1 experiment = 30 larvae per vial, 3 vials per genotype; 4 independent experiments). Pupation rate was determined by counting newly appeared pupae every 6 h and incremental percentage of number of pupae per total number of infected and control larvae at a particular time point postinfection was plotted; Log-rank survival analysis was used for comparison. For resistance, we first dissected 20 larvae per experiment from each genotype to count fully melanized wasp eggs (winning host) or surviving wasp larvae (winning parasitoid). Second, we counted all emerged adult flies as surviving the infection and flies without any egg (i.e., uninfected individuals) were excluded from the total number in the experiment. Adult wasps emerged from the vial were counted as adult parasitoid winners.

Gene Expression

Expression was analyzed by quantitative real-time PCR. Samples were collected from three independent infection experiments with three technical replicates for each experiment. Expression was normalized to Ribosomal protein *Rp49*.

^{14}C-glucose Distribution

Larvae were fed either 73 h AEL or 91 h AEL for 20 min a diet containing D[U-^{14}C]-glucose (10.6 Gbq/mmol; Amersham Biosciences) in yeast. Samples were collected 5 h later. Each sample contained tissues from 30 larvae—all hemolymph was collected by ripping larvae in PBS, centrifuging them, and dividing them into pelleted hemocytes and hemolymph fractions; brains with attached discs and wing discs, whole guts, whole fat bodies, and lymph glands were separated by dissection, and the rest were used as carcass. Macromolecular fractions were separated from tissue homogenates according to [58] for saccharides and lipids and by TCA treatment for proteins. Part of the homogenate was used for measurement of total absorbed amount of ^{14}C molecules. Number of ^{14}C disintegrations per minute was detected by liquid scintillator.

Metabolites Measurement

Glucose, trehalose, and glycogen were measured as described [59], using GAGO-20 kit (Sigma). Lipids extracted with chlorophorm:methanol were quantified by HPLC and mass spectrometry.

Imaginal Disc Size Measurement

Wing discs were dissected from larvae at 90 h AEL (18 hpi), and their size was determined from micrographs by FIJI software.

Data Analysis

Data were analyzed by GraphPad Prism 6 (GraphPad Software, Inc.).

Extended Materials and Methods are available in S1 Text.

Supporting Information

S1 Data. Compressed ZIP file containing 17 dataset files with original data in GraphPad PRISM 6 format. Fig 1 —data.pzfx: Immune response to parasitoid wasp intrusion. Fig 2 —data.pzfx: Metabolic changes during immune response in *w* flies. Fig 3 —data.pzfx: Gene expression during immune response of *w* larvae measured by q-PCR. Fig 4 —data.pzfx: Effects of blocking signaling through adenosine receptor (*adoR*) on immune response. Fig 5 —data.pzfx: Metabolic changes and developmental effects of AdoR deficiency. Fig 6 —data.pzfx: Effects of blocking adenosine transport in immune cells by *ENT2* RNAi. S2 Fig—data.pzfx: Statistical analysis of metabolite changes. S3 Fig—data.pzfx: Gene expression analysis of glycolytic and citrate cycle genes in fat body by q-PCR. S4 Fig—data.pzfx: Gene expression analysis of glycolytic and citrate cycle genes in circulating hemocytes by q-PCR. S5 Fig—data.pzfx: Gene expression analysis of glycolytic and citrate cycle genes in lymph gland by q-PCR. S7 Fig—data.pzfx: Recognition of parasitoid wasp egg by plasmatocytes is not affected by *adoR*. S8 Fig—data.pzfx: Total absorption of 14C from food. S9–S10 Fig—data.pzfx: Comparison of relative ^{14}C-tissue distribution between infected and uninfected larvae and between *w* and *adoR*. S11 Fig—data.pzfx: q-PCR expression analysis of genes involved in transport and metabolism of glucose and trehalose in *w* and *adoR*. S12 Fig—data.pzfx: Number of lamellocytes in flies with

knocked-down equilibrative nucleoside transporters ENT1 and ENT2 in different tissues. S14 Fig—data.pzfx: Relative ^{14}C incorporation into macromolecules in *w* and Srp>ENT2-RNAi at 6 hpi. S15 Fig—data.pzfx: Expression analysis of genes involved in regulation of lamellocytes differentiation by q-PCR.
(ZIP)

S1 Fig. Timescale of experimental procedures. Top timescale—sampling and treatment description for experiments with ^{14}C-labeled glucose. Middle timescale—sample collection and treatment for experiments characterizing reaction to infection. Bottom timescale—sample collection for experiments characterizing metabolites.
(TIF)

S2 Fig. Statistical analysis of metabolite changes. A) Statistical analysis of infection-induced changes in circulating trehalose between infection and control in particular time points (upper table) and between different time points either in control or infection (lower table); tested by two-way ANOVA, B) comparison of incorporation of ^{14}C into macromolecules (saccharides, lipids, and proteins), and C) into three distinguished processes (development and growth, cellular immunity, and circulation) in *w* and *adoR*; tested by two-way ANOVA. Uninfected individuals marked as CON (grey columns), infected individuals marked as INF (black columns). Graphs show mean values ± SEM of three independent experiments. Asterisks show statistical significance ($^{*}<0.05$; $^{**}<0.005$; $^{***}<0.0005$).
(TIF)

S3 Fig. Gene expression analysis of glycolytic and citrate cycle genes in fat body by q-PCR. Infection-induced difference in gene expression was analyzed in *w* and *adoR*, 6 and 18 hpi. Uninfected individuals are represented by grey columns (CON), infected individuals by black columns (INF). Graphs show mean values relative to Rp49 ± SEM of three independent experiments. Asterisks show statistical significance ($^{*}<0.05$; $^{**}<0.005$; $^{***}<0.0005$); tested by one-way ANOVA. Gene symbols and the corresponding genes can be found in S1 Table.
(TIF)

S4 Fig. Gene expression analysis of glycolytic and citrate cycle genes in circulating hemocytes by q-PCR. Infection-induced difference in gene expression was analyzed in *w* and *adoR*, 6 and 18 hpi. Uninfected individuals are represented by grey columns (CON), infected individuals by black columns (INF). Graphs show mean values relative to Rp49 ± SEM of three independent experiments. Asterisks show statistical significance ($^{*}<0.05$; $^{**}<0.005$; $^{***}<0.0005$); tested by one-way ANOVA. Gene symbols and the corresponding genes can be found in S1 Table.
(TIF)

S5 Fig. Gene expression analysis of glycolytic and citrate cycle genes in lymph gland by q-PCR. Infection-induced difference in gene expression was analyzed in *w* and *adoR*, 6 and 18 hpi. Uninfected individuals are represented by grey columns (CON), infected individuals by black columns (INF). Graphs show mean values relative to Rp49 ± SEM of three independent experiments. Asterisks show statistical significance ($^{*}<0.05$; $^{**}<0.005$; $^{***}<0.0005$); tested by one-way ANOVA. Gene symbols and the corresponding genes can be found in S1 Table.
(TIF)

S6 Fig. Comparison of glycolytic and citrate cycle genes expressions in *w* and *adoR* summarized by heat map. Comparison of infection-induced differences in gene expression between w and *adoR* in three different tissues (hemocytes, lymph gland, and fat body) and two different time points postinfection (6 and 18 hpi). Green squares—increased expression, red squares—

decreased expression, grey squares—no significant difference, white squares—not analyzed. Level of significance $p < 0.05$; one-way ANOVA.
(TIF)

S7 Fig. Recognition of parasitoid wasp egg by plasmatocytes is not affected by *adoR*. (A) Percentage of eggs with certain number of plasmatocytes (none, 1–10, 10–20, or >20) attached to their surface within the first 2 hpi and 4–6 hpi in *w* and *adoR* mutant larvae. (B) Examples of attached Hml>GFP-labeled hemocytes (green fluorescence) to parasitoid wasp egg within the first 2 hpi and 4–6 hpi in *w* and *adoR* mutant larvae.
(TIF)

S8 Fig. Total absorption of ^{14}C from food. Larvae were fed ^{14}C-glucose (in blue dye-labeled diet) for 20 min and then transferred to normal diet for 5 h in which they absorbed ^{14}C-glucose and cleared their guts. They were then homogenized to analyze how much ^{14}C-glucose they absorbed. There is no difference in absorption between control *w* and control *adoR* or infected *w* and infected *adoR* both at 6 and 18 hpi (labeled NS for not significant). Interestingly, infected larvae (both *w* and *adoR*) absorbed less ^{14}C than control larvae indicating anorexia upon infection. Graph shows uninfected *w* (grey columns), infected *w* (black columns), uninfected *adoR* (pink columns), and infected *adoR* (red columns) mean values of disintegration of ^{14}C per minute (dpm) per sample ± SEM of three independent experiments, tested by one-way ANOVA. Asterisks show statistical significance ($^{*}<0.05$; $^{**}<0.005$; $^{***}<0.0005$).
(TIF)

S9 Fig. Comparison of relative ^{14}C-tissue distribution between infected and uninfected larvae. This figure serves as an alternative for Fig 5B to visualize statistical significance. Compared values: uninfected *w* (grey columns) with infected *w* (black columns) and uninfected *adoR* (pink columns) with infected *adoR* (red columns). Graph shows mean values ± SEM of three independent experiments. Tested by one-way ANOVA with Arc-Sin transformation. Asterisks show statistical significance ($^{*}<0.05$; $^{**}<0.005$; $^{***}<0.0005$).
(TIF)

S10 Fig. Comparison of relative ^{14}C-tissue distribution between *w* and *adoR*. This figure serves as an alternative for Fig 5B to visualize statistical significance. Compared values: uninfected *w* (grey columns) with uninfected *adoR* (pink columns) and infected *w* (black columns) with infected *adoR* (red columns). Graph shows mean values ± SEM of three independent experiments. Tested by one-way ANOVA with Arc-Sin transformation. Asterisks show statistical significance ($^{*}<0.05$; $^{**}<0.005$; $^{***}<0.0005$).
(TIF)

S11 Fig. q-PCR expression analysis of genes involved in transport and metabolism of glucose and trehalose in *w* and *adoR*. Graphs display infection-induced differences in expression level of Trehalose transporter TreT1-1, Glucose transporter 1 (Glut1), Glycogen synthase (Gsyn), and Glycogen phosphorylase (Gps) in fat body, lymph gland, and circulating hemocytes at 6 and 18 hpi. Uninfected individuals marked as CON (grey columns), infected individuals marked as INF (black columns). Graph shows mean values ±SEM of three independent experiments. Asterisks show statistical significance ($^{*}<0.05$; $^{**}<0.005$; $^{***}<0.0005$; ns for non-significant difference); tested by one-way ANOVA.
(TIF)

S12 Fig. Number of lamellocytes in flies with knocked-down equilibrative nucleoside transporters ENT1 and ENT2 in different tissues. RNAi was induced by driving *UAS-Ent1-RNAi* (VDRC ID 109885) and *UAS-Ent2-RNAi* (VDRC ID 100464) by various Gal4 drivers: *Srp-Gal4*

expressed in all cells of hematopoietic lineage and fat body, *Upd3-Gal4* and *Hml-Gal4* in differentiated hemocytes and *C7-Gal4* in fat body. Lamellocytes were counted based on morphology using DIC at 24 hpi. Only combination of *Srp>Ent2-RNAi* significantly decreased lamellocytes. Results were tested by one-way ANOVA, each point in graph represents number of lamellocytes in one individual larva. Asterisks show statistical significance ($^{*}<0.05$; $^{**}<0.005$; $^{***}<0.0005$; NS for nonsignificant difference).
(TIF)

S13 Fig. Expression of SrpD-Gal4 driver in 72-h-old larvae. *Srp-Gal4* driver expression was visualized by crossing to *UAS-GFP*. Strong expression was detected in all cells of hematopoietic lineage as demonstrated by the GFP fluorescence in circulating hemocytes and all cells in the lymph gland. The expression was also detected in fat body but it was undetectable in the brain besides weak expression in nerve cords. Left panels show DIC image corresponding to GFP fluorescence images on right.
(TIF)

S14 Fig. Relative ^{14}C incorporation into macromolecules in *w* and Srp>ENT2-RNAi at 6 hpi. Comparison of incorporation of ^{14}C into macromolecules (saccharides, lipids, and proteins) tested by two-way ANOVA. Uninfected individuals are marked as control (grey columns), infected individuals are marked as infected (black columns). Graphs show mean values ± SEM of three independent experiments. Asterisks show statistical significance ($^{*}<0.05$; $^{**}<0.005$; $^{***}<0.0005$; ns for not significant).
(TIF)

S15 Fig. Expression analysis of genes involved in regulation of lamellocytes differentiation by q-PCR. RNA was isolated from dissected lymph glands at 6 hpi of control (grey) and infected (black) larvae. Graphs show the reciprocal changes in expression of Jak-Stat receptor *Domeless* and its negative coreceptor *Latran* and turning off *Unpaired3* (*Upd3*) upon infection. This hallmark of induction of lamellocyte differentiation does not differ in *adoR* or *Srp>ENT2-RNAi* compared to *w*. Graph shows mean values ± SEM of three independent experiments. Differences were tested by one-way ANOVA; results shown below the graphs—ns = not significant; $^{*}<0.05$; $^{**}<0.005$; $^{***}<0.0005$; $^{****}<0.00005$).
(TIF)

S16 Fig. Expression of lamellocyte-specific MSNF9>GFP marker. (A) Expression of MSNF9>GFP (green) together with plasmatocytes-specific P1 marker (red) in the lymph gland upon infection at 12 and 18 hpi. Both *w* and *adoR* express the lamellocyte marker indicating that *adoR* is able to differentiate lamellocytes but there is usually less MSNF9>GFP signal in *adoR* at 12 hpi. While *w* sometimes already releases lamellocytes into circulation at 18 hpi (as demonstrated by disintegrated lymph gland in DIC picture), *adoR* has lymph gland still compact at 18 hpi, but with increasing number of MSNF9>GFP positive cells further demonstrating ability of *adoR* to differentiate lamellocytes but with lower speed. Top—DIC, bottom—fluorescence confocal image. (B) MSNF9>GFP positive lamellocytes in circulation at 27 hpi are present in both *w* and *adoR* and their morphology is indistinguishable. Fluorescence and DIC-combined micrographs.
(TIF)

S17 Fig. Morphology of the lymph gland in 72-h-old larvae. Morphology and zonation of the lymph gland in 72-h-old larvae (corresponding to time of infection) was checked by expression of medullary zone-specific *Dome>GFP* marker (prohemocyte containing zone; green) and differentiated plasmatocyte-specific P1 marker for cortical zone (red) in *w* and *adoR*. Only P1

marker was used in *Srp>ENT2-RNAi* and DAPI (nuclear staining) for overall morphology to define medullary zone by the absence of P1. In all three genotypes, the zonation and morphology was comparable for multiple samples indicating that there is no gross effect of the used genetic manipulations on the lymph gland development prior to infection.
(TIF)

S1 Table. Genes, gene symbols, and primers used for q-PCR analysis.
(XLSX)

S1 Text. Extended materials and methods.
(DOCX)

Acknowledgments

We thank the Vienna *Drosophila* RNAi Center, Michele Crozatier for flies, wasps, and antibodies and Bruno Lemaitre for flies. We thank Marek Jindra for help with writing the manuscript and David Schneider and members of Schneider laboratory for inputs and discussions.

Author Contributions

Conceived and designed the experiments: AB TD. Performed the experiments: AB KK LJ AT IS TD. Analyzed the data: AB AT TD. Contributed reagents/materials/analysis tools: AT IS JO. Wrote the paper: AB TD.

References

1. Fong YM, Marano M a, Moldawer LL, Wei H, Calvano SE, Kenney JS, et al. The acute splanchnic and peripheral tissue metabolic response to endotoxin in humans. J Clin Invest. 1990; 85: 1896–1904. PMID: 2347917
2. Straub RH, Cutolo M, Buttgereit F, Pongratz G. Energy regulation and neuroendocrine-immune control in chronic inflammatory diseases. J Intern Med. 2010; 267: 543–560. doi: 10.1111/j.1365-2796.2010.02218.x PMID: 20210843
3. Cheng S-C, Quintin J, Cramer RA, Shepardson KM, Saeed S, Kumar V, et al. mTOR- and HIF-1α–mediated aerobic glycolysis as metabolic basis for trained immunity. Science. 2014; 345: 1250684. doi: 10.1126/science.1250684 PMID: 25258083
4. Delmastro-Greenwood MM, Piganelli JD. Changing the energy of an immune response. Am J Clin Exp Immunol. 2013; 2: 30–54. PMID: 23885324
5. Pfeiffer T, Schuster S, Bonhoeffer S. Cooperation and competition in the evolution of ATP-producing pathways. Science. 2001; 292: 504–507. PMID: 11283355
6. Clark RI, Tan SWS, Péan CB, Roostalu U, Vivancos V, Bronda K, et al. MEF2 Is an In Vivo Immune-Metabolic Switch. Cell. 2013; 155: 435–447. doi: 10.1016/j.cell.2013.09.007 PMID: 24075010
7. Hartman ZC, Kiang A, Everett RS, Serra D, Yang XY, Clay TM, et al. Adenovirus infection triggers a rapid, MyD88-regulated transcriptome response critical to acute-phase and adaptive immune responses in vivo. J Virol. 2007; 81: 1796–1812. PMID: 17121790
8. Rynes J, Donohoe CD, Frommolt P, Brodesser S, Jindra M, Uhlirova M. Activating Transcription Factor 3 Regulates Immune and Metabolic Homeostasis. Mol Cell Biol. 2012; 32: 3949–3962. doi: 10.1128/MCB.00429-12 PMID: 22851689
9. Yoo J-Y, Desiderio S. Innate and acquired immunity intersect in a global view of the acute-phase response. Proc Natl Acad Sci U S A. 2003; 100: 1157–1162. PMID: 12540827
10. Calder PC. Feeding the immune system. Proc Nutr Soc. 2013; 72: 299–309. doi: 10.1017/S0029665113001286 PMID: 23688939
11. Matarese G, La Cava A, Sanna V, Lord GM, Lechler RI, Fontana S, et al. Balancing susceptibility to infection and autoimmunity: a role for leptin? Trends Immunol. 2002; 23: 182–187. PMID: 11923112
12. Rauw WM. Immune response from a resource allocation perspective. Front Genet. 2012; 3: 267–267. doi: 10.3389/fgene.2012.00267 PMID: 23413205

13. Arsenijevic D, Garcia I, Vesin C, Vesin D, Arsenijevic Y, Seydoux J, et al. Differential roles of tumor necrosis factor-a and interferon-g in mouse hypermetabolic and anorectic responses induced by LPS. Eur Cytokine Netw. 2000; 11: 662–668. PMID: 11125311

14. Matarese G, La Cava A. The intricate interface between immune system and metabolism. Trends Immunol. 2004; 25: 193–200. PMID: 15039046

15. Tracey KJ, Cerami A. Tumor Necrosis Factor and Regulation of Metabolism in Infection: Role of Systemic versus Tissue Levels. Exp Biol Med. 1992; 200: 233–239. PMID: 1579588

16. Tsigos C, Papanicolaou DA, Kyrou I, Defensor R, Mitsiadis CS, Chrousos GP. Dose-dependent effects of recombinant human interleukin-6 on glucose regulation. J Clin Endocrinol Metab. 1997; 82: 4167–4170. PMID: 9398733

17. Wolowczuk I, Verwaerde C, Viltart O, Delanoye A, Delacre M, Pot B, et al. Feeding our immune system: impact on metabolism. Clin Dev Immunol. 2008; 2008: 639803. doi: 10.1155/2008/639803 PMID: 18350123

18. Chambers MC, Song KH, Schneider DS. Listeria monocytogenes infection causes metabolic shifts in Drosophila melanogaster. PLoS ONE. 2012; 7: e50679. doi: 10.1371/journal.pone.0050679 PMID: 23272066

19. Dionne MS, Pham LN, Shirasu-Hiza M, Schneider DS. Akt and FOXO dysregulation contribute to infection-induced wasting in Drosophila. Curr Biol. 2006; 16: 1977–1985. PMID: 17055976

20. Dionne M. Immune-metabolic interaction in Drosophila. Fly (Austin). 2014; 8: 1–5.

21. Hull-Thompson J, Muffat J, Sanchez D, Walker DW, Benzer S, Ganfornina MD, et al. Control of metabolic homeostasis by stress signaling is mediated by the lipocalin NLaz. PLoS Genet. 2009; 5: e1000460. doi: 10.1371/journal.pgen.1000460 PMID: 19390610

22. Buck LT. Adenosine as a signal for ion channel arrest in anoxia-tolerant organisms. Comp Biochem Physiol Part B. 2004; 139: 401–414. PMID: 15544964

23. Newby AC. Adenosine and the concept of "retaliatory metabolites." Trends Biochem Sci. 1984; 9: 42–44.

24. Bours MJL, Swennen ELR, Di Virgilio F, Cronstein BN, Dagnelie PC. Adenosine 5'-triphosphate and adenosine as endogenous signaling molecules in immunity and inflammation. Pharmacol Ther. 2006; 112: 358–404. PMID: 16784779

25. Da Silva CG, Jarzyna R, Specht A, Kaczmarek E. Extracellular nucleotides and adenosine independently activate AMP-activated protein kinase in endothelial cells: involvement of P2 receptors and adenosine transporters. Circ Res. 2006; 98: e39–47. PMID: 16497986

26. Fishman P, Bar-Yehuda S, Barer F, Madi L, Multani AS, Pathak S. The A3 Adenosine Receptor as a New Target for Cancer Therapy and Chemoprotection. Exp Cell Res. 2001; 269: 230–236. PMID: 11570815

27. Jinka TR, T?ien? ivind, Drew KL. Season primes the brain in an arctic hibernator to facilitate entrance into torpor mediated by adenosine A1 receptors. J Neurosci. 2011; 31: 10752–10758. doi: 10.1523/JNEUROSCI.1240-11.2011 PMID: 21795527

28. Krumschnabel G, Biasi C, Wieser W. Action of adenosine on energetics, protein synthesis and K(+) homeostasis in teleost hepatocytes. J Exp Biol. 2000; 203: 2657–2665. PMID: 10934006

29. Pék M, Lutz PL. Role for adenosine in channel arrest in the anoxic turtle brain. J Exp Biol. 1997; 200: 1913–1917. PMID: 9232005

30. Cortés D, Guinzberg R, Villalobos-Molina R, Piña E. Evidence that endogenous inosine and adenosine-mediated hyperglycaemia during ischaemia–reperfusion through A3 adenosine receptors. Auton Autacoid Pharmacol. 2009; 29: 157–164. doi: 10.1111/j.1474-8665.2009.00443.x PMID: 19740086

31. Martin C, Leone M, Viviand X, Ayem ML, Guieu R. High adenosine plasma concentration as a prognostic index for outcome in patients with septic shock. Crit Care Med. 2000; 28: 3198–3202. PMID: 11008982

32. Kumar V, Sharma A. Adenosine: an endogenous modulator of innate immune system with therapeutic potential. Eur J Pharmacol. 2009; 616: 7–15. doi: 10.1016/j.ejphar.2009.05.005 PMID: 19464286

33. Dolezal T, Dolezelova E, Zurovec M, Bryant PJ. A role for adenosine deaminase in Drosophila larval development. PLoS Biol. 2005; 3: e201. PMID: 15907156

34. Dolezelova E, Nothacker H-P, Civelli O, Bryant PJ, Zurovec M. A Drosophila adenosine receptor activates cAMP and calcium signaling. Insect Biochem Mol Biol. 2007; 37: 318–329. PMID: 17368195

35. Fenckova M, Hobizalova R, Fric ZF, Dolezal T. Functional characterization of ecto-5'-nucleotidases and apyrases in Drosophila melanogaster. Insect Biochem Mol Biol. 2011; 41: 956–967. doi: 10.1016/j.ibmb.2011.09.005 PMID: 21996016

36. Knight D, Harvey PJ, Iliadi KG, Klose MK, Iliadi N, Dolezelova E, et al. Equilibrative nucleoside transporter 2 regulates associative learning and synaptic function in Drosophila. J Neurosci Off J Soc Neurosci. 2010; 30: 5047–5057.

37. Zurovec M, Dolezal T, Gazi M, Pavlova E, Bryant PJ. Adenosine deaminase-related growth factors stimulate cell proliferation in Drosophila by depleting extracellular adenosine. Proc Natl Acad Sci U S A. 2002; 99: 4403–4408. PMID: 11904370

38. Zuberova M, Fenckova M, Simek P, Janeckova L, Dolezal T. Increased extracellular adenosine in Drosophila that are deficient in adenosine deaminase activates a release of energy stores leading to wasting and death. Dis Model Mech. 2010; 3: 773–784. doi: 10.1242/dmm.005389 PMID: 20940317

39. Novakova M, Dolezal T. Expression of Drosophila adenosine deaminase in immune cells during inflammatory response. PLoS ONE. 2011; 6: e17741. doi: 10.1371/journal.pone.0017741 PMID: 21412432

40. Keebaugh ES, Schlenke TA. Insights from natural host–parasite interactions: The Drosophila model. Dev Comp Immunol. 2014; 42: 111–123. doi: 10.1016/j.dci.2013.06.001 PMID: 23764256

41. Krzemien J, Oyallon J, Crozatier M, Vincent A. Hematopoietic progenitors and hemocyte lineages in the Drosophila lymph gland. Dev Biol. 2010; 346: 310–319. doi: 10.1016/j.ydbio.2010.08.003 PMID: 20707995

42. Kacsoh BZ, Schlenke TA. High Hemocyte Load Is Associated with Increased Resistance against Parasitoids in Drosophila suzukii, a Relative of D. melanogaster. PLoS ONE. 2012; 7: e34721. doi: 10.1371/journal.pone.0034721 PMID: 22529929

43. Sorrentino RP, Melk JP, Govind S. Genetic Analysis of Contributions of Dorsal Group and JAK-Stat92E Pathway Genes to Larval Hemocyte Concentration and the Egg Encapsulation Response in Drosophila. Genetics. 2004; 166: 1343–1356. PMID: 15082553

44. Reyes-DelaTorre A, Teresa M, Rafael J. Carbohydrate Metabolism in Drosophila: Reliance on the Disaccharide Trehalose. In: Chang C-F, editor. Carbohydrates—Comprehensive Studies on Glycobiology and Glycotechnology. InTech; 2012. Available: http://www.intechopen.com/books/carbohydrates-comprehensive-studies-on-glycobiology-and-glycotechnology/carbohydrate-metabolism-in-drosophila-reliance-on-the-disaccharide-trehalose

45. Ayres JS, Schneider DS. The role of anorexia in resistance and tolerance to infections in Drosophila. PLoS Biol. 2009; 7: e1000150–e1000150. doi: 10.1371/journal.pbio.1000150 PMID: 19597539

46. Machado J, Abdulla P, Hanna WJB, Hilliker AJ, Coe IR. Genomic analysis of nucleoside transporters in Diptera and functional characterization of DmENT2, a Drosophila equilibrative nucleoside transporter. Physiol Genomics. 2007; 28: 337–347. PMID: 17090699

47. Brand a H, Perrimon N. Targeted gene expression as a means of altering cell fates and generating dominant phenotypes. Dev Camb Engl. 1993; 118: 401–415.

48. Peters A, Schweiger U, Pellerin L, Hubold C, Oltmanns KM, Conrad M, et al. The selfish brain: competition for energy resources. Neurosci Biobehav Rev. 2004; 28: 143–180. PMID: 15172762

49. Straub RH. Insulin resistance, selfish brain, and selfish immune system: an evolutionarily positively selected program used in chronic inflammatory diseases. Arthritis Res Ther. 2014; 16: S4. doi: 10.1186/ar4688 PMID: 25608958

50. Mondal BC, Mukherjee T, Mandal L, Evans CJ, Sinenko SA, Martinez-Agosto JA, et al. Interaction between differentiating cell- and niche-derived signals in hematopoietic progenitor maintenance. Cell. 2011; 147: 1589–1600. doi: 10.1016/j.cell.2011.11.041 PMID: 22196733

51. Morin-Poulard I, Vincent A, Crozatier M. The Drosophila JAK-STAT pathway in blood cell formation and immunity. JAK-STAT. 2013; 2: e25700. doi: 10.4161/jkst.25700 PMID: 24069567

52. Makki R, Meister M, Pennetier D, Ubeda J-M, Braun A, Daburon V, et al. A short receptor downregulates JAK/STAT signalling to control the Drosophila cellular immune response. PLoS Biol. 2010; 8: e1000441–e1000441. doi: 10.1371/journal.pbio.1000441 PMID: 20689801

53. Andersen S. The roles of insulin and hyperglycemia in sepsis pathogenesis. J Leukoc Biol. 2004; 75: 413–421. PMID: 14657207

54. Faulhaber-Walter R, Jou W, Mizel D, Li L, Zhang J, Kim SM, et al. Impaired Glucose Tolerance in the Absence of Adenosine A1 Receptor Signaling. Diabetes. 2011; 60: 2578–2587. doi: 10.2337/db11-0058 PMID: 21831968

55. Figler RA, Wang G, Srinivasan S, Jung DY, Zhang Z, Pankow JS, et al. Links Between Insulin Resistance, Adenosine A2B Receptors, and Inflammatory Markers in Mice and Humans. Diabetes. 2011; 60: 669–679. doi: 10.2337/db10-1070 PMID: 21270276

56. Németh ZH, Csóka B, Wilmanski J, Xu D, Lu Q, Ledent C, et al. Adenosine A2A Receptor Inactivation Increases Survival in Polymicrobial Sepsis. J Immunol. 2006; 176: 5616–5626. PMID: 16622031

57. Sullivan GW, Fang G, Linden J, Scheld WM. A2A Adenosine Receptor Activation Improves Survival in Mouse Models of Endotoxemia and Sepsis. J Infect Dis. 2004; 189: 1897–1904. PMID: 15122527

58. Bligh EG, Dyer WJ. A rapid method of total lipid extraction and purification. Can J Biochem Physiol. 1959; 37: 911–917. PMID: 13671378

59. Tennessen JM, Barry W, Cox J, Thummel CS. Methods for studying metabolism in Drosophila. Methods. 2014; 68: 105–115. doi: 10.1016/j.ymeth.2014.02.034 PMID: 24631891

Paper IV

Separation and identification of lipids in the photosynthetic cousins of Apicomplexa *Chromera velia* and *Vitrella brassicaformis*.

Tomčala, A., Kyselová, V., Schneedorferová, I., Opekarová, I., Moos, M., Urajová, P., Kručinská, J., Oborník, M.

Journal of Separation Science, 40: 3402–3413

2017

ISSN 1615-9306 · JSSCCJ 40 (17) 3369–3564 (2017) · Vol. 40 · No. 17 · September 2017 · D 10609

JSS

JOURNAL OF

SEPARATION SCIENCE

17|17

VOLUME 40

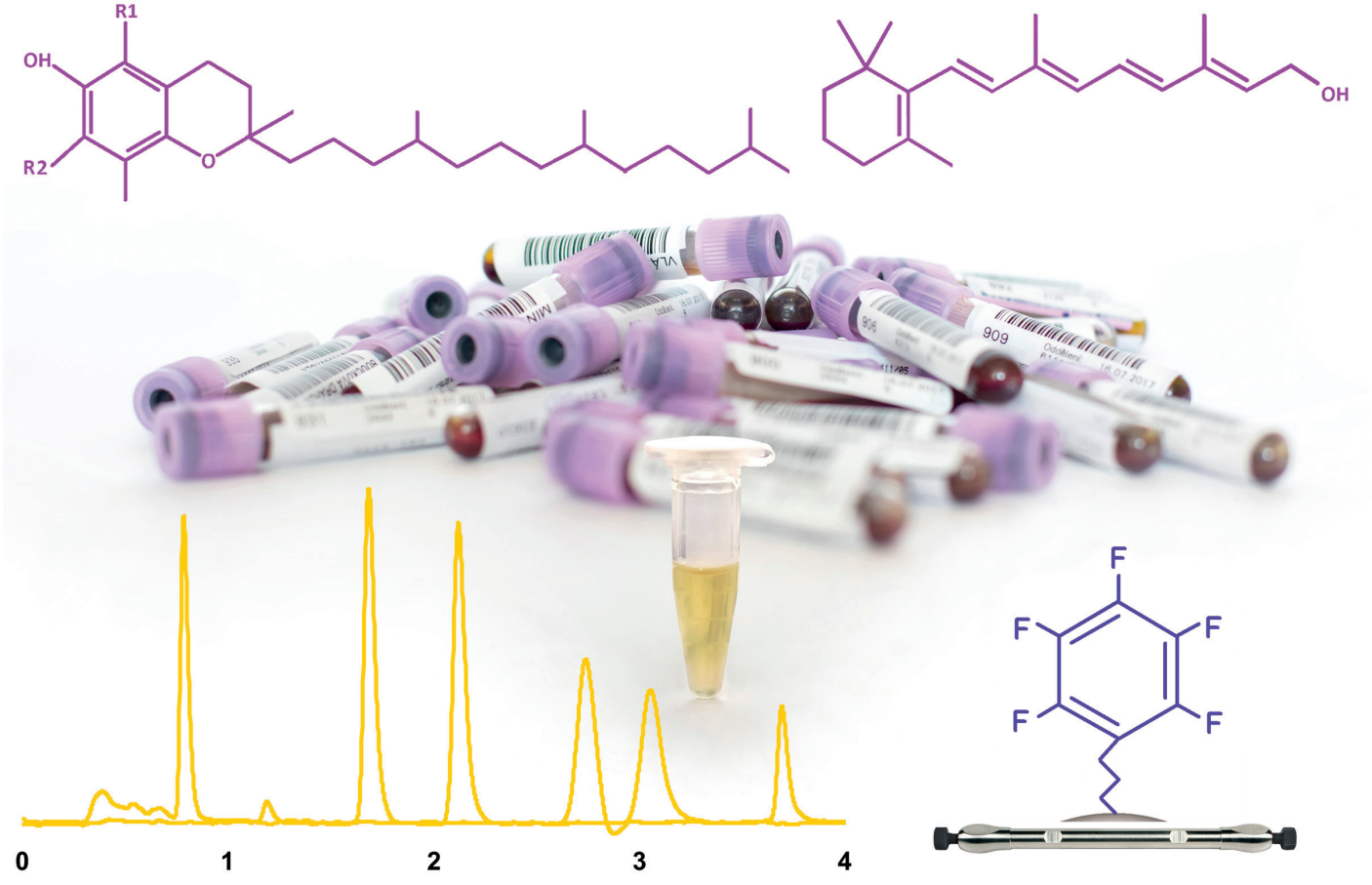

Methods
Chromatography · Electroseparation

Applications
Biomedicine · Foods · Environment

www.jss-journal.com

WILEY-VCH

Received: 13 February 2017 | Revised: 31 May 2017 | Accepted: 23 June 2017

DOI: 10.1002/jssc.201700171

RESEARCH ARTICLE

JOURNAL OF SEPARATION SCIENCE

Separation and identification of lipids in the photosynthetic cousins of Apicomplexa *Chromera velia* and *Vitrella brassicaformis*

Aleš Tomčala[1] | Veronika Kyselová[1,2] | Ivana Schneedorferová[1,2] | Iva Opekarová[3,4] | Martin Moos[3] | Petra Urajová[5] | Jitka Kručinská[1,2] | Miroslav Oborník[1,2,5]

[1]Biology Centre CAS, v.v.i., Institute of Parasitology, Laboratory of Evolutionary Protistology, České Budějovice, Czech Republic

[2]Faculty of Science, University of South Bohemia, České Budějovice, Czech Republic

[3]Biology Centre CAS, v.v.i., Institute of Entomology, Laboratory of Analytical Biochemistry, České Budějovice, Czech Republic

[4]University of Chemistry and Technology, Faculty of Food and Biochemical Technology, Department of Chemistry of Natural Compounds, Prague, Czech Republic

[5]Institute of Microbiology CAS, Laboratory of Algal Biotechnology, Třeboň, Czech Republic

Correspondence
Dr. Aleš Tomčala, Biology Centre CAS, v.v.i., Institute of Parasitology, Laboratory of Evolutionary Protistology, Branišovská 31, 370 05 České Budějovice, Czech Republic.
Email: a.tomcala@centrum.cz

The alveolate algae *Chromera velia* and *Vitrella brassicaformis* (chromerids) are the closest known phototrophic relatives to apicomplexan parasites. Apicomplexans are responsible for fatal diseases of humans and animals and severe economic losses. Availability of the genome sequences of chromerids together with easy and rapid culturing of *C. velia* makes this alga a suitable model for investigating elementary biochemical principals potentially important for the apicomplexan pathogenicity. Such knowledge allows us to better understand processes during the evolutionary transition from a phototrophy to the parasitism in Apicomplexa. We explored lipidomes of both algae using high-performance liquid chromatography with mass spectrometry or gas chromatography with flame ionization detection. A single high-performance liquid chromatography with mass spectrometry analysis in both ionization modes was sufficient for the separation and semi-quantification of lipids in chromerid algae. We detected more than 250 analytes belonging to five structural lipid classes, two lipid classes of precursors and intermediates, and triacylglycerols as storage lipids. Identification of suggested structures was confirmed by high-resolution mass spectrometry with an Orbitrap mass analyzer. An outstandingly high accumulation of storage triacylglycerols was found in both species. All the investigated aspects make *C. velia* a prospective organism for further applications in biotechnology.

KEYWORDS

Chromera velia, glycerolipids, mass spectrometry, *Vitrella brassicaformis*

1 | INTRODUCTION

Chromera velia [1] and *Vitrella brassicaformis* [2] known as chromerids were isolated from stony corals in Australia. Even though both organisms are photosynthetic, accumulating phylogenetic evidence [1] revealed their close relationship with parasitic Apicomplexa. Such phylogenetic position is also supported by other features such as the presence of cortical alveoli [1] and a pseudoconoid [3], non-canonical code for tryptophan in plastid-encoded proteins [1,4], and non-canonical arrangement of heme pathway with δ-aminolevulinate synthesized by the mitochondrial C4 pathway [5]. Recent analyses of chromerid genomes and

Abbreviations: CCA, constrained correspondence analysis; CID, collision-induced dissociation; DGDG, digalactosyldiacylglycerols; DGTS, diacylglyceryltrimethylhomoserine; FA, fatty acid; FAME, methyl esters of fatty acids; FID, flame ionization detection; HRMS, high-resolution mass spectrometry; LD, lipid droplet; LysoDGTS, lyso diacylglyceryltrimethylhomoserine; MGDG, mogalactodiacylglycerol; PC, phosphatidylacholine; PG, phosphatidylglycerol; RDA, redundancy analysis; SQDG, sulfoquinosyldiacylglycerol; TG, triacylglycerol

Conflict of interest: The authors have declared no conflict of interest.

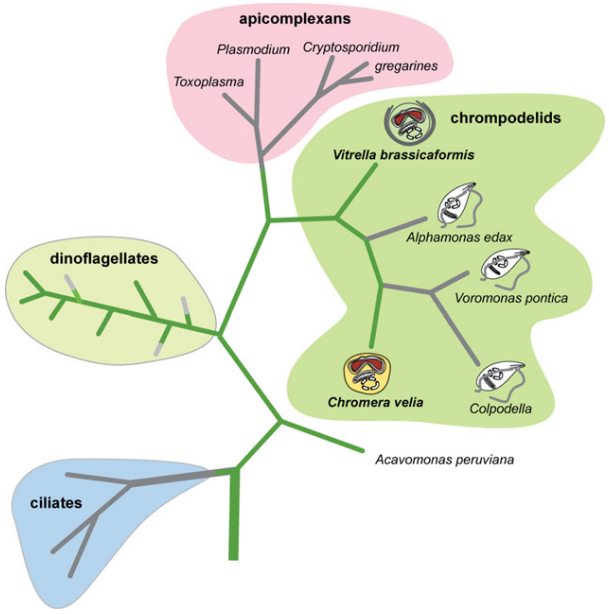

FIGURE 1 Phylogeny of chromerids and their relatives (modified according to Oborník and Lukeš 2015)

transcriptomes defined chromerids as a polyphyletic group of alveolate phototrophs forming a monophyletic clade with colpodellids, microscopic marine predators, with the entire group called chrompodellids [6] (Fig. 1).

In apicomplexan parasites, lipids are located to the cytoplasmic membrane and membrane of the apicoplast. Microscopic studies also revealed a presence of small cytoplasmic lipid structures of 0.1–1.5 μm in diameter in *Plasmodium falciparum*. The accumulation of such lipid inclusions filled with triacylglycerols (TGs) increases with the maturation of trophozoites [7]. The membrane lipidome of apicomplexan parasites is composed of glycerolipids, sphingolipids, and sterols. Glycerolipids are prevailing, mainly in the form of phospholipids such as phosphatidylcholine, phosphatidylethanolamine, phosphatidylserine, phosphatidylinositol, and phosphatidylglycerol (PG). Parasites uptake these phospholipids from a host [8]. In contrast, synthesis of plastid galactolipids in *Toxoplasma gondii* and *P. falciparum* parasites, namely digalactosyldiacylglycerols (DGDG), was reported [9]. However, the HPLC–MS/MS studies of purified apicoplast of *P. falciparum* did not reveal any detectable traces of galactolipids. It seems that the evolution of an apicomplexan ancestor to the parasite was accompanied by a replacement of galactolipids essential for photosynthetic membranes with phospholipids. This replacement is complicated by the loss of ability to synthesize phospholipids in the phototrophic ancestor of Apicomplexa, so, parasites must scavenge phospholipids from their hosts. Phosphatidylcholines cover almost 50% of all structural lipids in Apicomplexa, followed by phosphatidylethanolamines with 30% [10].

Typical photosynthetic membranes in biological entities from cyanobacteria to plastids of seed plants consist of mogalactodiacylglycerol (MGDG), DGDG as major components and by anionic PG and sulfoquinosyldiacylglycerol (SQDG) providing a negatively charged lipid–water interface [11]. Broad separation techniques are employed to isolate intact lipids from the crude lipid plant or algal extract, for instance, TLC [11–13] and SPE [14–16]. However, reverse HPLC is the most preferred [15,17–24]. For better separation of the particular lipid species, a combination of the methods mentioned above is also occasionally applied [15,16,24]. Analytical methods utilized for a lipidome analysis should provide information concerning lipid classes, lipid species, localization of the fatty acyl chain in the glycerol backbone [12], and the localization of particular double bonds in fatty acid (FA). The detection of particular lipids is provided by means of light chemistry: UV detector [15], IR detector [23], diode array detector [21], and evaporative light scattering detector [25]. Structure elucidation is then completed by NMR spectroscopy [11,14,21,22] and/or by means of MS/MS with different ionization techniques including matrix-assisted laser desorption [22], fast atom bombardment [26], atmospheric-pressure chemical ionization (APCI) [16], but mostly by ESI [12,16,17,19–21,23,24,27]. Fragmentation of MGDG and DGDG sodium adducts provides information about the *sn*-position of particular FA [17,21,22,24,28]. Xu and coworkers showed that FA attached to the *sn*-2 position is preferably cleaved from the deprotonated SQDG [17]. The position of a double bond in a fatty acid chain is usually investigated by GC with flame ionization detection (FID). Derivatization of intact molecules to methyl esters of fatty acids (FAME) is essential for this technique [21].

The lipid composition of thylakoid membranes in *C. velia* plastid was investigated by Botté and colleagues [27]. Using HPTLC, they showed an occurrence of three lipid classes in *C. velia*: MGDG, DGDG, and SQDG. An accurate structural determination of the first two classes was later completed by the use of sodium adducts MS in positive mode ESI [28]. Three species of MGDG and four species of DGDG were described. Some of these lipids occurred only in cultures grown in a higher cultivation temperature (30°C). The synthetic pathway of galactolipids was also proposed: the glycerol backbone is assembled in the lumen of the endoplasmic reticulum in the form of phosphatidylcholine and subsequently transported to the lumen of plastid, where the synthesis of galactolipids is finished [28]. However, further mass spectrometric studies of *C. velia* and *V. brassicaformis* lipidome have not been published yet.

TEM of *C. velia* cells [3] revealed the presence of lipid droplets (LDs) in the cytoplasm. A structural model of LDs was originally proposed for maize grains in 1992 [29] but seems to hold true for LDs isolated from divergent kingdoms [30]. Such LD usually consists of a storage neutral lipid

core mostly represented by TGs surrounded by a monolayer of structural polar lipids, usually phosphatidylcholines, and decorated by proteins. It was shown that lipids containing sulfur (SQDG) or nitrogen i.e. diacylglyceryltrimethylhomoserine (DGTS) are likely to replace phospholipids in a membrane in the phosphorus deficient environment: in the microsymbiotic α-proteobacterium *Rhizobium meliloti de novo* synthesis of structural DGTS lipids was observed when phosphate was the limiting factor for growth [31,32]. In eukaryotes, synthesis of DGTS molecules was reported in green (primary) algae such as chlorophytes and prasinophytes [33], and in algae with secondary red-derived plastids, particularly eustigmatophytes [34], haptophytes [35], and diatoms [36], again in the phosphorus-limited environment. In the mentioned algae, betaine lipids were obviously present not only in the plastid envelope but also in other cellular membranes [35]. For the separation of betaine lipids (DGTS), TLC is usually used followed by fast atom bombardment [26], with the determination and quantification of DGTS achieved by ESI-MS [36–39].

The aim of this study was an investigation of lipidomes of chromerid algae *C. velia* and *V. brassicaformis* as inferred by HPLC–(ESI)-MS/MS in a single analysis. We determined the *sn*-positions of particular galactolipids by an additional experiment with sodium adducts fragmentation in the case of MGDG and DGDG. The position of a double bond in the FA carbon chain was investigated through the GC–FID technique. The introduced methodology represents an easy and efficient method for routine algal or plant lipid measurements in a single analysis.

2 | MATERIALS AND METHODS

2.1 | Growth conditions

C. velia and *V. brassicaformis* cultures were grown in the f/2-enriched seawater medium (Marine Reef Salt, Sera, Heinsberg, Germany) under artificial light with a photoperiod 12h/12h and light exposure 30–50 μmol/m^2/s and at a temperature of 26°C. One mL of *C. velia* stationary culture was added to each 25 cm^2 flask with 40 mL of f/2 solution. The cultures were grown for 70 days and harvested by centrifugation. Pellets were stored at −20°C for lipid extraction.

2.2 | BODIPY® marker staining

Cells were harvested by filtration and subsequent gentle centrifugation (1000 rcf) for 10 min. The supernatant was removed, and the visible pellet was mixed with 1 mL of phosphate buffer saline. BODIPY® (Thermo Fisher) staining solution was added (1 μL/1 mL) and the microtube was covered in aluminum foil to prevent bleaching of the dye. The cells were incubated for approximately 12 h in 26°C. The confocal microscopes, Olympus FluoView^{TM} FV1000 and Imaris software (Olympus, Japan), were employed for BODIPY® visualization.

2.3 | Lipids extraction

Lipids were extracted with chloroform and methanol solution modified by Košťál and Šimek [40]. Homogenization of the algal sample was achieved by TissueLyser LT (Qiagen, Hilden, Germany) and glass beads in extraction solution. Homogenates were dried, weighted, and resolved in 500 μL of chloroform and methanol (1:1). From each sample extract, 100 μL aliquots were used for the lipid determination.

2.4 | Lipids HPLC

The liquid chromatograph Accela (Thermo Fisher Scientific, San Jose, CA, USA) was used for HPLC. The samples (5 μL) were injected and separated on the Gemini column 250 × 2 mm; id 3 μm (Phenomenex, Torrance, CA, USA). The mobile phase consisted of (A) 5 mM ammonium acetate in methanol, (B) water, and (C) 2-propanol. The analysis was completed within 85 min with a flow rate of 250 μL/min by the following gradient: 0–5 min 92% A and 8% B, 5–12 min 100% A, 12–50 min 100–40% A and 0–60% C, 50–65 min 40% A and 60% C, and 65–85 min back to the 92% A and 8% B. Column temperature was 30°C and autosampler temperature 15°C.

2.5 | Lipids TLC

TLC methodology was used for excluding the presence of phosphatidylacholine (PC) in *C. velia* lipid extracts. The detailed description of this technique was published by Zahradnickova and colleagues [41], the shorter version follows: TLC plates were washed step by step with methanol, chloroform/methanol (2:1, v/v), and hexane. After drying, the samples were applied to TLC plates and then washed several times in MP I (hexane/diethyl ether/acetic acid, 80:18:2, v/v/v) to remove neutral lipids. The samples were developed gradually in two MPs—MP II consisting of chloroform/methanol/acetic acid/water (60:35:2:1, v/v/v/v), developing path 9 cm, and MP III containing chloroform/methanol/acetic acid/water (50:30:8:4, v/v/v/v), developing path 6 cm. The spots of phospholipids were visualized by iodine vapors.

2.6 | Lipids MS

Linear ion trap LTQ-XL mass spectrometer (Thermo Fisher Scientific, San Jose, CA, USA) was used in both positive and negative ion ESI mode detection with the following settings: capillary temperature of 250°C, vaporizer temperature of 320°C, capillary voltage ±3,5 kV, nitrogen served as a

sheath gas (15) and auxiliary gas (5). The full scan lipid spectra were collected in the range 140–1400 Da with spectra rate 2 Hz. For the dependent MS/MS experiments, the collision-induced dissociation (CID) energy was 35 eV for both polarities.

The high-resolution information was obtained by Orbitrap Q-Exactive Plus with Dionex Ultimate 3000 XRS pump and Dionex Ultimate 3000 XRS Open autosampler (all by Thermo Fisher Scientific). The Orbitrap spectrometer was set as follows: the spray voltage was 3 kV in positive mode with probe temperature 350°C, capillary temperature 250°C, and S-Lens level at 60. Nitrogen was employed as sheath gas (30), auxiliary gas (10), and sweep gas (1). Mass range 400–1100 Da was scanned with resolving power 70 000 and $3{\cdot}10^6$ automatic gain control target and maximum ion injection time was 100 ms.

The data from both instruments were acquired and processed using Xcalibur software version 2.1 (Thermo Fisher Scientific, San Jose, CA, USA). Phosphatidylcholine 17:0/17:0 was used as an internal standard. The fragmentation patterns and quantification of particular lipid classes were studied by the external standards SQDG, DGDG, MGDG, and PG (all Larodan, Solna, Sweden), DGTS 16:0/16:0 (Avanti Polar Lipids, Inc., Alabama, USA), TG 14:0/18:1/16:0, and DG 16:0/18:0 (Sigma–Aldrich).

2.7 | Fatty acids GC–FID

Raw lipid extract was transformed to the FAMEs to enable the application of the GC technique. For this purpose, sodium methoxide was employed as a transesterification reagent, as described previously [41]. FAMEs were then analyzed by GC–FID. Hexacosane ($C_{26}H_{54}$) (Sigma–Aldrich–Supelco, St. Louis, MO, USA) was chosen as an internal standard. Chromatography was performed using the gas chromatograph GC–2014 (Shimadzu Corporation, Kyoto, Japan) equipped with column BPX70 (SGE, Victoria, Australia) 0.22 mm ID; 0.25 μm film; 30 m length. One μL of the derivatized sample was injected by an autosampler AOC—20i (Shimadzu Corporation, Kyoto, Japan) and applied on a column in a split mode (split ratio 10). The temperature of the injector was 220°C. The starting temperature of the column was 120°C and maintained for 4 min. Then the temperature was increased to 180°C at a rate of 10°C per min, and after that to 230°C at a rate of 7°C per min. FID temperature was 260°C. The whole analysis took approximately 20 min. Hydrogen was used as a carrier gas. A mixture of 37 standards purchased from Supelco was used for the identification of particular FAs.

2.8 | Multivariate analysis

The obtained glycerolipids peak areas were statistically evaluated using ordination methods as follows: for all data—detrended correspondence analysis; for linear data—redundancy analysis (RDA), Monte-Carlo permutation test (unrestricted permutations, $n = 999$), and for unimodal data—constrained correspondence analysis (CCA), Monte-Carlo permutation test (unrestricted permutations, $n = 999$). The data was transformed by using internal standard peak area of the particular sample. For each, the transformed peak areas were calculated in the deconvoluted total sample and peak area. In the canonical analysis (RDA, CCA) the species stood as a categorical predictor. Monte-Carlo permutation test was used to statistical significance determination. Statistic software CANOCO 4.5 (Biometrics, Plant Research International, Wageningen UR, Netherlands) was used for the detrended correspondence analysis, CCA, RDA, and Monte-Carlo permutation test analyses.

3 | RESULTS AND DISCUSSION

3.1 | The separation of lipid species in a single run

HPLC of crude extract from chromerid algae allowed the separation of structural and storage lipid species in a single run. The separation of structural lipids was accomplished after 17 min of the procedure (Supporting Information Fig. S1), and the whole process took 80 min. This time seems to be quite long but methods introduced by Zábranská and coworkers [24] are comparably time-consuming: their methodology requires two 80 min runs for separation of particular MGDG and DGDG. Also, separation of galactolipids using TLC [28] followed by LC–MS set to neutral loss scanning mode takes more time [27]. TLC is a very robust method, however, in recent separation technique articles, it is usually replaced by HPLC to save time and work [41]. In our analyses, the elution of lyso diacylglyceryltrimethylhomoserine (LysoDGTS) was followed by the release of the rest of the structural lipids (Fig. S1). The particular lipid species were determined by *m/z* record and retention time; however, some lipid classes gave similar mass to charge ratio (*m/z*) values at different retention times. For instance, *m/z* 744 Da corresponds to MGDG 32:2 or PG 34:3 or DGTS 35:5. More information is needed for the classification of particular lipid classes. The ammonium environment enables all detected structural lipids to provide ions in both ionization modes. Therefore, sufficient data was produced by the behavior of a particular lipid class in positive and negative ionization mode. Ammonium acetate gave a rise of ammonium adduct ions of MGDG, DGDG, and SQDG in positive mode (Table 1), as also reported in *C. velia* and tobacco leaf [20,27], and acetate adduct in negative mode of MGDG, DGDG, and PG. On the other hand, protonated ions are typical for DGTS and deprotonated ions for SQDG and PG (Table 1). Deprotonated ions of SQDG and PG were described in diatom *Stephanodiscus* sp. [17].

TABLE 1 The ionization and fragmentation behavior of particular lipid classes

	ESI+				ESI−				
Lipid class	**Full scan**		**MS MS**		**Full scan**		**MS MS**		**See more**
MGDG	[M+NH_4]	[M+18]	[M+NH_4–sugar]	[M–179]	[M+CH_2COO]	[M+59]	[M–H]	[M+59–60]	Fig. 2
			[M–sugar–R2COOH]		[M–H]	[M–1]			
			[M–sugar–R1COOH]						
DGDG	[M+NH_4]	[M+18]	[M+NH_4–sugar]	[M–341]	[M+CH_2COO]	[M+59]	[M–H]	[M+59–60]	Suppl Fig. 2
			[M–sugar–R2COOH]		[M–H]	[M–1]			
			[M–sugar–R1COOH]						
SQDG	[M+NH_4]	[M+18]	[M–sugar]	[M–261]	[M–H]	[M–1]	[M–R2COOH]		Suppl Fig. 3
			[M–sugar–Rx]		[M+CH_2COO]	[M+59]	[M–R1COOH]		
			[M–MG]						
			[M–sugar–MG]						
PG	[M+NH_4]	[M+18]	[M]		[M–H]	[M–1]	[M–R2COOH]		Suppl Fig. 4
							[M–R1COOH]		
							[RxCOO]		
DGTS	[M+H]	[M+1]	[M–R2CH = O]		[M+CH_2COO]	[M+59]	[M–H]	[M+59–60]	Suppl Fig. 5
			[M–RxCOOH]						
LysoDGTS	[M+H]	[M+1]	[M–R2CH = O]		[M+CH_2COO]	[M+59]			
			[M–DG]						
DG	[M+NH_4]	[M+18]	[M–RxCOOH]		–				
TG	[M+NH_4]	[M+18]	[M–RxCOOH]		–				

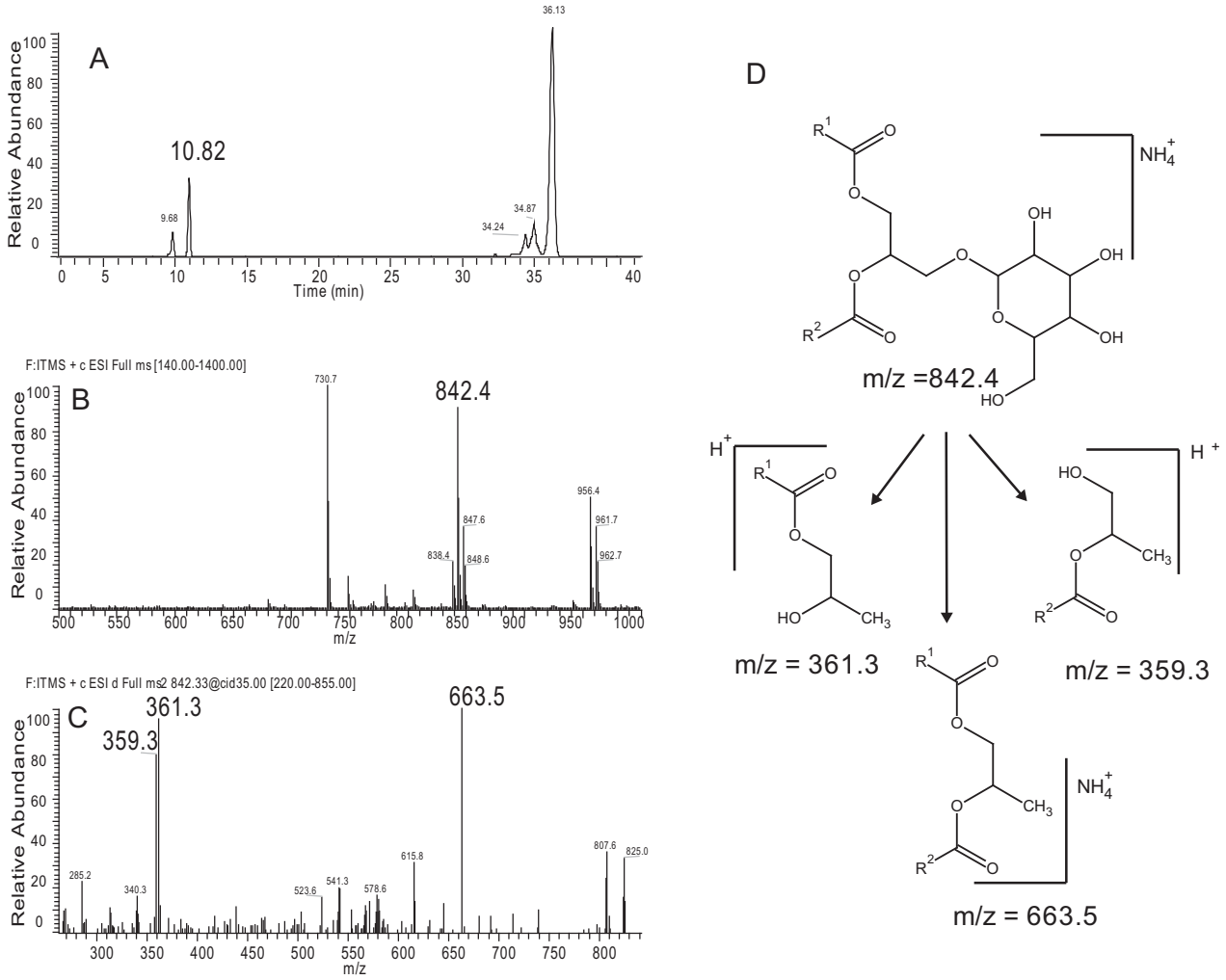

FIGURE 2 (A) Extracted chromatogram of *m/z* 842.4 Da corresponding to MGDG 20:5/20:4 in retention time 10.82 min. (B) Full MS spectrum for MGDG 20:5/20:4. (C) MS^2 spectrum *m/z* 842.4 Da (10.82 min). (D) Proposed fragmentation pattern of MGDG (ESI^+). All data obtained from *C. velia*

3.2 | The fragmentation of glycerolipids

The ionization and fragmentation behavior of particular glycerolipid classes is summarized for clarity in Table 1, particular glycerolipid fragmentation patterns are in Fig. 2 and Figs. S2–S5.

3.2.1 | Monogalactodiacylglycerols

The ionization of MGDG in the mobile phase contains ammonium acetate provided ions in both ionization modes (Fig. 2). An ammonium environment was also used by Li and colleagues, and Botté and colleagues [20,27]. In our analysis, the positive mode was represented by the ammonium adduct of MGDG $[M+18]^+$, the negative mode provided an acetate adduct of MGMG $[M+59]^-$ and a deprotonated ion of MGDG $[M-1]^-$. The signal of an ammonium adduct ion was approximately two hundred times more intensive than the deprotonated molecular ion and four times higher than the acetated ions. The positive fragmentation pattern provided sufficient information for the determination of the identity of attached FAs. The positive fragmentation resulted in the formation of the dominant ion *m/z* = 663.5 Da (Fig. 2; ammonium ion of the diacylglycerol molecule) indicating a loss of sugar moiety. The other ions (361.3, 359.3 Da) correspond to the protonated monoacylglycerol fragments with C20:4 and C20:5, respectively (for details see Fig. 2). Similar fragmentation of MGDG from *C. velia* was previously described [27]. The negative MS^2 spectrum also provided information concerning FAs identities. Deprotonated ions of particular FAs were observed (data not shown), which was also described in wheat MGDG [19].

3.2.2 | Digalactosyldiacylglycerols

The behavior of DGDG in the mobile phase containing ammonium acetate was the same as MGDG and provided ions in both ionization modes. The positive mode was

represented by the ammonium ion of DGDG $[M+18]^+$, negative mode gave a dominating acetate ion of DGDG $[M+59]^-$ and also a deprotonated ion of DGDG $[M-1]^-$. The response of the DGDG molecule in the positive mode was approximately four times greater than in the negative ionization in acetate ion form and more than three hundred times higher than the deprotonated ion. Positive ionization mode provided an easily readable fragmentation pattern of each particular DGDG molecule (Fig. S2). CID fragmented the molecules of DGDG to a sugar moiety (loss of 341 Da), and to the FA with a glycerol backbone. It is noticeable that the fragmentation patterns are similar for DGDG and MGDG, as was also described in sodium adducts of lipids in the diatom *Stephanodiscus* sp. [17], the dinoflagellate *Glenodinium sanguineum* [22] and in ammonium adducts of *C. velia* [27].

3.2.3 | Sulfoquinovosyldiacylglycerols

SQDG records were in chromerids provided in both polarities (Supporting Information Fig. S3). The positive mode was represented by the ammonium ion of SQDG $[M+18]^+$ and the negative mode was illustrated by the deprotonated ion of SQDG $[M-1]^-$. The intensities of positive and negative ions were comparable but slightly higher in the positive mode. Both polarity modes MS^2 experiments provided characteristic fragmentation patterns. Fragmentation in the positive mode provided three types of ions by the loss of sugar compound, ammonium carboxylic acid, and protonated carboxylic acid with a glycerol backbone. Negative MS^2 experiments gave two ions corresponding to losses of carboxylic acid from in the *sn*-1 position and from the *sn*-2 position, with the latter ion dominating, as reported for the diatom *Stephanodiscus* sp. [17].

3.2.4 | Phosphatidylglycerols

The behavior of PG in both positive and negative ionization mode was comparable with SQDG as it provided an ammonium adduct of PG $[M+18]^+$ and deprotonated ion in negative mode $[M-1]^-$, which was reported in the green alga *C. reinhardtii* [30]. Despite the fact that positive ionization provided three times more intense ion in the positive MS^2 experiment, it gave a rise of only protonated PG $[M+1]^+$ and was, therefore, not suitable for FA acyl characterization. Negative MS^2 experiments produced two major types of ions (Supporting Information Fig. S4), corresponding to a loss of acylium ion and a deprotonated FA. More intense loss of acylium ions originated from the *sn*-2 position. Such fragmentation patterns were also previously described in the soil bacterium *Sinorhizobium meliloti* [12] and the diatom *Stephanodiscus* sp. [17].

3.2.5 | Diacylglyceroletrimethylhomoserines

DGTS were ionized as protonated molecules in the positive ionization and as acetate adducts in the negative ionization mode. Positive ionization produced only protonated ions; the sodium adduct was not observed contrary to the literature [42]. The ions formed in the positive ionization mode were more intensive than the ions from the negative one. Therefore, the structure elucidation was performed by positive mode ionization MS^2 experiments in chromerids (Fig. S5). CID MS^2 scans of the $[M+H]^+$ precursor led to the two cleavage types. The first involves the loss of FA constituent at *sn-1* and *sn-2* position $[M+H-RCOOH]^+$. The second cleavage type arises from the instability of α-hydrogen in *sn-2* position, resulting in the more favorable formation of the $[M+H-R2-CH=O]^+$ ketene ion. The same fragmentation was also described in *C. reinhardtii* and [30] and in soil amoeba *Acanthamoeba castellanii* [26]. Negative ionization mode provided arise of the acetate adduct of DGTS $[M+59]^-$ and the MS^2 spectrum clearly shows the loss of acetate. The CID MS^3 technique is required for FA determination.

3.2.6 | Fragmentation of storage lipids

TGs do not possess any ionizable functional group, and only adducts with sodium or ammonia were observed in their ESI spectra. In mobile phases containing ammonium ion species, only ammonium adducts of TGs were detected in the positive ESI. The molecular weight of each TG determined the number of carbons and double bonds present in the investigated molecule. CID of $[M+NH_4]^+$ ions led to the neutral loss of NH_3 (i.e. $[M+H]^+$was observed), and acyl sidechain (carboxylic acid) generated a diacylglycerol product ion ($[M-RCOO]^+$). This fragmentation was characteristic for all molecular species of TG in chromerids and also for the precursor of DG (data not shown). The *sn*-position of a particular FA attached to a glycerol core was hard to examine by the ESI-MS method in chromerid algae. Additional information may be provided by a silver-ion HPLC [43] or ionization by APCI with a linear ion trap. The full scan TG in APCI showed very similar features, such as ESI MS^2 records as documented in the literature, e.g. [44].

3.3 | Lipidome of *C. velia* and *V. brassicaformis*

MS/MS provided a lipidomic record of glycerolipids from chromerids. In total, we detected 13 and 14 species of DGDG, 6 and 15 of MGDG, 3 and 2 of PG, 8 and 11 of SQDG, 20 and 13 of DGTS, 5 and 3 of LysoDGTS, 19 and 17 of DG, and 162 and 159 of TG in *C. velia* and *V. brassicaformis*, respectively (Table S1). The total yields of these lipids were 257 +/– 25 mg of lipid per 1 g dry mass of *C. velia* and 138 +/–16 mg of *V. brassicaformis* ($n = 5$). Previous work detected less MGDG and DGDG species in chromerids [45]; this might be caused by the better response of ammonium ions (Fig. S6). The mentioned lipid classes were identified by fragmentation patterns of particular molecules. Detected lipids are listed in Supporting Information Table S1. To prevent

misinterpretations of data, a high-resolution mass spectrometry (HRMS) Orbitrap mass analyzer was employed (Fig. S7). The double bond position was determined by GC–FID (Fig. S8). The quantification was achieved by a cocktail of external standards measured in six concentration levels. This quantification also provided a correction factor for particular lipid class ionization features. Proper quantification could be achieved by internal standard administration to prevent matrix effects; however, internal standards with appropriate FAs are not commercially available. Furthermore, this work is aimed for lipid species determination and description of fragmentation patterns rather than their quantification.

3.3.1 | Fatty acid composition

FAs from chromerids varied in length from 14 to 20 carbons with palmitic acid as the dominating compound (Supplementary Fig. 8). Two forms of monosaturated C16:1 (n-7 and n-9) were found in *C. velia*, but C16:1 n-9 was missing from *V. brassicaformis*. FA C16:1 n-7 occurs more commonly in chlorophytes [46], dinoflagellates [47], and diatoms [48]. However, FA C 16:1 n-9 has been detected only in diatoms so far and in very low amounts [48]. Monounsaturated FA with 18 carbons were recorded in both chromerids in two forms: C18:1 n-7 and C18:1 n-9. Contrary to Dahmen's group [28] presenting an identification of galactolipids with non-polyunsaturated FAs C18 in *C. velia*, FID methodology was able to found one type of FA C18:2 n-6 and two types of FA C18:3 n-6 and C18:3 n-3. All these FAs are present in different groups of marine photosynthetic organisms [46–48]. A quite high level of two essential FA, particularly arachidonic (20:4 n-6) and eicosapentaenoic (20:5 n-3) acid were recorded in all detected lipid classes of both chromerids with the exception of PG (Fig. 3). The levels of arachidonic acid were reaching more than 13% of all FA found in these alveolate algae. Such high abundance of arachidonic acid was recorded only in rhodophytes [46]. On the other hand, high amount of eicosapentaenoic acid is quite common in diatoms, dinoflagellates, and also in rhodophytes [46–48].

3.3.2 | Intact lipid molecules composition

Peak areas of intact lipids were recalculated and summarized to show the ratio of FA in particular lipid classes in chromerids. The whole process was described by Zahradníčková and coworkers [41]. Comparison of obtained data from GC–FID and recalculated data from HPLC–MS were carried out to test data deformation due to a recalculation itself (Fig. S9). The ratios of the particular FAs are comparable which was proved by RDA analysis ($p = 9.6\%$). Subtle variances can be explained by the SD and errors in the measurement. No significant differences were recorded in FA levels, however, CCA analysis of intact molecules dataset shows species-dependent differences ($p = 2.9\%$). The main glycerolipid class responsible for these differences was TG. The recalculated results (Fig. 3) demonstrate structural lipids of plastid membranes (Figs. 3A and D), structural lipids of droplet monolayer and their precursors or degradation products (Figs. 3B and E), and storage lipids and their precursors (Figs. 3C and F) in chromerids. The abundance of structural lipids responsible for the plastidial membrane formation was minor in both algae. However, *V. brassicaformis* contained three times more plastidial lipids than *C. velia*, reaching 2.6 mg of MGDGs, DGDGs, and PGs in 1 g of dry alga. From these three lipid species, DGDGs were the most abundant. Very low levels of PGs were recorded for *V. brassicaformis*; on the other hand, *C. velia* displayed surprisingly low levels of MGDGs (Figs. 3A and D). Low level of PG can be explained by a phosphorus limitation followed by the replacement of PG by SQDG; this phenomenon was described in cyanobacteria [32] and also in *C. reinhardtii* and *Arabidopsis thaliana* [49]. Low levels of MGDG in *C. velia* as inferred by high-performance TLC were recorded by Botté and colleagues [27]; however, their quantification is missing. Dahmen and coworkers [28] presented the relative abundance of MGDG ions reaching almost 40% of measured ions in *C. velia* extract, but no correction factor or other quantification approach was used. In our analyses, DGDG represented the dominating structural lipid class in *C. velia* and mostly consisted of palmitic and linoleic FA followed by 20 carbon polyunsaturated FAs. PGs were present only in unsaturated FAs reaching 18 carbons. The composition of FAs in *V. brassicaformis* was different when compared to *C. velia*, mainly due to the presence of MGDG containing myristic acid and lower abundance of FAs constituting 18 carbons chain.

Graphs B and E in Fig. 3 show DGTS, LysoDGTS, and SQDG. It is likely that as in *Chlamydomonas* and other algal species, DGTS and SQDG are responsible for the formation of the polar membrane surrounding LDs [39,42,50]. However, *V. brassicaformis* contained a significantly lower amount of storage lipids than *C. velia*, but both chromerids displayed similar levels of DGTS. Visualization of LDs in the chromerids cells using the BODIPY® marker explains this phenomenon: the experiment revealed several large LDs (marked by green) in *C. velia* (Fig. 4A) and many tiny LDs in *V. brassicaformis* (Fig. 4B). The droplets are covered by a monolayer of polar lipids, giving the vacuole shape and integrity. Therefore, a smaller droplet exhibits a higher ratio of surface area per unit of TG [51]. DGTS belongs to the betaine lipids family and the other most known are diacylglyceryl carboxyhydroxymethylcholine and diacylglyceryl hydroxymethyltrimethyl-β-alanine. No significant amounts of these betaine lipids with exception of DGTS were recorded by HPLC–MS.

The lack of PCs in chromerids is surprising but not unusual. Kato and colleagues [33] examined more than 40 species of marine algae for PC occurrence. PC were identified in all

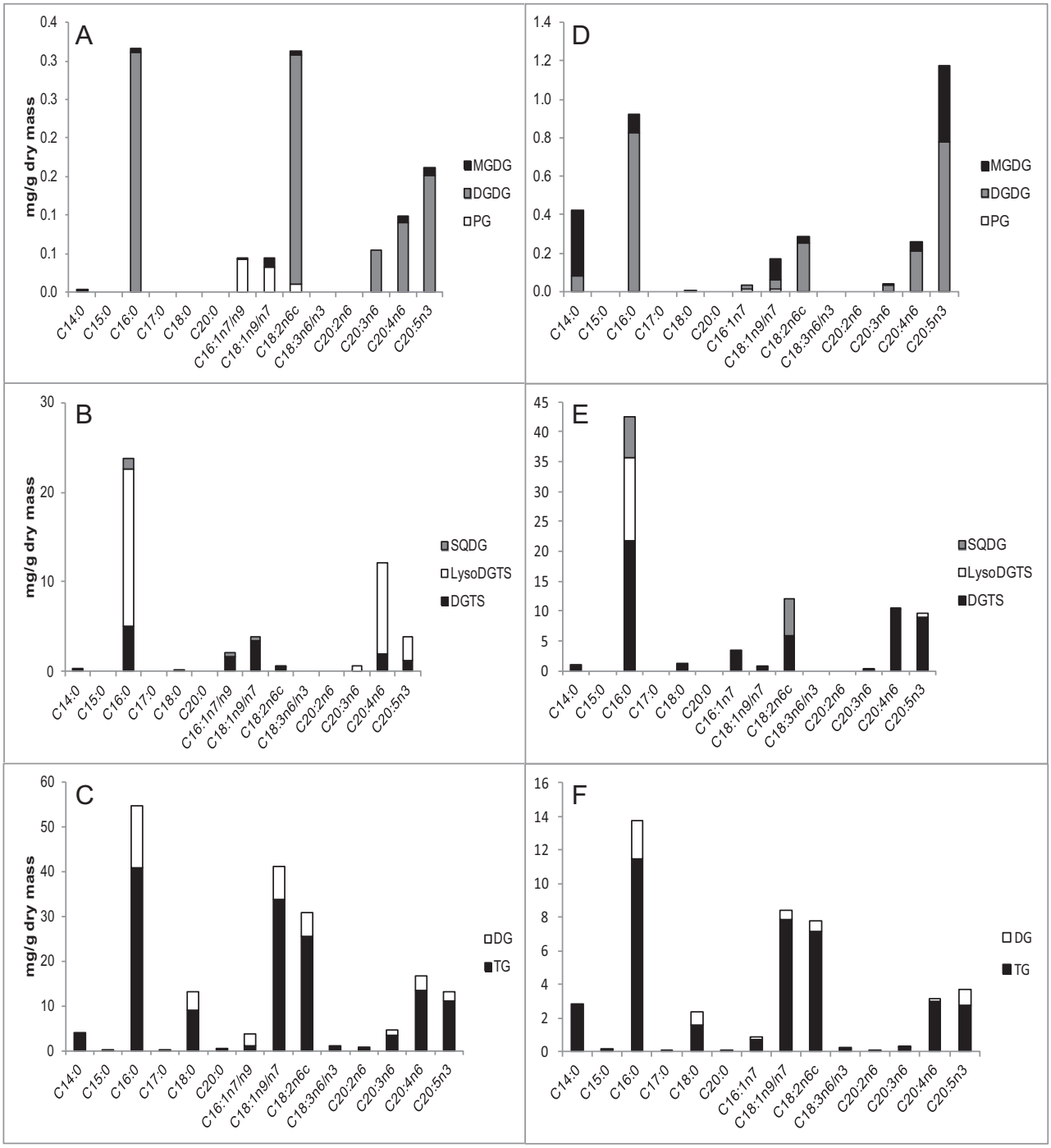

FIGURE 3 Ratio of particular fatty acids in lipid classes. A, B, and C are for *C. velia*; D, E, and F are for *V. brassicaformis*. Graphs A and D are dedicated to the structural lipids of plastid membrane, B and E represent the occurrence of DGTS, LysoDGTS, and SQDG. C and F are for storage lipids TG and their precursors DG

species of green algae except three chlorophytes: *Chlorococcum littorale*, *Chlorella saccharophila*, and *Halochlorococcum saccatum*. On the other hand, PC were absent from most haptophytes [33]. Due to very similar ionization behavior of DGTS and PC in positive and negative mode, these compounds could be simply commuted and misidentified. This situation prevents HRMS measurement (Table S1), which also revealed the presence of PC molecules in chromerids but only in trace amount (Table S2). TLC was performed to exclude the possibility of a strong effect of the matrix to ionization of PC. Fish lipid extract, a mixture of standards, and standard PC 16:0/18:1 were used for comparison with *C. velia* lipid extract. Obtained separation directly shows the presence of PC in all samples except *C. velia* lipid extract. However near the PC

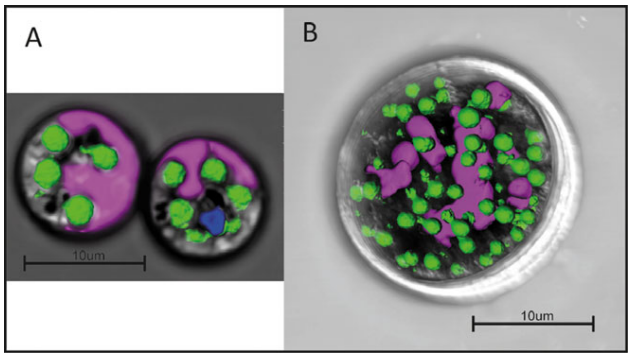

FIGURE 4 BODIPY® marker staining of *C. velia* (A) and *V. brassicaformis* (B). The plastid is colored by violet, nucleus by blue, and lipid droplets by green

region also some trace of lipids in *C. velia* occurred (Fig. S10). This trace was scratched and measured by high-resolution Orbitrap methodology, and the presence of PC in *C. velia* was excluded. The high abundance of LysoDGTS and DGTS likely replacing PC was described in most marine phototropic algae including organisms possessing secondary plastids such as diatoms *P. tricornutum* and *T. pseudonana* [33,36]. We suggest that phospholipids were replaced in the biological membranes of chromerids by non-phosphorus sulfur–(SQDG) and nitrogen–(DGTS) lipids. The HPLC–MS analysis did not reveal any significant clues for other phospholipids with exception of PG. Low levels of phospholipids in chromerids can thus be an adaptation to the phosphorus deficient environment in accordance with the hypothesis proposed for cyanobacteria, haptophytes, and diatoms [32]. Furthermore, PC were detected in traces and other phosphorus-containing lipids PG were recorded approximately in 100 times higher concentrations. PG seems to be essential for chlorophyll and photosystem I formation [52]. Therefore, we can speculate that most of the available phosphorus is consumed by PG biosynthesis.

Storage lipids and their precursor are depicted in Fig. 3, graphs C and F. These lipids represent the most abundant lipid classes in *C. velia*. Comparison of particular graphs shows a significantly higher abundance of TG and DG in *C. velia* cells, as was also reported by Woo and colleagues. The FA composition of storage lipids is comparable in both algae: palmitic acid dominates, followed by oleic, linoleic FA, and unsaturated FA contains 20 carbons. The ratio of FA in TGs is affected by the environment and particular supplemental elements rather than being a species-specific feature. This could be illustrated by the work of Danielewicz et al. [14] or Huang et al. [53], where diatom *P. tricornutum*, green alga *T. subcordiformis*, and eustigmatophyte *N. salina*, have very similar TG composition in similar environments, even though these three strains are phylogenetically distinct.

4 | CONCLUDING REMARKS

Here we introduce the methodology for the determination of plant and algal glycerolipids. This technique enabled us to determine the glycerolipid profile of chromerid algae *C. velia* and *V. brassicaformis* in a single run. Additional analyses provide information about *sn*-position of FA in the glycerol backbone, the position of the double bond in a particular FA, and test lipid identity by HRMS. More than 250 intact lipid molecules and 14 species of FA were detected in chromerids. Data interpretation and recalculation provided crucial information about particular lipid class functions, and the BODIPY staining experiment showed the location of storage lipids in the cells of chromerids. The glycerolipid profile of both algae was comparable and seems to reflect their lifestyles. *C. velia* grows fast and can rapidly accumulate an enormous amount of triacylglycerols, which is reflected by the high levels of storage and nitrogen containing structural lipid precursors and degradation products (DG and LysoDGTS). On the other hand, *V. brassicaformis* is a slow grower and levels of lipid intermediates are significantly lower. We suggest that sulfo- and betaine lipids replaced phospholipids in the biological membranes of chromerids as an evolutionary adaptation to the phosphorus deficient environment.

ACKNOWLEDGMENTS

This work was supported by Czech Science Foundation (P501-12-G055) and by Ministry of Education of the Czech Republic (project LM2015055) and National Programme of Sustainability I, ID: LO1416. We thank Laboratory of Analytical Biochemistry and Metabolomics (Biology Centre, Czech Academy of Sciences) for free access to LC–MS instruments and Natalie Czaban, M.A., for proofreading the manuscript.

REFERENCES

1. Moore, R. B., Obornik, M., Janouskovec, J., Chrudimsky, T., Vancova, M., Green, D. H., Wright, S. W., Davies, N. W., Bolch, C. J. S., Heimann, K., Slapeta, J., Hoegh-Guldberg, O., Logsdon, J. M. Jr., Carter, D. A., A photosynthetic alveolate closely related to apicomplexan parasites. *Nature* 2008, *451*, 959–963.
2. Obornik, M., Modry, D., Lukes, M., Cernotikova-Stribrna, E., Cihlar, J., Tesarova, M., Kotabova, E., Vancova, M., Prasil, O., Lukes, J., Morphology, ultrastructure and life cycle of *Vitrella brassicaformis* n. sp., n. gen., a novel chromerid from the Great Barrier Reef. *Protist* 2012, *163*, 306–323.
3. Obornik, M., Vancova, M., Lai, D.-H., Janouskovec, J., Keeling, P. J., Lukes, J., Morphology and ultrastructure of multiple life cycle stages of the photosynthetic relative of Apicomplexa, *Chromera velia*. *Protist* 2011, *162*, 115–130.
4. Janouskovec, J., Keeling, P.J., Photosynthetic alveolates and the evolution of apicomplexan parasites. *J. Phycol.* 2011, *47*, S58–S58.

5. Koreny, L., Sobotka, R., Janouskovec, J., Keeling, P. J., Obornik, M., Tetrapyrrole synthesis of photosynthetic chromerids is likely homologous to the unusual pathway of apicomplexan parasites. *Plant Cell* 2011, *23*, 3454–3462.
6. Janouskovec, J., Tikhonenkov, D. V., Burki, F., Howe, A. T., Kolisko, M., Mylnikov, A. P., Keeling, P. J., Factors mediating plastid dependency and the origins of parasitism in apicomplexans and their close relatives. *Proc. Natl. Acad. Sci. U. S. A.* 2015, *112*, 10200–10207.
7. Coppens, I., Vielemeyer, O., Insights into unique physiological features of neutral lipids in Apicomplexa: from storage to potential mediation in parasite metabolic activities. *Int. J. Parasitol.* 2005, *35*, 597–615.
8. Mazumdar, J., Striepen, B., Make it or take it: fatty acid metabolism of apicomplexan parasites. *Eukaryot. Cell* 2007, *6*, 1727–1735.
9. Marechal, E., Azzouz, N., de Macedo, C. S., Block, M. A., Feagin, J. E., Schwarz, R. T., Joyard, J., Synthesis of chloroplast galactolipids in apicomplexan parasites. *Eukaryot. Cell* 2002, *1*, 653–656.
10. Botte, C. Y., Yamaryo-Botte, Y., Rupasinghe, T. W. T., Mullin, K. A., MacRae, J. I., Spurck, T. P., Kalanon, M., Shears, M. J., Coppel, R. L., Crellin, P. K., Marechal, E., McConville, M. J., McFadden, G. I., Atypical lipid composition in the purified relict plastid (apicoplast) of malaria parasites. *Proc. Natl. Acad. Sci. U. S. A.* 2013, *110*, 7506–7511.
11. Al-Fadhli, A., Wahidulla, S., D'Souza, L., Glycolipids from the red alga Chondria armata (Kutz.) Okamura. *Glycobiology* 2006, *16*, 902–915.
12. Basconcillo, L. S., Zaheer, R., Finan, T. M., McCarry, B. E., A shotgun lipidomics approach in Sinorhizobium meliloti as a tool in functional genomics. *J. Lipid Res.* 2009, *50*, 1120–1132.
13. Sato, N., Is monoglucosyldiacylglycerol a precursor to monogalactosyldiacylglycerol in all cyanobacteria? *Plant Cell Physiol*. 2015, *56*, 1890–1899.
14. Danielewicz, M. A., Anderson, L. A., Franz, A. K., Triacylglycerol profiling of marine microalgae by mass spectrometry. *J. Lipid Res.* 2011, *52*, 2101–2108.
15. Norman, H. A., Mischke, C. F., Allen, B., Vincent, J. S., Semipreparative isolation of plant sulfoquinovosyldiacylglycerols by solid phase extraction and HPLC procedures. *J. Lipid Res.* 1996, *37*, 1372–1376.
16. Moreau, R. A., Doehlert, D. C., Welti, R., Isaac, G., Roth, M., Tamura, P., Nunez, A., The identification of mono-, di-, tri-, and tetragalactosyl-diacylglycerols and their natural estolides in oat kernels. *Lipids* 2008, *43*, 533–548.
17. Xu, J. L., Chen, D. Y., Yan, X. J., Chen, J. J., Zhou, C. X., Global characterization of the photosynthetic glycerolipids from a marine diatom Stephanodiscus sp. by ultra performance liquid chromatography coupled with electrospray ionization-quadrupole-time of flight mass spectrometry. *Anal. Chim. Acta* 2010, *663*, 60–68.
18. Djafi, N., Humbert, L., Rainteau, D., Cantrel, C., Zachowski, A., Ruelland, E., Multiple reaction monitoring mass spectrometry is a powerful tool to study glycerolipid composition in plants with different level of desaturase activity. *Plant Signal. Behav*. 2013, *8*, e24118.
19. Gil, J. H., Hong, J. K., Choe, J. C., Kim, Y. H., Analysis of fatty acyl groups of diacyl galactolipid molecular species by HPLC/ESI-MS with in-source fragmentation. *Bull. Korean Chem. Soc.* 2003, *24*, 1163–1168.
20. Li, L. L., Lu, X., Zhao, J. Y., Zhang, J. J., Zhao, Y. N., Zhao, C. X., Xu, G. W., Lipidome and metabolome analysis of fresh tobacco leaves in different geographical regions using liquid chromatography-mass spectrometry. *Anal. Bioanal. Chem.* 2015, *407*, 5009–5020.
21. Ma, A. C., Chen, Z., Wang, T., Song, N., Yan, Q., Fang, Y. C., Guan H. S., Liu, H. B., Isolation of the molecular species of monogalactosyldiacylglycerols from brown edible seaweed *Sargassum horneri* and their inhibitory effects on triglyceride accumulation in 3T3-L1 adipocytes. *J. Agric. Food Chem.* 2014, *62*, 11157–11162.
22. Guella, G., Frassanito, R., Mancini, I., A new solution for an old problem: the regiochemical distribution of the acyl chains in galactolipids can be established by electrospray ionization tandem mass spectrometry. *Rapid Commun. Mass Spectrom.* 2003, *17*, 1982–1994.
23. El Baz, F. K., El Baroty, G. S., Abd El Baky, H. H., Abd El-Salam, O. I., Ibrahim, E. A., Structural characterization and biological activity of sulfolipids from selected marine algae. *Grasas y Aceites* 2013, *64*, 561–571.
24. Zabranska, M., Vrkoslav, V., Sobotnikova, J., Cvacka, J., Analysis of plant galactolipids by reversed-phase high-performance liquid chromatography/mass spectrometry with accurate mass measurement. *Chem. Phys. Lipids* 2012, *165*, 601–607.
25. Jones, J., Manning, S., Montoya, M., Keller, K., Poenie, M., Extraction of algal lipids and their analysis by HPLC and mass spectrometry. *J. Am. Oil Chem. Soc.* 2012, *89*, 1371–1381.
26. Furlong, S. T., Leary, J. A., Costello, C. E., Dawidowicz, E. A., Isolation and identification of 1(3),2-diacylglyceryl-(3)-o-4'-(N,N,N-trimethyl)homoserine from the soil ameba, Acanthamoeba castellanii. *J. Lipid Res.* 1986, *27*, 1182–1189.
27. Botte, C. Y., Yamaryo-Botte, Y., Janouskovec, J., Rupasinghe, T., Keeling, P. J., Crellin, P., Coppel, R. L., Marechal, E., McConville, M. J., McFadden, G. I., Identification of plant-like galactolipids in *Chromera velia*, a photosynthetic relative of malaria parasites. *J. Biol. Chem.* 2011, *286*, 29893–29903.
28. Dahmen, J. L., Khadka, M., Dodson, V. J., Leblond, J. D., Mono- and digalactosyldiacylglycerol composition of dinoflagellates. VI. Biochemical and genomic comparison of galactolipid biosynthesis between *Chromera velia* (Chromerida), a photosynthetic alveolate with red algal plastid ancestry, and the dinoflagellate, *Lingulodinium polyedrum*. *Eur. J. Phycol.* 2013, *48*, 268–277.
29. Tzen, J. T. C., Huang, A. H. C., Surface structure and properties of plant seed oil bodies. *J. Cell Biol.* 1992, *117*, 327–335.
30. Yang, D. W., Song, D. H., Kind, T., Ma, Y., Hoefkens, J., Fiehn, O., Lipidomic analysis of chlamydomonas reinhardtii under nitrogen and sulfur deprivation. *PLoS One* 2015, *10*, e0137948.
31. Geiger, O., Rohrs, V., Weissenmayer, B., Finan, T. M., Thomas-Oates, J. E., The regulator gene phoB mediates phosphate stress-controlled synthesis of the membrane lipid diacylglyceryl-*N,N,N*-trimethylhomoserine in Rhizobium (Sinorhizobium) meliloti. *Mol. Microbiol.* 1999, *32*, 63–73.

32. Van Mooy, B. A. S., Fredricks, H. F., Pedler, B. E., Dyhrman, S. T., Karl, D. M., Koblizek, M., Lomas, M. W., Mincer, T. J., Moore, L. R., Moutin, T., Rappe, M. S., Webb, E. A., Phytoplankton in the ocean use non-phosphorus lipids in response to phosphorus scarcity. *Nature* 2009, *458*, 69–72.
33. Kato, M., Sakai, M., Adachi, K., Ikemoto, H., Sano, H., Distribution of betaine lipids in marine algae. *Phytochemistry* 1996, *42*, 1341–1345.
34. Banskota, A. H., Stefanova, R., Sperker, S., McGinn, P. J., New diacylglyceryltrimethylhomoserines from the marine microalga *Nannochloropsis granulata* and their nitric oxide inhibitory activity. *J. Appl. Phycol.* 2013, *25*, 1513–1521.
35. Eichenberger, W., Gribi, C., Lipids of *Pavlova lutheri*: cellular site and metabolic role of DGCC. *Phytochemistry* 1997, *45*, 1561–1567.
36. Canavate, J. P., Armada, I., Rios, J. L., Hachero-Cruzado, I., Exploring occurrence and molecular diversity of betaine lipids across taxonomy of marine microalgae. *Phytochemistry* 2016, *124*, 68–78.
37. Hsu, F.-F., Turk, J., Electrospray ionization with low-energy collisionally activated dissociation tandem mass spectrometry of glycerophospholipids: mechanisms of fragmentation and structural characterization. *J. Chromatogr. B* 2009, *877*, 2673–2695.
38. Yang, C. Y., Kim, J., Ahn, S. J., Kim, D. H., Cho, M. R., Identification of the female-produced sex pheromone of the plant bug *Apolygus spinolae*. *J. Chem. Ecol.* 2014, *40*, 244–249.
39. Li, S., Xu, J. L., Chen, J., Chen, J. J., Zhou, C. X., Yan, X. J., The major lipid changes of some important diet microalgae during the entire growth phase. *Aquaculture* 2014, *428*, 104–110.
40. Kostal, V., Simek, P., Changes in fatty acid composition of phospholipids and triacylglycerols after cold-acclimation of an aestivating insect prepupa. *J. Comp. Physiol. B* 1998, *168*, 453–460.
41. Zahradnickova, H., Tomcala, A., Berkova, P., Schneedorferova, I., Okrouhlik, J., Simek, P., Hodkova, M., Cost effective, robust, and reliable coupled separation techniques for the identification and quantification of phospholipids in complex biological matrices: application to insects. *J. Sep. Sci.* 2014, *37*, 2062–2068.
42. Sharma, D. K., Gautam, K., Jueppner, J., Giavalisco, P., Rihko-Struckmann, L., Pareek, A., Sundmacher, K., UPLC-MS analysis of *Chlamydomonas reinhardtii* and *Scenedesmus obliquus* lipid extracts and their possible metabolic roles. *J. Appl. Phycol.* 2015, *27*, 1149–1159.
43. Adlof, R., List, G., Analysis of triglyceride isomers by silver-ion high-performance liquid chromatography. Effect of column temperature on retention times. *J. Chromatogr. A* 2004, *1046*, 109–113.
44. Cvacka, J., Hovorka, O., Jiros, P., Kindl, J., Stransky, K., Valterova, I., Analysis of triacylglycerols in fat body of bumblebees by chromatographic methods. *J. Chromatogr. A* 2006, *1101*, 226–237.
45. Khadka, M., Dahmen, J. L., Salem, M., Leblond, J. D., Comparative study of galactolipid composition and biosynthetic genes for galactolipid synthases in *Vitrella brassicaformis* and *Chromera velia*, two recently identified chromerids with red algal-derived plastids. *Algological Studies* 2014, *144*, 73–93.
46. Zhukova, N. V., Aizdaicher, N. A., Fatty acid composition of 15 species of marine microalgae. *Phytochemistry* 1995, *39*, 351–356.
47. Mansour, M. P., Volkman, J. K., Jackson, A. E., Blackburn, S. I., The fatty acid and sterol composition of five marine dinoflagellates. *J. Phycol.* 1999, *35*, 710–720.
48. Viso, A. C., Marty, J. C., Fatty acids from 28 marine microalgae. *Phytochemistry* 1993, *34*, 1521–1533.
49. Plaxton, W. C., Shane, M. W., The role of post-translational enzyme modifications in the metabolic adaptations of phosphorus-deprived plants. In: Plaxton, W.C., Lambers H., (Eds.) Phosphorus Metabolism in Plants. Chichester: Wiley-Blackwell; 2015, 99–123.
50. Li-Beisson, Y., Beisson, F., Riekhof, W., Metabolism of acyl-lipids in *Chlamydomonas reinhardtii*. *Plant J.* 2015, *82*, 504–522.
51. Goold, H., Beisson, F., Peltier, G., Li-Beisson, Y., Microalgal lipid droplets: composition, diversity, biogenesis and functions. *Plant Cell Rep.* 2015, *34*, 545–555.
52. Kopecna, J., Pilny, J., Krynicka, V., Tomcala, A., Kis, M., Gombos, Z., Komenda, J., Sobotka, R., Lack of phosphatidylglycerol inhibits chlorophyll biosynthesis at multiple sites and limits chlorophyllide reutilization in *Synechocystis* sp. strain PCC 6803. *Plant Physiol.* 2015, *169*, 1307–1317.
53. Huang, X., Huang, Z., Wen, W., Yan, J., Effects of nitrogen supplementation of the culture medium on the growth, total lipid content and fatty acid profiles of three microalgae (*Tetraselmis subcordiformis*, *Nannochloropsis oculata* and *Pavlova viridis*). *J. Appl. Phycol.* 2013, *25*, 129–137.

SUPPORTING INFORMATION

Additional Supporting Information may be found online in the supporting information tab for this article.

How to cite this article: Tomčala A, Kyselová V, Schneedorferová I et al. Separation and identification of lipids in the photosynthetic cousins of Apicomplexa *Chromera velia* and *Vitrella brassicaformis*. *J Sep Sci*. 2017;40:3402–3413. https://doi.org/10.1002/jssc.201700171

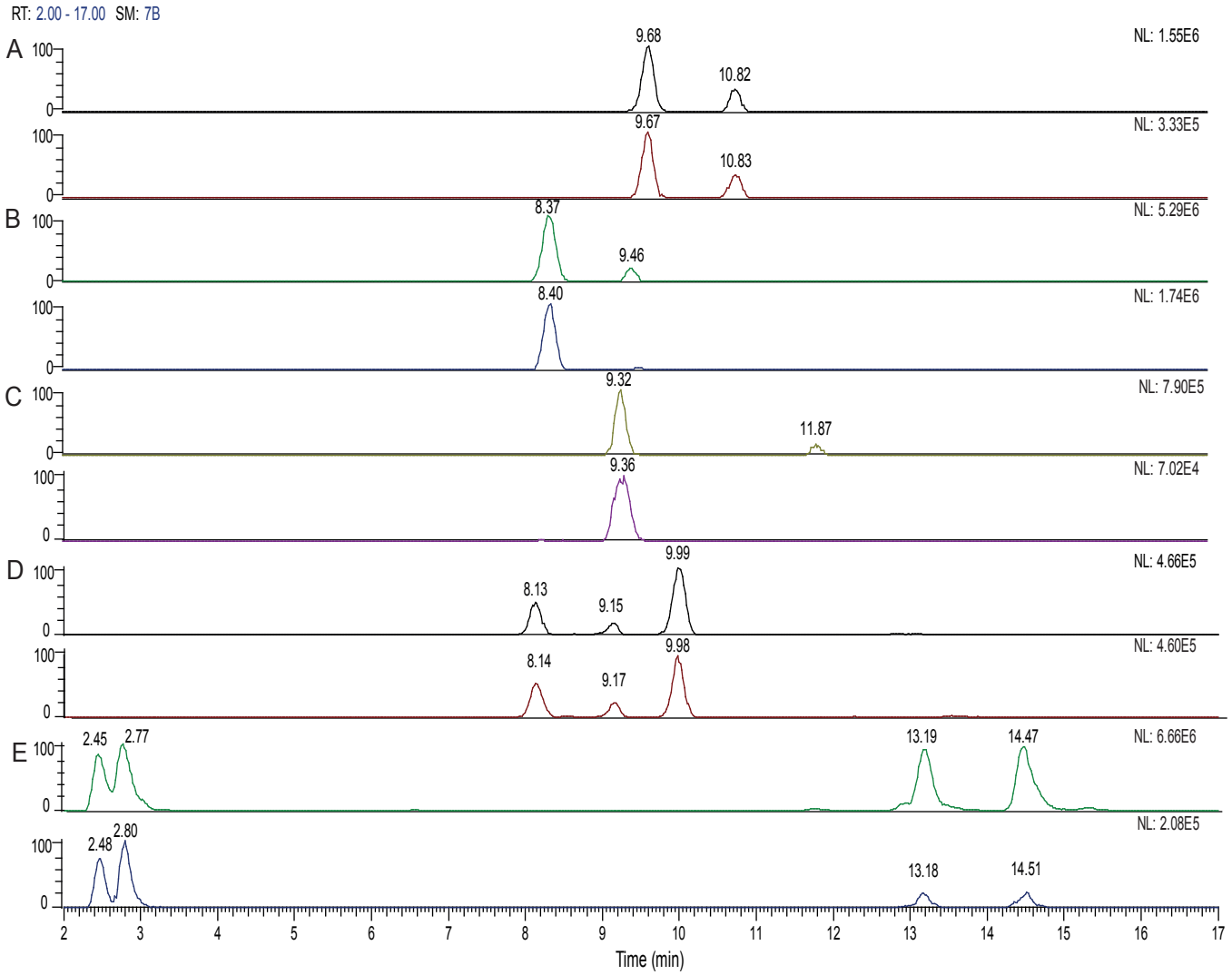

Supplementary Fig. 1.: HPLC of crude algal extract. Upper chromatograms represent positive ionization and bottom negative ionization mode. A) separation of MGDG 20:5/20:5 (Rt. 9.68 min), MGDG 20:4/20:5 (Rt. 10.82 min), B) DGDG 20:5/20:5 (Rt. 8.37 min), DGDG 20:4/20:5 (Rt. 9.46 min) C) PG 16:1/18:2 (Rt. 9.32 min), D) SQDG 16:0/20:5 (Rt. 8.13 min), SQDG 16:0/20:4 (Rt. 9.15 min), SQDG 16:0/20:3 (Rt. 9.99 min), E) LysoDGTS 20:5 (Rt. 2.45 min), LysoDGTS 20:4 (Rt. 2.77 min), DGTS 18:1/20:5 (Rt. 12.95 min), DGTS 18:2/20:4 (Rt. 13.19 min), DGTS 18:1/20:4 (Rt. 14.47 min).

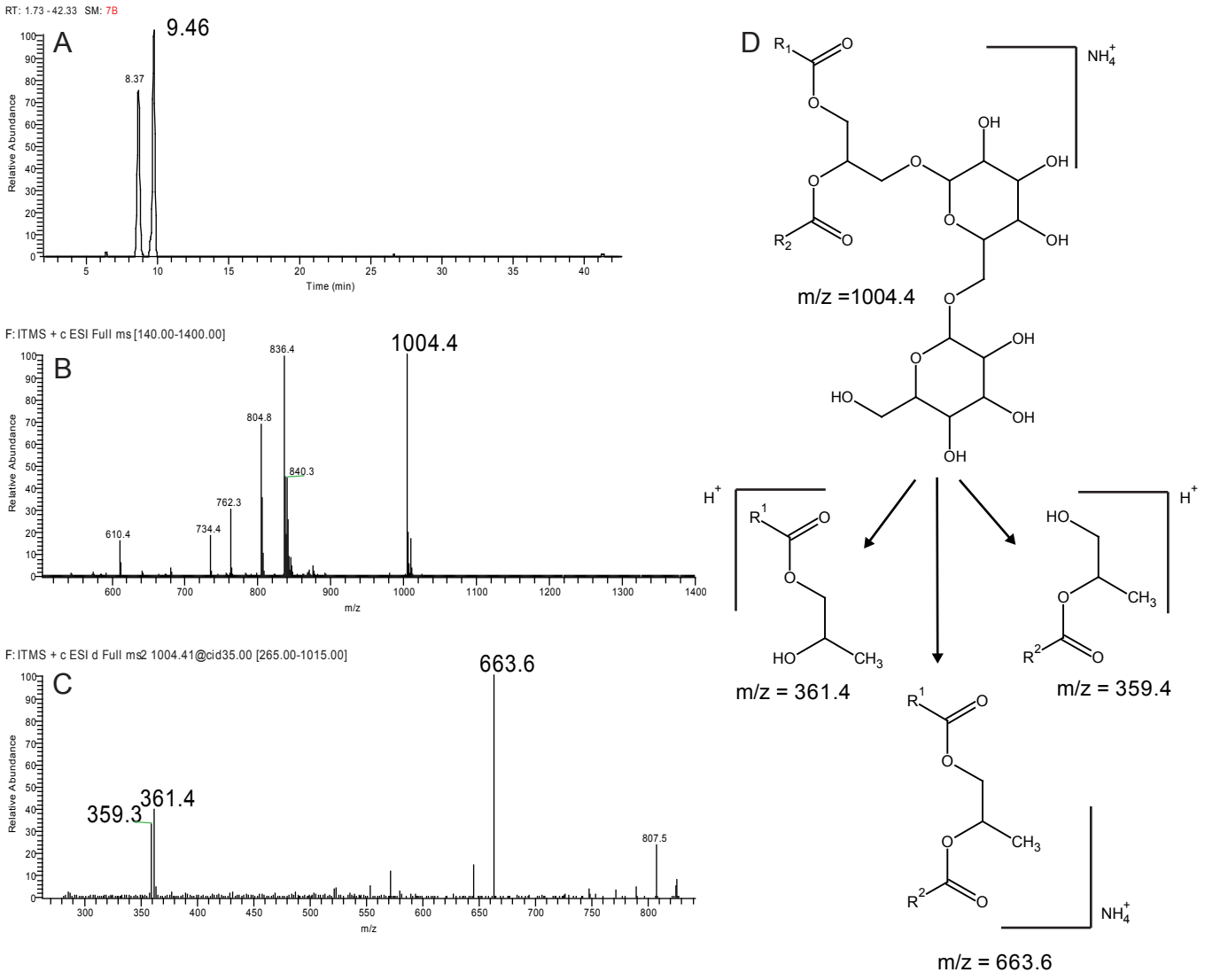

Supplementary Fig. 2.: A) Extracted chromatogram of m/z 1004.4 Da corresponding to DGDG 20:5/20:4 in retention time 9.46 min. B) Full ms spectrum for DGDG 20:5/20:4. C) MS^2 spectrum m/z 1004.4 Da (9.46 min). D) Proposed fragmentation pattern of DGDG (ESI+). CID fragmented the molecules of DGDG to sugar moiety (loss of 341 Da; Fig. 3 C. m/z = 663.6 Da), and to the fatty acid with glycerol backbone 359.3 Da corresponded to C20:5 and 361.4 Da to C20:4. All data is obtained from *C. velia*.

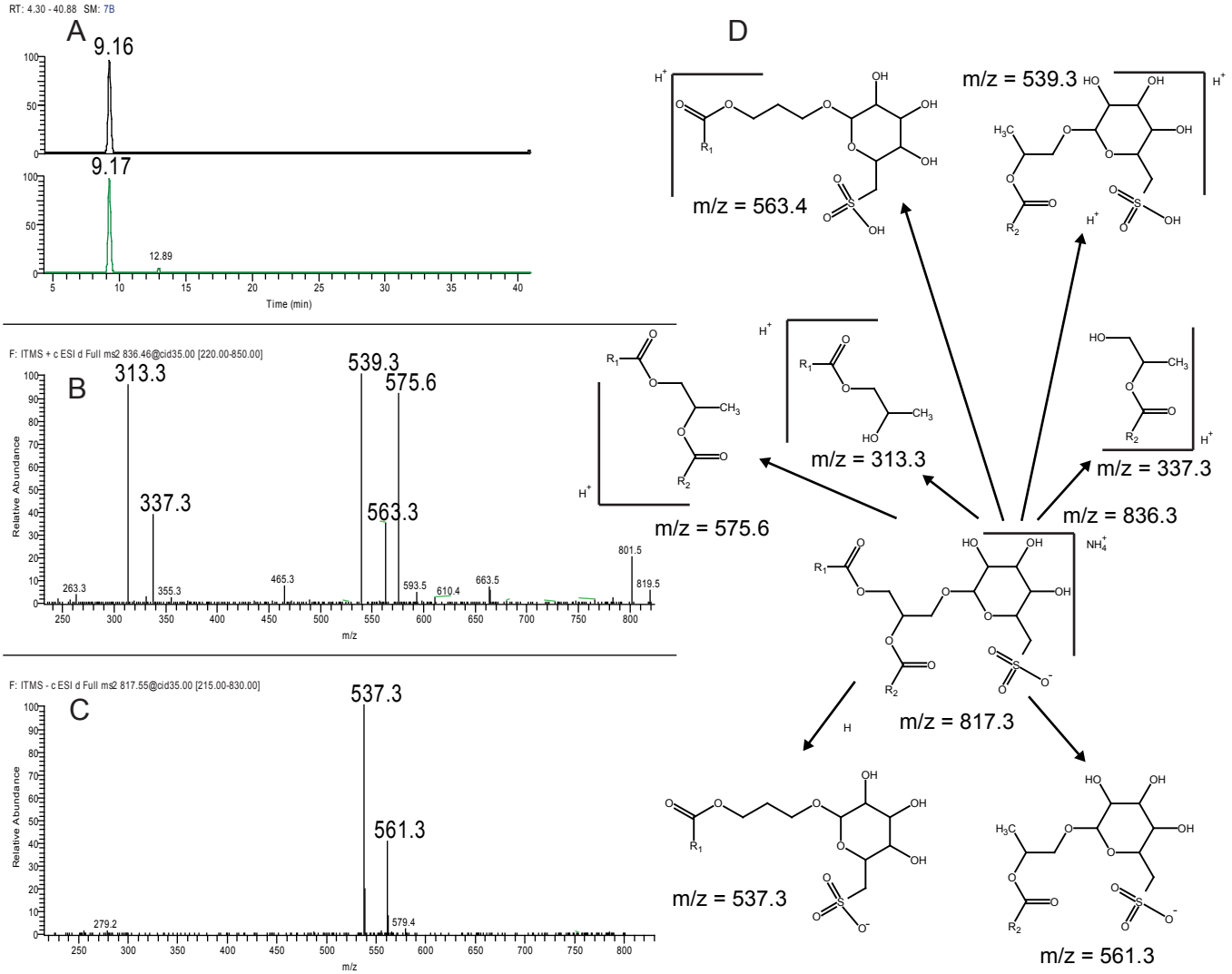

Supplementary Fig. 3.: A) Extracted chromatograms of m/z 836.5 Da in positive mode and m/z 817.5 Da in negative corresponding of SQDG 18:2/16:0 in retention time 9.16 min. B) Positive MS^2 spectrum of 9.16 min peak m/z 836.5 Da. C) MS^2 spectrum of 9.17 min. peak m/z 817.5 Da. D) Proposed fragmentation pattern of SQDG (up ESI+, bottom ESI-). Typical for positive ionization are following inos: loss of sugar part corresponding to ion 575.6 Da, and loss of ammonium carboxylic acid corresponding to ions 563.3 Da (C16:0) and 539.3 Da (C18:2), protonated carboxylic acid with glycerol backbone corresponding to ions 313.3 Da (C16:0) and 337.3 Da (C18:2). Negative MS^2 experiments give two ions the corresponding to a loss of carboxylic acid, 561.3 Da indicates loss of palmitic acid from in the *sn*-1 position and 537.3 Da gives a loss of linoleoyl acid from the *sn*-2 position. All data is obtained from *V. brassicaformis*.

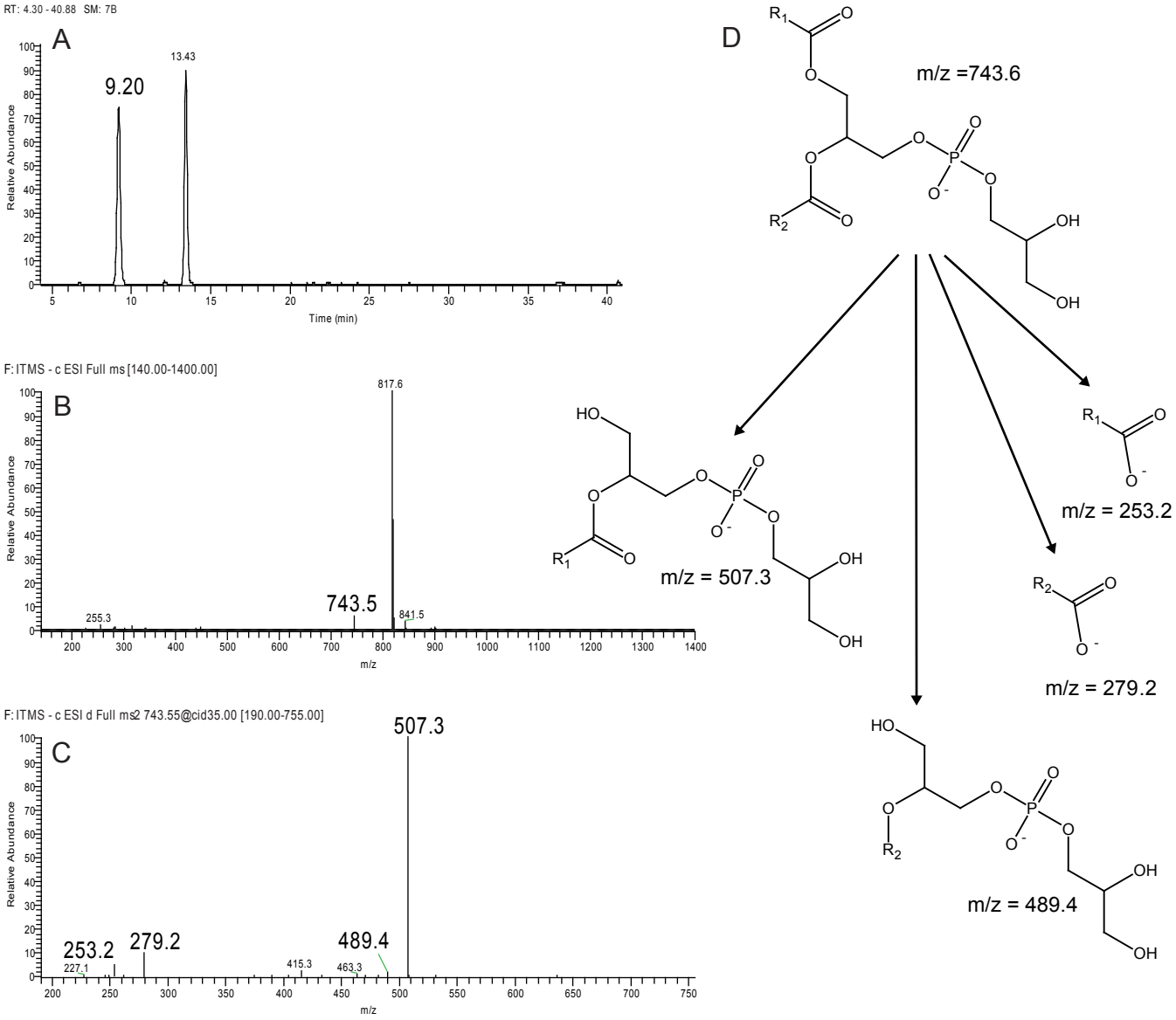

Supplementary Fig. 4.: A) Extracted chromatogram of peak m/z 743.5 Da corresponding to PG 18:2/16:1 in retention time 9.20 min. B) Negative full scan spectrum of PG 18:2/16:1 C) MS^2 spectrum of peak m/z 743.6 Da (9.20 min.) D) Proposed fragmentation pattern of PG (ESI-). The ions 507.3 Da and 489.4 Da correspond to a loss of acylium ion of palmitoleic acid and oleic acid respectively. More intense ion originate from loss of FA from sn-2 position. The ions 279.2 Da and 253.2 Da arise from deprotonated linoleic and palmitoleic acid respectively, resulting to identification of PG 18:2/16:1. All data is obtained from *V. brassicaformis*.

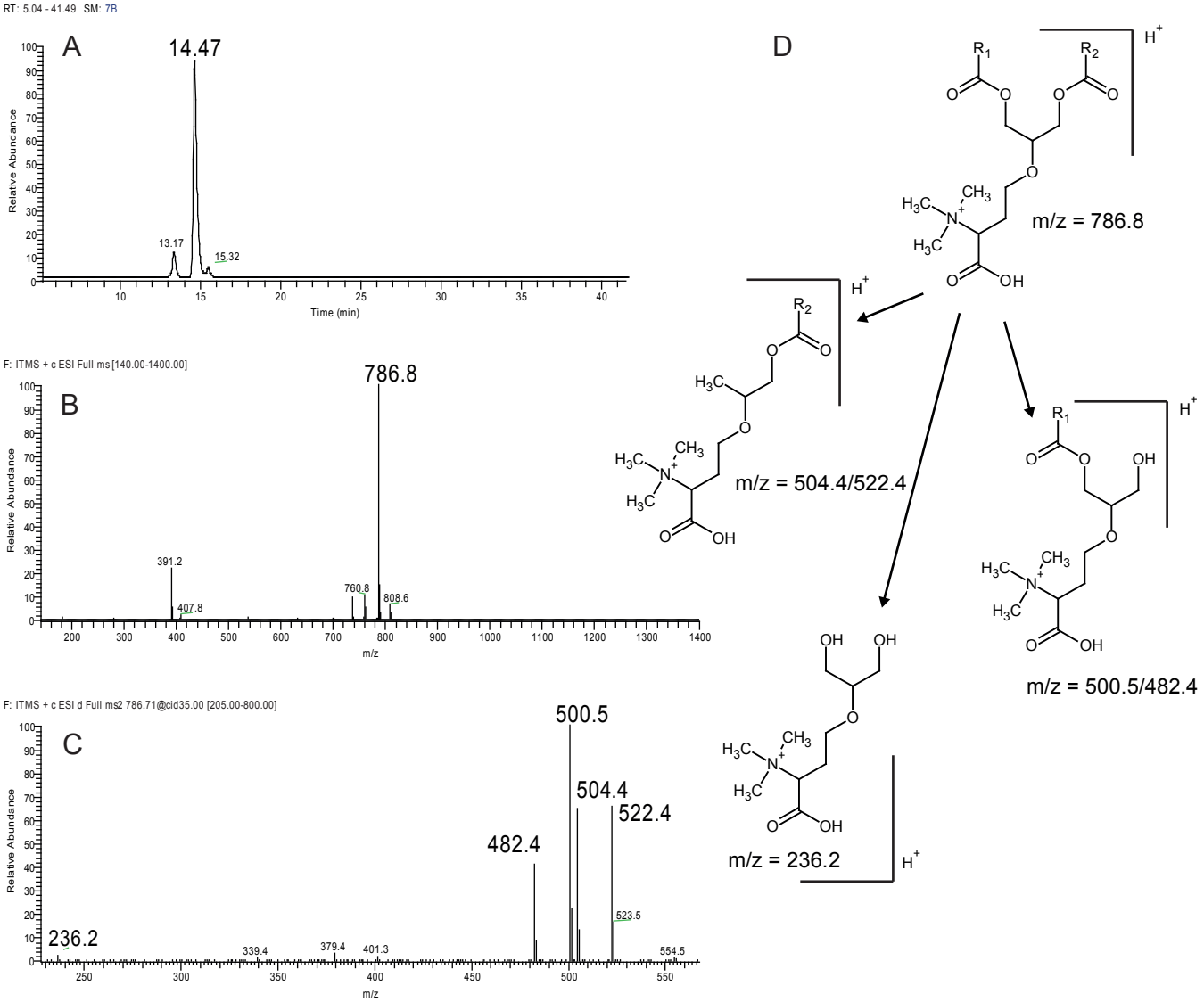

Supplementary Fig. 5.: A) Extracted chromatogram of m/z 786.8 Da corresponding to in retention time 14.47 min. B) Positive full scan spectrum of DGTS 20:4/18:1 and DGTS 18:1/20:4 C) MS^2 spectrum m/z 786.8 Da (14.47 min.) D) Proposed fragmentation pattern of DGTS (ESI+). In Fig. 5.C the ketene fragment ion with 500.5 Da and 482.4 Da is highly indicative for the *sn*-2 fatty acyl position of C20:4 and oleic acid respectively. Therefore, the algae sample contains a mixture of DGTS 20:4/18:1 and DGTS 18:1/20:4. The former molecule with eicosatetraenoic acid attached in *sn*-2 position dominates. All data is obtained from *C. velia*.

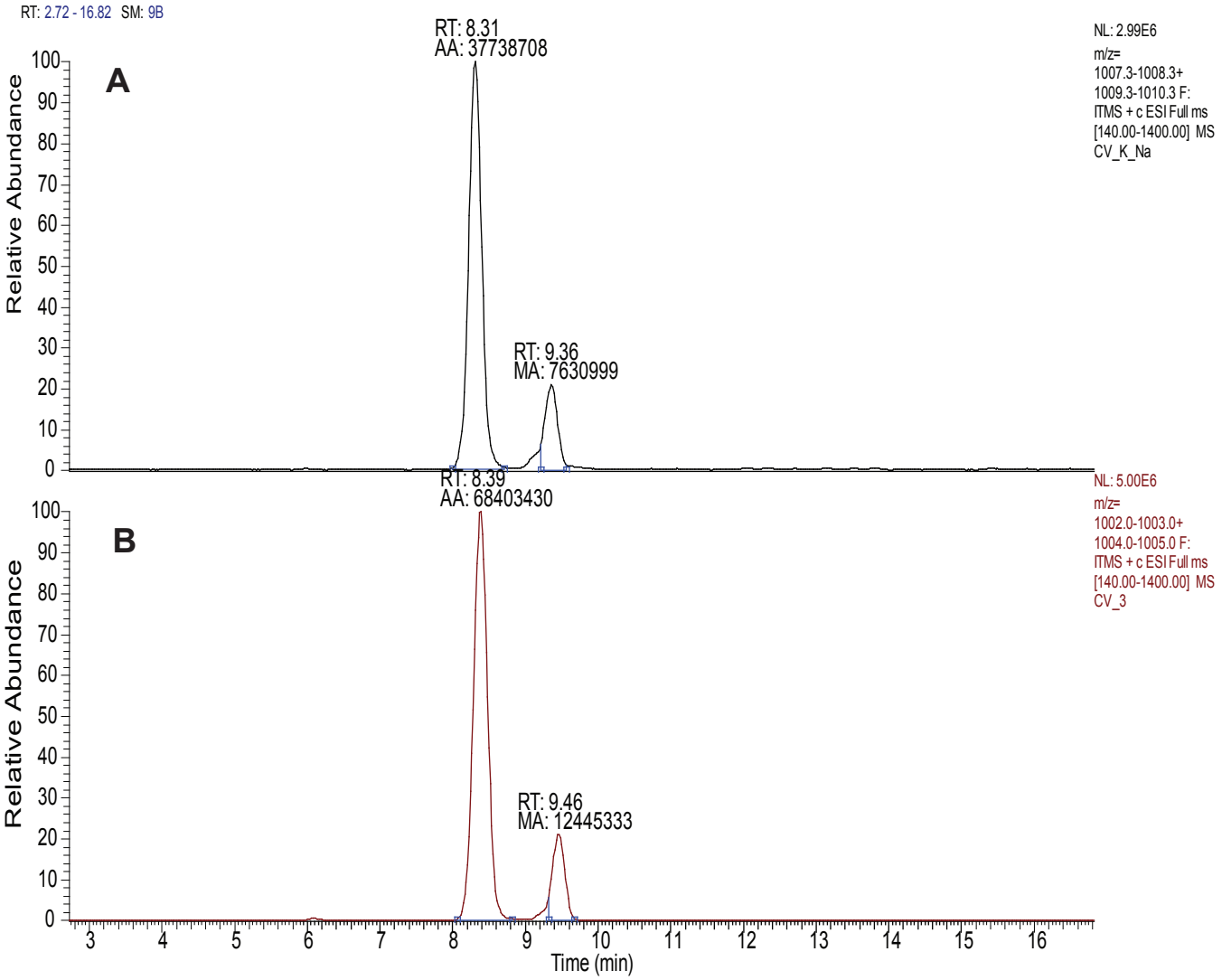

Supplementary Fig. 6.: comparison of responses of sodium $[M+Na]^+$ (A) and ammonium $[M+NH_4]^+$ (B) adducts of DGDG in positive ionization mode. The same sample provides approximately two times stronger intensities of ammonium adduct than sodium adduct.

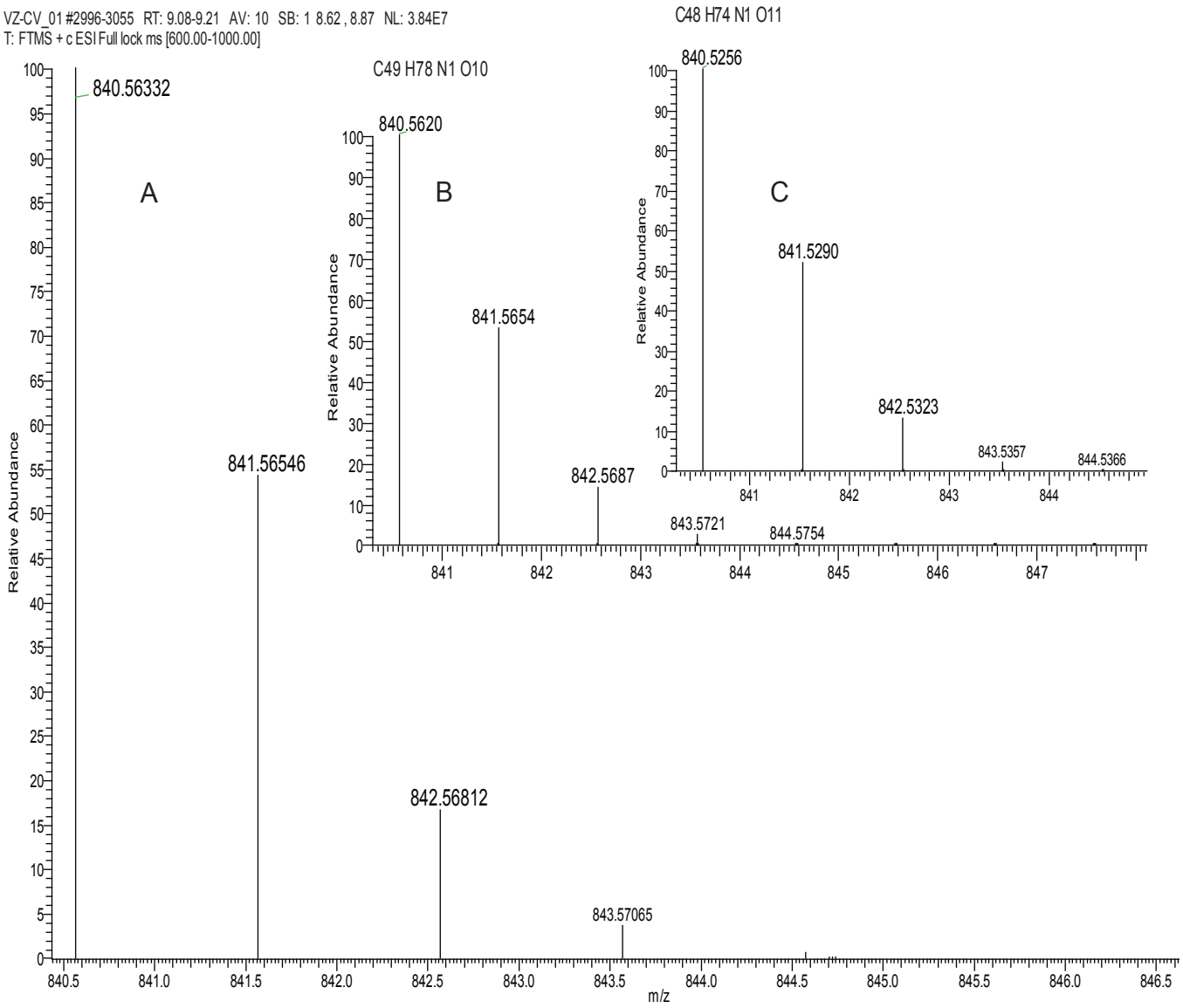

Supplementary Fig. 7.: comparison of acquired spectra of A) MGDG 20:5/20:5 from Orbitrap high resolution measurement of *C.velia* sample, B) calculated spectra of MGDG 20:5/20:5, C) calculated spectra of oxidized MGDG with same m/z.

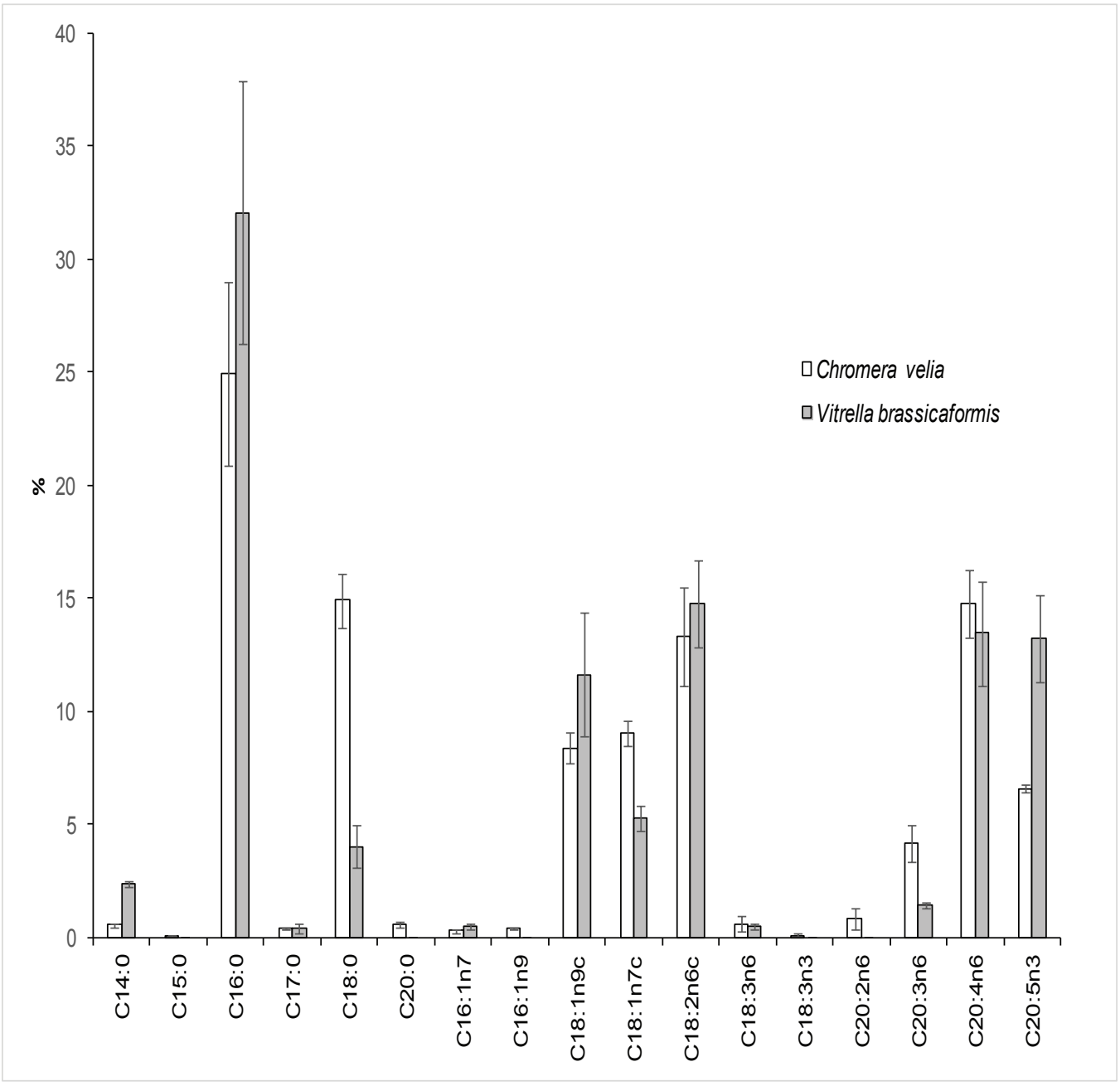

Supplementary Fig. 8.: FID record expressed by percentual ratio of FA (n=5).

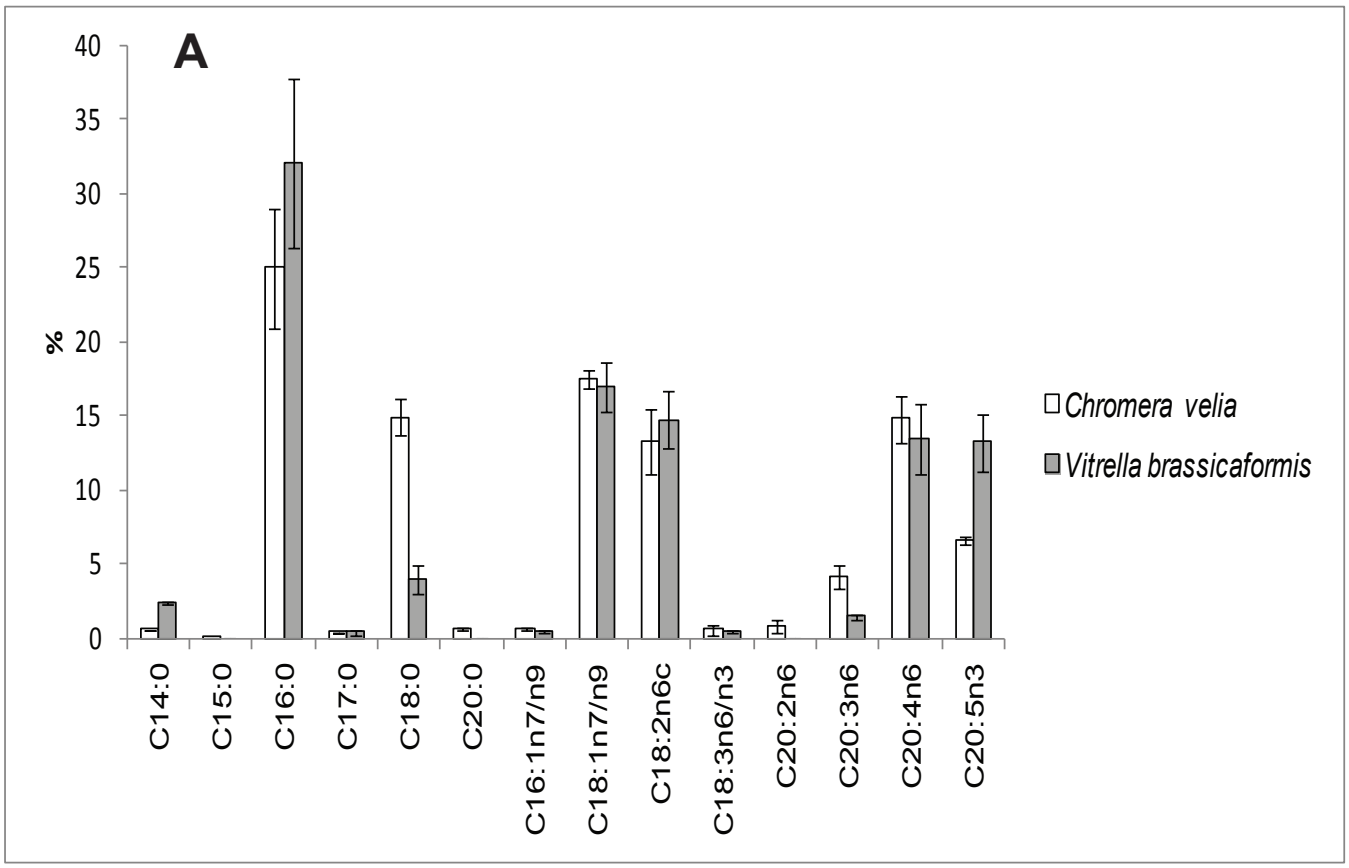

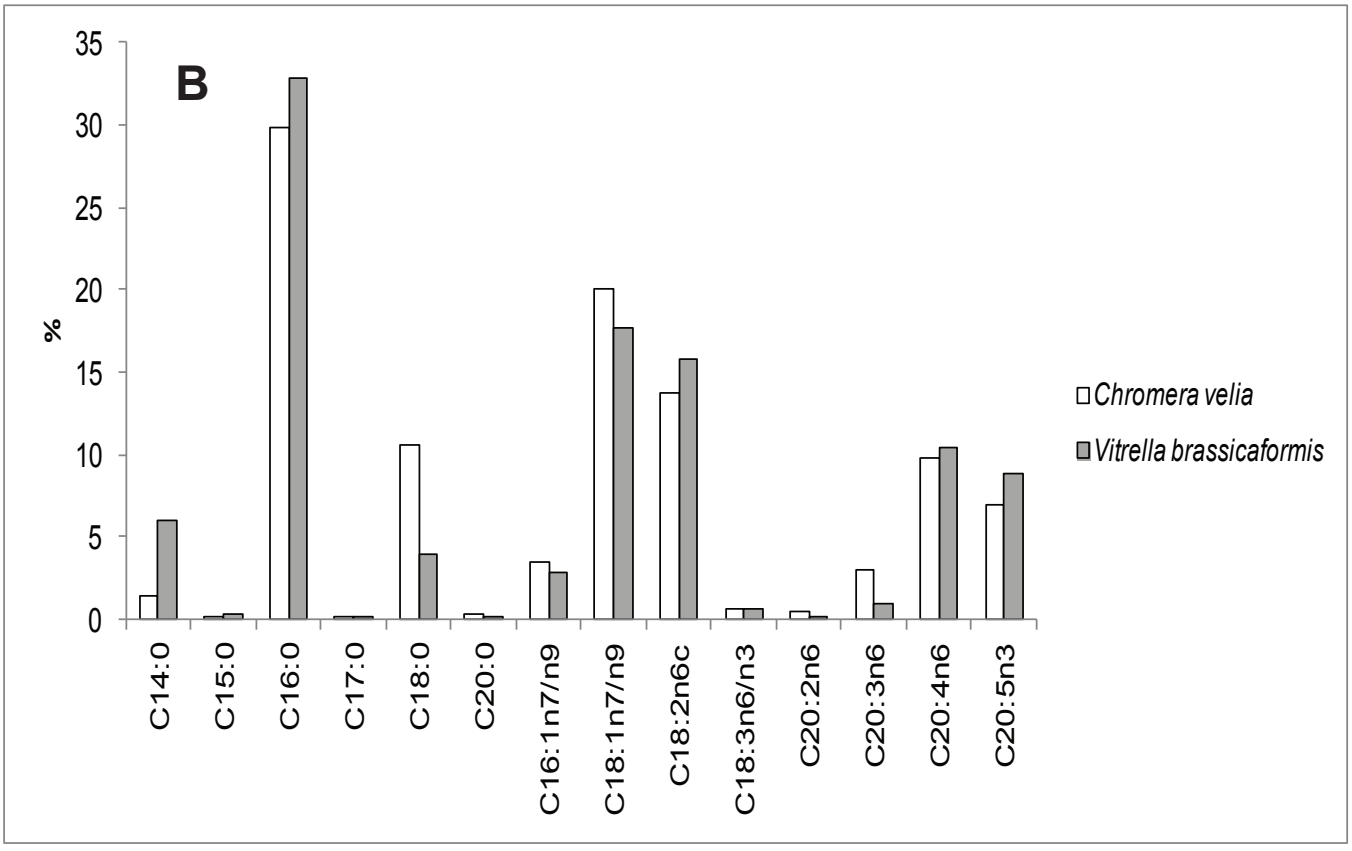

Supplementary Fig. 9.: FA ration in both algae: comparison of data obtained via GC FID (A) and data obtained via HPLC and recalculation (B).

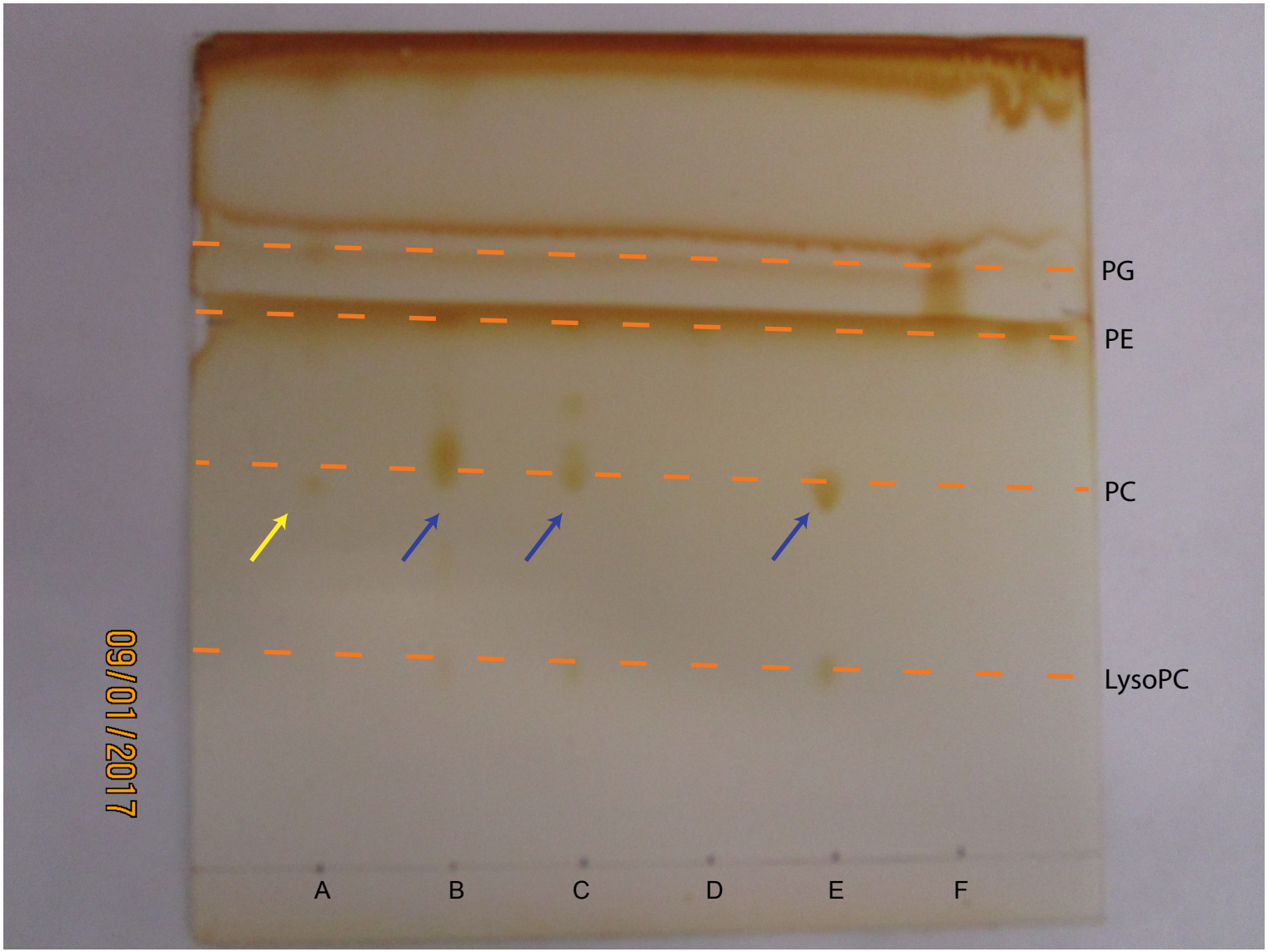

Supplementary Fig.10.: TLC plate with separated lipids. Lipid extracts of *Chromera velia* (A), *Danio rerio* (B), mixture of standards (C), phosphatidylethanolamine 16:0/18:2 (D), phosphatidylcholine 16:0/18:2 (E), and phosphatidylglycerol (F). Blue arrows poit to separated PC confirmed by HRMS Orbitrap, yellow arrow points to PC-like spot, but presence of PC was excluded by HRMS Orbitrap methodology.

Supplementary Table 1: List of identified glycerolipids in extract from *C. velia* and *V. brassicaformis* via fragmentation patterns and via high resolution mass spectrometry. (slash / is for known regioisomery /*sn*-1/*sn*-2 , and underscore _ is for unknown regioisomery)

ESI+	ESI-	Retention time	Identification	Ratio	ESI + HRMS simulation	ESI + HRMS measure.	Δ
586.3		20.23	DG 16:0_16:0				
610.4		18.10	DG 18:1_16:1				
610.4		18.26	DG 18:2_16:0				
612.4		20.66	DG 18:1_16:0				
614.4		23.64	DG 16:0_18:0				
632.4		15.92	DG 18:1_16:0				
634.4		17.79	DG 20:3_16:1				
634.4		17.94	DG 20:4_16:0				
636.4		18.69	DG 18:2_18:1				
636.4		19.27	DG 20:3_16:0				
638.5		21.70	DG 18:0_18:2				
638.5		21.19	DG 18:1_18:1				
640.5		24.26	DG 18:1_18:0				
656.4		14.55	DG 20:5_18:2				
658.4		16.05	DG 20:5_18:1				
660.4		17.44	DG 38:5				
660.4		18.10	DG 20:4_18:1				
678.3		12.79	DG 20:5_20:5				
682.4		15.62	DG 20:4_20:4				
1002.2	1043.20	8.78	DGDG 20:5/20:5		1002.61485	1002.61610	-0.00125
1004.2	1045.20	9.90	DGDG 20:4/20:5		1004.63050	1004.63123	-0.00073
1006.2	1047.20	10.82	DGDG 20:3/20:5		1006.64615	1006.64663	-0.00048
1006.2	1047.20	11.07	DGDG 20:4/20:4		1006.64615	1006.64637	-0.00022
1008.2	1047.20	12.12	DGDG 20:3/20:4		1008.66180	1008.66191	-0.00011
928.4	969.30	9.06	DGDG 14:0/20:5		928.59920	928.59984	-0.00064
934.6	973.20	12.81	DGDG 16:0/18:2		934.64615	934.64130	0.00485
954.5	995.50	11.06	DGDG 16:1/20:5		954.61484	954.61153	0.00331
956.2	997.20	11.22	DGDG 16:0/20:5		956.63049	956.63058	-0.00009
958.2	999.20	12.45	DGDG 16:0/20:4		958.64615	958.64604	0.00011
960.4	1001.30	13.35	DGDG 16:0/20:3		960.66180	960.66316	-0.00136
980.2	1021.20	10.14	DGDG 18:2/20:5		980.63050	980.63086	-0.00036
982.2	1023.20	11.38	DGDG 18:1/20:5		982.64615	982.64628	-0.00013
984.2	1025.20	11.76	DGDG 18:0/20:5		984.66180	984.66118	0.00062
710.7	768.70	14.66	DGTS 18:1/14:0//14:0/18:1	1:2	710.59292	710.59381	-0.00089
712.7	770.70	17.16	DGTS 16:1/16:1		712.60858	712.60938	-0.00080
730.8	788.80	10.67	DGTS 14:0/20:5//20:5/14:0	5:4	730.56163	730.56198	-0.00035
732.8	790.80	11.87	DGTS 14:0/20:4//20:4/14:0	5:4	732.67728	732.57801	0.09927
736.7	794.70	15.55	DGTS 16:0/18:2//18:2/16:0	4:3	736.60858	736.60881	-0.00023
738.7	796.70	17.51	DGTS 16:0/18:1//18:1/16:0	2:1	738.62423	738.62525	-0.00102
758.7	816.70	13.82	DGTS 16:0/20:5//20:5/16:0	2:1	758.59293	758.59357	-0.00064
758.7	816.70	13.16	DGTS 16:1/20:4//20:4/16:1	2:3	758.59293	758.59417	-0.00124
760.7	818.70	15.34	DGTS 16:0/20:4//20:4/16:0	4:3	760.60858	760.60967	-0.00109
762.8	820.80	12.30	DGTS 16:0/20:3//20:3/16:	1:1	762.62423	762.62374	0.00049
764.7	822.70	18.38	DGTS 16:0/20:2//20:2/16:0	1:2	764.63988	764.64055	-0.00067

ESI+	ESI-	Retention time	Identification	Ratio	ESI + HRMS simulation	ESI + HRMS measure.	Δ
764.7	822.70	17.94	DGTS 18:1/18:1		764.63988	764.64011	-0.00023
782.6	840.60	12.52	DGTS 18:2/20:5//20:5/18:2	2:3	782.59293	782.59344	-0.00051
784.6	842.60	14.13	DGTS 18:1/20:5//20:5/18:1	2:3	784.60858	784.60782	0.00076
784.6	842.60	14.47	DGTS 18:2/20:4//20:4/18:2	2:3	784.60858	784.60808	0.00050
784.6	842.60	13.90	DGTS 16:0/22:6/22:6/16:0	3:2	784.60858	784.60877	-0.00019
786.6	844.60	15.57	DGTS 20:4/18:1//20:4/18:1	2:3	786.62423	786.62444	-0.00021
786.7	844.70	16.47	DGTS 18:0/20:5//20:5/18:0	1:2	786.62423	786.62542	-0.00119
788.7	846.70	18.23	DGTS 18:0/20:4//20:4/18:0	2:3	788.63988	788.63996	-0.00008
788.7	846.70	16.80	DGTS 18:1/20:3//20:3/18:0	2:3	788.63988	788.64069	-0.00081
804.7	862.70	10.87	DGTS 20:5/20:5		804.57725	804.57806	-0.00081
806.7	864.70	12.15	DGTS 20:4/20:5//20:4/20:5	5:4	806.59293	806.59346	-0.00053
808.7	866.70	13.57	DGTS 20:4/20:4		808.60858	808.60861	-0.00003
474.4	532.40	2.30	LysoDGTS 16:0		474.37891	474.37848	0.00043
520.4	578.40	2.60	LysoDGTS 20:5		520.36326	520.36420	-0.00094
522.4	580.40	2.82	LysoDGTS 20:4		522.37891	522.37951	-0.00060
524.4	582.40	3.42	LysoDGTS 20:3		524.39455	524.39312	0.00143
766.4	807.40	10.01	MGDG 14:0/20:5		766.54634	766.54762	-0.00128
768.4	809.40	11.20	MGDG 14:0/20:4		768.56202	768.56261	-0.00059
772.3	813.30	15.05	MGDG 16:0/18:2		772.59332	772.59389	-0.00057
774.3	815.30	16.63	MGDG 16:0/18:1		774.60897	774.60766	0.00131
794.3	835.30	13.29	MGDG 16:0/20:5		794.57767	794.57776	-0.00009
796.3	837.30	12.60	MGDG 18:1/18:3		796.59332	796.59332	0.00000
798.3	839.40	14.10	MGDG 36:3		798.60897	798.60834	0.00063
818.3	859.30	12.09	MGDG 18:2/20:5		818.57767	818.57894	-0.00127
820.3	861.30	13.63	MGDG 18:1/20:5		820.59332	820.59323	0.00009
820.3	861.30	13.75	MGDG 18:2/20:4		820.59332	820.59369	-0.00037
822.4	863.40	14.99	MGDG 38:5		822.60890	822.60884	0.00006
840.3	881.30	10.52	MGDG 20:5/20:5		840.56202	840.56382	-0.00180
842.3	883.30	11.74	MGDG 20:4/20:5		842.57767	842.57820	-0.00053
844.3	885.30	12.77	MGDG 20:3/20:5		844.59332	844.59334	-0.00002
844.3	885.30	13.00	MGDG 20:4/20:4		844.59332	844.59331	0.00001
760.4	741.40	7.26	PG 16:1/18:3		760.51231	760.51312	-0.00081
762.3	743.30	7.65	PG 16:1/18:2		762.52796	762.52775	0.00021
764.3	745.30	8.71	PG 16:1/18:1		764.54361	764.54510	-0.00149
810.5	791.50	9.65	SQDG 16:0/16:1		810.53957	810.53982	-0.00025
812.5	793.50	9.94	SQDG 16:0/16:0		812.55522	812.55600	-0.00078
836.5	817.50	9.07	SQDG 18:2/16:0		836.55522	836.55551	-0.00029
838.5	819.50	9.97	SQDG 18:1/16:0		838.57087	838.57149	-0.00062
850.5	831.60	10.09	SQDG 18:2/17:0		850.57087	850.57068	0.00019
858.5	839.50	7.81	SQDG 20:5/160		858.53957	858.53961	-0.00004
860.5	841.50	8.90	SQDG 20:4/16:0		860.55522	860.55505	0.00017
862.5	843.50	9.75	SQDG 20:3/16:0		862.57087	862.57104	-0.00017
864.5	845.50	11.18	SQDG 18:2/18:0		864.58652	864.58777	-0.00125
866.5	847.50	12.56	SQDG 18:1/18:0		866.60217	866.59918	0.00299
904.6	885.60	6.20	SQDG 20:5/20:5		904.52392	904.52249	0.00143
906.6	887.60	7.13	SQDG 20:4/20:5		906.53957	906.54006	-0.00049

ESI+	ESI-	Retention time	Identification				
1006.8		45.67	TG 22:5_ 21:5_ 20:4				
1010.8		49.67	TG 20:4_ 24:0_ 18:1				
1030.8		45.89	TG 22:6_ 21:4_ 22:6				
1030.8		44.56	TG 65:16				
656.5		42.40	TG 12:0_12:0_12:0				
768.5		40.29	TG 14:0_ 14:0_ 16:0				
770.6		41.70	TG 45:6				
772.5		50.74	TG 15:2_ 15:2_ 15:1				
772.7		42.58	TG 45:5				
782.7		49.39	TG 46:3				
782.7		39.47	TG 46:3				
792.5		41.33	TG 14:0_ 18:2_ 14:0				
794.6		42.35	TG 14:0_ 18:1_ 14:0//16:1_ 16:0_ 14:0				
796.6		41.47	TG 48:0				
796.6		50.78	TG 16:0_ 14:0_ 16:0				
798.4		53.45	TG 17:2_ 17:3_ 13:1				
800.5		31.52	TG 17:2_ 17:2_ 13:1				
814.7		34.17	TG 14:0_ 14:0_ 20:5				
816.7		46.87	TG 14:0_ 14:0_ 20:4				
818.6		39.86	TG 48:3				
818.6		41.75	TG 16:0_ 18:2_ 14:1//18:2_ 16:1_ 14:0				
820.6		39.87	TG 16:1_ 18:1_ 14:0				
820.6		46.89	TG 16:0_ 18:2_ 14:0				
822.6		41.56	TG 16:0_ 18:1_ 14:0				
822.6		51.36	TG 16:0_ 16:0_ 16:1				
824.6		44.28	TG 48:0				
824.6		52.03	TG 16:0_ 16:0_ 16:0				
826.7		54.98	TG 16:2_ 16:2_ 17:2				
828.7		41.32	TG 17:2_ 17:2_ 15:1				
832.4		38.24	TG 16:1_ 18:1_ 15:1				
834.6		41.15	TG 18:2_ 15:0_ 16:0				
836.6		42.50	TG 16:0_ 18:1_ 15:0				
838.6		43.96	TG 16:0_ 17:0_ 16:0				
840.6		37.21	TG 20:5_ 16:1_ 14:0				
840.7		43.63	TG 16:0_ 18:1_ 14:0				
842.6		40.05	TG 48:5				
842.6		34.79	TG 20:5_ 16:0_ 14:0				
842.7		40.67	TG 20:4_ 16:1_ 14:0				
844.6		41.44	TG 18:2_ 18:2_ 14:0				
844.6		41.68	TG 20:4_ 14:0_ 16:0				
844.7		41.99	TG 18:3_ 18:1_ 14:0				
846.6		42.48	TG 18:2_ 18:1_ 14:0				
846.7		42.80	TG 18:0_ 18:0_ 14:3				
846.7		43.25	TG 50:3				
848.6		43.69	TG 16:0_ 18:2_ 16:0				
848.6		43.31	TG 18:1_ 18:1_ 14:0//18:1_ 16:0_ 16:1				

ESI+	ESI-	Retention time	Identification				
850.6		44.39	TG 16:0_ 18:1_ 16:0				
850.8		45.40	TG 50:1				
852.6		45.94	TG 16:0_ 16:0_ 18:0				
852.7		52.73	TG 50:0				
854.7		54.96	TG 51:5				
858.6		42.30	TG 51:4				
858.6		42.73	TG 51:4				
858.6		44.74	TG 51:4				
860.6		41.35	TG 18:2_ 18:1_ 15:0//18:2_ 17:1_ 16:0				
862.7		43.77	TG 18:1_ 15:0_ 18:1//18:1_ 16:0_ 17:1				
862.7		44.05	TG 18:2_ 17:0_ 16:0				
864.6		45.18	TG 17:0_ 18:1_ 16:0				
864.7		31.94	TG 20:5_ 18:3_ 14:0				
866.6		46.81	TG 52:8				
866.6		37.35	TG 20:5_ 18:2_ 14:0				
868.6		40.05	TG 20:4_ 18:2_ 14:0				
868.6		40.39	TG 20:5_ 18:1_ 14:0				
868.6		41.50	TG 52:4				
870.6		43.20	TG 52:5				
870.6		42.11	TG 16:0_ 16:0_ 20:5				
870.6		41.64	TG 20:4_ 16:1_ 16:0				
870.6		41.41	TG 20:4_ 18:1_ 14:0				
872.6		43.00	TG 16:0_ 16:0_ 20:4				
872.6		42.39	TG 18:1_ 18:2_ 16:1				
872.6		42.57	TG 18:2_ 18:2_ 16:0				
874.6		43.45	TG 18:2_ 18:1_ 16:0				
874.8		43.70	TG 16:0_ 16:0_ 20:3				
876.7		44.79	TG 18:0_ 18:2_ 16:0				
876.7		44.52	TG 18:1_ 18:1_ 16:0				
878.7		45.99	TG 18:0_ 18:1_ 16:0				
880.8		47.77	TG 18:0_ 18:0_ 16:0				
888.6		33.91	TG 20:5_ 14:0_ 20:5				
888.6		44.27	TG 18:1_ 18:2_ 17:0/18:1_ 19:2_ 16:0				
890.0		45.62	TG 53:2				
890.6		45.32	TG 18:0_ 17:0_ 18:2				
890.6		31.85	TG 20:4_ 14:0_ 20:5				
890.6		31.42	TG 20:5_ 16:1_ 18:3				
890.6		46.92	TG 54:9				
892.6		34.53	TG 18:0_ 18:1_ 17:0/18:1_ 19:0_ 16:0				
892.6		38.07	TG 20:5_ 18:2_ 16:1				
892.6		39.36	TG 20:5_ 20:4_ 14:1				
892.7		41.00	TG 20:4_ 14:0_ 20:4				
894.6		48.93	TG 20:5_ 18:2_ 16:0				
894.7		41.59	TG18:0_ 17:0_ 18:0				
896.7		42.08	TG 20:4_ 18:2_ 16:0				
896.7		41.35	TG 20:5_ 18:1_ 16:0				

ESI+	ESI-	Retention time	Identification				
896.6		43.15	TG 18:2_ 18:2_ 18:2				
898.6		41.20	TG 18:2_ 18:2_ 18:1				
898.7		42.77	TG 18:2_ 20:3_ 16:0//18:1_ 18:1_ 18:3				
898.7		44.52	TG 20:4_ 18:1_ 16:0				
900.6		43.57	TG 18:1_ 18:2_ 18:1				
900.7		43.85	TG 20:3_ 18:1_ 16:0				
900.7		44.30	TG 20:4_ 18:0_ 16:0				
902.7		44.95	TG 18:1_ 18:1_ 18:1				
902.5		45.25	TG 18:1_ 20:2_ 16:0				
902.6		46.14	TG 18:0_ 20:3_ 16:0				
904.6		46.49	TG 18:1_ 18:1_ 18:0				
904.7		47.86	TG 18:2_ 20:0_ 16:0				
906.6		49.90	TG 18:1_ 20:0_ 16:0/18:0_ 18:1_ 18:0				
908.8		35.96	TG 18:0_ 18:0_ 18:0				
914.6		30.34	TG 20:5_ 16:1_ 20:5				
914.7		31.55	TG 19:0_ 20:4_ 16:0				
914.7		36.38	TG 56:11				
916.6		37.03	TG 20:4_ 16:1_ 20:5				
916.6		45.31	TG 20:5_ 16:0_ 20:5				
916.6		39.30	TG 20:5_ 18:2_ 18:3				
918.7		39.04	TG 18:2_ 18:2_ 20:5				
918.7		39.75	TG 20:5_ 18:1_ 18:3				
918.7		40.50	TG 20:4_ 16:0_ 20:5				
920.6		41.30	TG 18:2_ 18:2_ 20:4				
920.6		40.63	TG 20:5_ 18:2_ 18:1				
920.6		41.72	TG 20:4_ 16:0_ 20:4				
920.7		49.02	TG 20:5_ 20:3_ 16:0				
920.7		41.85	TG 56:8				
922.7		42.22	TG 20:4_ 18:2_ 18:1				
922.7		51.20	TG 20:5_ 18:2_ 18:0				
922.7		42.49	TG 18:0_ 21:0_ 16:0				
924.6		42.88	TG 18:1_ 18:1_ 20:4				
924.6		43.24	TG 20:5_ 18:1_ 18:0				
924.7		44.62	TG 56:6				
926.6		43.54	TG 18:1_ 20:3_ 18:1				
926.6		43.95	TG 20:4_ 18:1_ 18:0				
926.6		45.34	TG 18:0_ 18:0_ 20:5				
928.6		45.10	TG 20:1_ 18:2_ 18:1/18:1_ 20:2_ 18:1				
928.6		43.84	TG 20:3_ 18:1_ 18:0				
928.7		46.12	TG 18:0_ 18:0_ 20:4				
930.7		46.10	TG 18:0_ 20:2_ 18:1/18:1_ 20:1_ 18:1				
930.7		46.94	TG 18:0_ 18:0_ 20:3/20:3_ 20:0_ 16:0				
932.7		47.99	TG 18:1_ 20:0_ 18:1				
932.7		48.38	TG 18:2_ 22:0_ 16:0				
934.8		52.47	TG 18:1_ 22:0_ 16:0				
936.8		49.94	TG 18:0_ 20:0_ 18:0				

ESI+	ESI-	Retention time	Identification				
938.5		33.16	TG 20:5_ 18:3_ 20:5				
940.6		35.76	TG 20:5_ 18:2_ 20:5				
940.7		36.00	TG 58:12				
940.7		44.54	TG 58:12				
942.6		35.28	TG 20:4_ 18:2_ 20:5				
942.6		38.36	TG 20:5_ 18:1_ 20:5				
944.5		38.94	TG 20:3_ 18:2_ 20:5				
944.6		39.40	TG 58:10				
944.5		40.18	TG 20:4_ 18:1_ 20:5				
944.5		40.44	TG 20:5_ 18:0_ 20:5				
946.5		41.66	TG 20:4_ 18:1_ 20:4				
946.5		41.35	TG 20:5_ 20:3_ 18:1				
946.7		42.5	TG 20:4_ 18:0_ 20:5				
948.6		42.35	TG 20:4_ 20:3_ 18:1				
948.6		42.35	TG 20:5_ 20:2_ 18:1				
948.7		42.64	TG 20:3_ 20:3_ 18:2				
954.7		43.20	TG 20:0_ 18:1_ 20:4				
954.7		44.40	TG 58:5				
956.6		11.61	TG 20:4_ 22:0_ 16:0				
956.7		47.95	TG 20:0_ 18:1_ 20:3				
958.7		48.05	TG 58:3				
958.7		48.53	TG 22:0_ 18:1_ 18:2				
960.7		48.91	TG 18:1_ 18:1_ 22:0				
960.8		50.10	TG 24:0_ 18:2_ 16:0				
962.6		31.50	TG 20:5_ 20:5_ 20:5				
962.8		50.59	TG 24:0_ 18:1_ 16:0				
964.6		31.56	TG 20:5_ 20:4_ 20:5				
964.6		55.33	TG 22:0_ 16:0_ 20:0/18:0_ 22:0_ 18:0				
966.6		36.66	TG 20:4_ 20:4_ 20:5				
966.6		42.22	TG 20:5_ 20:3_ 20:5				
968.6		37.22	TG 20:4_ 20:3_ 20:5				
968.6		39.54	TG 20:4_ 20:4_ 20:4				
968.6		50.50	TG 60:12				
970.6		40.83	TG 20:4_ 20:2_ 20:5				
970.8		41.30	TG 60:11				
970.8		42.01	TG 60:11				
970.8		47.28	TG 60:11				
972.8		40.41	TG 60:10				
972.8		40.93	TG 60:10				
972.8		48.34	TG 60:10				
978.7		44.17	TG 60:7				
978.7		44.55	TG 21:5_ 20:4_ 20:5				
980.7		45.79	TG 22:0_ 18:1_ 20:5				
982.8		46.90	TG 20:4_ 22:0_ 18:1				
984.6		48.79	TG 60:4				
988.8		49.40	TG 18:1_ 18:1_ 24:0				

Supplementary Table 2. List of detected phosphatidylcholines by LTQ Orbitrap high resolution mass spectrometr. Quantity of particular lipids and also their FA composition were not be able to obtain because all compounds were detected only in traces.

ESI+	Retention time	Identification	Chemical formula	ESI + HRMS simulation	ESI + HRMS measure.	Δ
730.4	10.81	C32:2	C40H77NO8P	730.5381312	730.5379	0.0002312
732.4	14.10	C32:1	C40H79NO8P	732.5537813	732.559	-0.0052187
734.4	16.31	C32:0	C40H81NO8P	734.5694313	734.5694	0.0000313
758.5	14.94	C34:2	C42H81NO8P	758.5694313	758.5679	0.0015313
760.5	16.61	C34:1	C42H83NO8P	760.5850514	760.5854	-0.0003486
780.6	13.35	C36:5	C44H79NO8P	780.5537813	780.5532	0.0005813
782.6	16.60	C36:4	C44H81NO8P	782.5694313	782.5667	0.0027313
786.4	16.96	C36:2	C44H85NO8P	786.6007315	785.5992	1.0015315
788.4	19.05	C36:1	C44H87NO8P	788.6163815	788.6139	0.0024815
804.4	12.13	C38:7	C46H79NO8P	804.5537813	804.5531	0.0006813
808.4	14.98	C38:5	C46H83NO8P	808.5850814	808.5849	0.0001814
818.4	15.50	C38:0	C46H93NO8P	818.6633317	818.6645	-0.0011683
826.4	10.55	C40:10	C48H77NO8P	826.5381312	826.5381	0.0000312
828.4	11.78	C40:9	C48H79NO8P	828.5537813	828.5544	-0.0006187
842.4	14.43	C40:2	C48H93NO8P	842.6633317	842.6606	0.0027317
844.4	15.80	C40:1	C48H95NO8P	844.6789818	844.6794	-0.0004182

ivana.schneedorferova@email.cz

Optimization and Application of Chromatographic and Mass Spectrometric Methods for Determination of Lipidome in Physiological, Nutritional and Biochemical Issues

Ph.D. Thesis, 2019

Printed in the Czech Republic by REPRO CO., v.o.s.
Edition of 5 copies

University of South Bohemia in České Budějovice
Faculty of Science
Branišovská 1760
CZ-37005 České Budějovice, Czech Republic

Phone: +420 387 776 201
www.prf.jcu.cz, e-mail: sekret-fpr@prf.jcu.cz